

Spring 2015

Formal Synthesis of CJ-12,954 and CJ-13,014 using Zinc-Mediated Tandem Chain Extension-Aldol Reaction and Synthesis and Investigation of Diastereoselectivity of Hydroxy-Cyclopropyl Peptide Isosteres

Yashoda Naga Deepthi Bhogadhi
University of New Hampshire, Durham

Follow this and additional works at: <https://scholars.unh.edu/dissertation>

Recommended Citation

Bhogadhi, Yashoda Naga Deepthi, "Formal Synthesis of CJ-12,954 and CJ-13,014 using Zinc-Mediated Tandem Chain Extension-Aldol Reaction and Synthesis and Investigation of Diastereoselectivity of Hydroxy-Cyclopropyl Peptide Isosteres" (2015). *Doctoral Dissertations*. 2204.

<https://scholars.unh.edu/dissertation/2204>

This Dissertation is brought to you for free and open access by the Student Scholarship at University of New Hampshire Scholars' Repository. It has been accepted for inclusion in Doctoral Dissertations by an authorized administrator of University of New Hampshire Scholars' Repository. For more information, please contact nicole.hentz@unh.edu.

I. FORMAL SYNTHESIS OF CJ-12,954 AND CJ-13,014 USING ZINC-MEDIATED TANDEM CHAIN EXTENSION-ALDOL REACTION

II. SYNTHESIS AND INVESTIGATION OF DIASTEREOSELECTIVITY OF HYDROXY-CYCLOPROPYL PEPTIDE ISOSTERES

BY

Yashoda Naga Deepthi Bhogadhi

M.S., University of South Dakota, 2009

DISSERTATION

Submitted to the University of New Hampshire

in Partial Fulfillment of the Requirements for the Degree of

Doctor of Philosophy

in

Chemistry

May, 2015

This dissertation has been examined and approved in partial fulfillment of the requirements for the degree of Doctor of Philosophy in Chemistry by

Dissertation Director, Charles K. Zercher
Professor of Chemistry

Gary R. Weisman, Professor of Chemistry

Glen P. Miller, Professor of Chemistry

Gonghu Li, Assistant Professor of Chemistry

Xiaowei Teng, Associate Professor of Chemical Engineering

On April 23, 2015

Original approval signatures are on file with the University of New Hampshire Graduate School

DEDICATION

*This dissertation is dedicated to
My grand parents*

Kammili Papaiah and Kammili Sarojini

*The love and respect I have for you both cannot be expressed in words.
Thank you for all your unconditional love, kindness, sacrifices which made what I am today.*

ACKNOWLEDGEMENTS

The entire department of chemistry at the University of New Hampshire has contributed in fulfilling my dream of receiving doctorate in chemistry. The first person I want to thank is my mentor and advisor, Professor Charles K. Zercher for accepting me into his group and providing me an opportunity to work on the challenging projects. My first introductory organic chemistry class at UNH was taught by Prof. Zercher and his extremely detailed and passionate teaching provided me all the basic knowledge needed throughout my graduate study. His immense support and guidance throughout my graduate study have been invaluable. He was extremely patient and helpful during the most difficult times, which will be remembered forever. I am continually amazed and inspired at the vast knowledge Prof. Zercher possesses for the field of organic syntheses.

I am extremely thankful to my committee members, Prof. Gary R. Weisman, Prof. Glenn P. Miller, Prof. Gonghu Li and Prof. Xiaowei Teng for their valuable suggestions and constructive criticism into my research. I had the fortune of taking class with Prof. Gary R. Weisman. His depth of knowledge and perfectionism in details always amazed me and is a constant source of inspiration. I am extremely grateful to Prof. Richard P. Johnson for all his generosity and computational help. I had the pleasure of taking classes with Prof. Arthur Greenberg, Prof. Roy Planalp, Prof. Howard R. Mayne, Prof. Sterling A. Tomellini and Prof. Erik Berda. Their valuable courses and guidance made my learning more exciting and memorable. I am very thankful to Dr. Patricia Wilkinson for all her assistance with the NMR spectrometer and other instrumentation. She is extremely patient and helpful in answering my questions. I want to thank John Briggs for taking time and running X-ray crystal

diffraction instrument. My sincere thanks to Cindi Rohwer, Peg Torch, Bob Constantine, Kristin Blackwell and Sue Small for keeping the chemistry department running smoothly.

I am extremely grateful to Jennifer Mazzone, who is a constant source of inspiration. I am very thankful to all Zercher group members, Alex Jacobine, Ian Taschner, Matt Mower, Peter Moran, Lindsey Daniels, Amanda St. Jean, Kimberly Drew, Kaushik Bala who all made my graduate school experience more memorable. I am very grateful to Carley Spencer for all her kindness and giving me the most memorable experience of arranging baby shower, which will be cherished forever. I want to thank Rekha Chhetri for being extremely helpful and supportive during my last days at UNH. My sincere thanks to all additional colleagues and friends, Justin Massing, Aida Ajaz, Kate Cahill, Jessica Morgan, Amanuel Ghidey, Erin McLaughlin, Julia Chan, Jared Pearl, Leon Wong, Barbara Wong, Sara Joiner who all contributed in their own ways to my experience at UNH.

I am greatly thankful to my parents Deva Rayalu and Venkateswaramma Bhogadhi without whom I wouldn't come this far. My mother made many sacrifices in her life in order for me to pursue my educational goals, for which I am ever grateful. I am very much indebted to my in-laws Mohan Rao and Krishna Veni Thamatam for their enormous support and love for me and my daughter Achintya. Without their immense support in my most crucial time this dissertation is not possible. I am very grateful to god for giving me Rajesh in my life. He is the best thing that happened in my life and I find no words to express my thanks for what all he did to me. My daughter Achintya is a bundle of joy, gifted by god. She made me a complete person and showed me the complete meaning of happiness.

Another important person to thank in this wonderful journey is Laura Zercher for immensely supporting me like a family when I started my new journey as a mother. Finally I want to thank Graduate school, University of New Hampshire for the graduate summer teaching fellowship and Department of Chemistry for all the awards and funding.

TABLE OF CONTENTS

DEDICATION	iii
ACKNOWLEDGEMENTS.....	iv
LIST OF SCHEMES.....	xiv
LIST OF FIGURES	xviii
LIST OF TABLES.....	xx
LIST OF ABBREVIATIONS.....	xxi
ABSTRACT.....	xxii
CHAPTER I.....	1
INTRODUCTION	1
Carbenoid.....	1
Zinc carbenoids.....	1
Zinc-mediated chain extension reaction	2
Mechanism of zinc-mediated chain extension.....	6
Zinc-mediated chain extension of β -diketones	8
Functionalization of β -position of the γ -keto backbone.....	12
Tandem chain extension protocols and their applications in natural product synthesis.....	16

Tandem chain extension-aldol reaction	17
CAN-mediated oxidative cleavage of hemiacetals	21
Tandem chain extension-oxidation-elimination reaction.....	22
Tandem chain extension-Mannich reaction	24
α -Methylation of γ -keto carbonyl	25
Tandem Chain Extension-Acylation Reaction.....	26
Summary	29
CHAPTER II.....	30
FORMAL SYNTHESIS OF CJ-12,954 AND CJ-13,014 USING ZINC-MEDIATED TANDEM CHAIN EXTENSION-ALDOL REACTION	30
Basic Ring-Systems of Spiroketal.....	30
Configuration and Stereochemistry in Spiroketal.....	31
CJ-12,954 and Its Congeners – New Anti- <i>Helicobacter pylori</i> Agents	32
First Reported Synthesis of <i>ent</i> -CJ-12,954 and <i>ent</i> -CJ-13,014.....	37
Aiken’s attempts towards the synthesis of CJ-12,954	39
Efforts towards the formal synthesis of CJ-12,954 and CJ-13,014	42
First Synthetic Approach Towards Spiroacetal Backbone	43
Attempts towards the synthesis of β -keto imide 159	44
DCC Coupling Route for the Synthesis of β -Keto imide 175	47

Tandem Chain Extension Aldol Reaction (TCEA):	49
Synthesis of (<i>R</i>)- γ -Valerolactone	50
DCC Coupling Route for the synthesis of β -keto imide 194	53
Barton decarboxylation of spiroketals 216 and 217	63
Characterization of spiroketals 206 and 207	70
 CHAPTER III	 80
 SYNTHESIS AND INVESTIGATION OF DIASTEREOSELECTIVITY OF HYDROXY- CYCLOPROPYL PEPTIDE ISOSTERES.....	 80
 Zinc-mediated chain extension reaction for the preparation of peptide isosteres.....	 81
 Cyclopropane peptide isosteres.....	 83
 Novel cyclopropanol peptide isosteres	 84
 Homologation-cyclopropanation reaction for the preparation of peptide isosteres..	 85
 Tandem homologation-cyclopropanation-rearrangement-lactonization (HCRL)	 88
 Taschner efforts for the stereochemical determination of major bicyclic lactone....	 93
 Current work	 95
 Synthesis of β -keto imide of phenyl carbamate protected proline.....	 96
 Chelation Model vs Felkin-Anh Model	 99
 NOE studies to determine the stereochemistry of major bicyclic lactone	 101
 Synthesis of bicyclic lactone from TMS cyclopropanol.....	 104

VT Experiment of TMS cyclopropanol 299	106
Effect of Evans auxiliary on the diastereoselectivity of formation of bicyclic lactones 290 and 291	112
Summary of TBAF mediated rearrangement of TMS cyclopropanols.....	116
Tosyl Protected Proline derived β -keto imides	117
Conclusions and Future Work.....	120
CHAPTER IV	122
EXPERIMENTALS.....	122
GENERAL EXPERIMENTAL SECTION	122
DETAILED EXPERIMENTAL SECTION	124
(R)-5-Methyldihydrofuran-2(3H)-one (181).....	124
(R)-tert-Butyldimethylsilyl 4-((tert-butyldimethylsilyl)oxy)pentanoate (190).....	125
(R)-4-((tert-Butyldimethylsilyl)oxy)pentanoic acid (191).....	126
4-(Dimethylamino)pyridin-1-ium (R)-4-((tert-butyldimethylsilyl)oxy)-1-(2,2-dimethyl-4,6-dioxo-1,3-dioxan-5-ylidene)pentan-1-olate DMAP salt (192)	127
(R)-4-((tert-Butyldimethylsilyl)oxy)-1-(2,2-dimethyl-4,6-dioxo-1,3-dioxan-5-ylidene)pentan-1-olate (193).....	127
(R)-1-((S)-4-Benzyl-2-oxooxazolidin-3-yl)-6-((tert-butyldimethyl silyl)oxy) heptane 1,3-dione (194)	128

(4 <i>S</i>)-4-Benzyl-3-((2 <i>R</i> ,3 <i>R</i>)-5-((<i>R</i>)-3-((<i>tert</i> -butyldimethylsilyl)oxy)butyl)-2-(3-((<i>tert</i> -butyldiphenylsilyl)oxy)propyl)-5-hydroxytetrahydrofuran-3-carbonyl)oxazolidin-2-one (210, 211)	129
(<i>S</i>)-4-Benzyl-3-((2 <i>R</i> ,3 <i>R</i> ,5 <i>R</i> ,7 <i>R</i>)-2-(3-((<i>tert</i> -butyldiphenylsilyl)oxy)propyl)-7-methyl-1,6-dioxaspiro[4.4]nonane-3-carbonyl)oxazolidin-2-one (212)	131
(<i>S</i>)-4-Benzyl-3-((2 <i>R</i> ,3 <i>R</i> ,5 <i>S</i> ,7 <i>R</i>)-2-(3-((<i>tert</i> -Butyldiphenylsilyl)oxy)propyl)-7-methyl-1,6-dioxaspiro[4.4]nonane-3-carbonyl)oxazolidin-2-one (213)	131
(2 <i>R</i> ,3 <i>R</i> ,5 <i>R</i> ,7 <i>R</i>)-2-(3-((<i>tert</i> -Butyldiphenylsilyl)oxy)propyl)-7-methyl-1,6-dioxaspiro[4.4]nonane-3-carboxylic acid (216)	132
(2 <i>R</i> ,3 <i>R</i> ,5 <i>S</i> ,7 <i>R</i>)-2-(3-((<i>tert</i> -Butyldiphenylsilyl)oxy)propyl)-7-methyl-1,6-dioxaspiro[4.4]nonane-3-carboxylic acid (217)	133
<i>tert</i> -Butyl(3-((2 <i>R</i> ,5 <i>R</i> ,7 <i>R</i>)-7-methyl-1,6-dioxaspiro[4.4]nonan-2-yl)propoxy)diphenylsilane (206)	135
<i>tert</i> -Butyl(3-((2 <i>R</i> ,5 <i>S</i> ,7 <i>R</i>)-7-methyl-1,6-dioxaspiro[4.4]nonan-2-yl)propoxy)diphenylsilane (207)	135
4-((<i>tert</i> -Butyldimethylsilyl)oxy)butan-1-ol (180)	137
4-((<i>tert</i> -Butyldimethylsilyl)oxy)butanal (176)	137
4-((<i>tert</i> -Butyldiphenylsilyl)oxy)butan-1-ol (208)	138
4-((<i>tert</i> -Butyldiphenylsilyl)oxy)butanal (209)	138
5-(1-hydroxyethylidene)-2,2-dimethyl-1,3-dioxane-4,6-dione (166)	139
(<i>S</i>)-1-(4-Benzyl-2-oxooxazolidin-3-yl)butane-1,3-dione (167)	140

(<i>S</i>)-3-Acetyl-4-benzyloxazolidin-2-one (169)	140
(<i>S</i>)-2-Amino-3-phenylpropan-1-ol (163)	141
(<i>S</i>)-Ethyl (1-hydroxy-3-phenylpropan-2-yl)carbamate (164)	142
(<i>S</i>)-4-benzyloxazolidin-2-one (161).....	142
(4 <i>S</i>)-4-benzyl-3-((2 <i>R</i> ,3 <i>R</i>)-5-((<i>R</i>)-3-((tert-butyl)dimethylsilyl)oxy)butyl)-2-(3-((tert-butyl)dimethylsilyl)oxy)propyl)-5-hydroxytetrahydrofuran-3-carbonyloxazolidin-2-one (177)	143
(<i>S</i>)-1-(Phenoxycarbonyl) pyrrolidine-2-carboxylic acid (286).....	144
4-(Dimethylamino)pyridin-1-ium(<i>S</i>)-(2,2-dimethyl-4,6-dioxo-1,3-dioxan-5-ylidene)(1-(phenoxycarbonyl)pyrrolidin-2-yl)methanolate (287)	145
(<i>S</i>)-phenyl 2-(3-oxo-3-(2-oxooxazolidin-3-yl)propanoyl)pyrrolidine-1-carboxylate (289)	146
(<i>S</i>)-phenyl 2-((1 <i>S</i> ,5 <i>S</i>)-3-oxo-2-oxabicyclo[3.1.0]hexan-1-yl)pyrrolidine-1-carboxylate (290) and (<i>S</i>)-phenyl 2-((1 <i>R</i> ,5 <i>R</i>)-3-oxo-2-oxabicyclo[3.1.0]hexan-1-yl)pyrrolidine-1-carboxylate (291)	147
(<i>S</i>)-phenyl-2-((1 <i>S</i> ,2 <i>S</i>)-2-(2-(benzylamino)-2-oxoethyl)-1-hydroxycyclopropyl)pyrrolidine-1-carboxylate (292) and (<i>S</i>)-phenyl 2-((1 <i>R</i> ,2 <i>R</i>)-2-(2-(benzylamino)-2-oxoethyl)-1-hydroxycyclopropyl)pyrrolidine-1-carboxylate (293)	148
(<i>S</i>)-Phenyl2-((1 <i>R</i> ,2 <i>R</i>)-2-(2-(benzylamino)-2-oxoethyl)-1-hydroxycyclopropyl)pyrrolidine-1-carboxylate.....	149

N-Benzyl-2-((1 <i>S</i> ,2 <i>S</i> ,7 <i>a'</i> <i>S</i>)-3'-oxotetrahydro-3'H-spiro[cyclopropane-1,1'-pyrrolo[1,2-c]oxazol]-2-yl)acetamide (297).....	150
(<i>S</i>)-phenyl 2-(3-((<i>S</i>)-4-benzyl-2-oxooxazolidin-3-yl)-3-oxopropanoyl)pyrrolidine-1-carboxylate (298)	150
(<i>S</i>)-phenyl 2-(2-((1 <i>R</i> ,2 <i>S</i>)-2-((<i>S</i>)-4-benzyl-2-oxooxazolidin-3-yl)-2-((trimethylsilyl)oxy)cyclopropyl)acetyl)pyrrolidine-1-carboxylate (299).....	151
TBAF rearrangement of TMS cyclopropanol (299)	152
(<i>S</i>)-phenyl 2-(3-((<i>R</i>)-4-benzyl-2-oxooxazolidin-3-yl)-3-oxopropanoyl)pyrrolidine-1-carboxylate (301)	153
(<i>S</i>)-phenyl 2-(2-((1 <i>S</i> ,2 <i>R</i>)-2-((<i>R</i>)-4-benzyl-2-oxooxazolidin-3-yl)-2-((trimethylsilyl)oxy)cyclopropyl)acetyl)pyrrolidine-1-carboxylate (302).....	154
TBAF rearrangement of TMS cyclopropanol (302)	155
(2 <i>S</i>)-phenyl 2-(2-(2-(2-oxooxazolidin-3-yl)-2-((trimethylsilyl)oxy)cyclopropyl)acetyl)pyrrolidine-1-carboxylate (320).....	156

LIST OF SCHEMES

Scheme 1. Discovery of Zinc-mediated chain extension reaction	3
Scheme 2. Zinc-mediated homologation of variety of β -dicarbonyl substrate	5
Scheme 3. Proposed mechanism for zinc-mediated homologation reaction supported both experimentally and computationally where $R^2 =$ ester, amide, phosphonates	7
Scheme 4. Formation of more reactive oxygen-bound zinc enolate in β -keto imides	8
Scheme 5. Chain extension-cyclopropanation of β -diketones.	9
Scheme 6. Proposed mechanism for the chain extension-cyclopropanation of β -diketones	10
Scheme 7. Homoallylic alcohol directed cyclopropanation using a methyl-substituted carbenoid	14
Scheme 8. Homoallylic alcohol as directing group in chain extension of L-serine derived β -keto ester	15
Scheme 9. Dissociation of <i>C</i> -bound zinc enolate to <i>O</i> -bound zinc enolate, <i>Z</i> -enolate 49 and <i>E</i> -enolate 50	17
Scheme 10. Zimmerman-Traxler closed transition state model for the favored <i>Z</i> -enolate of the chain extension aldol reaction	19
Scheme 11. <i>Z</i> - and <i>E</i> - Geometries for the imide enolate	20
Scheme 12. Open transition state for tandem chain extension-aldol of β -keto imide.....	20
Scheme 13. Equilibrium between open chain and closed hemiketal isomers	21
Scheme 14. CAN-mediated oxidative cleavage of hemiacetal to γ -lactone	22
Scheme 15. Synthesis of 3,4,5-trisubstituted γ -lactone by TCEA reaction and CAN-mediated oxidative cleavage	22
Scheme 16. Formal synthesis of (+)-Brefeldin A	23
Scheme 17. Total synthesis of patulolide A and B using chain-extension-oxidation-elimination reaction	24
Scheme 18. Tandem chain extension-imine capture reaction with diphenylphosphinoyl imine	25
Scheme 19. Tandem chain extension-imine capture reaction with Boc-activated imines	25
Scheme 20. Synthesis of α -methylated and α -iodomethylated γ -keto ester.....	26
Scheme 21. First reported synthesis of α -acylated γ -keto ester	27
Scheme 22. Paal-Knorr synthesis of highly functionalized heterocycles	27
Scheme 23. One-pot synthesis of spiroketal framework of Papyracillic acid B using tandem chain extension-acylation reaction	28

Scheme 24. Synthesis of spiroketal by cyclization of dihydroxy ketone.....	32
Scheme 25. Proposed Application of TCEA reaction in the synthesis of spiroketals via hemiacetal intermediate.....	32
Scheme 26a. Retrosynthetic analysis of CJ-13,015, CJ-13,102 and CJ-13,103	36
Scheme 27b. Retrosynthetic analysis of CJ-13,015, CJ-13,102, CJ-13,103, CJ-13,104 and CJ-13,108.....	37
Scheme 28. Brimble et al. approach for the synthesis of spiroketal backbone.....	38
Scheme 29. Brimble et al. approach towards the total synthesis of <i>ent</i> -CJ-12,954 and <i>ent</i> -CJ-13,014.	39
Scheme 30. Aiken's first synthetic approach towards the synthesis of CJ-12,954.....	41
Scheme 31. Aiken's second synthetic approach towards the synthesis of CJ-12,954.	41
Scheme 32. Brimble et al. approach towards synthesis of spiroacetals 34 and 35	43
Scheme 33. Retrosynthetic scheme for the synthesis of spiroacetal 153	44
Scheme 34. Synthesis of Evans chiral auxiliary from L-phenylalanine	46
Scheme 35. Synthesis of β -keto imide 167	46
Scheme 36. Failed synthesis of β -keto imide 159 via dianion route.....	46
Scheme 37. Failed synthesis of β -keto imide 159 via mixed-Claisen route	47
Scheme 38. DCC Coupling route for the synthesis of β -keto imide 175	48
Scheme 39. TCEA reaction of β -keto imide 175 derived from racemic γ -valerolactone 170	50
Scheme 40. Synthesis of aldehyde 176	50
Scheme 41. Attempted synthesis of (<i>R</i>)- γ -valerolactone (181) using Ipc ₂ BH (182)	52
Scheme 42. Synthesis of (<i>R</i>)- γ -valerolactone (181) from (<i>R</i>)-propylene oxide (187)....	53
Scheme 43. Synthesis of β -keto imide 194 as a single diastereomer.....	54
Scheme 44. TCEA reaction of β -keto imide 194 with aldehyde 176	55
Scheme 45. TCEA reaction of β -keto imide 197 by Lai.....	57
Scheme 46. Formation of <i>anti</i> -aldol product 195 from the transition state 200 of favored <i>Z</i> -.....	57
Scheme 47. Attempt towards spiroketals synthesis using deprotection followed by spiroketalization.....	58
Scheme 48. Synthesis of aldehyde 209	60
Scheme 49. TCEA reaction of β -keto imide 194 and TBDPSiCl protected aldehyde 209 60	
Scheme 50. Spirocyclization of TCEA product 211 using camphorsulfonic acid.....	61
Scheme 51. Lithium hydroperoxide mediated hydrolysis of carboximide of spiroketal 212	63

Scheme 52. Lithium hydroperoxide mediated hydrolysis of carboximide of spiroketal 213	63
Scheme 53. Barton decarboxylation	64
Scheme 54. TCEA reaction β -Keto imide 175 and aldehyde 209	65
Scheme 55. Attempted Barton decarboxylation on carboxylic acid 220	65
Scheme 56. Attempted Barton decarboxylation on spiroketal 216	66
Scheme 57. Lithium hydroperoxide mediated hydrolysis of carboximide of spiroketals 214 and 215	67
Scheme 58. Attempted Barton decarboxylation on carboxylic acids 222 and 223	67
Scheme 59. Barton decarboxylation on carboxylic acid 216 using chloroform as the hydrogen atom source.	69
Scheme 60. Barton decarboxylation on carboxylic acid 217 using chloroform as the hydrogen atom source.	69
Scheme 61. Aspartyl protease promoted peptide hydrolysis	80
Scheme 62. Synthesis of tripeptide 235	83
Scheme 63. Cyclopropanol byproduct formed during homologation-aldol reaction	86
Scheme 64. Proposed mechanism for the formation of cyclopropanol 241	86
Scheme 65. Silane reduction of cyclopropanol 241	87
Scheme 66. First incorporated cyclopropanol isostere	88
Scheme 67. Homologation-Lactonization of β -keto imide	89
Scheme 68. Proposed mechanism of the HCRL reaction	90
Scheme 69. Rearrangement-cyclization of TMS ether to bicyclic lactone	91
Scheme 70. TMAF induced desilylation-rearrangement-lactonization	91
Scheme 71. HCRL of β -keto imide 263	92
Scheme 72. HCRL of β -keto imide 264	92
Scheme 73. HCRL of Valine and Phenylalanine derived β -keto imides	93
Scheme 74. Hydrogenolysis of bicyclic lactone 271	93
Scheme 75. Attempt at rigid structure 277 for NOE studies	94
Scheme 76. Formation of bicyclic lactones followed by ring opening	95
Scheme 77. Potassium <i>tert</i> -butoxide mediated cyclization of 60	96
Scheme 78. Phenyl carbamate protection of proline	96
Scheme 79. DCC coupling route towards the synthesis of β -keto imide 289	97
Scheme 80. HCRL reaction of β -keto imide 289	98
Scheme 81. Benzyl amine opening of bicyclic lactones 290 and 291	98

Scheme 82. Rearrangement of zinc cyclopropanoxide to bicyclic lactones	99
Scheme 83. Potassium <i>tert</i> -butoxide mediated cyclization.....	101
Scheme 84. Synthesis of β -keto imide 298	104
Scheme 85. HCRL reaction of β -keto imide 298	104
Scheme 86. Synthesis of bicyclic lactones from the rearrangement of TMS ether	105
Scheme 87. Synthesis of TMS ether 299 from β -keto imide 298	105
Scheme 88. TBAF rearrangement of TMS cyclopropanol 299	107
Scheme 89. Deprotection of TMS cyclopropanol 299 to cyclopropanol 300	108
Scheme 90. Carbenoid facilitated rearrangement of cyclopropanol 300	108
Scheme 91. Synthesis of β -keto imide 301	108
Scheme 92. HCRL reaction of β -keto imide 301	109
Scheme 93. Synthesis of TMS cyclopropanol 302	109
Scheme 94. TBAF rearrangement of TMS cyclopropanol 302	112
Scheme 95. Synthesis of TMS ether 304 from β -keto imide 289	112
Scheme 96. TBAF rearrangement of β -keto imide to bicyclic lactones	112
Scheme 97. Proposed diastereoselective mechanism for the formation of 308	114
Scheme 98. Proposed diastereoselective mechanism for the formation of 314	115
Scheme 99. Formation of sulfonamide-derived β -keto imide 278	117
Scheme 100. Synthesis of chiral β -keto imide 320	119
Scheme 101. Synthesis and TBAF mediated rearrangement of TMS cyclopropanol 119	119

LIST OF FIGURES

Figure 1. Different types of carbenoids synthesized	2
Figure 2. Cyclopropanol rearrangement	11
Figure 3. Zinc-chelated sigmatropic rearrangement of methyl cyclopropanol to aryl cyclopropanol	11
Figure 4. The A, B and C Ring Systems of Spiroketal.	30
Figure 5. Conformation in Spiroketal	31
Figure 6. The Anomeric Effect in Spiroketal.....	31
Figure 7. Structures and helicobactericidal activities of phthalides 126a-g	34
Figure 8. Helicobactericidal compounds Spirolaxine.....	35
Figure 9. Spiroacetals synthesized by Brimble et al.....	42
Figure 10. Targeted spiroacetals 151 and 152 for formal synthesis	43
Figure 11. D-camphorsultam and Evans chiral auxiliary	45
Figure 12. Establishing C-7 stereocenter in 151 and 152 from (<i>R</i>)- γ -valerolactone	51
Figure 13. Methyl protons of a) racemic γ -valerolactone and b) (<i>R</i>)- γ -valerolactone with	53
Figure 14. Presence of three doublets in ¹ H NMR of TCEA product showing presence of open-chain and two diastereomers of hemiacetals.	56
Figure 15. Spiroacetals synthesized by Brimble et al.....	59
Figure 16. New targets for formal synthesis of CJ-12,954 and CJ-13,014	59
Figure 17. Spiroketal from the other possible <i>anti</i> -aldol product	61
Figure 18. ¹ H NMR spectra of spiroketals 206 (<i>R, R, R</i>) and 207 (<i>R, S, R</i>)	73
Figure 19. ¹³ C NMR spectrum of spiroketal 206	77
Figure 20. ¹³ C NMR spectrum of spiroketal 207	78
Figure 21. DEPT spectra a) DEPT-135 (CH ₃ , CH and CH ₂ carbons) b) DEPT-90 (CH carbons) c) DEPT-45 (all protonated carbons) of spiroketal 206	79
Figure 22. Ketomethylene and hydroxyethylene peptide isosteres	81
Figure 23. Peptidomimetic 236	84
Figure 24. Novel cyclopropanol peptide isostere	85
Figure 25. Unexpected cyclopropanol by-product	85
Figure 26. X-ray crystal structure depicting the absolute stereochemistry of cyclopropane of cyclopropanol 292	99
Figure 27. Chelation model predicting the stereochemistry of major bicyclic lactone	100

Figure 28. Felkin-Anh model would predict potential formation of the minor diastereomer	101
Figure 29. NOE of the tricyclic compound 297	102
Figure 30. NOE of the tricyclic compound 297	103
Figure 31. ^1H NMR of TMS cyclopropanol 299 at a) 70 °C b) 25 °C.....	106
Figure 32. VT ^1H NMR (500 MHz) experiment of TMS cyclopropanol 302 a) 70 °C b) 55 °C c) 25 °C	110
Figure 33. Determination of diastereomeric ratio of TMS cyclopropanol 302 using MestReNova line fitting	111
Figure 34. Model of TBAF mediated rearrangement of TMS protected cyclopropanol	114
Figure 35. Model of TBAF mediated rearrangement of TMS protected cyclopropanol	115
Figure 36. ^1H NMR of a) mixture of bicyclic lactones b) bicyclic lactone obtained from the TBAF rearrangement.....	120

LIST OF TABLES

Table 1. Conversion of β -keto esters to γ -keto esters using chain extension reaction.....	4
Table 2. Conversion of β -keto esters and amides to β -substituted γ -keto substrates using methyl and phenyl substituted carbenoids.....	13
Table 3. Diastereoselective synthesis of β -methyl γ -keto esters using an L-serine auxiliary	16
Table 4. Tandem-chain extension aldol reaction of β -keto esters and amides	18
Table 5. Scope of tandem chain extension-acylation reaction.....	29
Table 6. ^1H NMR assignment of spiroketals 206 and 207 compared to their enantiomers 134 and 135 reported by Brimble et al.	72
Table 7. ^{13}C NMR assignment of spiroketals 206 and 207 compared to their enantiomers 134 and 135 reported by Brimble et al. (The symbol * is used to denote either the (<i>S</i> , <i>R</i> , <i>S</i>) or the (<i>S</i> , <i>S</i> , <i>S</i>) isomer)	76
Table 8. Two-step synthesis of amino acid derived γ -keto methyl esters	82

LIST OF ABBREVIATIONS

CAN	Ceric Ammonium Nitrate
Cbz	Carbobenzyloxy
COSY	Correlation spectroscopy
DBU	1,8-Diazabicyclo[5.4.0]undec-7-ene
DCC	Dicyclohexylcarbodiimide
DEPT	Distortionless enhancement by polarization transfer
DMAP	4-Dimethylaminopyridine
DMSO	Dimethyl sulfoxide
HSQC	Heteronuclear single quantum coherence spectroscopy
LDA	Lithium Diisopropylamide
LiAlH ₄	Lithium aluminium hydride
NOE	Nuclear Overhauser Effect
Pmb	p-Methoxybenzyl
TBAF	Tetra-n-butylammonium fluoride
TBDMS	<i>tert</i> -Butyldimethylsilyl
TBDPS	<i>tert</i> -Butyldiphenylsilyl
THF	Tetrahydrofuran
TMSCl	Trimethylsilyl chloride
pTsOH	p-Toluenesulfonic acid
Ts	Tosyl

ABSTRACT

- I. **FORMAL SYNTHESIS OF CJ-12,954 AND CJ-13,014 USING ZINC-MEDIATED TANDEM CHAIN EXTENSION-ALDOL REACTION**

- II. **SYNTHESIS AND INVESTIGATION OF DIASTEREOSELECTIVITY OF HYDROXY- CYCLOPROPYL PEPTIDE ISOSTERES**

by

Yashoda Naga Deepthi Bhogadhi

University of New Hampshire, May 2015

A formal synthesis of the natural products CJ-12,954 and CJ-13,014 was successfully accomplished using the zinc-mediated tandem chain extension-aldol reaction methodology. This chemistry was performed on a chiral β -keto imide synthesized using a DCC coupling reaction. The diastereoselectivity of the aldol reaction was controlled by an Evans chiral auxiliary. Comparison between the reported and experimental spectral data for the spiroketals confirmed the structural assignment.

The diastereoselectivity of the homologation-cyclization-rearrangement-lactonization reaction of β -keto imide derived from phenyl carbamate-protected proline was studied. Tetra-*n*-butylammonium fluoride-mediated rearrangement of trimethylsilyl cyclopropanol demonstrated the role of chiral auxiliary and the amino acid stereocenter in controlling the diastereoselectivity of the bicyclic lactone formation.

CHAPTER I

INTRODUCTION

Carbenoid

The term 'carbenoid' was developed in the course of expanding new carbene precursors.¹
² A carbenoid is a synthetically useful version of a carbene that is stabilized by complexation to a metal.^{1,2} Carbenoids can be divided into two classes.

- 1) those of general structure MCH_2X , $M = Zn, Sm, Al$ etc.
- 2) those that belong to structure $M=CH_2$

Organozinc carbenoids that possess sp^3 -hybridized carbon are an extensively studied class of carbenoids owing to their excellent reactivity and their ambiphilic nature.³ Organozinc carbenoids can act both as nucleophiles and electrophiles in reactions like addition to C-C double bonds, 1,2-alkyl(aryl) migrations etc.³

Zinc carbenoids

The first zinc carbenoid ($IZnCH_2I$) was prepared by Emschwiller in 1929,⁴ but this zinc carbenoid did not attract significant attention until Simmons and Smith reported in 1958 that this reagent could be used for the stereospecific conversion of alkenes to cyclopropanes.^{5, 6} The Simmons-Smith cyclopropanation reaction uses iodomethylzinc iodide ($IZnCH_2I$), which is prepared by mixing a zinc/copper couple with CH_2I_2 in ether.^{5, 6} This reaction is widely used due to the stereospecificity with respect to the double bond geometry and its compatibility with a wide variety of functional groups.

Variants of this versatile cyclopropanating reagent have been developed by replacing the iodide substituent bonded to the zinc atom with an alternate R group. Many of the variants are summarized in **Figure 1**.⁷ One of those carbenoids that is a more practical and reproducible cyclopropanation reagent is EtZnCH₂I, which was developed by Furukawa in 1966 by mixing equimolar amounts of readily available diethylzinc with CH₂I₂.⁸⁻¹⁰ This reaction was particularly useful for the cyclopropanation of cationically polymerizable olefins such as vinyl ethers. The Simmons-Smith reaction gave lower yields due to polymerization.

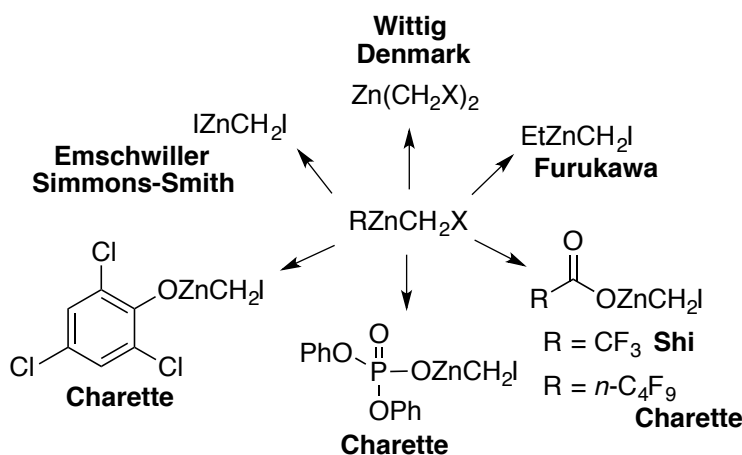
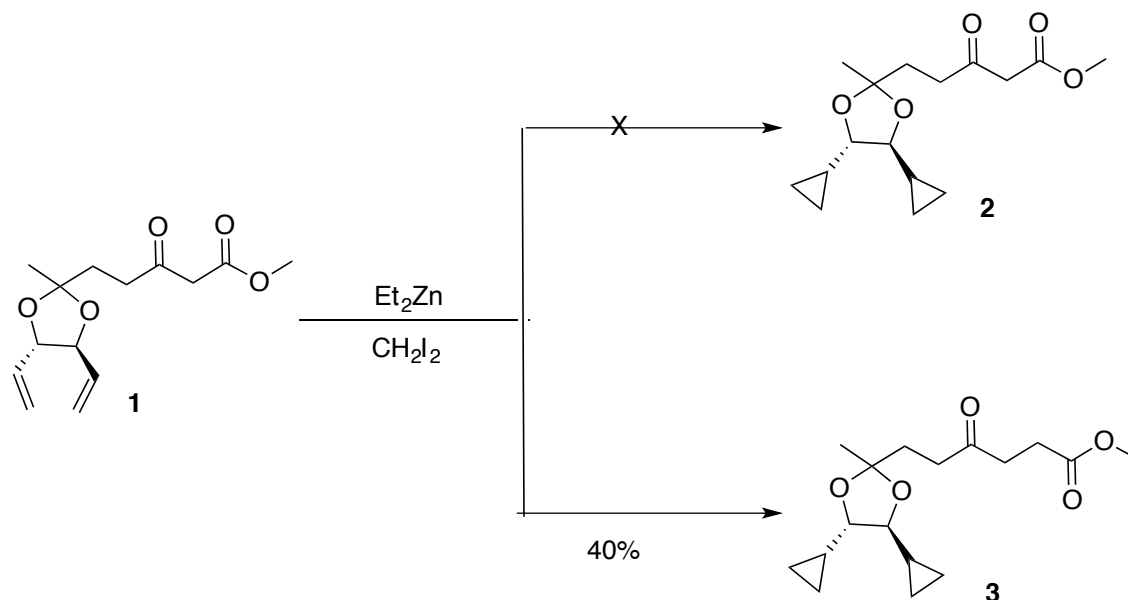


Figure 1. Different types of carbenoids synthesized

Zinc-mediated chain extension reaction

Another application of the Furukawa carbenoid (EtZnCH₂I) was not known until Brogan and Zercher in 1997 reported the one carbon homologation of β-keto esters to γ-keto esters.¹¹ This reaction was serendipitously discovered by Brogan and Zercher during an attempt to cyclopropanate the terminal olefins of ketal **1** (**Scheme 1**). Ketal **1**, when subjected to Furukawa carbenoid EtZnCH₂I, gave an unanticipated product **3**, which contained both the cyclopropane and an additional methylene unit between the two carbonyls. Similar methods have been reported for the synthesis of γ-keto carbonyls and all of the methods report the intermediacy of a

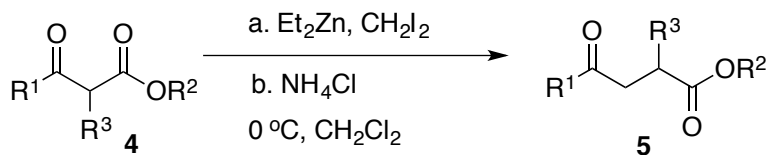
cyclopropane intermediate.¹²⁻¹⁶ However, the zinc-carbenoid-mediated homologation reaction, offers the advantages of being a mild, simple and efficient one-pot reaction.¹¹



Scheme 1. Discovery of Zinc-mediated chain extension reaction

A variety of β -keto esters, β -diketones and α -substituted β -keto esters were subjected to the zinc-mediated chain extension conditions to elucidate the scope of the reaction.¹¹ Several different β -keto esters **4a-i** (Table 1), when subjected to 5 equivalents of zinc carbenoid, derived from diethylzinc and diiodomethane, rendered their respective γ -keto ester homologues **5a-i**. All simple β -keto esters **4a-f** proceeded cleanly and efficiently to their corresponding γ -keto ester homologues in high yields. Olefin-containing β -keto esters **4g-h** tolerated the chain extension conditions, thus affording their respective olefin-containing γ -keto ester homologues **5g-h**. This result demonstrates that the chain extension reaction is more rapid than the cyclopropanation of olefins (**4g,h**). α -Substituted β -keto ester **4i** gave the corresponding chain-extended product **5i**,

albeit in low yield and with the emergence of multiple byproducts. However, β -diketones behaved differently and will be discussed later in this chapter.

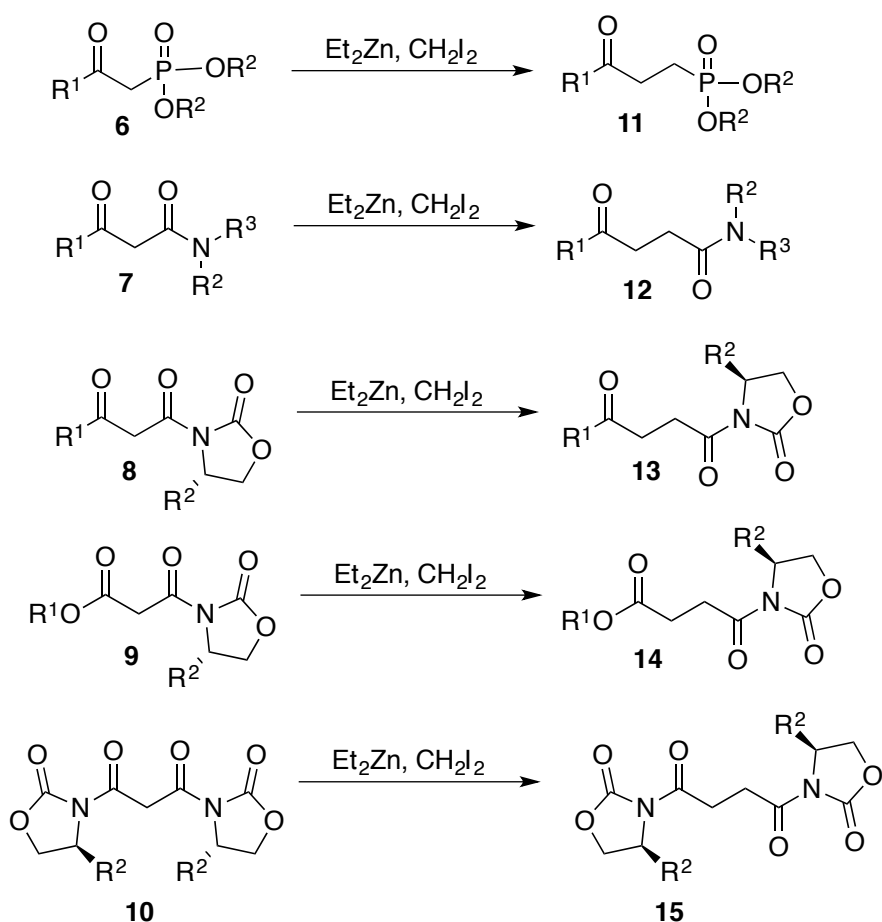


Entry	Starting material	R ¹	R ²	R ³	Yield (%)
1	4a	Me	Me	H	81
2	4b	Me	<i>t</i> -Bu	H	74
3	4c	<i>t</i> -Bu	Me	H	71
4	4d	Ph	Et	H	58
5	4e	<i>i</i> -Pr	Et	H	68
6	4f	Ph(CH ₂) ₂ -	Et	H	73
7	4g	CH ₂ = CH(CH ₂) ₂ -	Me	H	74
8	4h	PhCH = CH-	Me	H	68
9	4i	Me	Me	Me	26

Table 1. Conversion of β -keto esters to γ -keto esters using chain extension reaction

The scope of the zinc-mediated chain extension reaction has been extended to variety of β -dicarbonyl substrates (**Scheme 2**).¹⁷ Some of those early substrates studied were β -keto phosphonates (**6**) (**Scheme 2**).¹⁸ γ -Keto phosphonates are present in molecules that possess diverse biological activity ranging from antihypertensive agents,¹⁹ fungicidal and herbicidal

activity and this functionality could be obtained cleanly from the corresponding β -keto phosphonates in one step using the zinc carbenoid chain extension reaction. While β -keto esters undergo chain-extension in minutes, β -keto phosphonates required longer reaction times for chain extension.



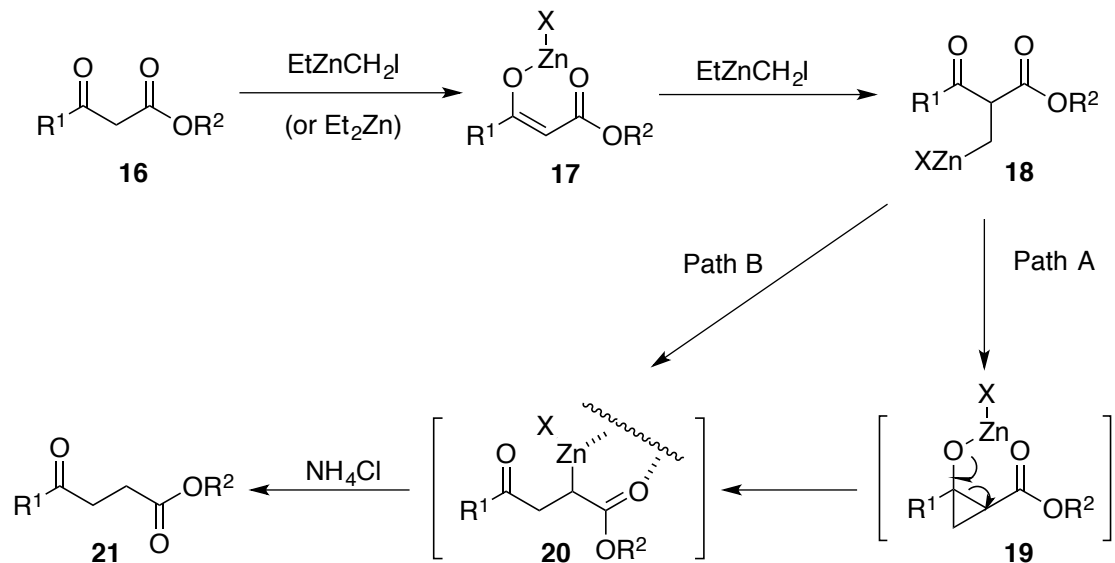
Scheme 2. Zinc-mediated homologation of variety of β -dicarbonyl substrate

A wide variety of β -keto amides (7),²⁰ including primary, secondary and tertiary amides were chain extended to their respective γ -keto amides in good yields. While β -keto tertiary amides provided products in good yields (42-88%), secondary and primary amides generated products in lower yields, possibly due to the acidic hydrogen on amide and/or difficulty in

extracting water-soluble products after aqueous work-up. Other substrates like β -keto imides (**8**),²¹⁻²³ α -carboxyester imides (**9**)^{24, 25} and α -carboxydiimides (**10**)²⁴ were studied and shown capable of undergoing zinc-mediated homologation (**Scheme 2**), thus broadening the scope of this reaction.

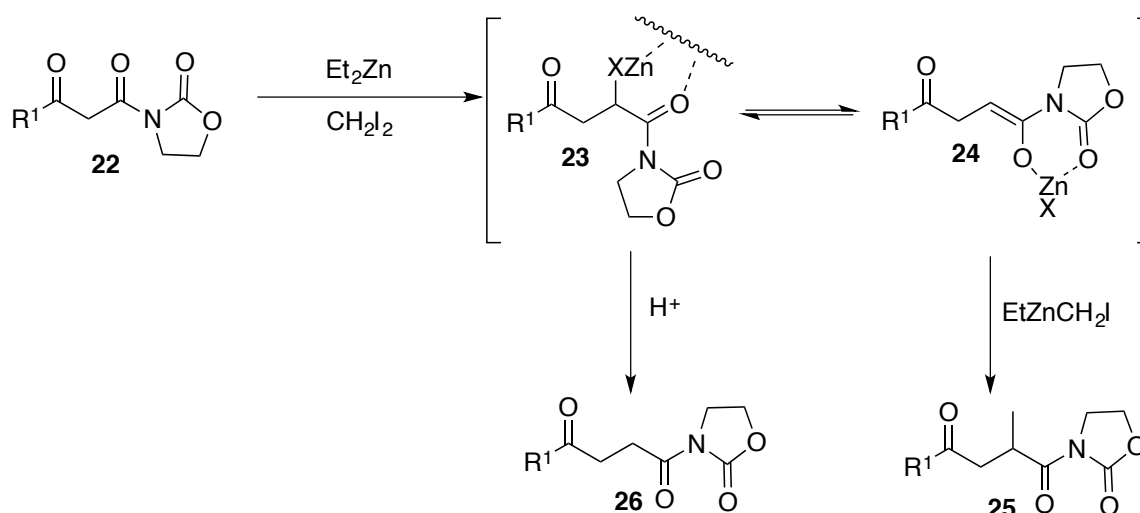
Mechanism of zinc-mediated chain extension

The mechanism of the zinc-mediated homologation reaction has been studied experimentally, including by NMR and computational studies (**Scheme 3**).^{26, 27} The proposed mechanism is described below. The methylene between the 1,3-dicarbonyl (**16**) is deprotonated either by an ethyl residue of diethylzinc or zinc carbenoid, resulting in the formation of zinc enolate **17**. The enolate **17** then undergoes alkylation with a second equivalent of zinc carbenoid, resulting in the formation of homoenolate **18**. An intramolecular cyclization of the homoenolate **18** into the keto functionality generates a donor-acceptor cyclopropane intermediate **19** via path A, which undergoes fragmentation due to ring strain to provide organometallic intermediate **20**, similar to a Reformatsky-type intermediate. Cyclopropane intermediate **19** was not observed in the NMR studies. The computational studies support the intramolecular methylene transfer via cyclopropane intermediate, and show that the cyclopropane fragmentation has a very low activation barrier, suggesting that if intermediate **19** is formed, it has a very short lifetime.²⁶ The computational study also revealed an alternate mechanism for the formation of **20** via path B. This pathway does not include a donor-acceptor cyclopropane intermediate. Instead, the reaction proceeds via a 1,2-shift in which the homoenolate **18** is directly converted to Reformatsky type intermediate **20**. The inclusion of solvation in the computational model resulted in the donor acceptor pathway being lower in energy than path B; therefore, path A appears likely to be the operative pathway in solution.



Scheme 3. Proposed mechanism for zinc-mediated homologation reaction supported both experimentally and computationally where $\text{R}^2 = \text{ester, amide, phosphonates}$

The Reformatsky-type intermediate **20**, which contains anionic character at the position α to the ester, is considered as the resting state of the homologation reaction. Quenching with a mild acid like ammonium chloride gives the chain extended product **21**. NMR studies by Aiken revealed the oligomeric nature of the C-bound zinc intermediate **20**, which makes it less nucleophilic than a typical enolate; therefore, the zinc organometallic intermediate does not undergo alkylation with the excess carbenoid or the ethyl iodide present in the solution.²⁷ The mechanism suggests that two equivalents of carbenoid are required; however, in practice three equivalents are used for a typical chain extension reaction to ensure that the reaction goes to completion. The presence of any other acidic hydrogen in the substrate, like an NH or OH, requires additional carbenoid be present.



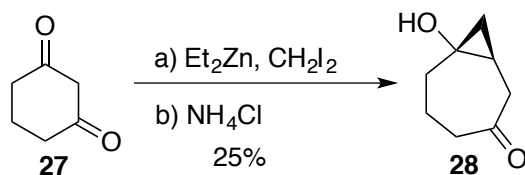
Scheme 4. Formation of more reactive oxygen-bound zinc enolate in β -keto imides

Slightly different product formation was observed in β -keto imide-derived systems (**Scheme 4**). The formation of α -methyl- γ -keto imide **25** as a byproduct during the chain extension of β -keto imides suggested a decreased stability of the organometallic intermediate.^{23, 28, 29} Such a byproduct is proposed to arise from the alkylation of Reformatsky-type intermediate **24** with the excess carbenoid in solution. This alkylation has not been observed in the case of β -keto esters. In the case of the imide functionality, intermediate **23** could be in equilibrium with enolate **24** due to potential chelation of the zinc between the two oxygen atoms. Oxygen-bound zinc enolate **24**, expected to be more reactive than carbon-bound zinc enolate **23**, could undergo alkylation with the excess carbenoid, and provide the α -methyl- γ -keto imide **25** as the byproduct. The amount of α -methylated by-product can be reduced by careful control of carbenoid stoichiometry and reaction time.

Zinc-mediated chain extension of β -diketones

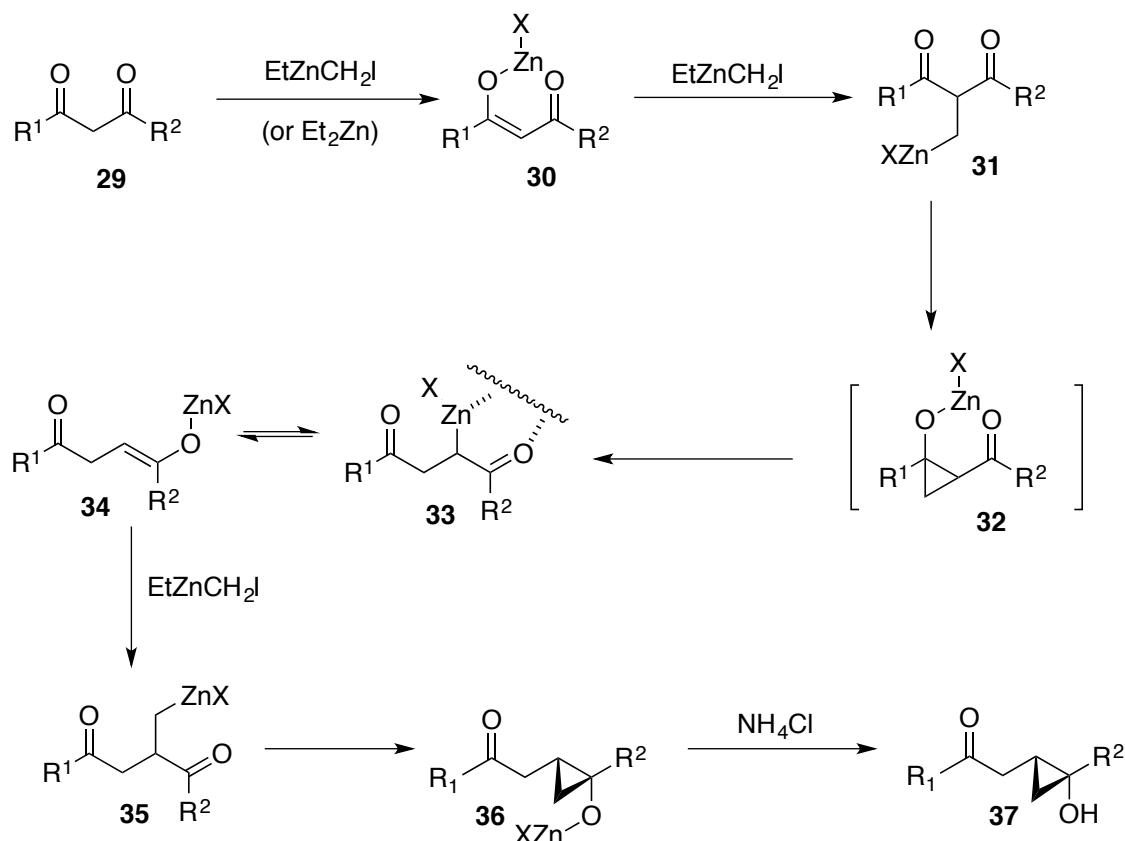
β -Diketones behave differently in zinc-mediated chain extension conditions. In the original work by Brogan and Zercher, exposure of 1,3-cyclohexanedione (**27**) to standard chain

extension conditions resulted in the formation of γ -keto cyclopropanol **28** (Scheme 5).¹¹ This product was produced by ring expansion followed by the rapid addition of the second methylene group. In a similar fashion, Xue and co-workers employed zinc carbenoid $\text{CF}_3\text{CO}_2\text{ZnCH}_2\text{I}$ for the homologation of β -diketones, resulting in the formation of γ -diketones and γ -keto cyclopropanols.³⁰



Scheme 5. Chain extension-cyclopropanation of β -diketones.

The proposed mechanism for the chain extension-cyclopropanation of β -diketones is similar to the one proposed for β -keto carbonyls, except that the zinc-enolate **34** reacts with a third equivalent of carbenoid to form the homoenolate **35** (Scheme 6). Homo enolate **35** undergoes intramolecular cyclization to generate zinc cyclopropoxide **36**, which on quenching with a mild acid generates the γ -keto cyclopropanol **37**. The key to cyclopropanol formation is the high reactivity of the zinc-enolate equivalent (**34**). Heathcock has shown that zinc-ketone enolate possesses oxygen-bound zinc, which makes the reactivity very different from the Reformatsky-like ester organometallic intermediate.³¹ Chain extension-cyclopropanation reactions of β -diketones and β -keto carbonyls have been developed for the preparation of novel cyclopropanol peptide isosteres, which will be discussed in detail in Chapter III.



Scheme 6. Proposed mechanism for the chain extension-cyclopropanation of β -diketones

A novel γ -keto cyclopropanol rearrangement has also been studied on the cyclopropanols resulting from the chain extension of β -diketones.^{29, 32} Xue and co-workers reported that two isomeric γ -keto cyclopropanols were formed from homologation-cyclopropanation of β -diketones that contains both aryl and aliphatic R groups.³⁰ Based on results by Xue³⁰ and Taschner²⁹ of the Zercher group, it was hypothesized that rearrangement of product regioisomers might be occurring during the homologation-cyclopropanation reaction. When benzoylacetone was subjected to zinc carbenoid for a short time period, the product mixture had the aryl cyclopropanol as the major product and the methyl cyclopropanol as the minor product (**Figure 2**).³² This major product would result from the preferential homoenolate **31** cyclization into the carbonyl α to an aliphatic moiety. When the above product mixture was exposed to a zinc

carbenoid, equilibration to a thermodynamic mixture containing methyl cyclopropanol as the major isomer and aryl cyclopropanol as the minor isomer resulted. A zinc-chelated sigmatropic rearrangement (**Figure 3**) was proposed and computational studies by Moran provided support for the proposed rearrangement.³³ Besides carbenoid, other organometallic bases like potassium *tert*-butoxide, sodium hydride, lithium diisopropylamide (LDA) and di-*n*-butyl magnesium have been successful in facilitating the rearrangement.³⁴

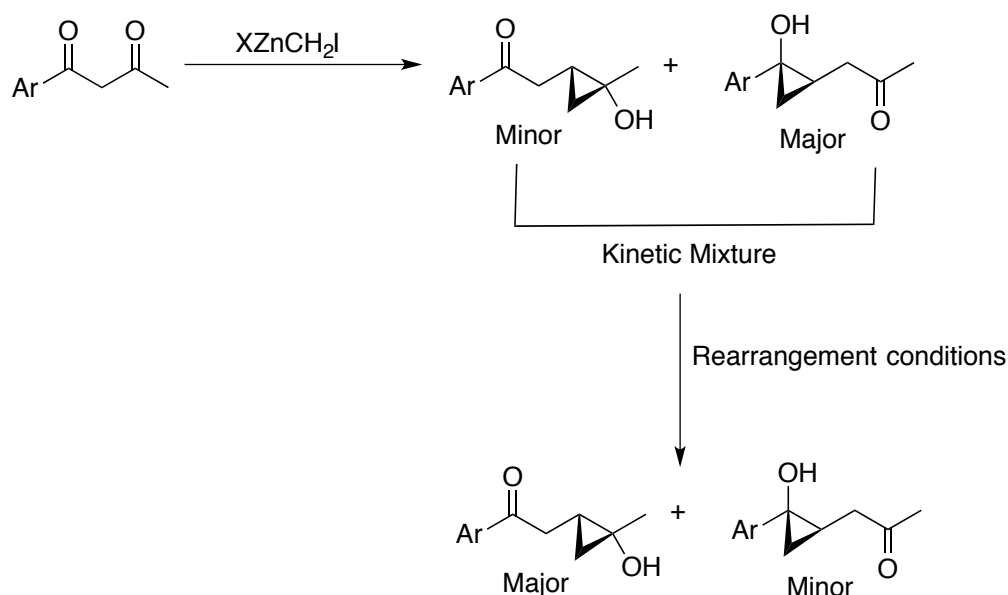


Figure 2. Cyclopropanol rearrangement

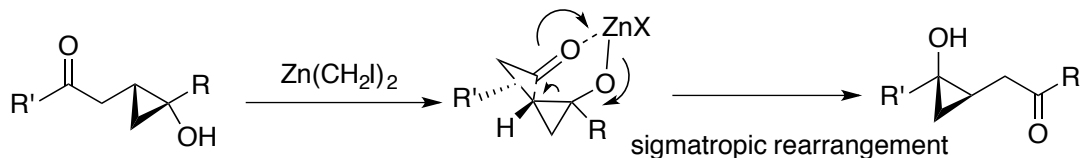


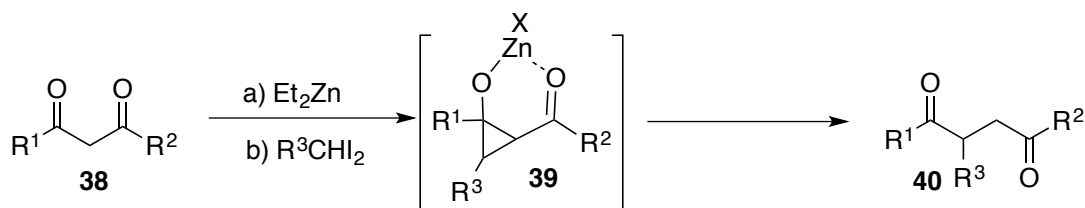
Figure 3. Zinc-chelated sigmatropic rearrangement of methyl cyclopropanol to aryl cyclopropanol

Functionalization of β -position of the γ -keto backbone

Selective functionalization of α and β carbons (carbons 2 and 3) of 1,4-dicarbonyls by deprotonation followed by electrophilic addition is not practical due to the similarity in pKa's of the α -protons adjacent to ketones, esters and amides. Zinc carbenoid-mediated chain extension reaction facilitates the incorporation of substituents at both of these positions either through the use of substituted carbenoids or by electrophile addition to the organometallic intermediate. As indicated from the proposed mechanism, the β -methylene of the homologated product arises from the insertion of zinc-carbenoid derived from 1,1-diiodomethane. On the basis of this knowledge, the β -position of the 1,4-dicarbonyl can be functionalized using a substituted carbenoid derived from *gem*-diiodoalkanes.

1,1-Diiodoethane and α,α -diiodotoluene were employed as the substituted carbenoids in the chain reaction, which resulted in the formation of β -substituted γ -keto carbonyls (**Table 2**).³⁵ Several methods are available for the preparation of *gem*-diiodoalkanes.^{36, 37} 1,1-Diiodoethane can be prepared by aluminum chloride-catalyzed reaction of 1,1-dichloroethane and ethyl iodide.³⁸ An alternative method for the preparation of 1,1-diiodoethane is conversion of acetaldehyde to its corresponding hydrazone followed by treatment of iodine in the presence of triethylamine.³⁹ α,α -Diiodotoluene can be prepared by subjecting benzaldehyde to trimethylsilyliodide.⁴⁰ Synthesis of substituted cyclopropanes employing substituted carbenoids derived from *gem*-diiodoalkanes has been reported by other groups,⁴¹ whereas synthesis of substituted donor-acceptor cyclopropanes employing substituted carbenoid has only been explored by the Zercher group.³⁵ β -Keto esters and amides were subjected to carbenoids generated from 1,1-diiodoethane to afford the corresponding β -methyl γ -keto esters or amides efficiently in one step via substituted donor-acceptor cyclopropane intermediate **39** (**Table 2**).³⁵

While β -keto esters reacted with substituted carbenoid efficiently, β -keto amides were less efficient. In addition to the methyl group, attempts to substitute phenyl group at the β -position by employing α,α -diiodotoluene was successful, however this reaction was less efficient (**Table 2**).



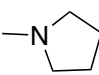
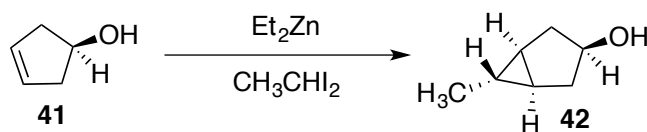
Entry	Starting material	R ¹	R ²	R ³	% yield
1	38a	Me	OMe	Me	76
2	38b	Me	O <i>t</i> -Bu	Me	88
3	38c	<i>t</i> -Bu	OMe	Me	82
4	38d	Me	OCH ₂ CH=CH ₂	Me	74
5	38e	Ph	OEt	Me	84
6	38f	Me	OBn	Me	80
7	38g	Me	—NH(Me) ₂	Me	67
8	38h	Me	—N 	Me	74
9	38i	Me	OMe	Ph	74
10	38j	Me	O <i>t</i> -Bu	Ph	44

Table 2. Conversion of β -keto esters and amides to β -substituted γ -keto substrates using methyl and phenyl substituted carbenoids.

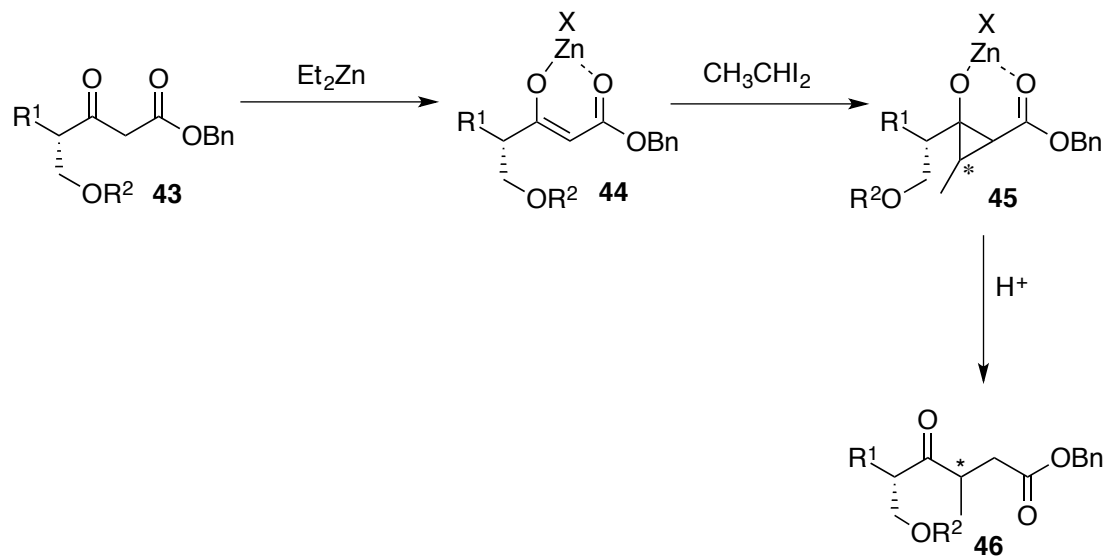
Functionalization of the β -position of 1,4-dicarbonyl generates a new stereocenter. Stereocontrol of this chiral center would broaden the scope of this reaction. Lin attempted to induce enantioselectivity in the reaction by employing a chiral ligand; however, these efforts resulted in the formation of a racemic mixture.²³ Evans auxiliaries, which resulted in a good diastereocontrol in tandem chain extension-aldol reactions, were not effective in controlling the

stereocenter at the β -position. It was hypothesized that the establishment of a chiral environment around the ketone could influence the stereochemical course of the intramolecular cyclization that produces the substituted donor-acceptor cyclopropane. Chiral allylic and homoallylic alcohols have been shown to provide modest to good stereocontrol in carbenoid cyclopropanation reactions with the selectivity attributed to hydroxyl-directing effects.⁴² For instance, treatment of 3-cyclopentenol (**41**) with methyl-substituted zinc-carbenoid produced *exo*-6-methyl-*cis*-3-hydroxybicyclo[3.1.0]hexane (**42**) as the only isomer out of four possible isomers (**Scheme 7**).⁴³ The mechanism of this reaction is proposed to involve complexation of the hydroxyl group with the zinc carbenoid, thereby facilitating stereoselective ethylidene transfer to the most accessible face of the alkene.⁴³



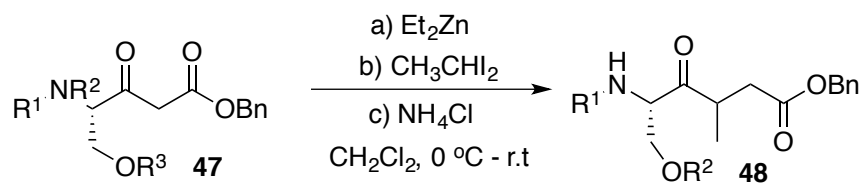
Scheme 7. Homoallylic alcohol directed cyclopropanation using a methyl-substituted carbenoid

The diastereoselective incorporation of the methyl-substituted zinc carbenoid in a chain extension reaction was probed by Mazzone, who studied reactions of L-serine-derived β -keto esters.⁴⁴ It was proposed that the L-serine-derived β -keto ester **43** would generate intermediate **44**, which contains a homoallylic hydroxyl group (**Scheme 8**).⁴⁴ Upon addition of carbenoid this homoallylic alcohol was anticipated to influence diastereoselectivity in the formation of substituted donor-acceptor cyclopropane **45**. Fragmentation of the cyclopropane intermediate **45** would retain the stereochemistry of the methyl substituent, whereas the other two cyclopropane stereocenters are destroyed upon fragmentation.



Scheme 8. Homoallylic alcohol as directing group in chain extension of L-serine derived β -keto ester

Mazzone studied the diastereomeric ratio of the β -methyl- γ -keto esters prepared from the use of a methyl-substituted carbenoid in the chain extension reaction of L-serine-derived β -keto esters (**Table 3**).⁴⁴ Substrates **47a-c** gave high diastereomeric ratios, whereas substrate **47e**, which contained a cyclic five-membered ring, gave no diastereocontrol. Therefore, it was concluded that the hydroxyl functionality of the L-serine group can serve a crucial role in the high diastereocontrol observed during the zinc carbenoid-mediated chain extension reaction using a methyl-substituted carbenoid.



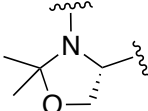
Entry	Starting material	R ¹	R ²	R ³	dr
1	47a	Boc	H	Bn	20:1
2	47b	Boc	H	TBDMS	20:1
3	47c	Boc	H	MOM	15:1
4	47d	-C(O)OCH ₃	H	Et	3:1
5	47e	Boc			1:1

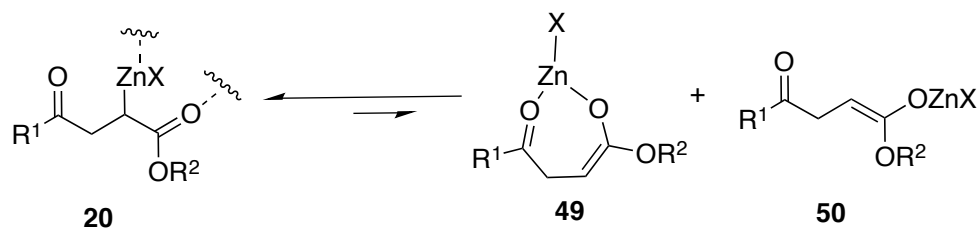
Table 3. Diastereoselective synthesis of β -methyl γ -keto esters using an L-serine auxiliary

Tandem chain extension protocols and their applications in natural product synthesis

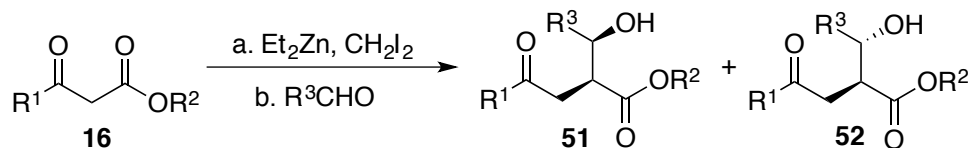
Functionalization of the α -position of 1,4-dicarbonyls through deprotonation followed by electrophilic addition is not practical; however, zinc-mediated chain extension of a 1,3-dicarbonyl generates a versatile organometallic intermediate **20**, that has anionic character α to the ester, amide or imide. Various electrophiles like aldehydes,²¹ ketones,²¹ imines,^{45, 46} iminium ions, excess carbenoid,⁴⁷ iodine,^{23, 28, 48} and anhydrides^{44, 45, 49} have been captured by the organometallic intermediate in a zinc-mediated tandem-chain extension reaction. In an effort to widen the scope of these tandem processes, methods for stereoselective functionalization of α -position were also developed. Many of these tandem processes were implemented as a key step in the synthesis of natural products. The development and application of tandem chain extension processes are described below.

Tandem chain extension-aldol reaction

The chain extension-aldol reaction was the first tandem protocol to be developed.²¹ The diastereoselectivity of the chain extension-aldol reaction was studied extensively. Chain extension-aldol reaction of β -keto esters and amides favored formation of the *syn*-isomer over the *anti*-isomer (**Table 4**). As mentioned earlier the zinc organometallic intermediate **20** is similar to the zinc-Reformatsky intermediate,^{50, 51} however, the high *syn*-selectivity of the zinc ester enolate was unprecedented. The lower reactivity of organometallic intermediate **20** compared to a traditional enolate with respect to alkylation is believed to be due to the organometallic oligomeric nature,^{50, 51} however, addition of an aldehyde to this carbon-bonded zinc intermediate may be responsible to its isomerization to the more reactive oxygen-bonded zinc enolate.⁵² The *O*-bound enolate can exist in two geometries, *Z*-enolate **49** and *E*-enolate **50** (**Scheme 9**). The ketone functionality in intermediate **20** is believed to play a vital role in favoring formation of the *Z*-enolate thus leading to the formation of *syn*-isomer with high diastereoselectivity via a closed (Zimmerman-Traxler) transition state (**Table 4**).⁵³



Scheme 9. Dissociation of *C*-bound zinc enolate to *O*-bound zinc enolate, *Z*-enolate **49** and *E*-enolate **50**

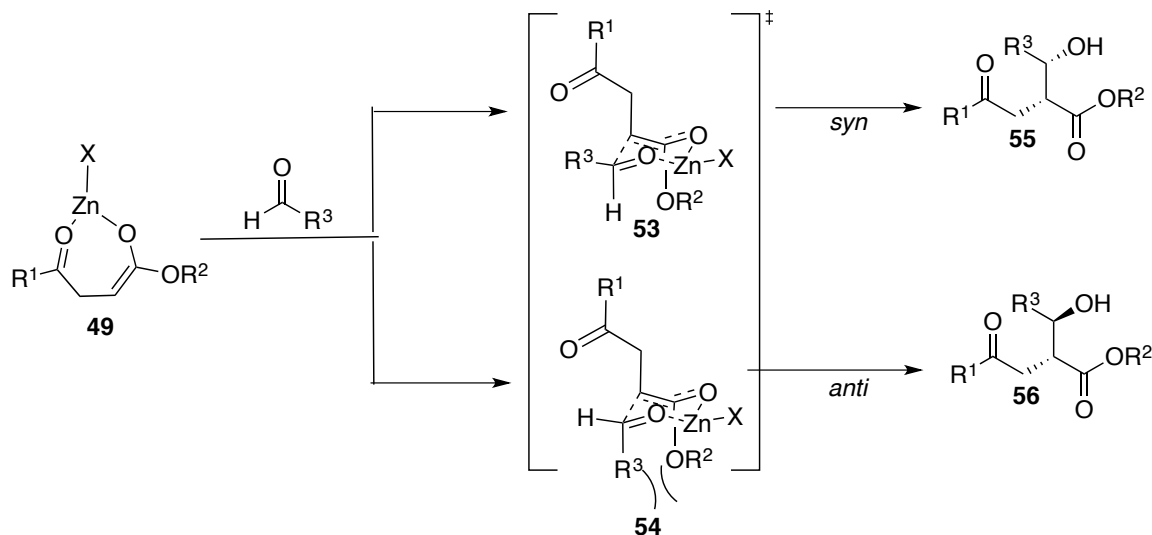


Entry	R ¹	R ²	R ³	Yield %	syn:anti
16a	tBu	OMe	Ph	97	12:1
16b	tBu	OMe	Ar	61	9:1
16c	Ar	OEt	Ar	57	7:1
16d	Me	OMe	tBu	85	>20:1
16e	Me	OMe	Ph	61	15:1
16f	Me	NPhMe	Me	46	3:1

Table 4. Tandem-chain extension aldol reaction of β -keto esters and amides

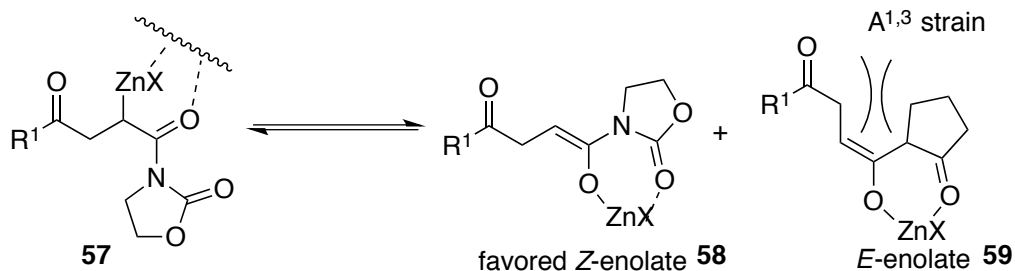
A Zimmerman-Traxler model has been used to predict stereochemistry of aldol reactions that are believed to proceed through a closed chair-like transition state.⁵³ If *Z*-enolate **49** reacts with an aldehyde in a chair-like transition state (**Scheme 10**), the stereochemical outcome of the aldol reactions will be dictated by the facial selectivity of the aldehyde. When the R³ substituent of the aldehyde approaches the enolate in the pseudo-equatorial position **53**, formation of the *syn*-isomer **55** would be predicted (**Scheme 10**); however, if the aldehyde approaches with the R³ substituent in the pseudo-axial position **54**, formation of the *anti*-isomer **56** could be predicted. In general, formation of *anti*-isomer **56** is less favored, which is rationalized by the undesired 1,3-diaxial interactions in the transition state. The high diastereoselectivity of the tandem chain extension-aldol reaction of β -keto esters and amides favoring *syn*-aldol product **55** suggests that the reaction proceeds via a *Z*-enolate in a chair-like transition state.

Computational investigation also supported the assertion that the aldol reaction proceeds through a six-membered closed transition state.⁵⁴



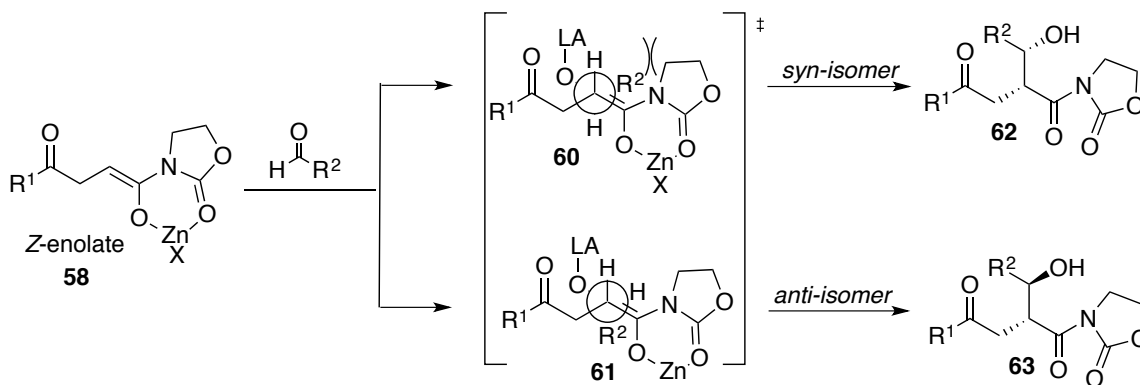
Scheme 10. Zimmerman-Traxler closed transition state model for the favored *Z*-enolate of the chain extension aldol reaction

Tandem chain extension-aldol reactions (TCEA) involving β -keto imides (acylated Evans auxiliaries) also have been studied. The diastereoselectivity of this reaction favors formation of the *anti*-isomer over the *syn*-isomer.⁵⁵ The formation of *anti*-isomer as the major product can be rationalized by the Heathcock open-transition state model.⁵⁶ The presence of excess Lewis acid and an extra Lewis basic site on the oxazolidinone is proposed as necessary for the reaction to proceed through an open-transition state, where one equivalent of Lewis acid chelates to the two imide carbonyls and the other equivalent of Lewis acid activates the aldehyde. The carbon-bound zinc organometallic (**57**) may be in equilibrium with two enolate isomers, however the *Z*-enolate **58** is favored over the *E*-enolate **59** due to the absence of undesired A^{1,3} strain observed with the *E*-geometry (**Scheme 11**).⁵⁷



Scheme 11. *Z*- and *E*- Geometries for the imide enolate

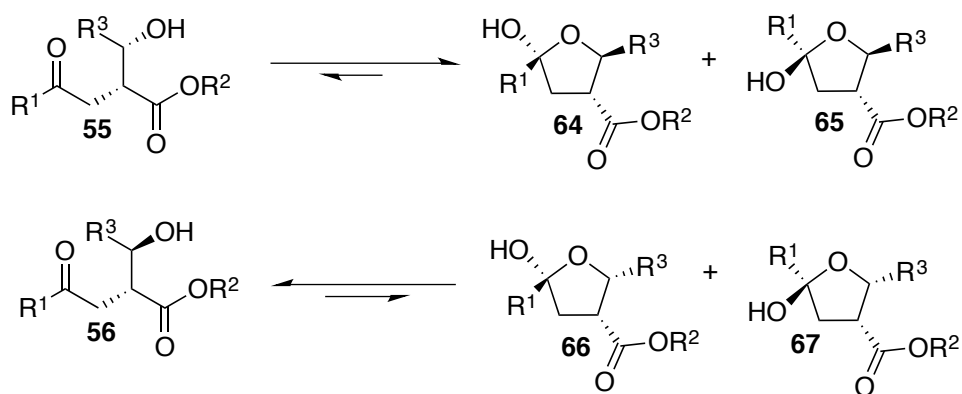
The diastereoselectivity in tandem chain extension-aldol reactions of β -keto imides is also dictated by the facial approach of the aldehyde in the open transition state. If the *Z*-enolate attacks on the face of the aldehyde where the steric interactions are minimized as in the transition state **61**, *anti*-isomer **63** is formed.⁵⁵ If attack of the *Z*-enolate takes place on the opposite face of the aldehyde, where steric interactions between R group of the aldehyde and the imide are maximized as in transition state **60**, *syn*-isomer **62** is formed (**Scheme 12**).



Scheme 12. Open transition state for tandem chain extension-aldol of β -keto imide

The analysis of the diastereomeric ratio of products generated in the tandem chain extension-aldol reactions is often difficult to analyze by NMR due to the equilibrium existing between the open and closed (hemiketal) forms. Both the *syn* and *anti*-isomers exist in

equilibrium with their hemiketals (**Scheme 13**). The *syn*-aldol **55** exists in equilibrium with hemiketal **64** where the substituents R² and the ester functionality are *trans* to each other. The product exists mostly in the hemiketal form. The *anti*-aldol **56** also exists in equilibrium with hemiketal **66**, however the substituents R² and the ester groups are *cis* to each other in the hemiacetal form. A greater proportion of the open form is observed for the *anti*-aldol isomer. This equilibrium provides the means by which the closed forms can be converted to a spiroketal framework through acid mediated cyclization. This methodology was key to the formal synthesis of spiroketal-based natural products CJ-12,954 and CJ-13,014 ,which will be discussed in detail in **Chapter II**.

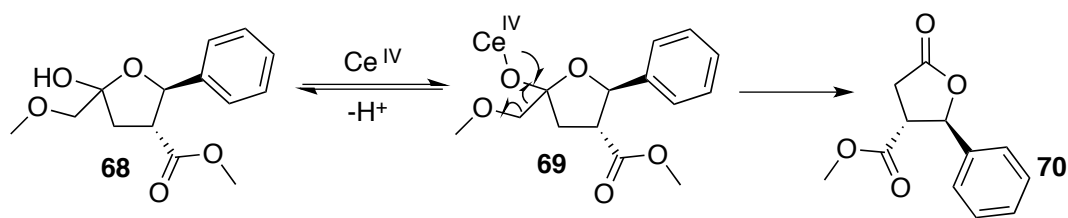


Scheme 13. Equilibrium between open chain and closed hemiketal isomers.

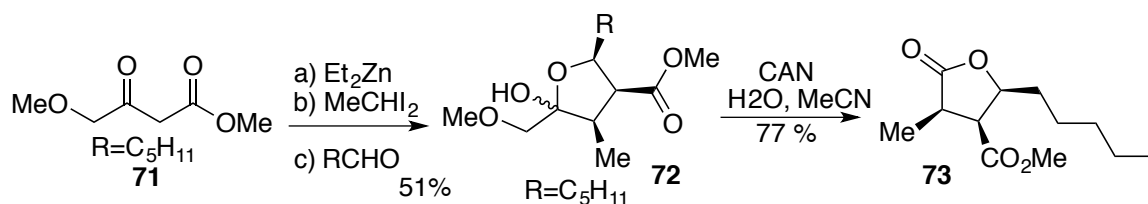
CAN-mediated oxidative cleavage of hemiacetals

During an attempt to remove a para-methoxybenzyl (Pmb) protecting group, Lin serendipitously discovered a ceric ammonium nitrate (CAN)-mediated oxidative cleavage of hemiacetals that results in formation of substituted γ -lactones.²³ The reaction requires the presence of a heteroatom vicinal to the hemiacetal hydroxyl group. Complexation of the hydroxyl group of the hemiacetal **68** derived from the tandem chain extension-aldol reaction with the cerium (IV) is followed by single electron transfer and cleavage of the carbon-

carbon bond, which affords the corresponding γ -lactone **70** (Scheme 14). The proposed mechanism predicts that the stereocenters established during the TCEA reaction would not be impacted during the cleavage process, which was also confirmed experimentally with no epimerization of those stereocenters being observed. Jacobine employed both the TCEA reaction and CAN-mediated oxidative cleavage methodologies to access the paraconic acid family of natural products (Scheme 15).^{45, 58}



Scheme 14. CAN-mediated oxidative cleavage of hemiacetal to γ -lactone

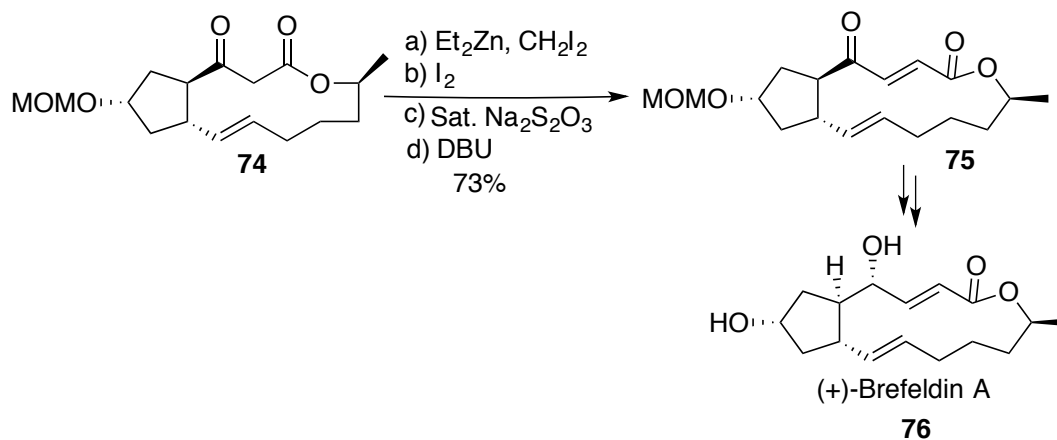


Scheme 15. Synthesis of 3,4,5-trisubstituted γ -lactone by TCEA reaction and CAN-mediated oxidative cleavage

Tandem chain extension-oxidation-elimination reaction

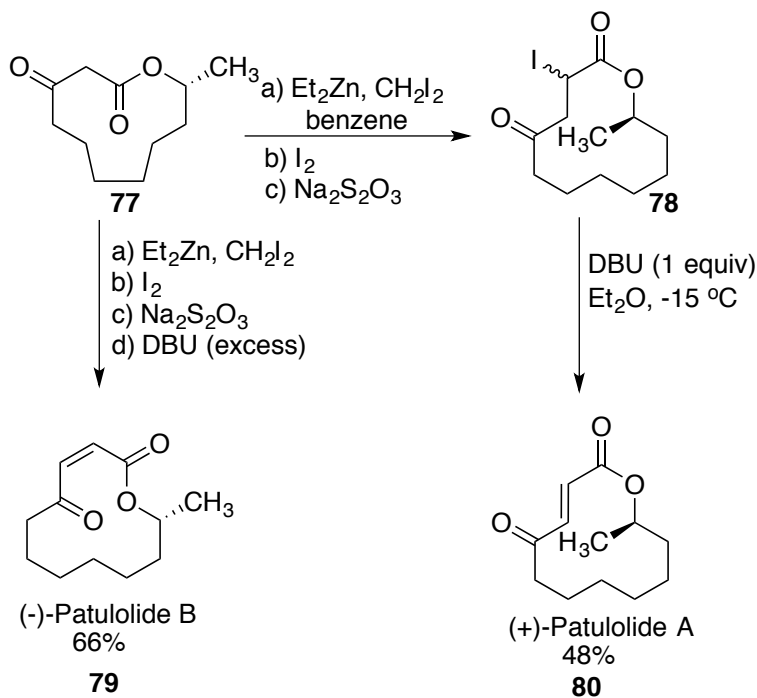
A rapid one-pot conversion of β -keto carbonyls to the corresponding α,β -unsaturated γ -keto carbonyls employing sequential chain extension-oxidation-elimination was developed.⁴⁸ The organometallic intermediate **20** was trapped with iodine to generate the corresponding α -halogenated γ -keto carbonyl, which was then treated with a base (DBU was used frequently) to form an α,β -unsaturated γ -keto carbonyl with very high *E* selectivity.⁴⁸ Substrates with olefins

also tolerated this reaction. Amino acid substrates afforded the corresponding α,β -unsaturated products, although epimerization of the stereocenter took place. This method was successfully employed in the formal syntheses of 16-membered dilactone natural product (-)-pyrenophorin⁴⁸ and in the formal synthesis of (+)-brefeldin A (**79**)²³ (**Scheme 16**).



Scheme 16. Formal synthesis of (+)-Brefeldin A

The tandem chain extension-oxidation-elimination reaction has also been key to the total syntheses of macrocyclic β -keto lactones (+)-patulolide A and (-)-patulolide B (**Scheme 17**).⁵⁹ The stereochemistry of alkenes was controlled by use of kinetic and thermodynamic conditions in the elimination reaction. Use of excess base followed by stirring the reaction mixture at room temperature resulted in formation of the *Z*-olefin in (-)-patulolide B, whereas using one equivalent of base at lower temperature (-15 °C) resulted in *E*-olefin in (+)-patulolide A.⁵⁹ Whereas chain extension was sluggish in these macrocyclic systems, change of solvent from dichloromethane to benzene accelerated the chain extension reaction.

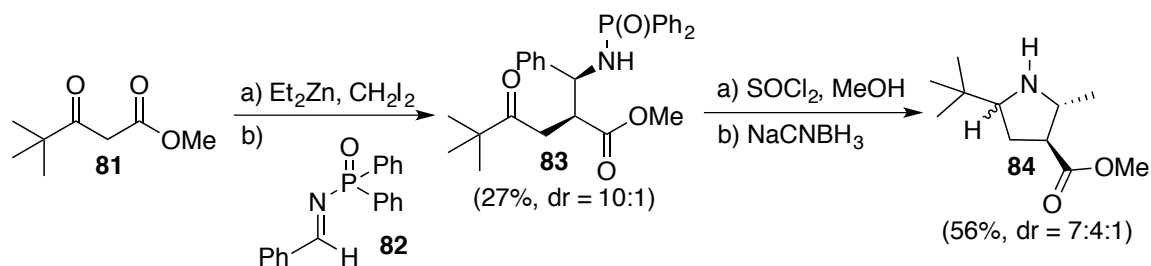


Scheme 17. Total synthesis of patulolide A and B using chain-extension-oxidation-elimination reaction

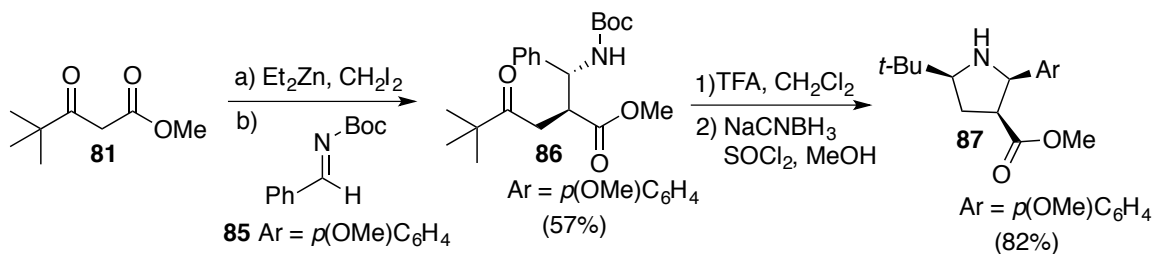
Tandem chain extension-Mannich reaction

One of the more recently developed tandem protocols involves the use of activated imines for the capture of organometallic intermediate **20**.⁴⁶ Jacobine developed the tandem chain extension-Mannich reaction as a novel method to synthesize β -proline derivatives. The organometallic intermediate generated from the chain extension was trapped with *N*-phosphinoylimine **82** to generate the respective β -amino acid **83**, which was deprotected and reduced to afford β -proline derivative **84** (**Scheme 18**).⁴⁶ The efficiency and yield of the tandem chain extension-Mannich reaction was improved by changing from phosphinoyl imines to Boc-activated aryl imines. Trifluoroacetic acid-mediated Boc-deprotection followed by reductive cyclization using sodium cyanoborohydride rendered the β -proline derivatives in good yields (**Scheme 19**). The nitrogen-protecting groups controlled the diastereoselectivity of the chain

extension-imine capture reaction. While the Mannich reaction with the phosphinoyl imines gave *syn*-aldol like stereochemistry, the Boc-protected imines favored formation of “*anti*-aldol” β -amino esters. The tandem chain extension-Mannich reaction of chiral β -keto imides gave β -proline derivatives with absolute stereocontrol. The tandem chain extension-Mannich reaction using sulfone-activated imines is currently under investigation.⁶⁰



Scheme 18. Tandem chain extension-imine capture reaction with diphenylphosphinoyl imine

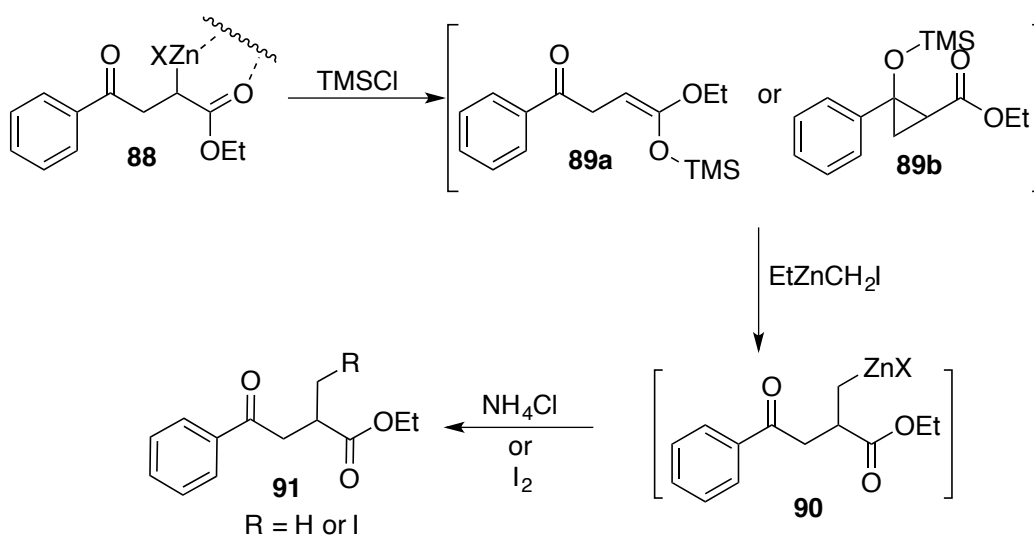


Scheme 19. Tandem chain extension-imine capture reaction with Boc-activated imines

α -Methylation of γ -keto carbonyl

Synthesis of α -methylated γ -keto esters by trapping the zinc organometallic intermediate **20** with alkyl halides like methyl iodide or methyl bromide cannot be achieved due to the reduced nucleophilicity of **20** compared to a traditional enolate. However, indirect methylation can be achieved by addition of trimethylsilylchloride (TMSCl) in the presence of excess carbenoid. Addition of TMSCl is believed to promote the fragmentation of the dimeric

Reformatsky-type intermediate **88** (Scheme 20),^{20, 47, 61} which results in the formation of a nucleophilic species like **89a** or **89b**. Capture of the excess carbenoid by these nucleophiles generates homoenolate **90**, which may be quenched with a mild acid to form α -methylated γ -keto carbonyl^{47, 61} or with iodine to form α -iodomethylated γ -keto carbonyl.²⁸ Synthesis of α -iodomethylated γ -keto carbonyls provided opportunities for both cross coupling reactions and nucleophilic displacement of the iodine, both of which can lead to diversification of the substitution pattern of the γ -keto carbonyl.

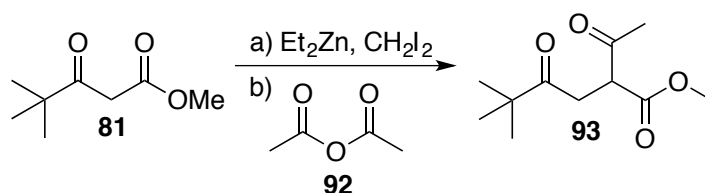


Scheme 20. Synthesis of α -methylated and α -iodomethylated γ -keto ester

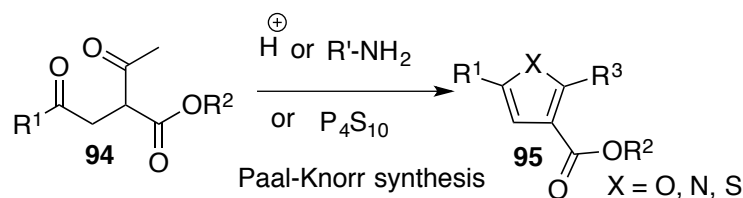
Tandem Chain Extension-Acylation Reaction

The scope of the zinc-mediated chain extension reaction was broadened when Jacobine reported the synthesis of α -acylated γ -keto ester **93** by trapping the zinc organometallic intermediate **20** with acetic anhydride (Scheme 21).⁴⁵ Taddei and co-workers synthesized a similar α -acylated γ -keto ester by subjecting the aldol product derived from tandem chain extension homologation-aldol reaction to PCC oxidation.⁶² Synthesis of highly functionalized heterocycles like furans, pyrroles and thiophenes from α -acylated γ -keto carbonyl using a Paal-

Knorr synthesis enhances the potential utility of the tandem chain extension-acylation reaction (**Scheme 22**). Mazzone used cyclic anhydrides as acylating agents to synthesize spiroketals,⁴⁴ which are found in many natural products.⁶³ Mazzone employed this methodology to target the papyracillic acid family of natural products.⁶⁴ The spiroketal framework of 4-*epi*-papyracillic acid B (**99**) and Papyracillic acid B (**100**) was synthesized in one step by exposing methyl acetoacetate (**96**) to ethyl(iodomethyl)zinc and then trapping the organometallic intermediate with methoxymaleic anhydride (**97**) (**Scheme 23**).⁶⁴ A similar approach was employed by Spencer recently in the synthesis of papyracillic acid A.⁴⁹

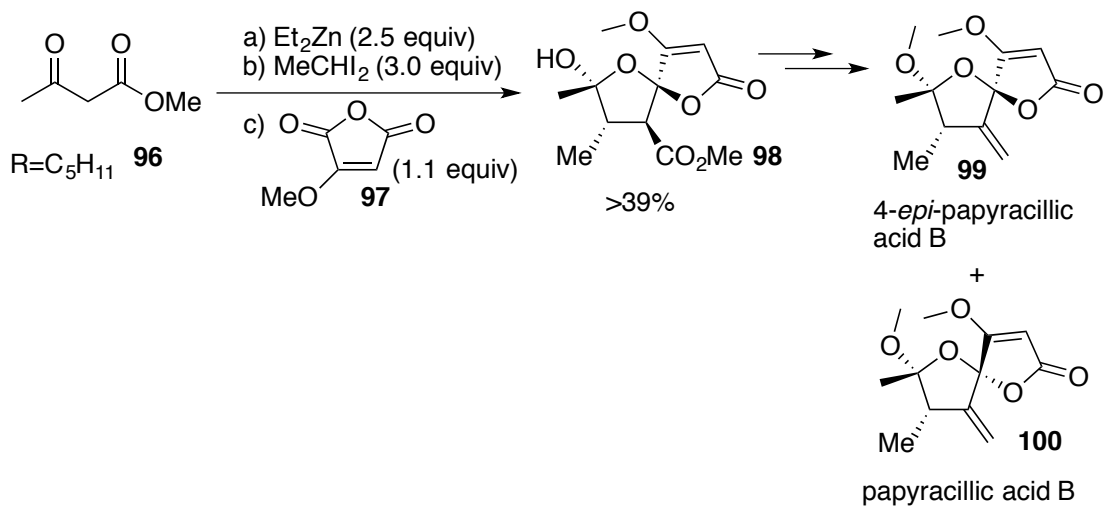


Scheme 21. First reported synthesis of α -acylated γ -keto ester

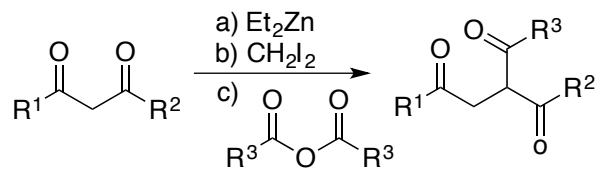


Scheme 22. Paal-Knorr synthesis of highly functionalized heterocycles

Spencer subjected various β -keto esters to diverse anhydrides in a study designed to understand the scope of tandem chain extension-acylation reaction (**Table 5**).⁴⁹ These studies determined that the presence of bulky or aromatic substituents⁴⁹ on the ketone or ester functionalities do not decrease the efficiency of the reaction.



Scheme 23. One-pot synthesis of spiroketal framework of Papyracillic acid B using tandem chain extension-acylation reaction



Starting material	R ¹	R ²	R ³	Product	Yield (%)
81	<i>t</i> -Bu	OMe	Me	101	63
81	<i>t</i> -Bu	OMe	<i>i</i> -Pr	102	80
81	<i>t</i> -Bu	OMe	Ph	103	95
104	Me		Me	105	36
104	Me		Ph	106	51
107	Me	OAllyl	Me	108	44
107	Me	OAllyl	Ph	109	73
110	Ph	OMe	Me	111	55
110	Ph	OMe	Ph	112	51
113	Me	NPhMe	Ph	114	62
115			Ph	116	80

Table 5. Scope of tandem chain extension-acylation reaction

Summary

Development of the zinc-mediated chain extension reaction provides a facile method for the synthesis of γ -keto carbonyls. The versatile zinc organometallic intermediate generated during the chain extension reaction can be trapped with various electrophiles, thus opening new avenues for the various tandem processes discussed above. The diastereoselectivity in many tandem processes, like the aldol, Mannich and iodination-elimination reaction was also controlled efficiently. Application of this versatile zinc-mediated chain extension reaction to more novel methodologies and target-guided synthesis is currently being investigated.

CHAPTER II

FORMAL SYNTHESIS OF CJ-12,954 AND CJ-13,014 USING ZINC-MEDIATED TANDEM CHAIN EXTENSION-ALDOL REACTION

Basic Ring-Systems of Spiroketal

Spiroketals occur as the main backbone in many natural products with pharmacological activity. Different ring arrangements of spiroketals exist, however, three different types are predominantly found.⁶³ They are ring systems A, B and C (**Figure 4**). The ring system A is 1,7-dioxaspiro[5.5]undecane **117**, which consists of two six membered rings fused at carbon 6. The ring system B is 1,6-dioxaspiro[4.5]decane **118**, which consists of a six and five membered rings fused at carbon 5. The ring system C is 1,6-dioxaspiro[4.5]decane **119**, which consists of two five membered rings fused at carbon 5.

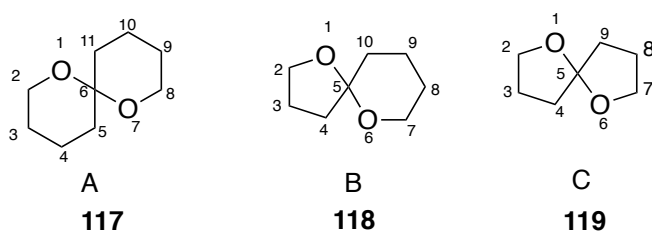


Figure 4. The A, B and C Ring Systems of Spiroketal.

Spiroketals are obtained from many sources including insects, microbes, plants, fungi and marine organisms. The biological activity of spiroketal-based natural products and also the role of spiroketals in protecting group chemistry^{65, 66} has been extensively studied. Many novel and flexible approaches have been designed for the synthesis of spiroketal frameworks.⁶⁷⁻⁶⁹ The stereochemistry associated with the pivotal O-C-O linkage offers challenge in these compounds.

Configuration and Stereochemistry in Spiroketal

Four all-chair conformers are available for the spiro[5.5] ring systems (**Figure 5**).⁷⁰ However, the one where the individual C-O bonds of the O-C-O bonding system are positioned axially relative to the ring unit to which they are connected is the most thermodynamically favored conformer of the spiroketal. This stability has been ascribed to the anomeric effect, which outweighs the more sterically favored equatorial orientation (**Figure 6**). The anomeric effect is the stabilizing overlap between the oxygen lone-pair orbital with the exocyclic C-O bonds constituting the O-C-O bonding system, and the stabilization is maximized when the two are positioned antiperiplanar to one another allowing for optimal overlap.⁷¹ The anomeric effect has been extensively studied in spiro[5.5] ring systems, whereas this effect is less consistent and predictable in spiro[4.5] and spiro[4.4] ring systems due to lack of well-defined axial or equatorial positions in five-membered rings.⁷²

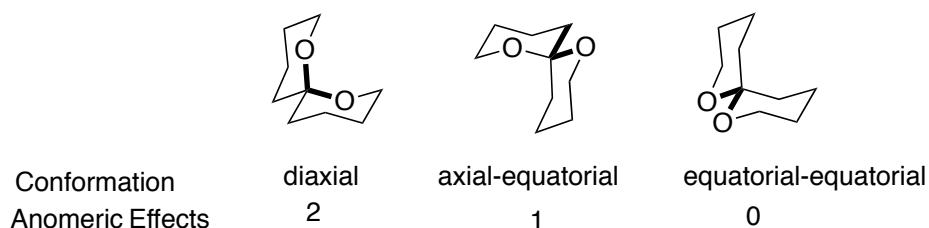


Figure 5. Conformation in Spiroketals

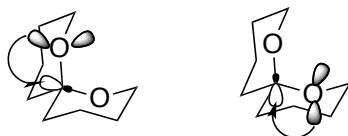
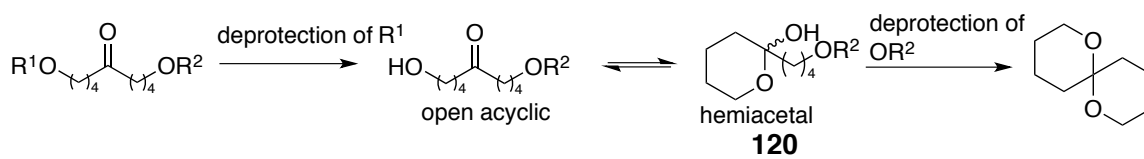


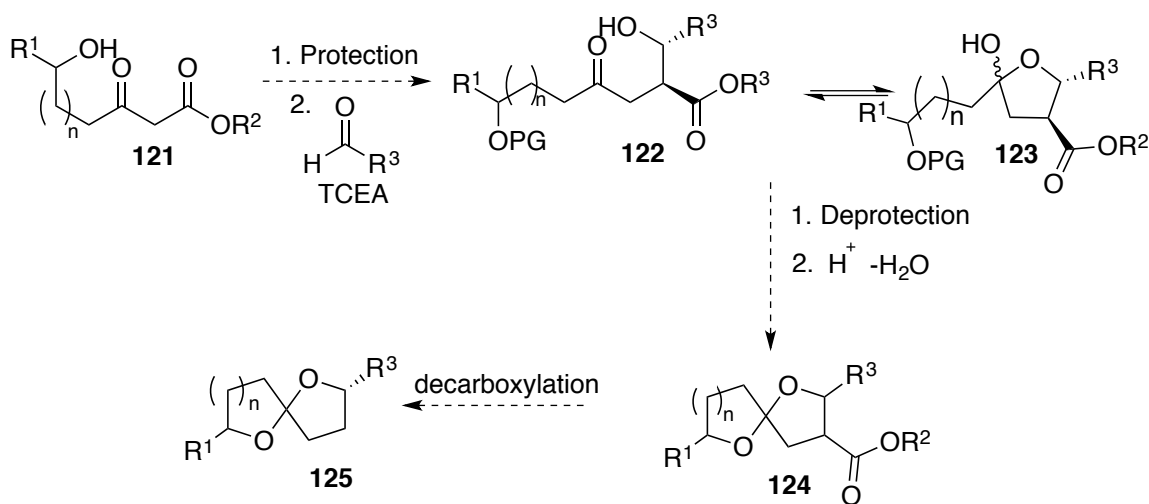
Figure 6. The Anomeric Effect in Spiroketals

Cyclization of dihydroxyketones is one of the most commonly employed synthetic approaches towards spiroketal synthesis (**Scheme 24**).⁶³ This method involves the hemiacetal

120 as the key intermediate, which loses water to form oxocarbenium ion followed by attack of the other alcohol to access the spiroketal framework. The tandem chain extension aldol reaction (TCEA) as discussed in **Chapter 1** was the first tandem chain extension protocol developed. The aldol products from tandem chain extension-aldol reaction (TCEA) exist in both the open chain form and its hemiacetal (**Scheme 25**). Hence the TCEA reaction can provide easy access to the hemiacetal **123**, which is key intermediate in spiroketal synthesis.



Scheme 24. Synthesis of spiroketal by cyclization of dihydroxy ketone.

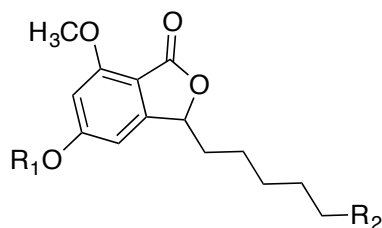


Scheme 25. Proposed Application of TCEA reaction in the synthesis of spiroketals via hemiacetal intermediate

CJ-12,954 and Its Congeners – New Anti-*Helicobacter pylori* Agents

In a screening program to discover safe and effective compounds having excellent anti-*Helicobacter pylori* activity Dekker et al. extracted seven phthalide compounds **126a-g** (**Figure 7**) from the basidiomycete *Phanerochaete velutina*.⁷³ *Helicobacter pylori*, a Gram-negative bacterium, lives beneath the mucus layer of stomach and causes gastric and duodenal ulcers.⁷⁴

Current treatment methods employ one or two broad spectrum antibiotics combined with a proton pump inhibitor or a bismuth salt.⁷⁵ Prolonged course of therapy is required for complete eradication of *H.pylori* related infections.⁷⁶ However, long-term treatment in these patients can result in side-effects due to toxic bismuth salts and also build-up of drug resistance due to the use of antibiotics. Hence, compounds with specific anti-*H.pylori* activity, but that are inactive against other Gram-positive and –negative bacteria, are highly desired. Hence, in the early stage of their screening program Dekker et al. eliminated other extracts having antibacterial activity which can be obtained by common antibiotics.⁷³ The phthalide compounds were found to be effective only against *Helicobacter pylori* and showed no antimicrobial activity against other microorganisms such as *Bacillus stearothermophilus*, *Staphylococcus aureus* and others.

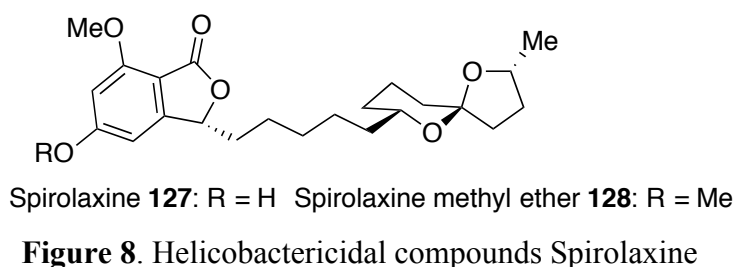


	R1	R2	Activity ($\mu\text{g}/\text{disk}$ that gives a 15 mm zone)
CJ-12,954 (126a)	Me		0.02
CJ-13,014 (126b)	Me		0.02
CJ-13,015 (126c)	Me		2
CJ-13,102 (126d)	Me		0.5
CJ-13,103 (126e)	Me		50
CJ-13,104 (126f)	Me		500
CJ-13,108 (126g)	Me		10

Figure 7. Structures and helicobactericidal activities of phthalides **126a-g**.

Dekker et al. elucidated the structures of the seven phthalide extracts including CJ-12,954 (**126a**) and CJ-13,014 (**126b**) using ^1H NMR, ^{13}C NMR, COSY, NOE difference, DEPT and HREI-MS data. CJ-12,954 (**126a**) contains a 5,5-spiroacetal ring joined through a polymethylene chain to the phthalide unit. CJ-13,014 (**126b**) was identified to be an isomer of **126a** and has the same planar structure by all spectroscopic methods. Hence CJ-13,014 was identified as the epimer of CJ-12,954 at the spiroketal carbon. The structures of both CJ-12,954 (**126a**) and CJ-

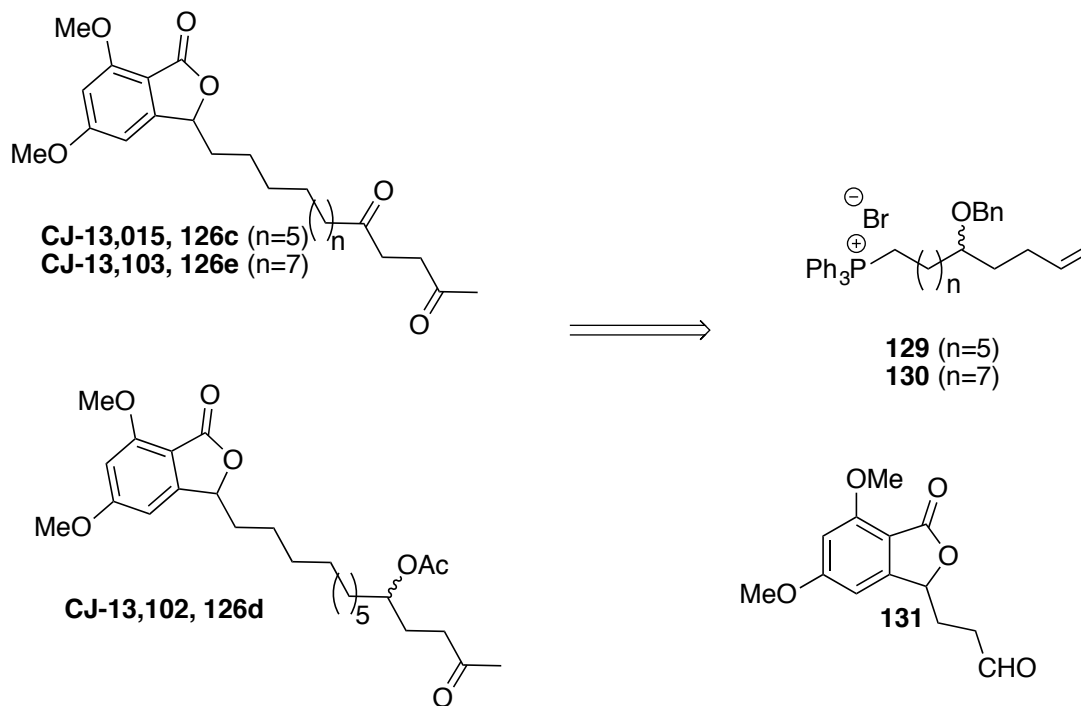
13,014 (**126b**) were also confirmed by the comparison of their spectral data with the structurally related helicobactericidal compounds spiroloxine **127** and its methyl ether **128**, which also contains a 6,5-spiroacetal ring joined through a polymethylene chain to a phthalide unit (**Figure 8**).⁷⁷ Whilst Dekker et al. assigned the relative stereochemistry of the three stereogenic centers on spiroketal ring of (**126a**) and (**126b**), they were unable to elucidate the absolute stereochemistry of the four stereocenters of the natural products CJ-12,954 (**126a**) and CJ-13,014 (**126b**).



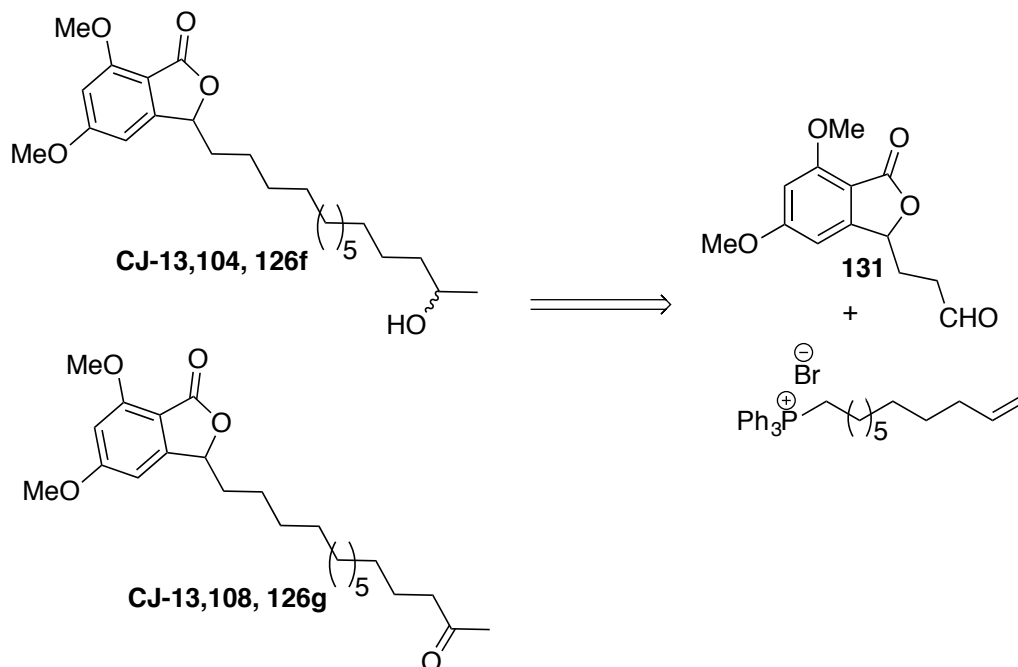
Based on the antimicrobial assay, it was observed that the helicobactericidal activities of the phthalide compounds strongly depend on their structures (**Figure 7**). Among the seven phthalide extracts, the spiroketal-containing CJ-12,954 (**126a**) and CJ-13,014 (**126b**) were found to be the two most potent anti-*Helicobacter pylori* agents.⁷³ While the change in stereochemistry of the spiroketal backbone has no effect on antibacterial activity, the ring opening of spiroketal to γ -diketone **126c** reduced the potency by 100-fold. This supports the significance of spiroketal framework towards helicobactericidal activity. Hence these spiroketal-containing phthalide compounds, CJ-12,954 (**126a**) and CJ-13,014 (**126b**) can be considered as potential new leads for the treatment of *H. pylori* related diseases.

The total synthesis of (\pm)-CJ-13,015 (**126c**), one among the seven phthalide-extracts was first reported by Argade and Mondal.⁷⁸ The total synthesis was accomplished in six steps with an overall yield of 65%; however, their methodology lacks the intrinsic flexibility

necessary to synthesize the other structurally similar compounds of the series. Brimble et al. later reported the racemic total syntheses of five of the *Phanerochaete. velutina* series of phthalide antibiotics **126c-g** (Scheme 26a,b).⁷⁹ The indole analogues of these anti-*Helicobacter pylori* compounds were also synthesized.⁸⁰



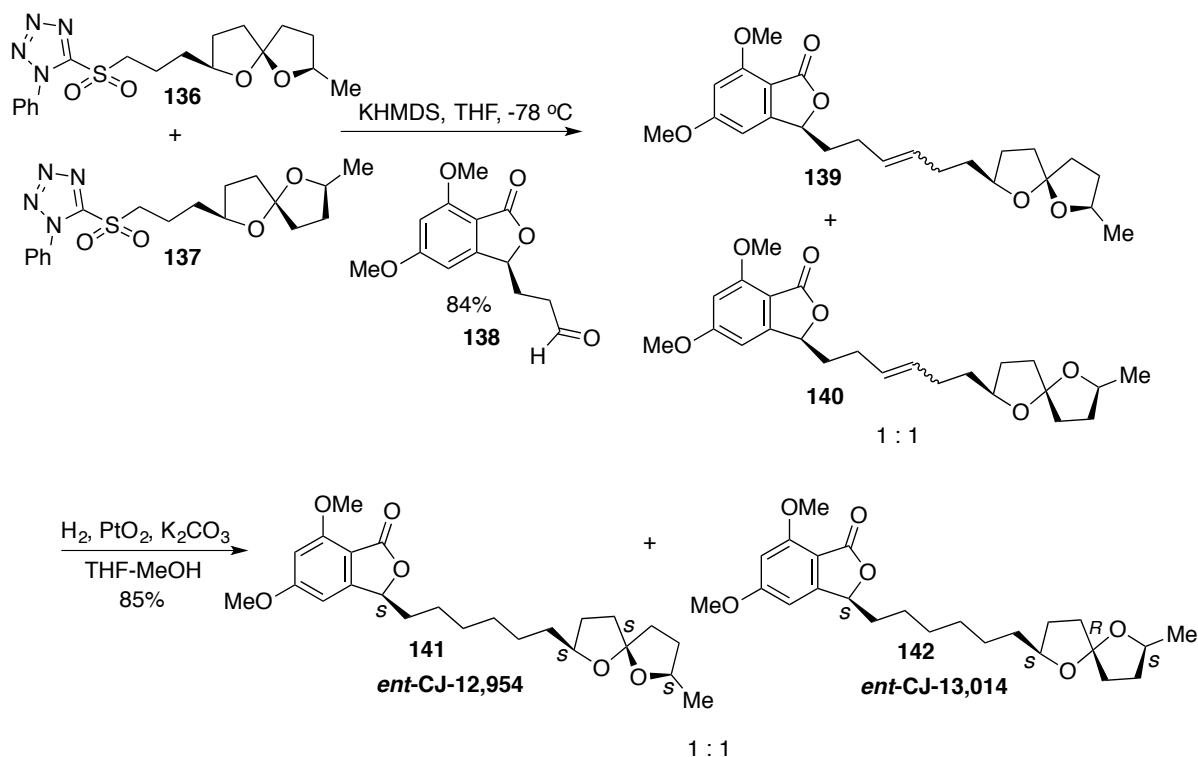
Scheme 26a. Retrosynthetic analysis of CJ-13,015, CJ-13,102 and CJ-13,103



Scheme 27b. Retrosynthetic analysis of CJ-13,015, CJ-13,102, CJ-13,103, CJ-13,104 and CJ-13,108

First Reported Synthesis of *ent*-CJ-12,954 and *ent*-CJ-13,014

Brimble et al. in 2006 first reported the enantioselective total syntheses of the spiroacetal-containing helicobactericidal antibiotics CJ-12,954 (**126a**) and CJ-13,014 (**126b**).⁸¹ The spiroketal backbone of *ent*-CJ-12,954 (**141**) and *ent*-CJ-13,014 (**142**) was synthesized by deprotection followed by spirocyclization of diprotected dihydroxy ketone **133** which resulted an inseparable 1 : 1 mixture of spiroketals **134** and **135** (**Scheme 27**).^{81, 82} The key step in their total syntheses involves convergent union of 1:1 mixture of heterocycle-activated spiroketal sulfones **136** and **137** with (3*S*)-phthalide aldehyde **138** (**Scheme 28**). Hydrogenation of the mixture of alkenes **139** and **140** afforded an inseparable 1 : 1 mixture of *ent*-CJ-12,954 (**141**) and *ent*-CJ-13,014 (**142**).⁸² The presence of the 5,5-spiroacetal ring was confirmed by characteristic resonances at δ 114.3 and 114.7.



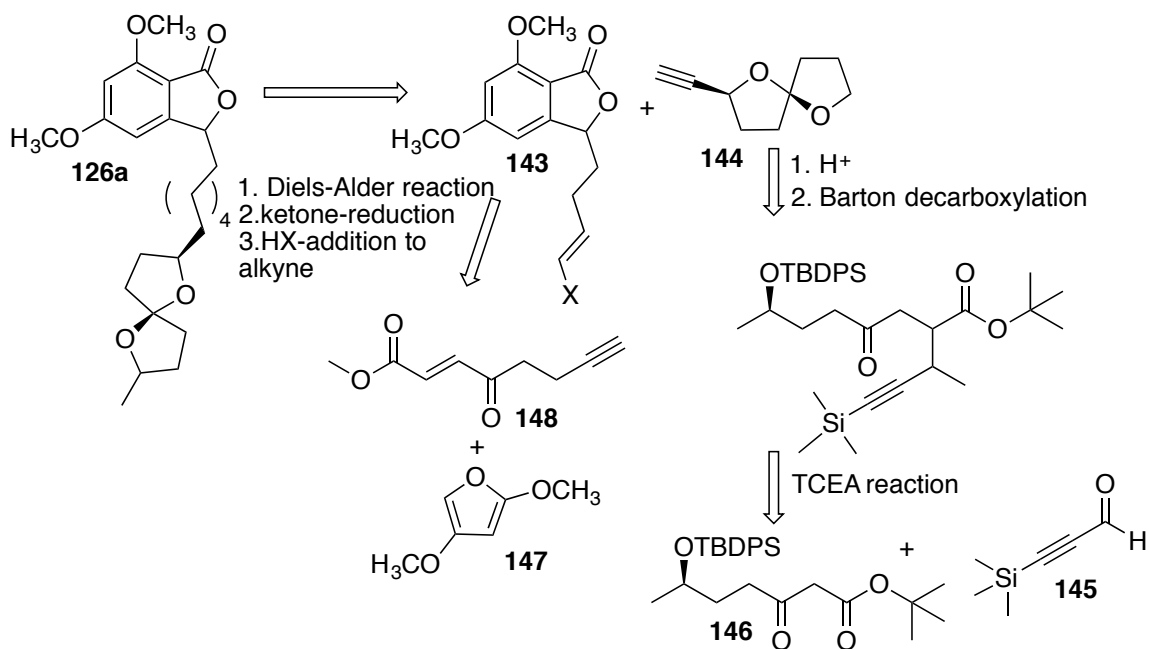
Scheme 29. Brimble et al. approach towards the total synthesis of *ent*-CJ-12,954 and *ent*-CJ-13,014.

Aiken's attempts towards the synthesis of CJ-12,954

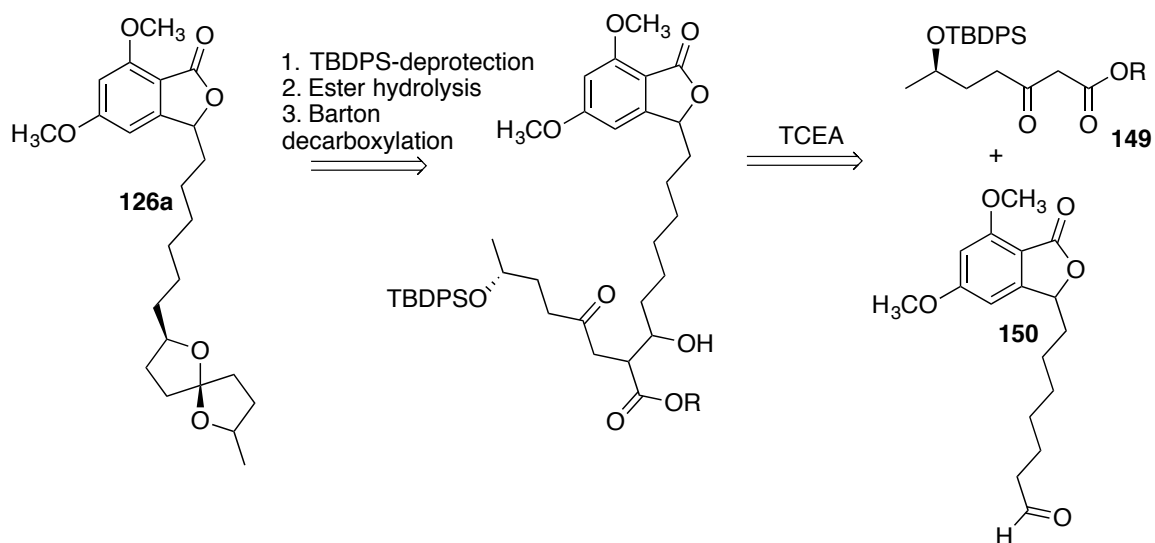
Karelle Aiken of the Zercher group has reported efforts to synthesize natural product CJ-12,954 (**126a**) employing zinc-mediated tandem chain extension as the key methodology.²⁷ Aiken attempted two different approaches for the synthesis of CJ-12,954. When Aiken initiated her efforts towards the total synthesis of CJ-12,954, the absolute stereochemistry of neither the phthalide unit nor the spiroketal were known. Only the relative stereochemistry of the spiroketal backbone had been determined by Dekker et al.⁷³ Since the absolute stereochemistry of the natural product CJ-12,954 was unknown, Aiken's efforts were directed towards the total syntheses of the natural product and to the establishment of the absolute stereochemistry of the natural product. The first synthetic approach involved a palladium-mediated coupling reaction between phthalide unit **143** and a spiroketal unit **144** (**Scheme 29**). The spiroketal **144** needed for palladium coupling was synthesized by a tandem chain extension aldol (TCEA) reaction between

TMS-propynal **145** and β -keto ester **146**, followed by deprotection and decarboxylation. The phthalide unit **143** needed for palladium coupling was proposed to be synthesized from a Diels Alder reaction between a 2,4-dimethoxyfuran (**147**) and an α,β -unsaturated γ -keto ester **148**, which can be accessed from the tandem chain extension-oxidation-elimination reaction (**Scheme 29**). However Aiken's attempts towards the synthesis of desired 2,4-dimethoxyfuran (**147**) were unsuccessful. Hence a different approach was designed for the synthesis of CJ-12,954 (**126a**).

As mentioned earlier the TCEA reaction of a hydroxy β -keto ester **121** was proposed as a means to access the key spiroketal framework. Hence Aiken's second synthetic approach proposed that CJ-12,954 (**126a**) could be accessed by a TCEA reaction between a phthalide aldehyde **150** and a TBDPS-protected hydroxy β -keto ester **149**, followed by TBDPS-deprotection, an ester hydrolysis and Barton decarboxylation (**Scheme 30**). While Aiken's efforts towards the synthesis of spiroketal unit employing TCEA reaction were successful, the absolute stereochemistry of the natural product was unknown until 2006, when Brimble et al. established the absolute stereochemistry of the natural products CJ-12,954 and CJ-13,014.⁸¹ The anticipated stereochemistry of the Aiken synthesis was diastereomeric to the natural product stereochemistry. Furthermore, the efficiency of the synthetic effort could be improved, which led to the second generation approach discussed in this thesis.



Scheme 30. Aiken's first synthetic approach towards the synthesis of CJ-12,954.



Scheme 31. Aiken's second synthetic approach towards the synthesis of CJ-12,954.

Efforts towards the formal synthesis of CJ-12,954 and CJ-13,014

The zinc-mediated tandem chain extension aldol (TCEA) reaction was employed as the key step towards the formal synthesis of CJ-12,954 (**126a**). Spiroacetals **134** and **135** (**Figure 9**) were the advanced intermediates synthesized by Brimble et al. which were eventually converted to the enantiomers of the natural products *ent*-CJ-12,954 (**141**) and *ent*-CJ-13,014 (**142**) respectively.^{81, 82} In the Brimble syntheses spirocyclization of protected dihydroxy ketone **133** using camphorsulfonic acid afforded inseparable 1:1 mixture of spiroacetals **134** and **135** (**Scheme 31**); however, total synthesis of the natural products CJ-12,954 (**126a**) and CJ-13,014 (**126b**) has not been reported to date. Hence, formal synthesis of the advanced intermediates **151** and **152** (**Figure 10**) with the natural stereochemistry as the natural products CJ-12,954 and CJ-13,014 was attempted using TCEA as the key methodology. Thus it was proposed that these advanced intermediates could be converted to natural products using the synthetic strategy followed by Brimble et al. with minor modifications.

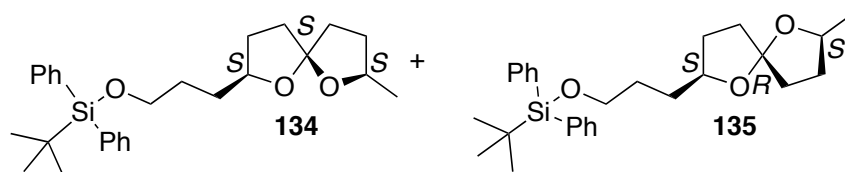
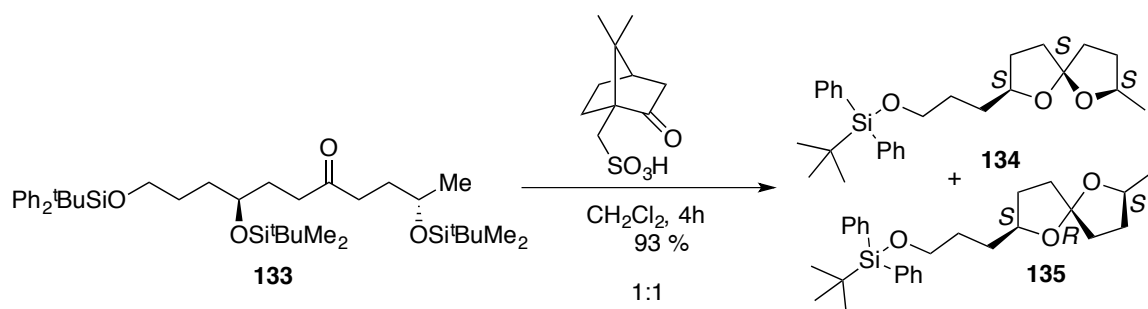


Figure 9. Spiroacetals synthesized by Brimble et al.



Scheme 32. Brimble et al. approach towards synthesis of spiroacetals **34** and **35**

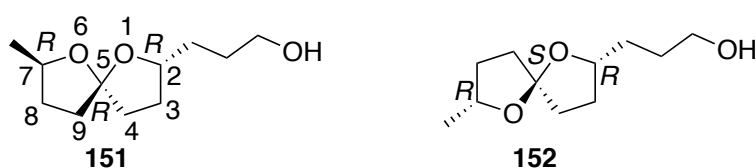
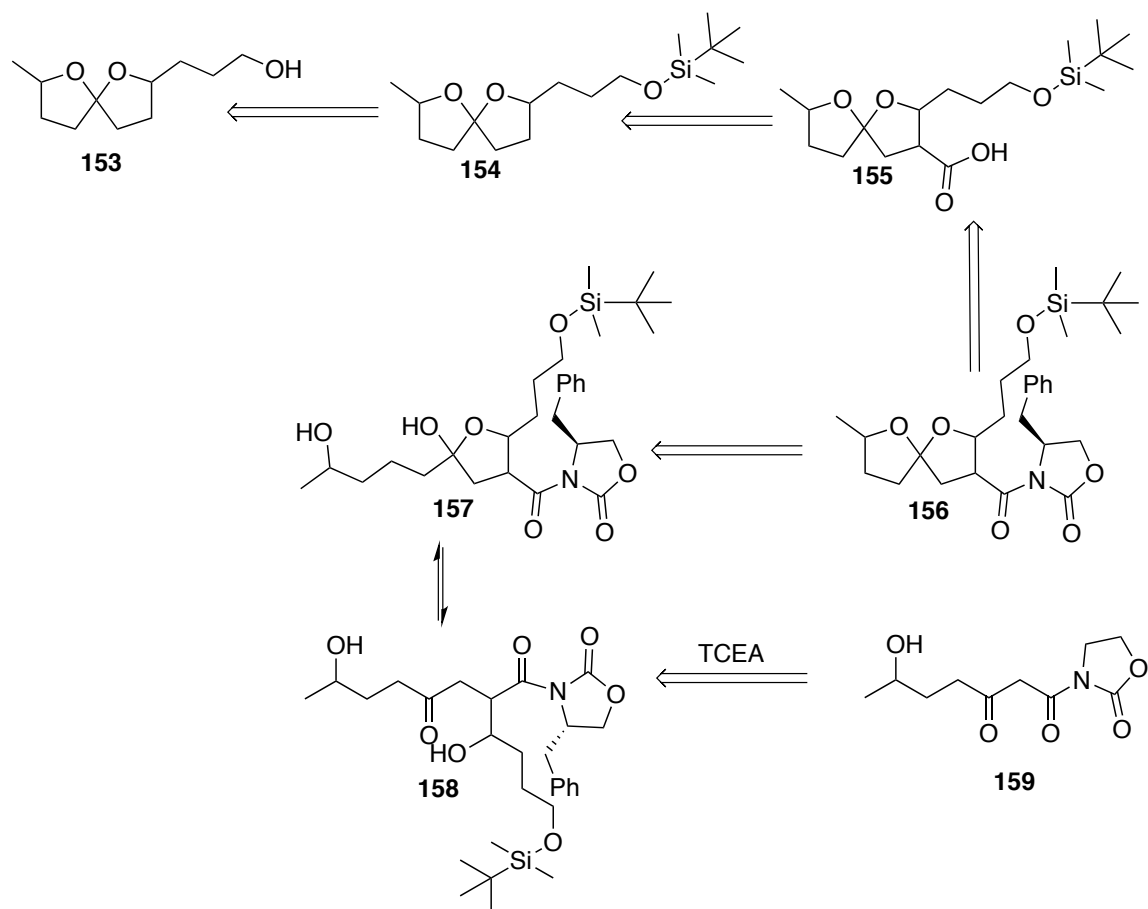


Figure 10. Targeted spiroacetals **151** and **152** for formal synthesis

First Synthetic Approach Towards Spiroacetal Backbone

The initial attempt towards the formal synthesis involved the targeting of spiroacetal alcohol **153**, which would come from cleavage of the *tert*-butyldimethylsilyl ether **154** with tetrabutylammonium fluoride as illustrated in the retrosynthetic analysis (**Scheme 32**). The silyl ether **154** would come from Barton decarboxylation of spiroketal carboxylic acid **155**. The hydrolysis of imide carbonyl functionality of **156** would give carboxylic acid **155**. Acid-mediated spirocyclization followed by dehydration of the hemiacetal **157** would afford spiroketal **156**. The zinc-mediated chain extension of β -keto imide **159** derived from an Evans chiral auxiliary would give the chain extended aldol product **158** which exists in equilibrium with its closed form hemiacetal **157**. Thus the tandem chain extension-aldol reaction offers a novel method for the synthesis of spiroketal framework.



Scheme 33. Retrosynthetic scheme for the synthesis of spiroacetal **153**

Attempts towards the synthesis of β -keto imide **159**

β -Keto imide **159** is the key intermediate required for the synthesis of spiroacetal **153**. β -Keto imide substrates that incorporate the Evans chiral auxiliary, when subjected to TCEA reaction, favor formation of the *anti* aldol-isomer over *syn* aldol-isomer.²¹ The aldol component of the TCEA reaction of a β -keto imide is believed to proceed through an open transition state as discussed in **Chapter 1**. Based on the synthetic approach, stereochemistry of the carboxylic acid side chain (C-3) was not relevant to the final product; however the *anti*-aldol isomer was targeted in order to establish the C-2 stereocenter. Hence, the stereochemistry of the β -keto imide starting material was chosen to control the necessary *anti*-selective aldol TCEA reaction that would provide the desired stereochemistry at C-2 of the spiroacetals **151** and **152**. Aiken had attempted

to induce asymmetry into the TCEA reaction using the chiral auxiliary D-camphorsultam (**160**) (**Figure 11**). However, the desired stereochemistry could not be established with D-camphorsultam; therefore, the chiral auxiliary employed in the synthetic effort described below was the Evans chiral auxiliary **161** derived from L-phenylalanine (**162**) (**Figure 11**).

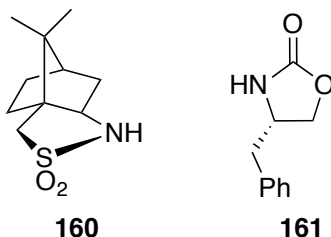
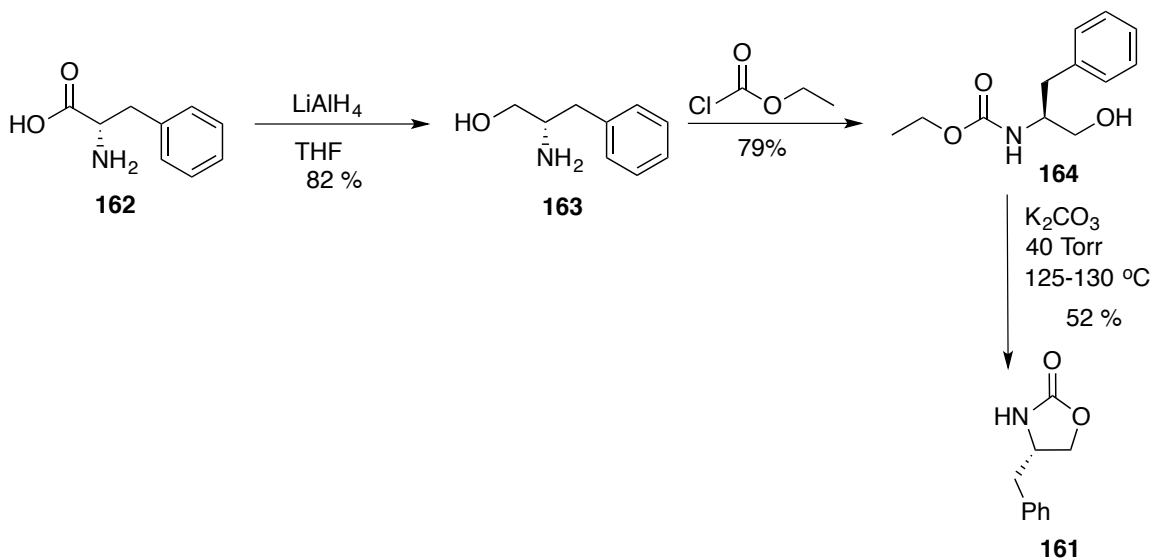


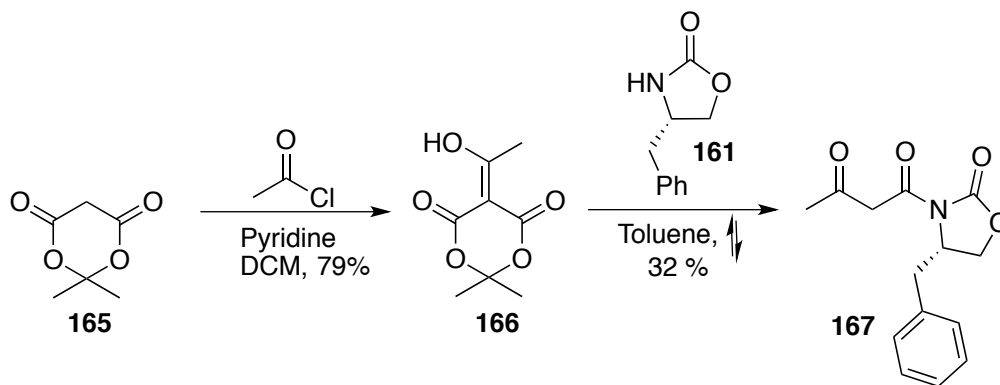
Figure 11. D-camphorsultam and Evans chiral auxiliary

Chiral-2-oxazolidinones, also known as Evans chiral auxiliaries, are versatile chiral auxiliaries with broad application in asymmetric synthesis.⁸³⁻⁸⁷ Evans chiral auxiliary **161** was synthesized from L-phenylalanine (**162**) following the method developed by Wu and Shen (**Scheme 33**).⁸⁸ L-Phenylalanine (**162**) was reduced with LiAlH_4 to amino alcohol **163** which was then treated with ethyl chloroformate to give carbamate **164**. The carbamate **164** was then cyclized on heating in the presence of potassium carbonate under vacuum to afford the chiral-2-oxazolidinone **161** in 52% yield. This chiral oxazolidinone was then reacted with acetylated Meldrum's acid **166** in refluxing toluene to afford the β -keto imide **167** (**Scheme 34**), which was further used in the preparation of hydroxy-substituted β -keto imide **159**. The dianion of the β -keto imide **167** was formed by treating **167** with 1.1 equiv of sodium hydride followed by 2.5 equiv of *n*-butyllithium (**Scheme 35**). The generation of a dianion of β -keto imide **167**, indicated by the deep orange reaction mixture, was treated with racemic propylene oxide in an effort to give the hydroxy-substituted β -keto imide **159**, which would be anticipated to exist in

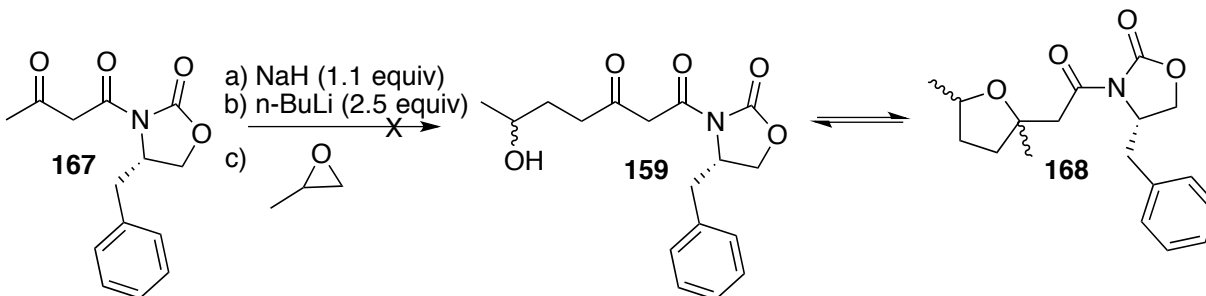
equilibrium with hemiacetal **168**. However, the ^1H and ^{13}C NMR of the crude reaction mixture did not show any evidence of the product.



Scheme 34. Synthesis of Evans chiral auxiliary from L-phenylalanine

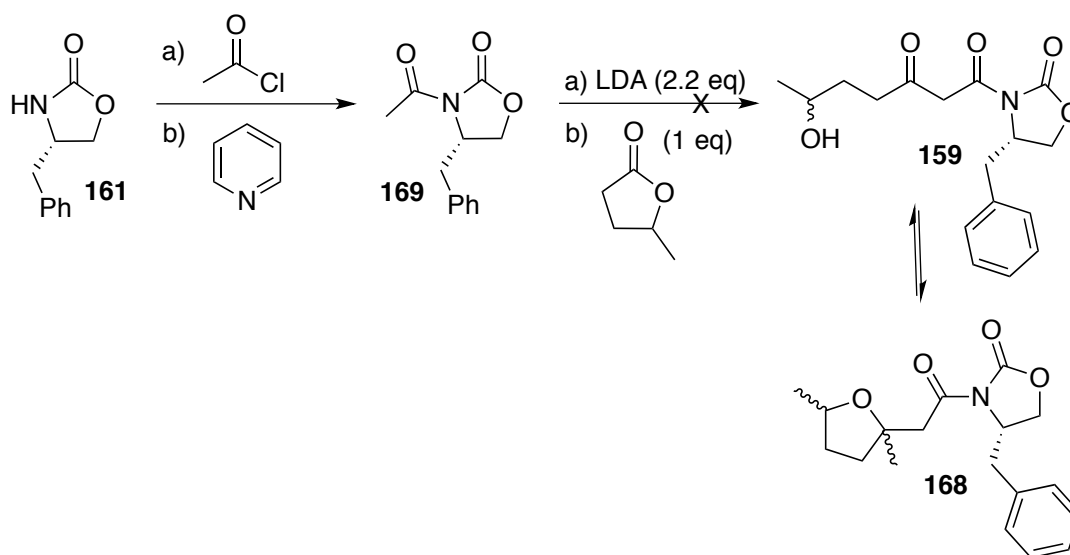


Scheme 35. Synthesis of β -keto imide **167**



Scheme 36. Failed synthesis of β -keto imide **159** via dianion route

An alternative attempt to synthesize hydroxy-substituted β -keto imide **159** made use of a mixed-Claisen reaction (**Scheme 36**). Chiral oxazolidinone **161** was refluxed with acetyl chloride in pyridine to yield acylated chiral oxazolidinone **169**. Acylated chiral oxazolidinone **169** was treated with Lithium diisopropylamine (LDA) in THF at $-78\text{ }^{\circ}\text{C}$ to form the corresponding lithium enolate. The lithium enolate was treated with γ -valerolactone to yield the hydroxy-substituted β -keto imide **159**. Once again, the ^1H and ^{13}C NMR of the crude reaction mixture did not show evidence of the desired product.

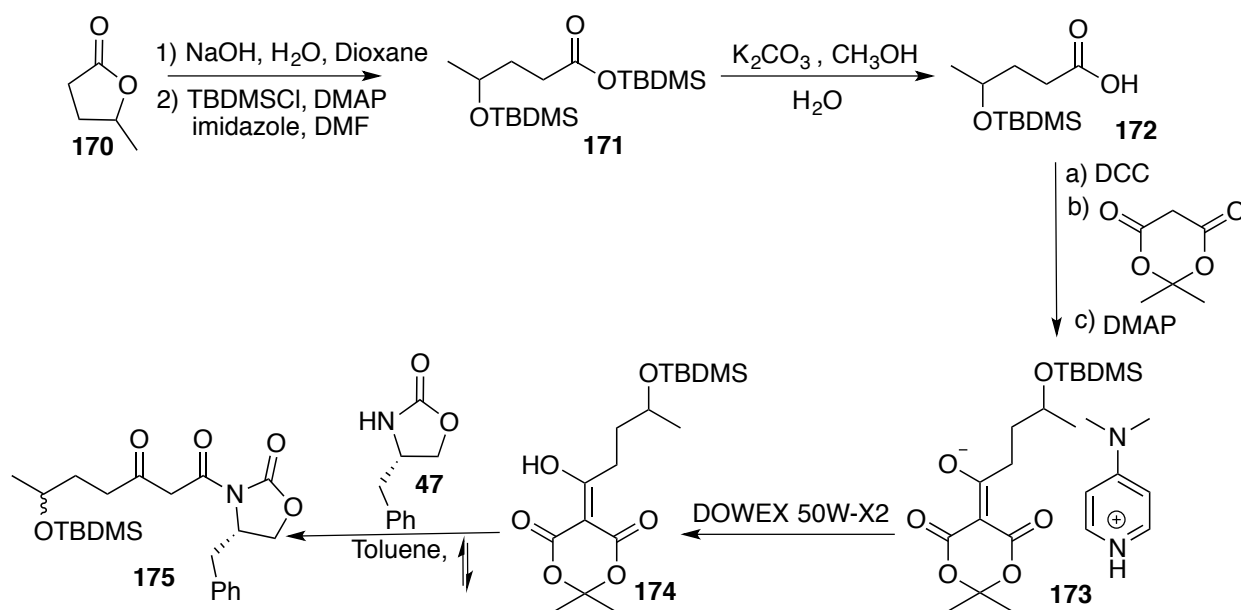


Scheme 37. Failed synthesis of β -keto imide **159** via mixed-Claisen route

DCC Coupling Route for the Synthesis of β -Keto imide **175**

An alternative and ultimately successful method for the synthesis of hydroxy-protected β -keto imide **175** was based upon a DCC-mediated condensation reaction (**Scheme 37**). The reaction was first attempted with racemic γ -valerolactone **170** to test the feasibility of the reaction. Racemic γ -valerolactone **170** was saponified with sodium hydroxide, then diprotected with *tert*-butyldimethylsilane to form the corresponding bis-TBDMS derivative **171**.⁸⁹ Selective deprotection of **171** with potassium carbonate in methanol yielded carboxylic

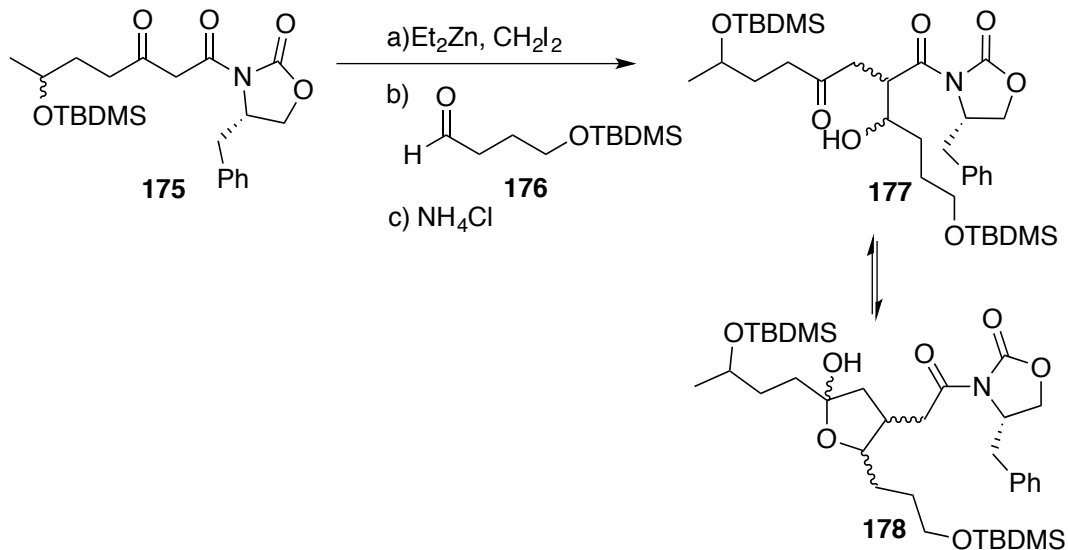
acid **172**.⁹⁰ Carboxylic acid **172** was then subjected to DCC, Meldrum's acid and 4-dimethylaminopyridine in dichloromethane to yield the corresponding stable 4-dimethylaminopyridine (DMAP) salt **173** in 94 % yield (**Scheme 37**).⁹¹ Removal of DMAP salt with aqueous acid followed by solvent extraction and evaporation can lead to product decomposition, therefore the non-aqueous protocol developed by Raillard and co-workers was followed.⁹¹ The DMAP salt **173** was dissolved in dichloromethane and stirred with DOWEX 50W-X2 resin (a polystyrene based sulfonic acid, an acidic H⁺ cation exchanger) to afford the respective free acid **174**.⁹¹ The free acid **174** is an unstable oil, which, without any further purification, was refluxed with chiral oxazolidinone **161** in toluene to afford the desired hydroxy-protected β -keto imide **175** as a 1:1 mixture of diastereomers in 45% yield after purification. The ¹H NMR of the β -keto imide **175** showed the characteristic AB of the diastereotopic methylene protons. However the hydroxy protected β -keto imide **175** does not exist in equilibrium with its hemiacetal form as in the case of hydroxy substituted β -keto imide **159** due to the TBDMS protection in **175**.



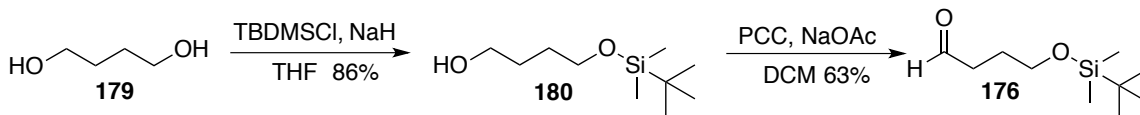
Scheme 38. DCC Coupling route for the synthesis of β -keto imide **175**

Tandem Chain Extension Aldol Reaction (TCEA):

The zinc-mediated tandem chain extension-aldol reaction (TCEA) is the key step designed to synthesize the spiroketal framework of the natural products CJ-12,954 and CJ-13,014. As discussed in **Chapter I** the reactivity and diastereoselectivity of TCEA of β -keto esters, amides and imides were extensively studied. In contrast to β -keto esters and amides, β -keto imides give more side products under zinc carbenoid-mediated chain extension reactions. β -Keto imide **175** was subjected to tandem chain extension-aldol reaction using aldehyde **176** to study the feasibility of the reaction (**Scheme 38**). Aldehyde **176** was synthesized by monosilylation of 1,4-butanediol (**179**) followed by PCC oxidation (**Scheme 38**).^{92, 93} In an initial attempt β -keto imide **175** was added to the preformed carbenoid, stirred for 30 min to allow for chain extension followed by addition of aldehyde **176**. The TCEA reaction involving β -keto imide **175**, which exists as a mixture of diastereomers, with aldehyde **176** was proposed to give the aldol product **177**, which in turn would exist in equilibrium with its hemiacetal **178** (**Scheme 38**). The ^1H NMR of the crude reaction mixture was difficult to analyze for the presence of TCEA product due to the presence of diastereomeric open-chain and hemiacetal forms. However, the presence of tandem chain extension-aldol product in the crude reaction mixture was confirmed by the ^{13}C NMR spectroscopy signal of the hemiacetal carbon in CDCl_3 . Four different signals in the range δ 110-113 ppm corresponding to four different hemiacetal carbons were observed. Based on these initial results, it was confirmed that application of TCEA reaction of the β -keto imide **175** for the synthesis of the spiroketal backbone is feasible. However, since β -keto imide **175** had been derived from the racemic γ -valerolactone **170**, a mixture of diastereomeric products were generated. Future attempts were focused on the synthesis and utilization of desired enantiopure (R)- γ valerolactone (**181**).



Scheme 39. TCEA reaction of β -keto imide **175** derived from racemic γ -valerolactone **170**



Scheme 40. Synthesis of aldehyde **176**

Synthesis of (*R*)- γ -Valerolactone

The C-7 stereocenter (**Figure 10**) in the targeted spiroketals **151** and **152** has *R* stereochemistry. As illustrated in the retrosynthetic analysis, this stereocenter comes from the γ -carbon next to the keto functionality in β -keto imide **175**, which ultimately is derived from the γ -carbon of the γ -valerolactone (**Figure 12**). Since *R* stereochemistry is desired, (*R*)- γ -valerolactone (**181**) is the necessary starting material for the synthesis of β -keto imide **194**, which would be the substrate for the tandem chain extension aldol reaction. Hence formal synthesis of CJ-12,954 and CJ-13,014 required access to (*R*)- γ -valerolactone (**181**).

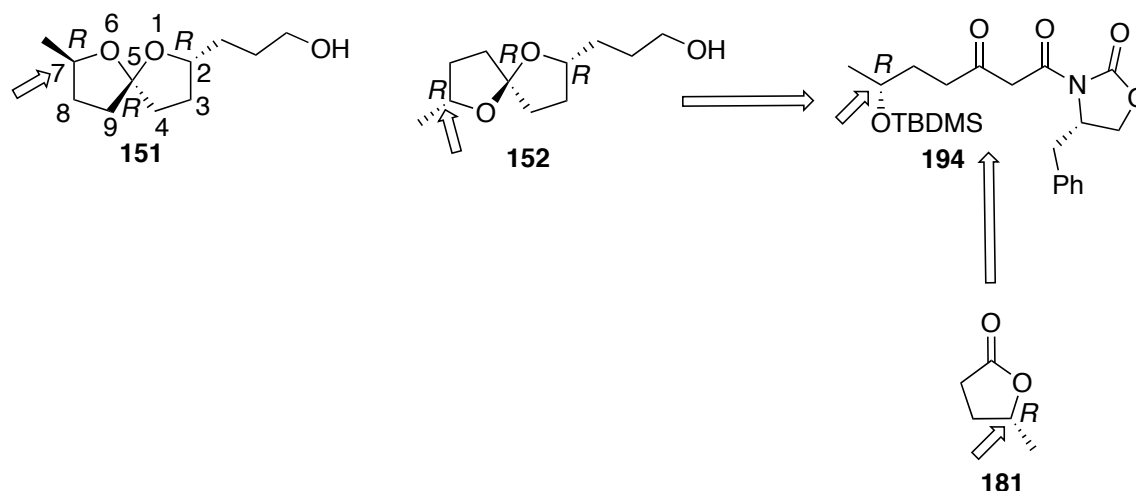
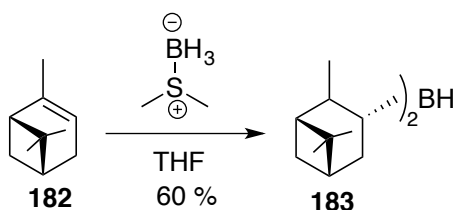
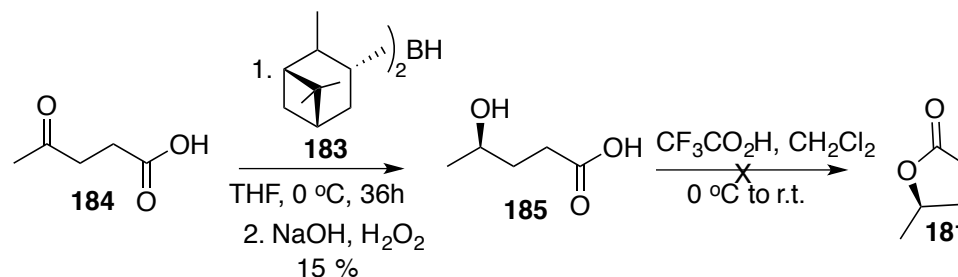


Figure 12. Establishing C-7 stereocenter in **151** and **152** from (*R*)- γ -valerolactone

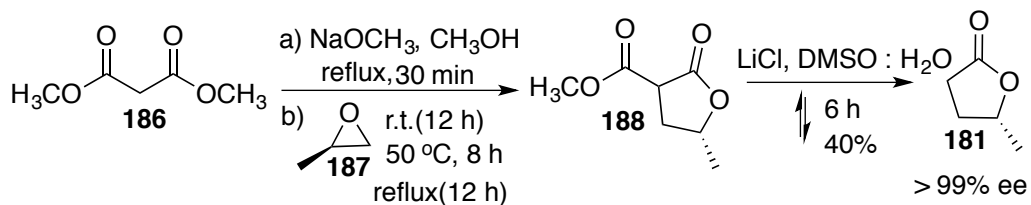
Attempts to synthesize enantiopure (*R*)- γ -valerolactone (**181**) involved following the literature protocol reported by Brown et al.⁹⁴ Optically pure diisocamphenylborane (Ipc_2BH) (**183**) was synthesized from commercially available (+)- α -pinene (**182**) (91% ee) and borane-methyl sulfide (BMS) by asymmetric hydroboration (**Scheme 40**).⁹⁴ Asymmetric reduction of the keto acid **184** with Ipc_2BH **183** yielded the hydroxy acid **185**, although in very low yield (**Scheme 40**).⁹⁵ Attempts to increase the yield of the reaction were unsuccessful. Efforts to lactonize the hydroxy acid **185** to the corresponding (*R*)- γ valerolactone (**181**) through treatment with trifluoroacetic acid were unsuccessful.⁹⁵



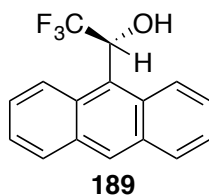


Scheme 41. Attempted synthesis of (*R*)- γ -valerolactone (**181**) using Ipc₂BH (**182**)

An alternative approach for the synthesis of (*R*)- γ -valerolactone (**181**) involved the use of a chiral epoxide.⁹⁶ The condensation of dimethyl malonate (**186**) with commercially available (*R*)-propylene oxide (**187**) with 99% ee gave lactone ester **188**, which upon Krapcho decarboxylation afforded the desired (*R*)- γ -valerolactone (**181**) in 40% yield (**Scheme 41**).⁹⁶ An optical rotation was obtained for (*R*)- γ -valerolactone (**181**) and was calculated to be $[\alpha]_D^{20} +24.8^\circ$ (c 0.23, CH₂Cl₂), which was compared to literature $+31.4^\circ$ (c 1, CH₂Cl₂). A positive specific rotation correlates to (+)-(*R*)- γ -valerolactone (**181**), although the optical rotation data suggested the ee of the product may be modest. The enantiomeric excess of the synthesized (*R*)- γ -valerolactone (**181**) was also determined by NMR spectroscopy using two equivalents of Pirkle's alcohol **189** (**Figure 13**). The enantiotopic methyl protons of the racemic γ -valerolactone (**170**), when introduced into the chiral environment using Pirkle's alcohol, become diastereotopic and show two different signals as two doublets ($J = 6.2$ Hz) in ¹H NMR analysis. In contrast, the synthetic (+)-(*R*)- γ valerolactone (**181**) shows only one signal as a doublet ($J = 6.2$ Hz) when introduced into the chiral environment using Pirkle's alcohol **189** (**Figure 13**), which established the ee of the lactone as >99%.



Scheme 42. Synthesis of (*R*)- γ -valerolactone (**181**) from (*R*)-propylene oxide (**187**)



(*R*)-(-)-Pirkle's alcohol

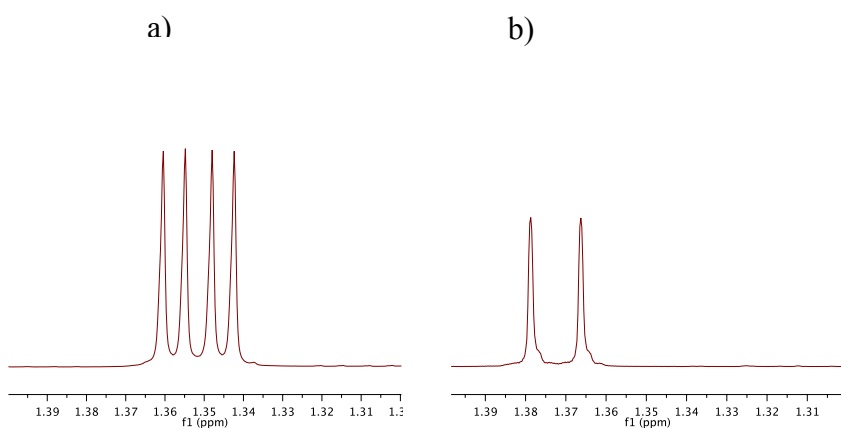
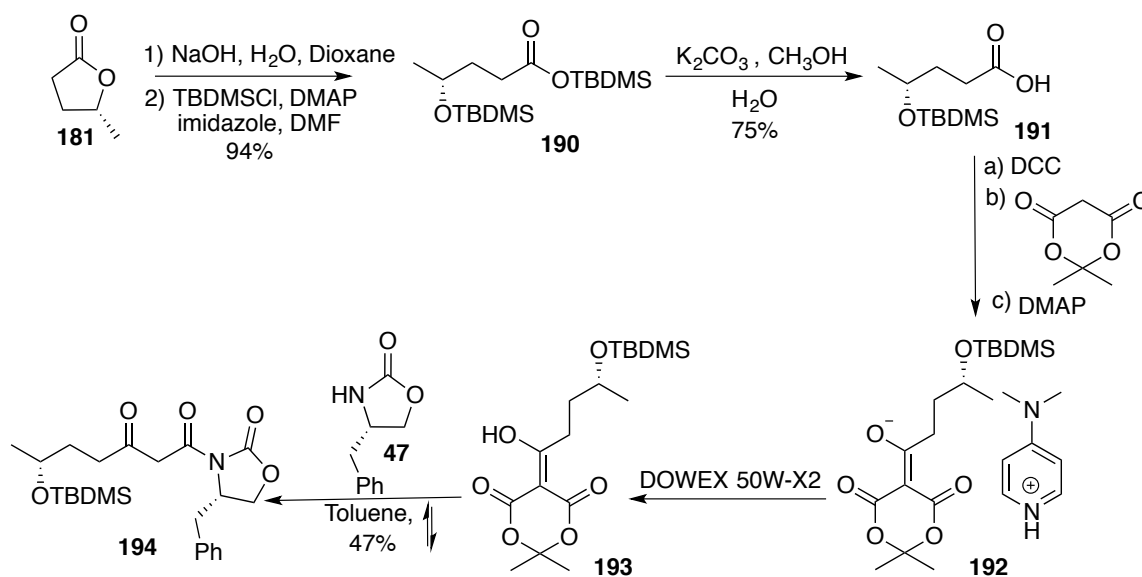


Figure 13. Methyl protons of a) racemic γ -valerolactone and b) (*R*)- γ -valerolactone with (*R*)-(-)-Pirkle's alcohol in CDCl₃

DCC Coupling Route for the synthesis of β -keto imide **194**

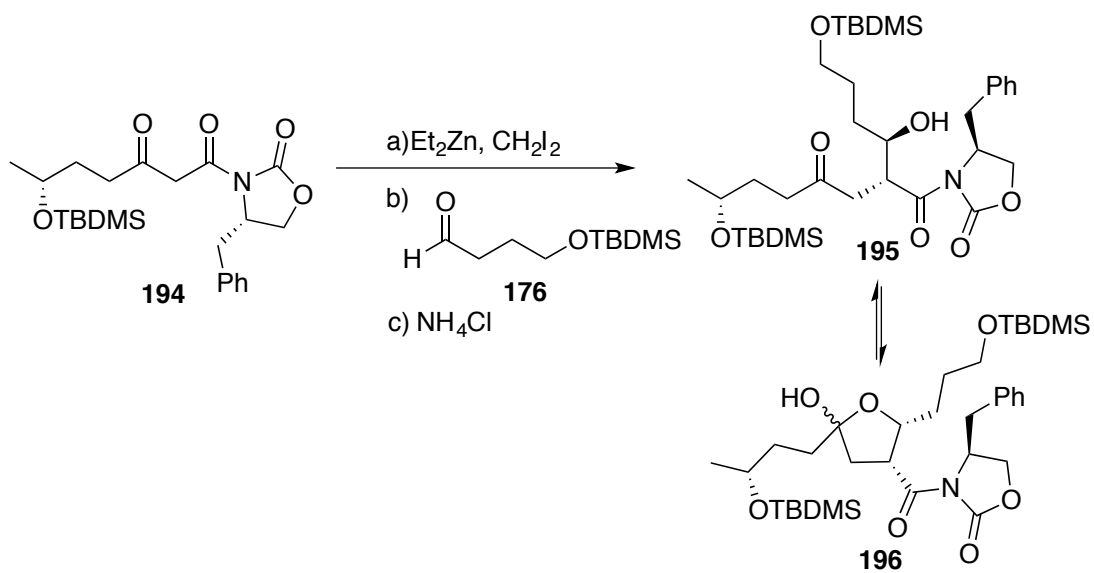
The DCC coupling method used earlier to synthesize β -keto imide **61** was applied for the synthesis of β -keto imide **194** as a single diastereomer, starting with enantiopure (*R*)- γ -valerolactone (**181**) (Scheme 42).⁹¹ The β -keto imide **194** was obtained as a single diastereomer in 47% yield as a light yellow colored solid. The AB spin system of the two methylene protons

between the keto and imide carbonyls and the presence of enolic protons around 13.6 ppm suggests the presence of β -keto imide **194** in both keto and enolic forms.



Scheme 43. Synthesis of β -keto imide **194** as a single diastereomer

The zinc-mediated tandem chain extension-aldol reaction of β -keto imide **194** with aldehyde **176** afforded an aldol product, presumed to be **195** and its hemiacetal **196** (**Scheme 43**). The presence of open chain form **195** and two possible diastereomers of hemiacetal **196** was confirmed by ¹H NMR spectroscopy where three methyl doublets with coupling constant of 6.1 Hz were observed (**Figure 14**). The doublets indicate the presence of isomeric forms, but it is unclear whether the doublet are all derived from the same aldol product or whether they are from other aldol isomers. The ¹³C NMR analysis showed two signals at 111.8 and 112.3 ppm, which would correspond to the two hemiacetal carbons of the two possible diastereomers of **196**.



Scheme 44. TCEA reaction of β -keto imide **194** with aldehyde **176**

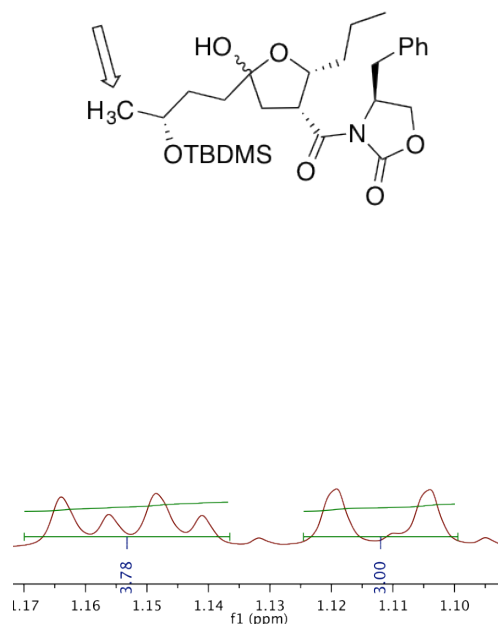
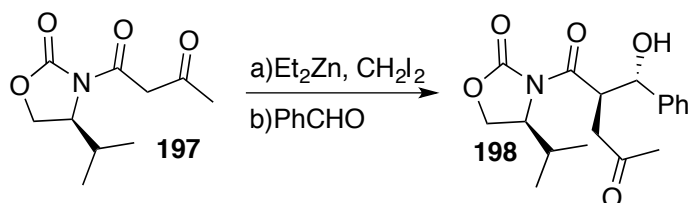


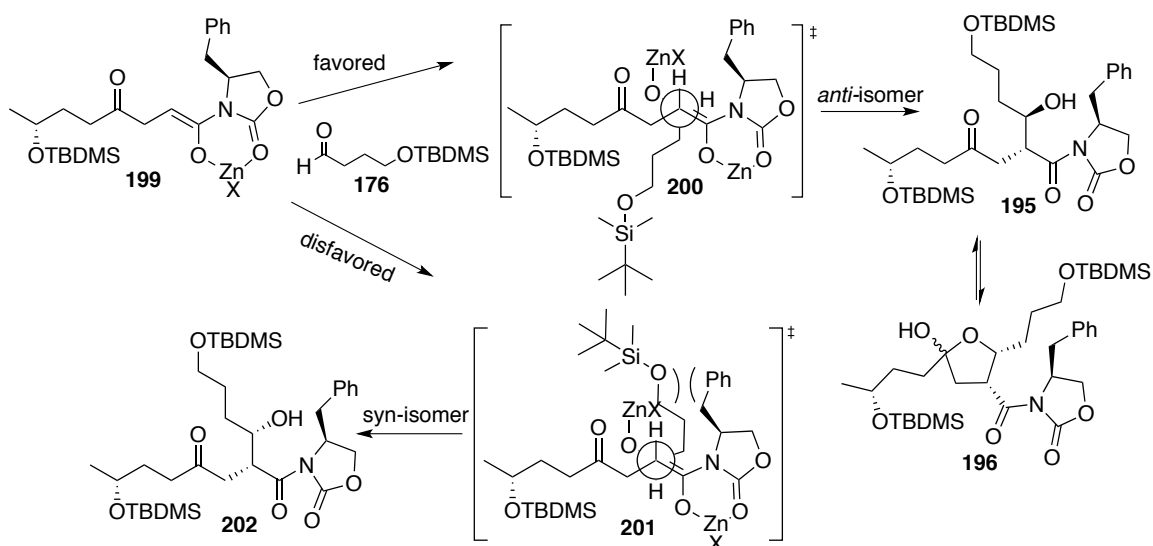
Figure 14. Presence of three doublets in ^1H NMR of TCEA product showing presence of open-chain and two diastereomers of hemiacetals.

Sujen Lai, a previous group member, extensively studied the zinc-mediated tandem chain extension-aldol reaction, including reaction of β -keto imides. Lai observed that *anti*-aldol product **198** was the only isomer formed during the TCEA reaction of β -keto imide **197** with benzaldehyde (**Scheme 44**). Lai confirmed the stereochemistry of the *anti*-aldol product **198** unambiguously by X-ray crystallography. Hence, previous studies by Lai, Aiken and also the Heathcock model³¹ provides good evidence that the zinc-mediated tandem chain extension-aldol reaction involving β -keto imides react with aldehyde via an open transition state. Based on these results the favored *Z*-enolate of β -keto imide **199** is proposed to attack aldehyde **176** from the *si*-face through an open transition state **200**, leading to the *anti*-aldol product **195**, which exists in equilibrium with its hemiacetal **196** (**Scheme 45**). The *syn*-aldol product **202**, which would result from the attack of *Z*-enolate of β -keto imide **194** on the *re*-face of aldehyde **176**, is less likely to form due to an undesired steric interaction between the alkyl chain of the aldehyde and the

oxazolidinone ring in the transition state **201** (**Scheme 45**). The *syn*-isomer could also result from reaction via a closed transition state.



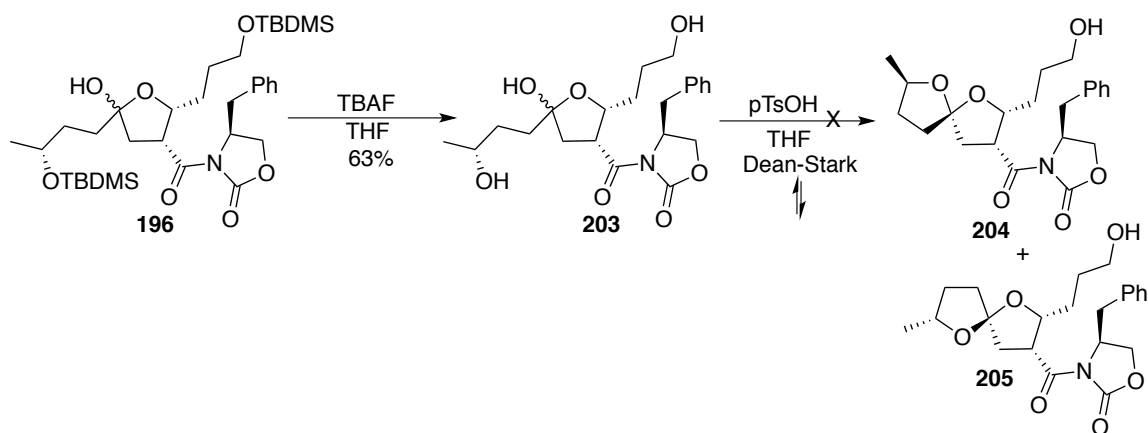
Scheme 45. TCEA reaction of β -keto imide **197** by Lai.



Scheme 46. Formation of *anti*-aldol product **195** from the transition state **200** of favored *Z*-enolate **199**

Tetrabutylammonium fluoride (TBAF) mediated deprotection of TCEA product **196** followed by spirocyclization using *p*-toluenesulfonic acid (*p*TsOH) should afford the desired spiroketal backbone of the natural product. In the initial attempt, the TCEA product was deprotected using TBAF and the crude reaction mixture was treated with *p*TsOH and refluxed in THF using a Dean-Stark trap to effect spiroketalization (**Scheme 46**). However, these attempts

did not afford the desired spiroketals and the ^1H NMR analysis showed mostly the deprotected starting material.



Scheme 47. Attempt towards spiroketals synthesis using deprotection followed by spiroketalization

An alternative approach for spiroketalization was desired. Careful review of the total syntheses of *ent*-CJ-12,954 **141** and *ent*-CJ-13,014 **142** reported by Brimble et al. suggested a different approach. The spiroacetals **134** and **135** synthesized by Brimble et al. (**Figure 15**) are advanced intermediates in the total synthesis of *ent*-CJ-12,954 **141** and *ent*-CJ-13,014 **142**.⁸¹ The presence of two different protecting groups in this alternate approach would allow for selective deprotection. The *tert*-butyldiphenyl protecting group would be expected to be stable under the conditions used for TBDMS removal, which can make the selective formation of spiroacetals possible. Hence the spiroketals **206** and **207** are considered as the new targets for the formal synthesis (**Figure 16**).

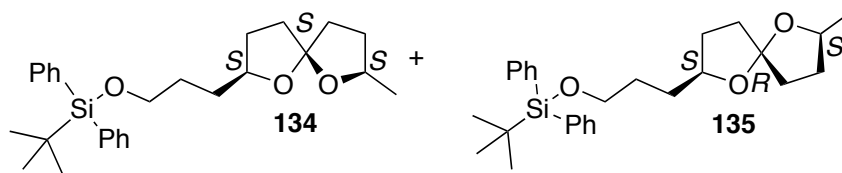


Figure 15. Spiroacetals synthesized by Brimble et al.

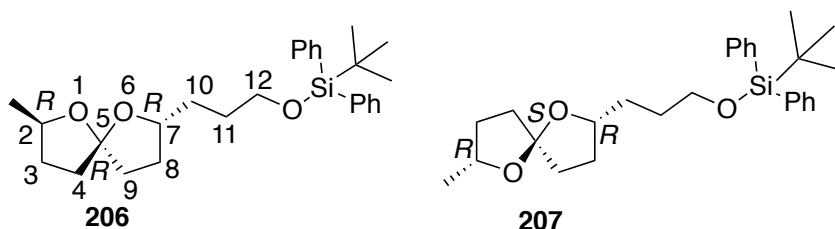
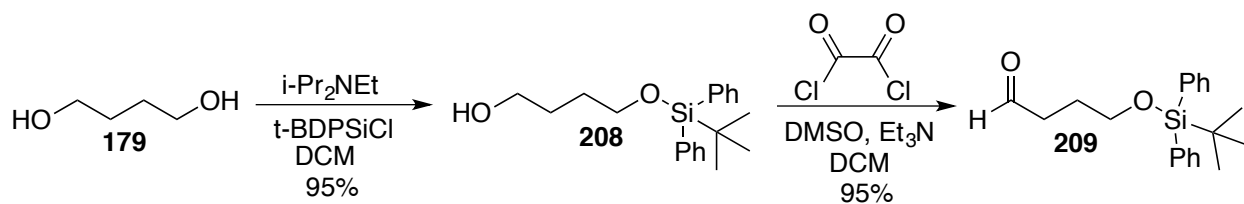
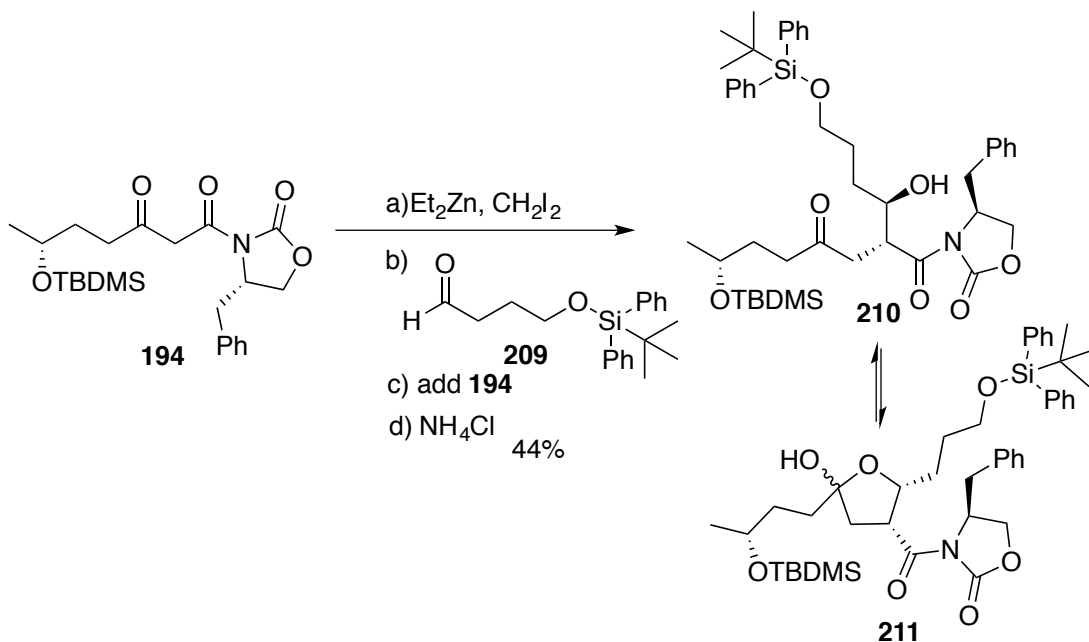


Figure 16. New targets for formal synthesis of CJ-12,954 and CJ-13,014

The new target for formal synthesis employs aldehyde **209** in the zinc-mediated tandem chain extension-aldol reaction. Monoprotection of 1,4-butanediol (**179**) as *tert*-butyldiphenylsilyl ether **208** followed by Swern oxidation afforded the desired aldehyde **209** for TCEA reaction (**Scheme 47**).^{97, 98} Tandem chain extension-aldol reaction of β -keto imide **194** and aldehyde **209** did not afford efficient formation of the desired aldol product **210**. After repeated formation of a complex reaction mixture from the TCEA reaction with very low yield of the product, it was postulated that the reaction's complexity was due to reactivity of the β -keto imide. From previous studies as discussed in **Chapter 1**, exposure of β -keto imides to zinc carbenoid for extended reaction times resulted in the formation of two major by-products, which were identified as α -methylated γ -keto imide **25** and bicyclic lactone which will be discussed in **Chapter 3**.^{29, 99} Hence a modified TCEA reaction was performed. Aldehyde **209** was added to the carbenoid prior to addition of the β -keto imide **194**. This experimental modification yielded the desired TCEA product **210** and its hemiacetal (**211**) isomers (**Scheme 48**). The presence of the desired TCEA product was confirmed by ¹H and ¹³C NMR analysis.



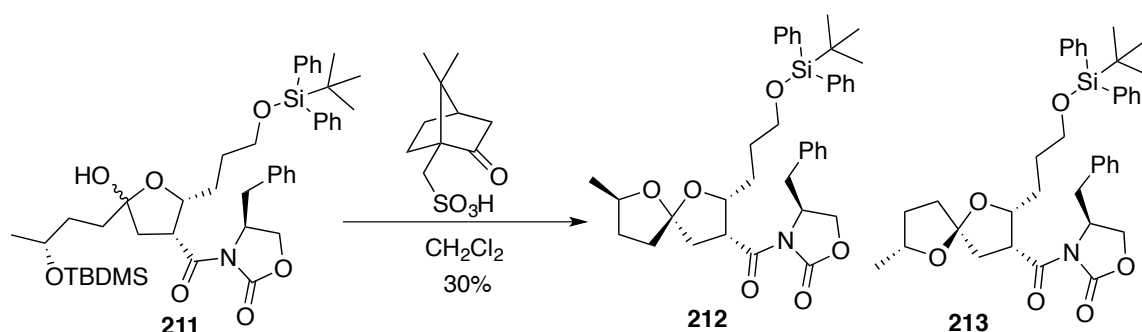
Scheme 48. Synthesis of aldehyde **209**



Scheme 49. TCEA reaction of β -keto imide **194** and TBDPSiCl protected aldehyde **209**

The presence of two different silyl ethers, *tert*-butyldimethylsilyl and *tert*-butyldiphenylsilyl, in the TCEA product offers the opportunity to selectively deprotect one silyl ether while leaving the other silyl ether intact. Brimble et al. employed this strategy to access the spiroketals **134** and **135** from protected dihydroxy ketone **133**, where the *tert*-butyldimethylsilyl ether was deprotected using camphorsulfonic acid while the *tert*-butyldiphenylsilyl ether was unaffected (**Scheme 31**).^{81, 82} Following a similar protocol, the hemiacetal **211** was subjected to spirocyclization using camphorsulfonic acid (**Scheme 49**). The successful deprotection of the TBDMS ether afforded four different spiroketals, as determined by both TLC and ¹H analysis. The NMR analysis suggested the presence of two major and two minor isomers. Spiroketals **212** and **213** are the isomers expected from the deprotection of hemiacetal **211**. The other two

spiroketals **214** and **215** are believed to have resulted from minor amounts of the other possible *anti*-aldol isomers (**Figure 17**). *Syn* aldol products could also be the source of the minor isomers, although these possible products are not illustrated. No studies were done to confirm the origin of the two other spiroketals. Spiroketals **212** and **213** are tentatively identified as the desired spiroketals by comparison of their ^1H and ^{13}C NMR spectra to the spiroketals reported by Brimble et al. A key difference is the absence of an acyl oxazolidinone as part of the Brimble intermediate.



Scheme 50. Spirocyclization of TCEA product **211** using camphorsulfonic acid

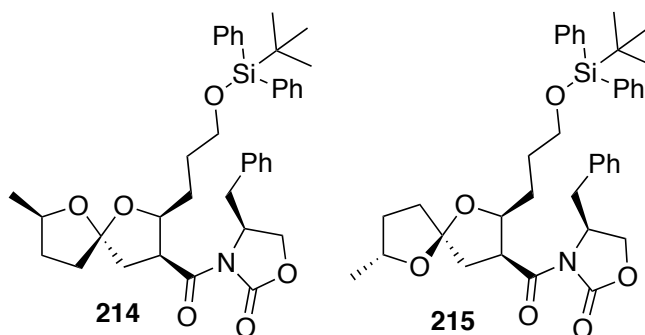


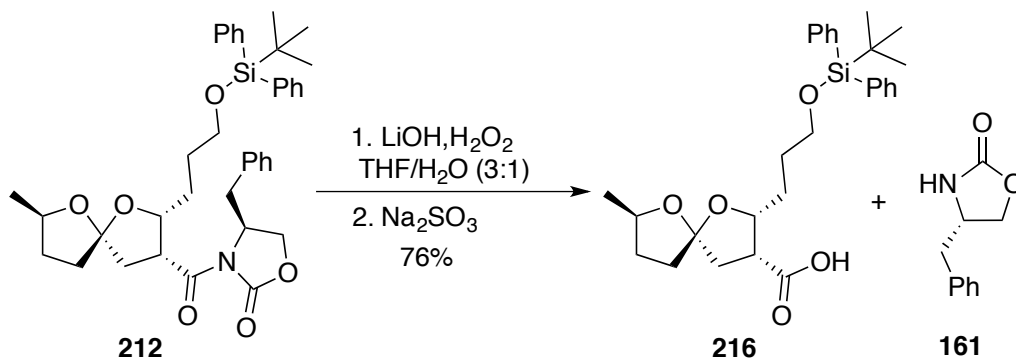
Figure 17. Spiroketals from the other possible *anti*-aldol product

The spiroketals **212** and **213** were purified by column chromatography. Hydrolysis of the imide followed by decarboxylation was expected to afford the final spiroketals **206** and **207**, thus completing the formal synthesis (**Figure 16**). Brimble et al. obtained equal quantities of spiroacetals **134** and **135** (**Figure 15**) as an inseparable mixture, which was attributed to the lack

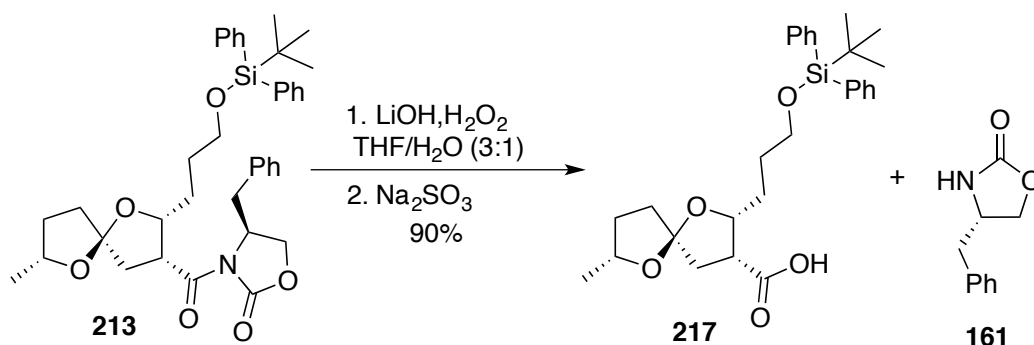
of stereocontrol from anomeric and steric effects. Hence the Brimble team completed the synthesis using a 1:1 mixture of spiroacetals **134** and **135**, obtaining an inseparable 1:1 mixture of *ent*-CJ-12,954 and *ent*-CJ-13,014 at the end of their total synthesis. Our ability to separate compounds **206** and **207** offers an advantage in that each isomer could be cleanly transformed into their respective natural products, assuming that the reaction conditions used for completing the synthesis of the natural product did not result in epimerization of the ketal stereocenter.

Lithium hydroperoxide-mediated removal of the oxazolidinone of spiroketal **212** afforded the carboxylic acid **216** (Scheme 50).¹⁰⁰ Following the reported procedure developed by Evans et al., the spiroketal **212** was dissolved in a 3:1-THF/H₂O mixture and treated with hydrogen peroxide followed by lithium hydroxide. Lithium hydroperoxide is formed and cleaves the exocyclic carbonyl of the acyl oxazolidinone to provide carboxylic acid **216** and oxazolidinone **161** (Scheme 50).¹⁰⁰ The reaction was quenched and buffered to pH 10 with aqueous sodium bicarbonate. The volatile solvent was evaporated and the aqueous residue was extracted with dichloromethane in an effort to remove the deacylated chiral oxazolidinone **161**. The aqueous layer was acidified to pH 1 and extracted with ethyl acetate in an unsuccessful effort to isolate the carboxylic acid **216**. Both the carboxylic acid **216** and chiral oxazolidinone **161** were recovered from the dichloromethane layer. Repeated extraction protocols were investigated in an effort to separate **216** and **161**, however no suitable conditions were identified. While the compounds were found to have a similar R_f in the majority of solvent systems, thus making chromatographic separation challenging, flash column chromatography using gradient mobile phase of methyl *tert*-butyl ether (MTBE) and hexane eventually afforded the carboxylic acid **216** as a pure compound free from chiral oxazolidinone **161**. Following the similar protocol

spiroketal **213** was subjected to hydrolysis and purified by chromatography to afford the carboxylic acid **217** (**Scheme 51**).



Scheme 51. Lithium hydroperoxide mediated hydrolysis of carboximide of spiroketal **212**

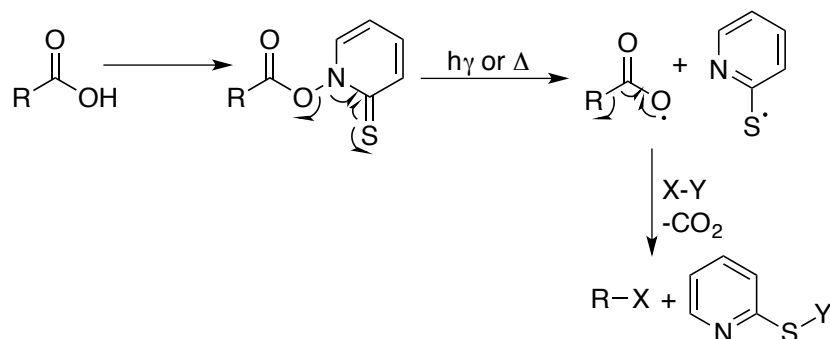


Scheme 52. Lithium hydroperoxide mediated hydrolysis of carboximide of spiroketal **213**

Barton decarboxylation of spiroketals **216** and **217**

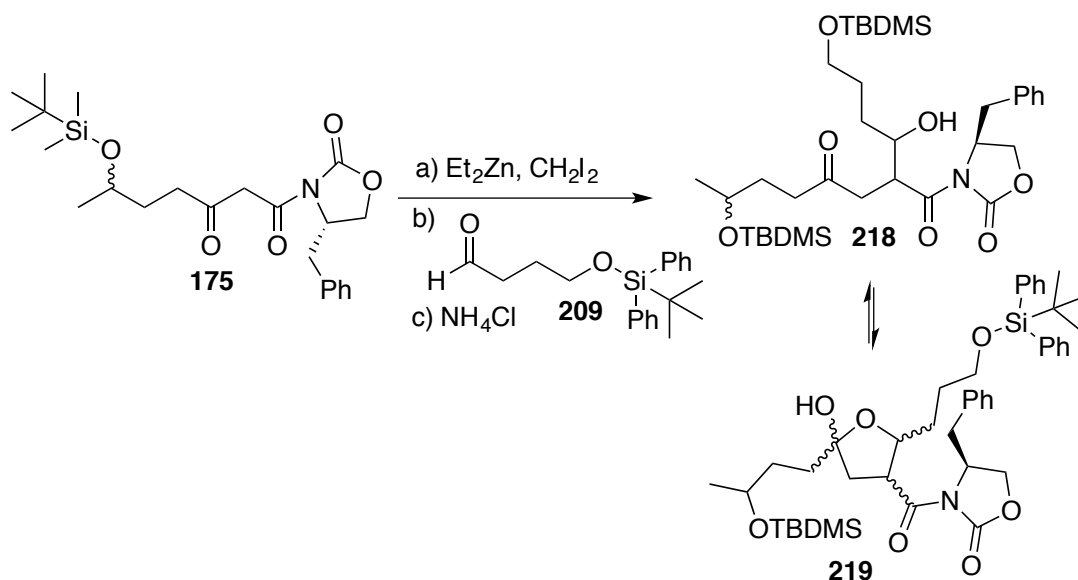
Barton decarboxylation is a valuable synthetic tool to convert alkyl carboxylic acids to various different functionalities. In the Barton decarboxylation, a carboxylic acid is converted to its thiohydroxamate ester (often called a Barton ester), which undergoes homolytic cleavage, generally initiated by light or heat, to generate 2-pyridylthiyl radical and acyloxy radical (**Scheme 52**).¹⁰¹ The alkyl radical generated by radical decarboxylation of acyloxy radical can react with various radical-trapping species (X-Y) to generate the trapped product bearing a new

functional group. Barton reductive radical decarboxylation can be achieved by treating alkyl radical with a hydrogen donor.

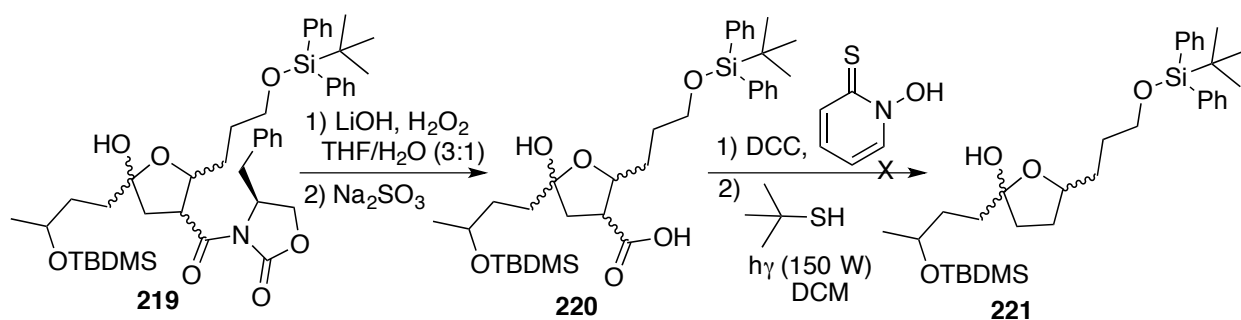


Scheme 53. Barton decarboxylation

In order to develop experience with the Barton decarboxylation methodology, initial reactions were not performed on either spiroketals **216** or **217**. Decarboxylation was first attempted on the hemiacetal **220**, obtained from the hydrolysis of carboximide of hemiacetal **219** (**Scheme 54**).²⁷ The hemiacetal **219** was obtained from the TCEA reaction of β -keto imide **175** derived from racemic γ -valerolactone (**170**) and aldehyde **209** (**Scheme 53**), therefore **219** was a mixture of diastereomers. Barton decarboxylation of the hemiacetal **220** gave a complex reaction mixture (**Scheme 54**). ¹H and ¹³C NMR spectra of the crude reaction mixture and NMR analysis of fractions obtained from preparative thin layer chromatography showed the presence of Barton ester generated from **220** and starting carboxylic acid **220**.



Scheme 54. TCEA reaction β -Keto imide **175** and aldehyde **209**

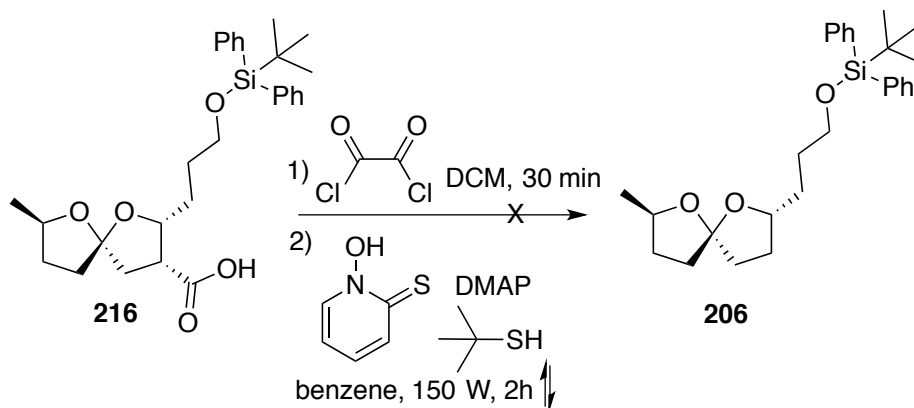


Scheme 55. Attempted Barton decarboxylation on carboxylic acid **220**

Though the reasons for unsuccessful Barton decarboxylation of carboxylic acid **220** were unknown, hemiacetal **220** was likely not an ideal substrate for decarboxylation due to the presence of the hemiacetal. Our next attempt was focused on the carboxylic acid **216** prepared from spiroketal **212**. Barton decarboxylation of carboxylic acid **216** was expected to afford the desired spiroketal **206**, which would complete the formal synthesis. Following the procedure reported by Thomas et al., carboxylic acid was treated with oxalyl chloride to give the corresponding acyl chloride (**Scheme 55**).¹⁰² The acyl chloride was then dissolved in anhydrous benzene and added dropwise to a magnetically stirred and irradiated (150 W, tungsten light)

refluxing suspension of 2-mercaptopyridine *N*-oxide in anhydrous benzene containing DMAP and *tert*-butyl thiol (**Scheme 55**).¹⁰² After a two-hour reflux with irradiation, the reaction mixture was worked up. The ¹H and ¹³C NMR spectra of the crude reaction mixture did not show any traces of the desired product.

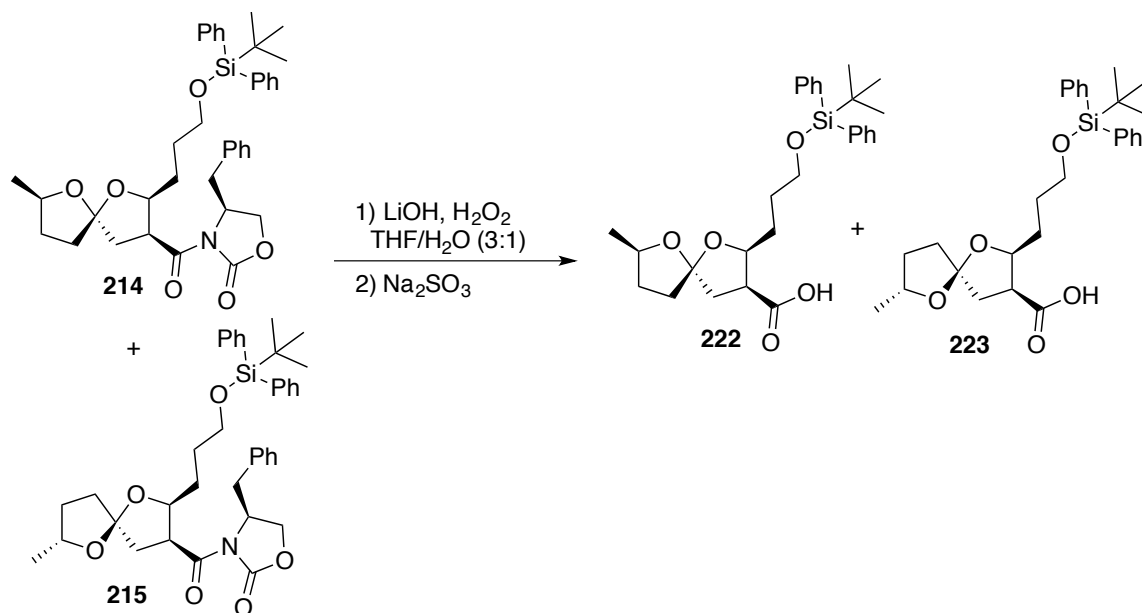
Tsanaktsidis et al. reported the use of chloroform as the hydrogen atom source in a Barton decarboxylation reaction, thus reducing the cost, toxicity and/or smell of traditional Barton decarboxylation reaction, which uses tributyltin hydride or *tert*-butyl thiol as the hydrogen source.¹⁰³ Barton decarboxylation with chloroform as the hydrogen source was attempted on carboxylic acids **222** and **223**, which were obtained from the hydrolysis of spiroketals **214** and **215** (**Scheme 56**) using the procedure reported by Tsanaktsidis et al (**Scheme 57**).¹⁰³ The stereochemistries at C-7 and C-8 of spiroketals **214** and **215** are not known..



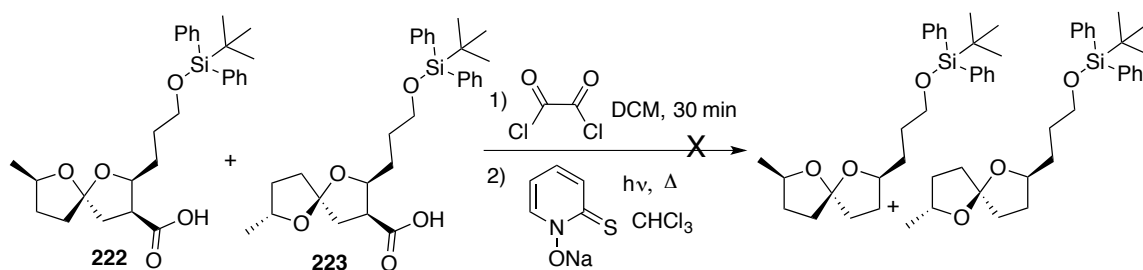
Scheme 56. Attempted Barton decarboxylation on spiroketal **216**

Since the earlier attempts of Barton decarboxylation were unsuccessful, it was important to confirm formation of the acid chloride from the carboxylic acid. The mixture of carboxylic acids **222** and **223** were treated with oxalyl chloride in anhydrous dichloromethane (**Scheme 57**). The formation of acyl chloride from carboxylic acid was monitored by ¹H NMR, ¹³C NMR and IR spectroscopy. In the ¹³C NMR spectrum, the acid chloride carbonyl was observed slightly

upfield of the carbonyl in the carboxylic acids **222** and **223**, which confirmed formation of the acid chloride. The acid chloride was then added drop-wise to the refluxing suspension of 1-hydroxypyridine-2(1H)-thione sodium salt and DMAP in chloroform with concomitant irradiation from a halogen lamp.



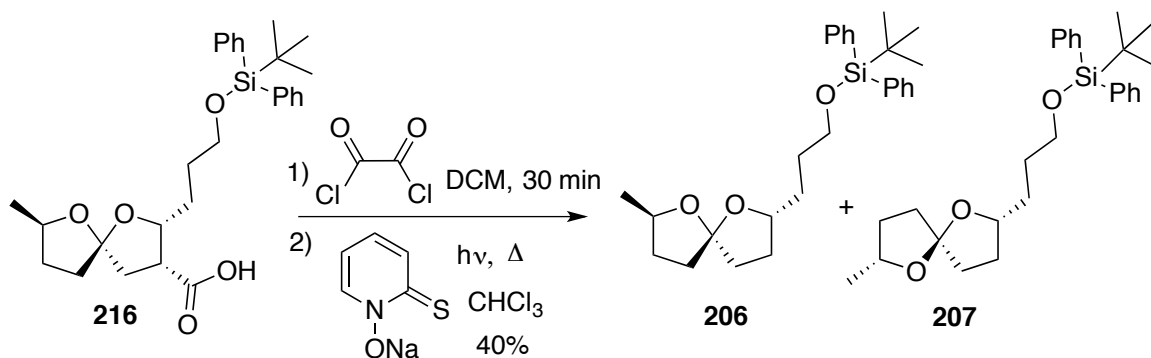
Scheme 57. Lithium hydroperoxide mediated hydrolysis of carboximide of spiroketals **214** and **215**



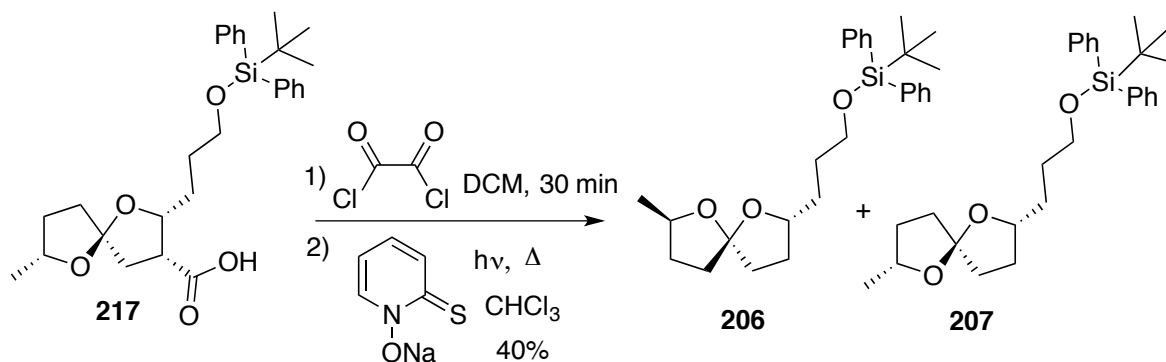
Scheme 58. Attempted Barton decarboxylation on carboxylic acids **222** and **223**

The crude reaction mixture obtained after work-up did not show any evidence of decarboxylated product from ^1H and ^{13}C NMR analysis. Barton decarboxylation using chloroform as the hydrogen atom source was next attempted on the carboxylic acid **216** with minor modifications (**Scheme 58**).

Commercial chloroform includes ethanol as the stabilizer to enhance solvent shelf life. However, addition of ethanol will increase the polarity of the solvent and can impact certain chemical reactions. In order to remove the traces of ethanol, chloroform was washed with water, dried over potassium carbonate and distilled over P_2O_5 . *N*-Mercaptopyridine oxide sodium salt was dried under high vacuum prior to use. The carboxylic acid **216** was treated with oxalyl chloride in anhydrous dichloromethane for 30 min. The resulting acid chloride was dried under high vacuum for 10 min to remove any excess oxalyl chloride. The crude acid chloride was dissolved in distilled chloroform and added drop-wise over 10 min to a refluxing white suspension of 1-hydroxypyridine-2(1H)-thione sodium salt and DMAP in distilled chloroform with concomitant irradiation from a halogen lamp (**Scheme 58**). The reaction mixture turned from a white suspension to a light yellow colored mixture upon addition of the acid chloride. The crude reaction mixture showed the presence of two spiroketals. The crude reaction mixture was separated by preparative thin layer chromatography to afford spiroketal **206** and its epimer at the spiroketal carbon **207** in 40% yield. Barton decarboxylation of carboxylic acid **217** gave the spiroketals **206** and **207** (**Scheme 59**).



Scheme 59. Barton decarboxylation on carboxylic acid **216** using chloroform as the hydrogen atom source.



Scheme 60. Barton decarboxylation on carboxylic acid **217** using chloroform as the hydrogen atom source.

Brimble et al. synthesized the spiroketals **134** and **135**, which are the enantiomers of spiroketals **206** and **207**, as key intermediates in their total synthesis of *ent*-CJ-12,954 (**141**) and *ent*-CJ-13,014 (**142**). However, they were unable to separate the 1:1 mixture of spiroketals **134** and **135**. In our attempt towards the formal synthesis of CJ-12,954 (**126a**) and CJ-13,014 (**126b**), decarboxylation of the carboxylic acid **216** afforded the two spiroketals, **206** and its epimer at the spiroketal carbon **207**.

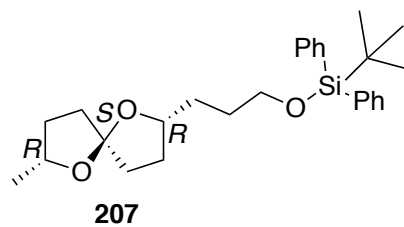
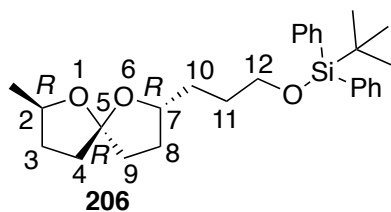
Characterization of spiroketals **206** and **207**

In a similar fashion to the hydrolysis of spiroketal **212** to afford the carboxylic acid **216**, spiroketal **213** was hydrolyzed to the carboxylic acid **217**. The carboxylic acids **216** and **217** were subjected to Barton decarboxylation using chloroform as the hydrogen atom source to afford the desired spiroketals **206** and **207**. While application of the model for predicting stereochemistry of the TCEA reaction and the known stereochemistry of the starting material suggested that **206** and **207** were enantiomers to Brimble's **134** and **135**, careful comparison of NMR spectra was necessary to confirm the prediction.

The ^1H and ^{13}C NMR of the synthesized spiroketals **206** and **207** are compared to the spiroketals **134** and **135** reported by Brimble et al (**Table 6**). Since Brimble et al. were unable to separate the two spiroketals **134** and **135**, some of the ^1H and ^{13}C resonances were not assigned to a specific spiroketal. However, the characteristic resonances of quaternary spiroketal carbons at δ 114.3 and 114.7 were assigned to spiroketals **134** and **135** respectively (**Table 7**). These assignments were made by Brimble et al., on comparison of their spectral data with the Dekker et al. data for the natural products. Based on this information, we have characteristic resonances at δ 114.4 and 114.6 corresponding to the two quaternary carbon resonances in the ^{13}C NMR spectrum to spiroketals **206** and **207**, respectively.

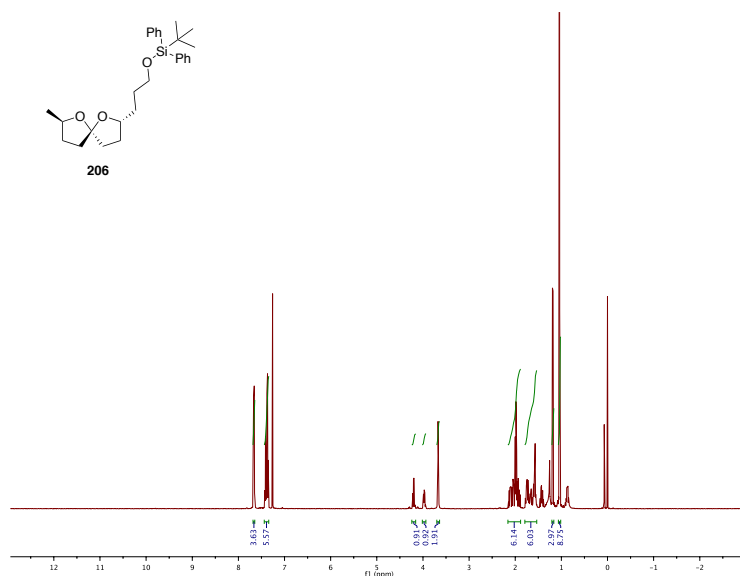
Brimble et al. also matched the spectral data of ^1H doublets assigned to the methyl group with the natural product spectral data. However this comparison was made on the final products (*ent*-CJ-12,954 and *ent*-CJ-13,014 and natural products CJ-12,954 and CJ-13,014) and not on the spiroketals **134** and **135**. The 1:1 mixture of spiroketals **134** and **135** showed doublets at δ 1.23 and 1.29 ppm; however, resonances are not matched to a specific spiroketal. Based on this spectral data we characterized the doublets at δ 1.20 and 1.26 ppm ($J = 6.2$ Hz), corresponding to

the methyl group in spiroketals **206** and **207** respectively. Hence, the spectral data of the key quaternary carbons and doublets due to the methyl groups are in general, good agreement with the data reported by Brimble et al. (**Table 6** and **Figure 18**). The stereocenter C2 was derived from (*R*)- γ -valerolactone (**181**) and the stereocenter incorporated in Brimble's study was *S*; the excellent match of these resonances is consistent with the enantiomeric relationship of the spiroketals. Hence the synthesized spiroketals **206** and **207** are enantiomers of the spiroketals **134** and **135**, prepared in the Brimble's work.



H atom	Brimble et al. Spiroketal 134 and 135 (<i>S, S, S</i>) and (<i>S, R, S</i>)	Spiroketal 206 (<i>R, R, R</i>)	Spiroketal 207 (<i>R, S, R</i>)
Si ^t BuPh ₂	1.07 (s, 9H)	1.04 (s, 9H)	1.04 (s, 9H)
Me	1.23 (d, <i>J</i> = 6.2 Hz, 1.5H) 1.29 (d, <i>J</i> = 6.2 Hz, 1.5H)	1.2 (d, <i>J</i> = 6.2 Hz, 3H)	1.26 (d, <i>J</i> = 6.2 Hz, 3H)
3, 4, 8	1.43-1.78 (m, 6H)	1.53-1.80 (m, 6H)	1.42-1.77 (m, 6H)
9, 10, 11	1.91-2.17 (m, 6H)	1.88-2.16 (m, 6H)	1.86-2.16 (m, 6H)
12	3.70 (t, <i>J</i> = 6.2 Hz, 2H)	3.67 (t, <i>J</i> = 6.3 Hz, 2H)	3.62-3.72 (m, 2H)
7	4.06-4.13 (m, 1H)	4.0-3.97 (m, 1H)	
2	4.20 (qd, <i>J</i> = 6.3, 6.3 Hz, 1H)	4.20 (sextet, <i>J</i> = 6.3 Hz, 1H)	4.06-4.22 (m, 2H)
Si ^t BuPh ₂ , <i>m</i> and <i>p</i>	7.37-7.45 (m, 6H)	7.34-7.44 (m, 6H)	7.34-7.44 (m, 6H)
Si ^t BuPh ₂ , <i>o</i>	7.69 (dd, <i>J</i> = 7.3, 1.4 Hz)	7.64-7.68 (m, 4H)	7.64-7.69 (m, 4H)

Table 6. ¹H NMR assignment of spiroketals **206** and **207** compared to their enantiomers **134** and **135** reported by Brimble et al.



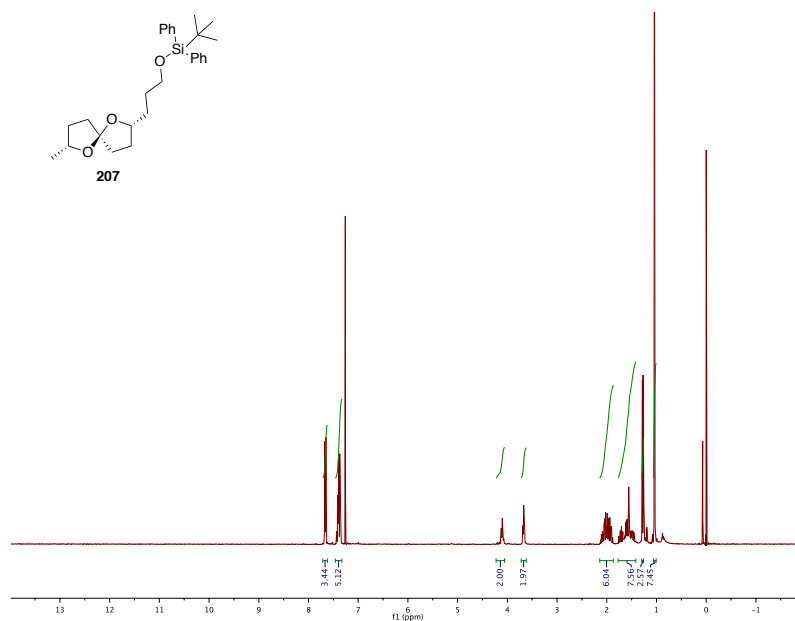


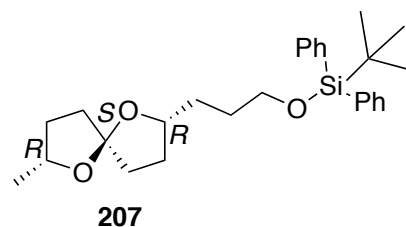
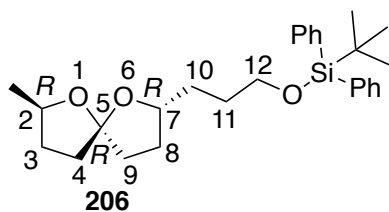
Figure 18. ^1H NMR spectra of spiroketals **206** (*R, R, R*) and **207** (*R, S, R*)

There are 21 distinct carbons in each of the spiroketals **206** and **207** including the two diastereotopic phenyl groups, however 17 carbon resonances were observed by the ^{13}C NMR (**Figure 19** and **Figure 20**). A DEPT 135 spectrum was also obtained for the spiroketal **206** (**Figure 21**). DEPT was used as a valuable tool to confirm the transformation of spiroketal **212** to carboxylic acid **216** and ultimately to decarboxylated spiroketal **206**. Two methyl carbons, seven methylene, five methine and two quaternary carbons in spiroketal **206** were confirmed by the DEPT spectrum. The disappearance of the two quaternary carbons from the ^{13}C NMR spectrum (**Figure 19**) in the DEPT spectrum (**Figure 21**) also confirms the resonances for the quaternary spiroketal carbon and quaternary carbon of the phenyl group.

The resonances of the spiroketals **206** and **207** are in good agreement with the spiroketals **134** and **135**. Since the methyl (C1), quaternary (C5) and the two methine (C2 and C7) could be unambiguously identified by DEPT analysis, the resonances were compared. The methine carbon C7 of spiroketals **134** and **135** was assigned by Brimble to the resonances at δ 79.7 and 77.9, respectively. Similar to these assignments, the methine carbon C7 of spiroketals **206** and **207** also showed resonances at δ 79.7 and 77.9 ppm, respectively. The methine carbon C2 of spiroketals **134** and **135** was assigned for the resonances at δ 75.8 and 74.0 ppm, respectively, by Brimble et al (Table 7, Figure 19 and 20). In contrast to their assignments, the methine carbon C2 of spiroketals **206** and **207** showed the resonances at δ 73.7 and 75.8 ppm, respectively. Brimble et al. assigned the resonance for methyl carbon in ^{13}C NMR at δ 23 ppm for spiroketal **134** (*S, S, S*) and at δ 21.2 ppm for spiroketal **135** (*S, R, S*). In contrast to their assignments the targeted spiroketals **206** (*R, R, R*) and **93** (*R, S, R*) showed resonances for the methyl carbon in ^{13}C NMR at δ 21.2 ppm and 23 ppm respectively (Table 7, Figure 19 and 20). However these assignments were made by Brimble et al., on a 1:1 mixture of **134** and **135**. Hence they may not have been able to appropriately assign specific resonances to a particular spiroketal. It might be possible that the assignments made by Brimble et al. for the methyl carbon and the methine C2 carbon was incorrect. Requests were made for reported data and samples from Brimble, however, she reported that the data was no longer available. All the other ^1H and ^{13}C NMR resonances are in excellent agreement with the reported values by Brimble et al.

In summary, successful synthesis of spiroketals **206** and **207** completed the formal synthesis of the natural products CJ-12,954 and CJ-13,014. The spectral data of the spiroketals **206** and **207** are in good agreement with the spiroketals **134** and **135** (enantiomers of **206** and **207**) synthesized by Brimble et al. The stereochemistry at C7 carbon was controlled by zinc-

mediated tandem chain extension aldol reaction. Extensive studies by Aiken and Lai on zinc-mediated chain extension-aldol reaction of β -keto imides suggest that an *anti*-aldol isomer is formed, possibly through an open transition state. Hence, we believe that the stereochemistry at C7 is *R*, consistent with an *anti*-aldol isomer and facial selectivity imparted by the oxazolidinone. However, no X-ray crystallographic data was obtained to confirm the stereochemistry of the aldol reaction. Previous studies in Zercher group and excellent agreement of our spectral data with Brimble et al. can be used to support that the synthesized spiroketals **206** and **207** and enantiomers of spiroketals **134** and **135** synthesized by Brimble et al.



Carbon atom	¹³ C NMR Brimble et al. spiroketals 134 (<i>S, S, S</i>) and 135 (<i>S, R, S</i>)	Spiroketal 206 (<i>R, R, R</i>)	Spiroketal 207 (<i>R, S, R</i>)
quat., Si ^t BuPh ₂	19.2	19.2	19.3
Me	21.2 (135) and 23.0 (134)	21.3	22.9
CH ₃ , Si ^t BuPh ₂	26.9	26.9	26.9
CH ₂ , C11	29.0		29.1
CH ₂ , C11	29.3*	29.3	
CH ₂ , C8	30.2		30.1
CH ₂ , C8	30.8*	30.8	
CH ₂ , C3	32.0	31.8	
CH ₂ , C3	32.2*		32.1
CH ₂ , C10	33.7*	33.7	33.7
CH ₂ , C4	35.6	35.5	35.2
CH ₂ , C9	36.1		
CH ₂ , C9	36.5*	36.3	36.8
CH ₂ , C12	63.9	64.0	64.0
CH, C2	74.0 (135) and 75.8 (134)	73.7	75.8
CH, C7	77.9		77.9
CH, C7	79.7 (134)	79.7	
quat, C5	114.7 (135) and 114.3 (134)	114.4	114.6
CH, Si ^t BuPh ₂ , <i>m</i>	127.6	127.6	127.6
CH, Si ^t BuPh ₂ , <i>p</i>	129.5	129.5	129.6
quat., Si ^t BuPh ₂	134.1	134.1	134.1
CH, Si ^t BuPh ₂ , <i>o</i>	135.6	135.6	135.6

Table 7. ¹³C NMR assignment of spiroketals **206** and **207** compared to their enantiomers **134** and **135** reported by Brimble et al. (The symbol * is used to denote either the (*S, R, S*) or the (*S, S, S*) isomer)

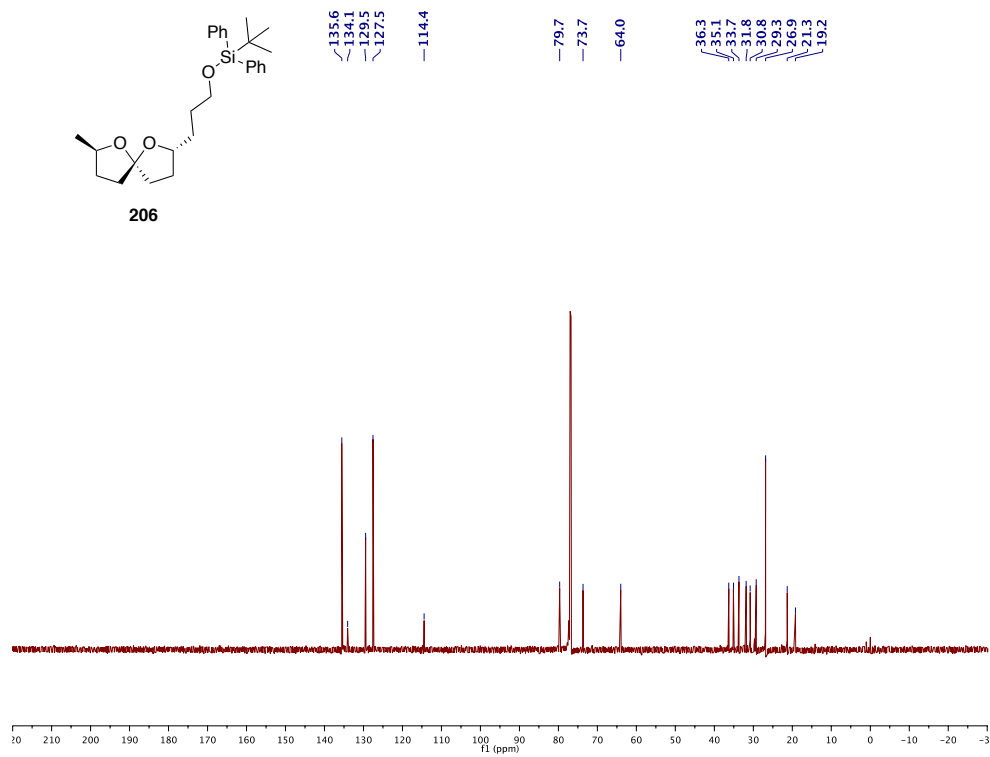


Figure 19. ^{13}C NMR spectrum of spiroketal **206**

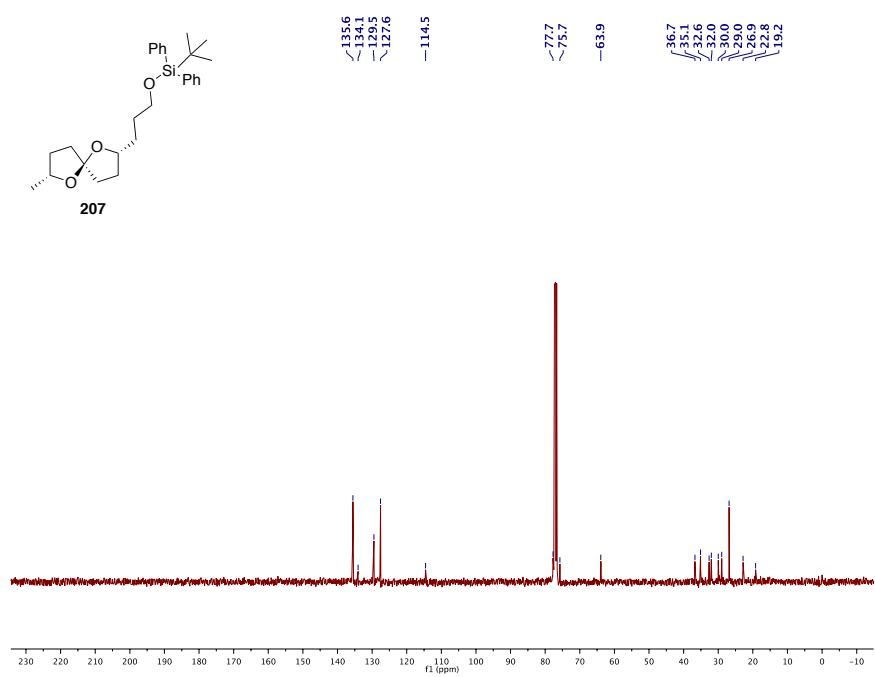


Figure 20. ¹³C NMR spectrum of spiroketal **207**

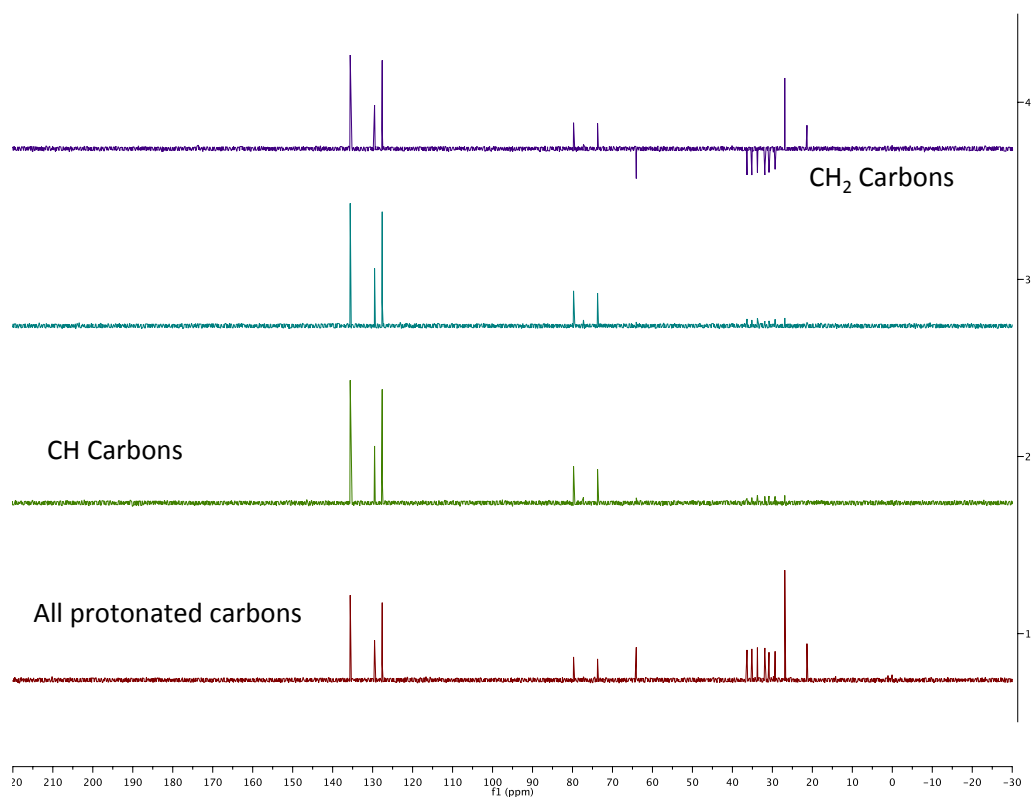


Figure 21. DEPT spectra a) DEPT-135 (CH₃, CH and CH₂ carbons) b) DEPT-90 (CH carbons) c) DEPT-45 (all protonated carbons) of spiroketal **206**

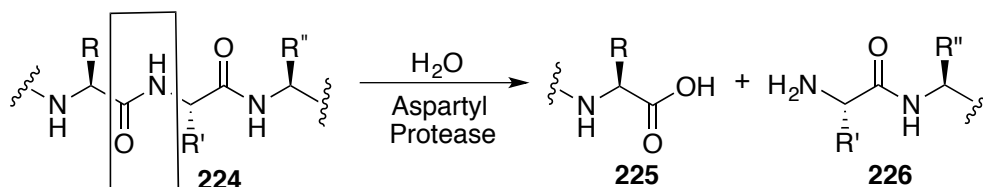
In summary, zinc-mediated tandem chain extension-aldol reaction methodology was successfully used for the formal synthesis of the spiroketals **206** and **207**. Spiroketals **206** and **207** are the enantiomers of spiroketals **134** and **135**, which are the key intermediates in the total synthesis of *ent*-CJ-12,954 (**141**) and *ent*-CJ-13,014 (**142**). The spiroketals **206** and **207** are characterized by ¹H, ¹³C and DEPT spectra. Since spiroketals **206** and **207** have the desired stereochemistry as the natural products CJ-12,954 (**126a**) and CJ-13,014 (**126b**), **206** and **207** can also be converted to the natural products (**126a**) and (**126b**) using the synthetic route followed by Brimble et al. Other spiroketal based natural products can also be targeted using this zinc-mediated tandem chain extension-aldol reaction methodology.

CHAPTER III

SYNTHESIS AND INVESTIGATION OF DIASTEREOSELECTIVITY OF HYDROXY-CYCLOPROPYL PEPTIDE ISOSTERES

Peptide isosteres were developed to increase the metabolic stability of oligopeptides and in some cases to reduce their conformational flexibility. Peptidomimetics are mimics of naturally occurring peptides that contain synthetically-derived peptide isosteres. In 1919 Langumir first described the term ‘isostere’, which refers to two molecules containing the same number of atoms and valence electrons.¹⁰⁴ Peptide isosteres are attractive tools for the analysis of enzyme and substrate interactions.¹⁰⁵ Proteases are a class of enzymes promoting the hydrolysis of peptide bonds.

Peptide isosteres have proven to be effective in the inhibition of a variety of proteases including HIV aspartyl protease.^{106, 107} HIV aspartyl proteases plays a vital role in the replication of HIV virus by site-specific cleavage of a polypeptide chain into peptide fragments (**Scheme 60**). Despite successful inhibition of the aspartyl proteases through peptide isosteres, the highly mutative nature of the HIV virus mandates continued development of novel peptide isosteres with increased efficiency to expand the therapeutic opportunities.¹⁰⁸ The protease targets often require the development of a wide array of peptide mimics.



Scheme 61. Aspartyl protease promoted peptide hydrolysis

A variety of functional groups like (*E*)-alkenes,¹⁰⁹ silanols¹¹⁰ and dihydroxy ethylene¹¹¹ have been used to mimic the peptide bond. Various factors such as functionality, bond angles, hybridization of the amide mimic, stereochemistry and hydrogen bonding capabilities influence the efficiency of the peptide isosteres. Efforts have been mainly directed towards replacing the amide bond with functionalities resistant to hydrolysis, while maintaining recognition for the active site.

The replacement of the amide nitrogen of a peptide bond with a methylene unit results in formation of a ketomethylene peptide isosteres **227**.^{112, 113} An advantage of the ketomethylene isostere is that the ketone adopts the tetrahedral geometry upon nucleophilic attack, yet this isostere is hydrolytically stable unlike an amide bond. While amide resonance results in restricted rotation and a strong conformational bias in an amide bond, ketomethylene peptide isosteres possess lower barrier rotation around the isosteric carbon-carbon bond, thereby lacking the rigidity needed for optimized binding to an active site. Another common peptide isostere extensively explored in protease inhibition is the hydroxyethylene isostere **228**.¹¹³⁻¹¹⁵ Hydroxyethylene isosteres have the advantages of hydrolytic stability and also hydrogen-bonding capability in the enzyme's active site; however, carbon-carbon bond rotation is facile and non-binding conformations are extensively populated.

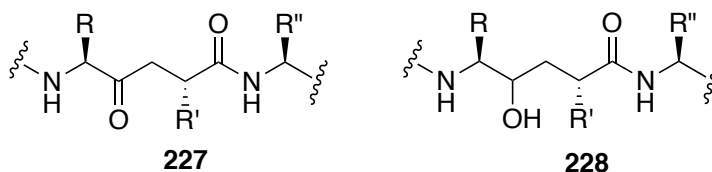
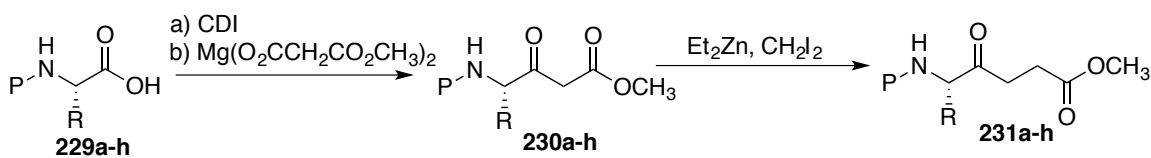


Figure 22. Ketomethylene and hydroxyethylene peptide isosteres

Zinc-mediated chain extension reaction for the preparation of peptide isosteres

Peptide isosteres are known to be effective for enzyme inhibition; however, synthesis of

these isosteres can be challenging. Lengthy synthetic routes and limited stereocontrol make the synthesis of many peptide isosteres difficult. The Zercher research group has developed an efficient approach to the synthesis of ketomethylene isosteres employing a zinc carbenoid-mediated chain extension reaction (**Table 8**).¹¹⁶ Various amino acids were converted to the corresponding ketomethylene isosteres. The C-terminus of the *N*-protected amino acid was converted to a β -keto ester using a mixed Claisen protocol. The derivatized amino acid was subjected to zinc carbenoid-mediated chain extension conditions to afford the corresponding γ -keto ester. This reaction showed high tolerance towards variety of amino acids. A single enantiomer of selected amino acids was subjected to this sequence of reactions. The substrates underwent little racemization during the formation of the β -keto ester and no racemization during chain extension conditions.

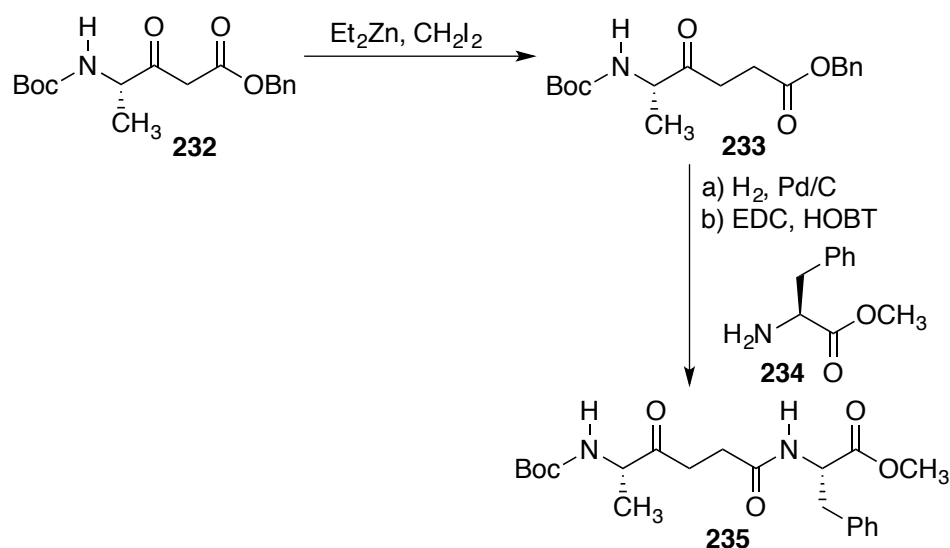


Entry	P	R	230 (%Yield)	231 (%Yield)
229a	Boc	H	91	25
229b	Boc	Me	70	48
229c	Cbz	H	65	60
229d	Cbz	Me	66	60
229e	Bz	H	65	58
229f	Bz	Me	47	58
229g	Fmoc	H	65	55
229h	Fmoc	Me	76	57

Table 8. Two-step synthesis of amino acid derived γ -keto methyl esters

The tripeptide mimic **235** was synthesized using the chain extension strategy to further demonstrate the scope of the reaction. No epimerization of the amino acid stereocenters in the final product was observed by NMR or chiral HPLC (**Scheme 61**).¹¹⁶ A stereocontrolled

approach for the formation of ketomethylene isosteres using zinc carbenoid-mediated chain extension reactions was also developed.¹¹⁷ Lin, a previous Zercher group member, reported the synthesis of a single diastereomer **235** using a zinc-mediated homologation reaction. A stereoselective synthesis of a functionalized dipeptide isostere employing zinc-carbenoid mediated chain extension reaction has been reported by Zercher group.¹¹⁸



Scheme 62. Synthesis of tripeptide **235**

Cyclopropane peptide isosteres

Although ketomethylene and hydroxyethylene peptide isosteres were found to have good affinity to bind HIV-1 protease inhibitors, decreased conformational rigidity by restriction of free rotation around carbon-carbon bond was suggested as a route to enhance binding. Research into the development of more rigid isosteric replacement to the amide bond led to the development of cyclopropyl peptide isosteres. Wipf and Xiao first prepared the cyclopropyl isosteres from alkenyl dipeptide isosteres.¹¹⁹ Martin and co-workers synthesized a C_2 -symmetrical α -tri-substituted cyclopropyl peptide isostere **236** for inhibition of aspartic protease of HIV-1 (**Figure 23**).¹⁰⁶ The bound conformation of peptide isosteres to HIV-1 protease was determined through

X-ray analysis. The cyclopropanes in these peptide isosteres were designed to maintain conformational integrity of the chain and be hydrolytically stable.

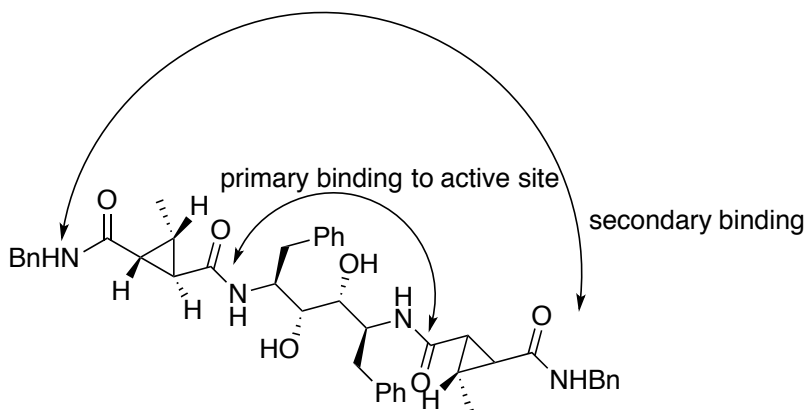


Figure 23. Peptidomimetic **236**

Novel cyclopropanol peptide isosteres

A novel cyclopropanol peptide isostere **237** has been designed by the Zercher group (**Figure 24**).²⁹ This novel peptide isostere containing the cyclopropanol moiety as a replacement for the amide linkage is envisioned to be non-hydrolyzable, conformationally-biased and capable of hydrogen-bonding. The individual carbons of this cyclopropanol peptide isostere are also capable of being functionalized stereoselectively, which offers the potential to design more efficient inhibitors for mutation-prone proteases. The cyclopropanol moiety is provided by adaptation of the zinc-mediated reaction sequence that results in the formation of bicyclic lactones, which upon opening releases a cyclopropanol. The use of amino acids as starting materials provides the environment for inclusion of the cyclopropanol as part of the proposed peptide isosteres. This strategy and reaction will be discussed in detail in this chapter.²⁹

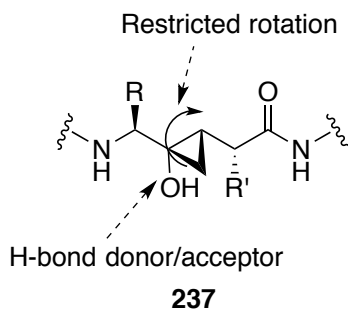


Figure 24. Novel cyclopropanol peptide isostere

Homologation-cyclopropanation reaction for the preparation of peptide isosteres

Both Lin and Pu, previous Zercher group members, observed the formation of a cyclopropanol **238** as a minor byproduct during the tandem homologation-aldol and tandem homologation-homoenolate formation reaction of β -keto imides, respectively (**Figure 25**).^{23, 28} The unique structure of this byproduct was envisioned as a potential synthetic building block. Taschner observed formation of a similar product and explored this transformation in more detail, which resulted in the identification of mechanistic insights and the preparation of an array of cyclopropanol products.²⁹

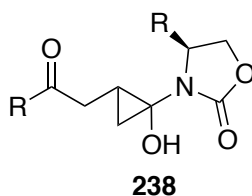
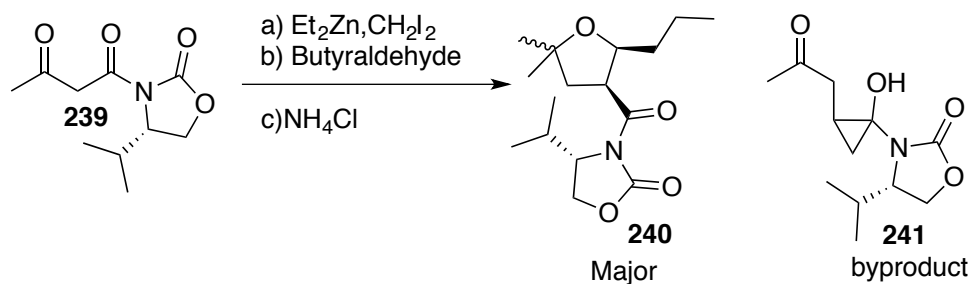


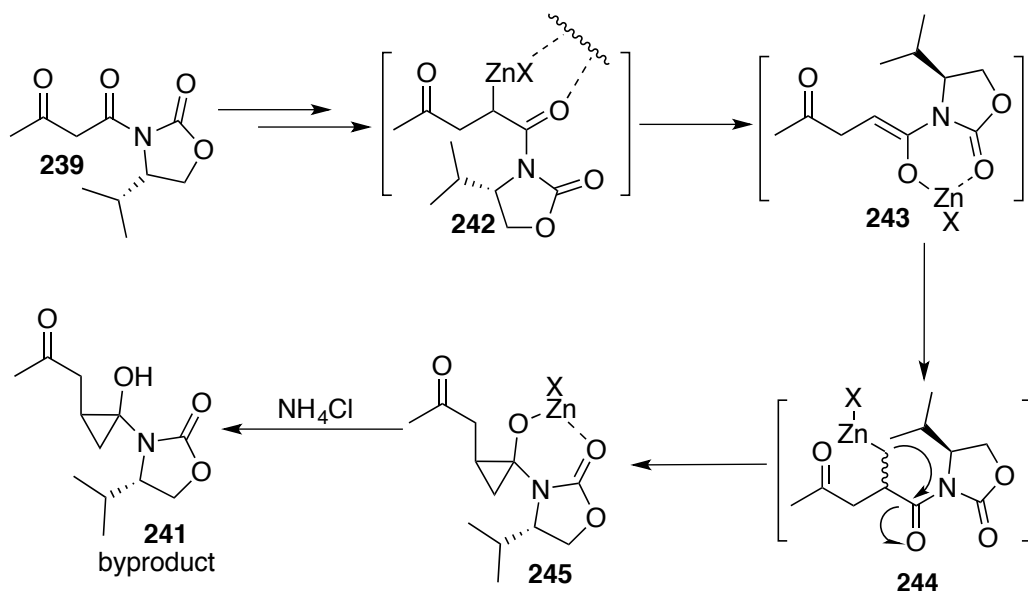
Figure 25. Unexpected cyclopropanol by-product

A homologation-aldol reaction of β -keto imide **238** was performed by Taschner during his efforts to synthesize the plakortether backbone. A cyclopropanol byproduct **241**, with undetermined stereochemistry, was isolated in small quantities (**Scheme 62**). The cyclopropanol byproduct **241** was proposed to result from the intramolecular cyclization of the homoenolate (**244**) produced by carbenoid capture of the chain extended intermediate (**Scheme 63**). The

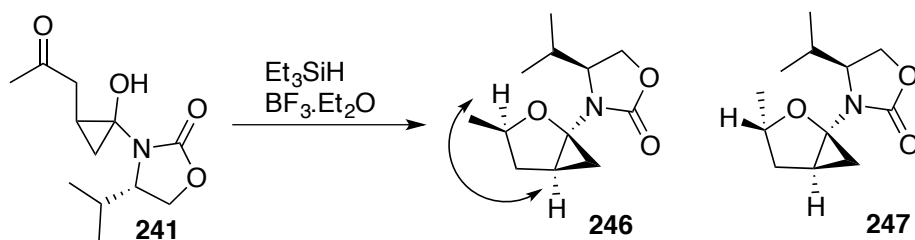
presence of the cyclopropanol byproduct was confirmed by the reduction of **241** using triethylsilane and boron trifluoride, which afforded two cyclopropylfuranyl diastereomers **246** and **247** (Scheme 64). The stereochemical assignment of the major isomer **246** was determined by an NOE experiment.²⁹



Scheme 63. Cyclopropanol byproduct formed during homologation-aldol reaction



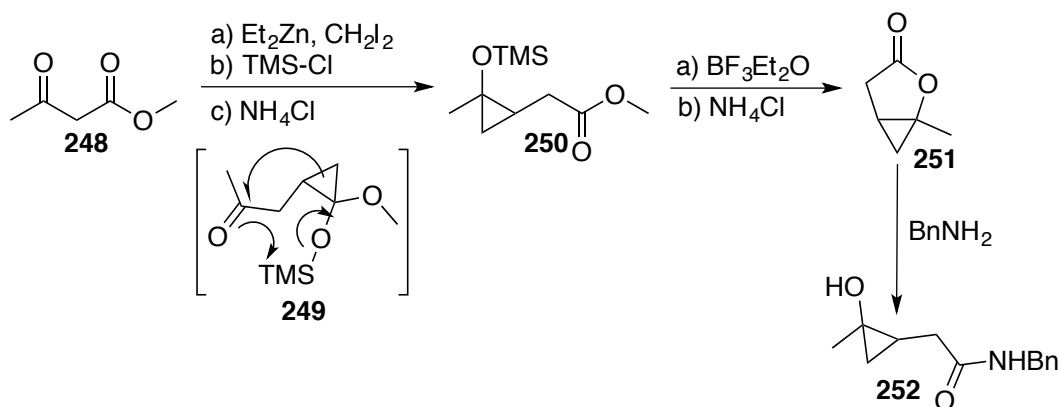
Scheme 64. Proposed mechanism for the formation of cyclopropanol **241**



Scheme 65. Silane reduction of cyclopropanol **241**

Various attempts by Taschner to increase the yield of cyclopropanol **241** resulted in the formation of minor quantities of **241** or no cyclopropanol product. Hilgenkamp reported that the use of TMS-Cl in the zinc-mediated chain extension enhanced formation of the homoenolate intermediate. The TMS-Cl was proposed to produce a more reactive zinc-bound enolate, which would react with excess zinc carbenoid to form the homoenolate.¹²⁰ Hence, Taschner attempted the homologation-cyclopropanation of β -keto ester **248** in the presence of stoichiometric TMS-Cl. The TMS-protected cyclopropanol **250** was generated in the reaction (**Scheme 65**). The relative stereochemistry of the TMS cyclopropanol **250** was not reported.

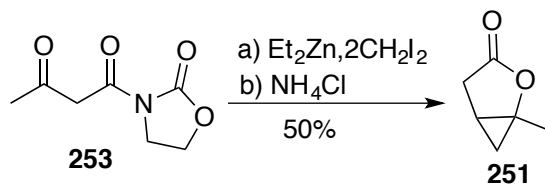
Cyclopropanol formation involving the keto moiety was opposite the result observed by Lin and Pu, for whom the cyclopropanol had been formed at the imide carbonyl. The unusual product reported by Taschner was proposed to result from rearrangement of silyl ether **249** during the TMS-promoted homologation-alkylation reaction (**Scheme 65**). Lewis acid-mediated cyclization of cyclopropylsilyl ether **250** produced bicyclic lactone **251**. Benzyl amine opening of the bicyclic lactone **251** to cyclopropanol **252**, which was the first compound to incorporate the cyclopropyl moiety as a potential isosteric replacement for the amide bond (**Scheme 65**). However, the low yield upon deprotection of silyl ether was a significant limitation to this method.



Scheme 66. First incorporated cyclopropanol isostere

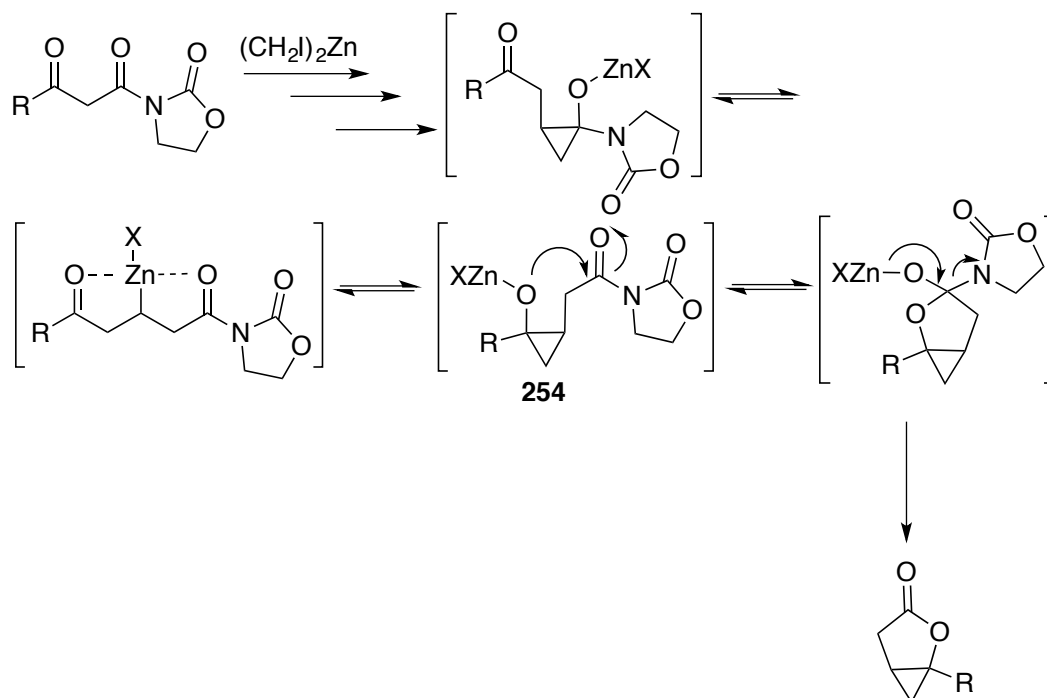
Tandem homologation-cyclopropanation-rearrangement-lactonization (HCRL)

Various studies were performed by Taschner in an effort to optimize the conditions for the preparation of the bicyclic lactone **251**. The ease of formation of zinc cyclopropanoxide in β -keto imides due to the electrophilicity of the imide carbonyl led to the use of β -keto imides in the place of β -keto esters for the preparation of bicyclic lactones. The lactonization reaction in the presence of TMS-Cl gave low yields, possibly due to the quenching of the carbenoid with any trace amounts of HCl present in the TMSCl . Taschner's study of the oxazolidinone starting materials resulted in complicated reaction mixtures and discovered that bis-carbenoid was better for lactone formation. Taschner identified that use of bis-carbenoid in place of the Furukawa carbenoid resulted in higher yield, presumably due to less by-product formation. Hence the optimized conditions for the homologation-lactonization reaction utilized five equivalents of the bis(iodomethyl)zinc carbenoid, and the yield of the bicyclic lactone was increased to 50% (**Scheme 66**).²⁹ The direct conversion of β -keto imide to bicyclic lactone was proposed to involve the rearrangement of the zinc cyclopropanoxide (**Scheme 67**).



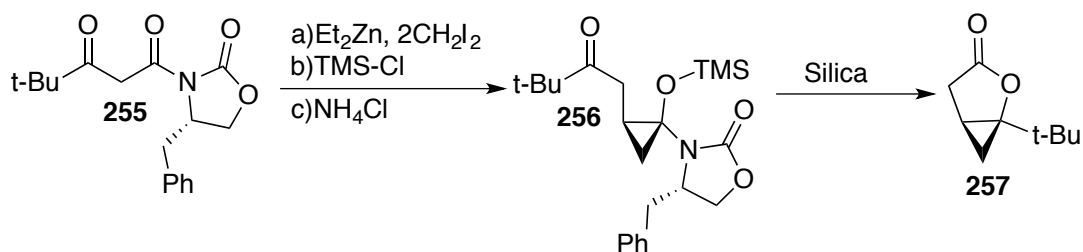
Scheme 67. Homologation-Lactonization of β -keto imide

The homologation-cyclopropanation reaction of β -diketones has been extensively studied in the Zercher research group and these studies were discussed in **Chapter 1**.^{32, 33} Equilibration of isomeric cyclopropoxide plays a role in product formation in the homologation-cyclopropanation reaction of β -diketones, and studies on these substrates provided mechanistic insights into the mechanism of homologation-lactonization reaction.³² The reaction mechanism that leads to bicyclic lactone formation is believed to be similar to the chain extension-cyclopropanation of β -diketones, but lactone formation requires both cyclopropoxide rearrangement and intramolecular acylation using the imide carbonyl (**Scheme 67**). Hence the cascade reaction that results in conversion of β -ketoimide to lactone has been termed the homologation-cyclopropanation-rearrangement-lactonization (HCRL) reaction.²⁹



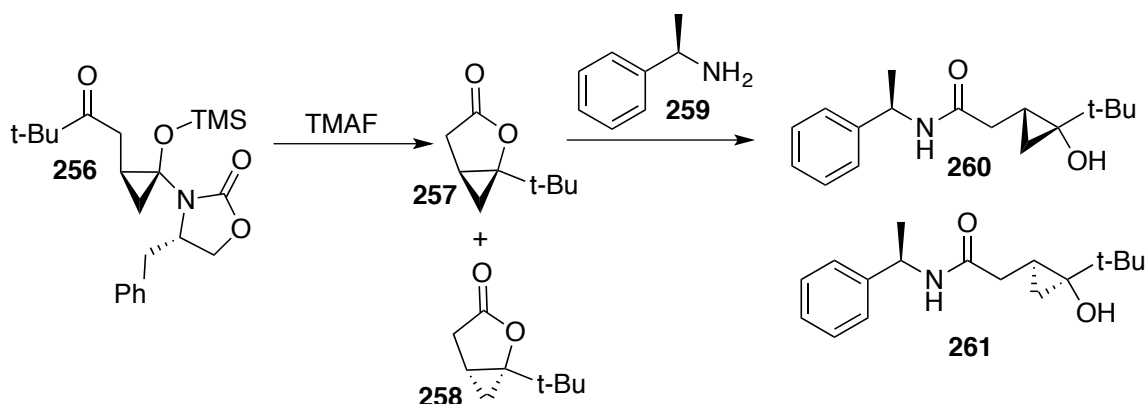
Scheme 68. Proposed mechanism of the HCRL reaction

The proposed cyclopropoxide rearrangement in the HCRL reaction was confirmed by trapping the initially formed cyclopropane intermediate with TMSCl . Taschner isolated the trapped silylcyclopropyl ether **256** as a single diastereomer and the stereochemistry was confirmed by X-ray crystal structure analysis (**Scheme 68**).²⁹ The silylcyclopropyl ether **256** was derived from enantiomerically pure β -keto imide **255** and the stereochemistry of the cyclopropane in **256** was controlled by the chiral auxiliary, in a fashion consistent with the enolate facial selectivity reported by Lin and Lai.^{23, 55}



Scheme 69. Rearrangement-cyclization of TMS ether to bicyclic lactone

The TMS-protected cyclopropanol **256** was treated with tetramethylammonium fluoride (TMAF) to afford the bicyclic lactones **257** and **258**. To determine the enantiomeric ratio of the bicyclic lactone resulting from diastereomer **256**, the lactones were opened with (*R*)-methyl benzyl amine. The diastereomeric ratio of the amide products was observed as 2.3:1. This result suggests that even though initial cyclopropanation was controlled by the chiral auxiliary, the stereochemistry of the bicyclic lactone was compromised by lack of stereocontrol in the cyclopropanation rearrangement (**Scheme 69**).

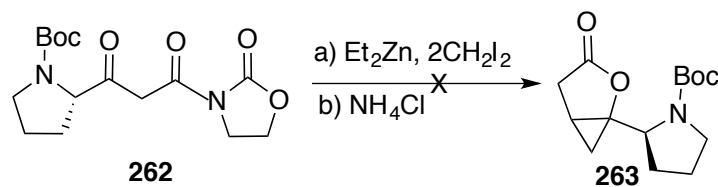


Scheme 70. TMAF induced desilylation-rearrangement-lactonization

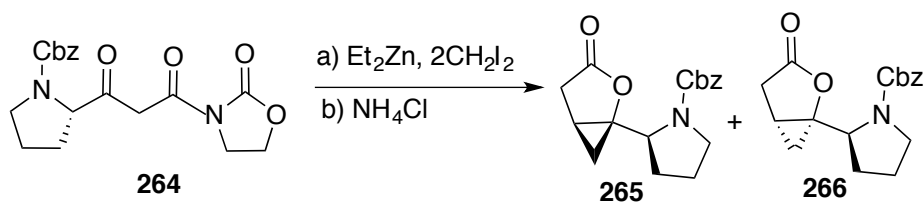
From the poor diastereomeric ratio of the cyclopropyl alcohol-containing amide, it was concluded that the chirality within the oxazolidone moiety provided insufficient stereocontrol. Hence Taschner used amino acid-derived β -keto imides for the HCRL reaction to study the role of the amino acid stereocenter in controlling the stereochemistry of the HCRL reaction. Taschner

incorporated an achiral oxazolidone into the β -keto imides. Taschner attempted different methods to synthesize the β -keto imide starting materials; however, the DCC-coupling route reported by Raillard and co-workers provided the best results.⁹¹

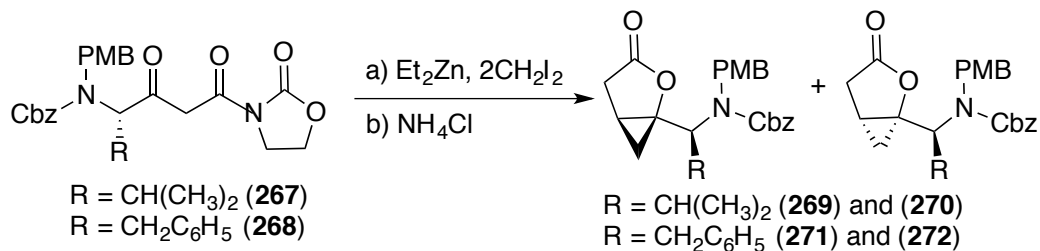
The first β -keto imide **262** synthesized using the DCC coupling method was derived from Boc-protected proline and an achiral oxazolidone. However, the HCRL reaction of **262** did not yield bicyclic lactone **263**, possibly due to the Boc-decomposition mediated by the Lewis acidic Zn(II) species present. The protecting group was changed from *t*-butyl carbamate (Boc) to benzyl carbamate (Cbz) **264**, and a mixture of bicyclic lactones **265** and **266** were generated (**Scheme 71**). The other β -keto imides studied were derived from valine **267** and phenylalanine **268**, which afforded the corresponding lactones from the HCRL reaction (**Scheme 72**).



Scheme 71. HCRL of β -keto imide **263**



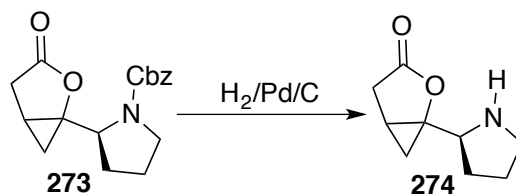
Scheme 72. HCRL of β -keto imide **264**



Scheme 73. HCRL of Valine and Phenylalanine derived β -keto imides

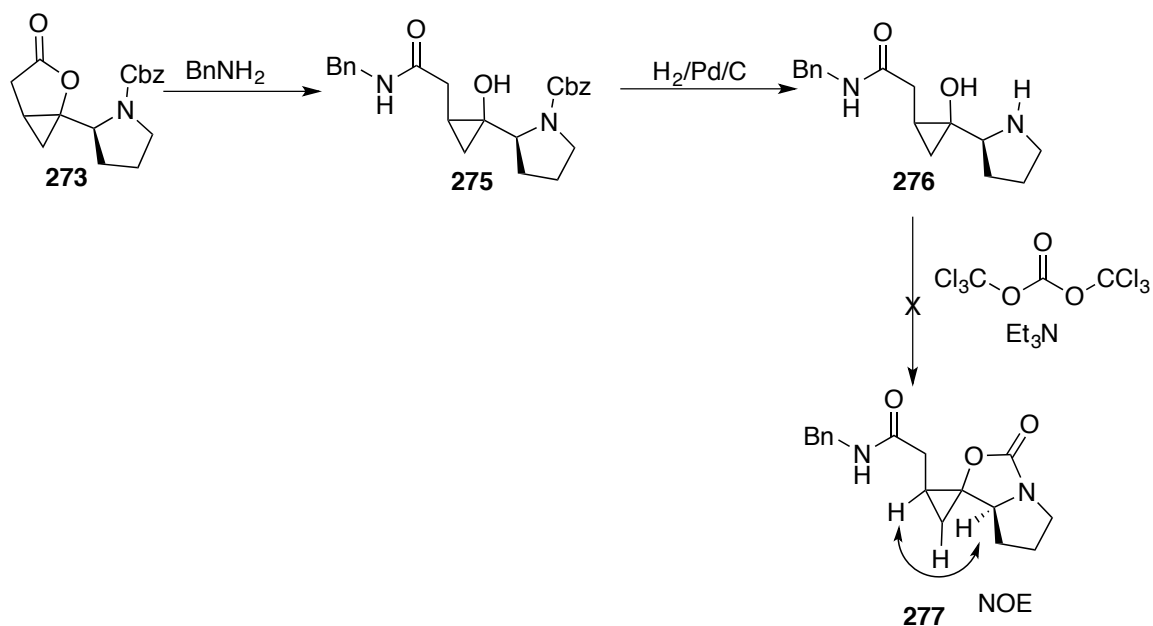
Taschner efforts for the stereochemical determination of major bicyclic lactone

In an effort to probe the diastereoselectivity of the reaction, Taschner attempted different strategies to identify the relative stereochemistry of the major diastereomer of the bicyclic lactone derived from the HCRL reaction of amino acid-derived β -keto imides. The first lactone to be studied was the Cbz-protected proline-derived lactone **273**. The major diastereomer of lactone **274** was subjected to a hydrogenolysis reaction to remove the benzyl carboxy protecting group. The deprotected lactone **274** was afforded as an oily solid (**Scheme 73**). Attempts to grow an X-ray quality crystal of lactone **274** were unsuccessful.



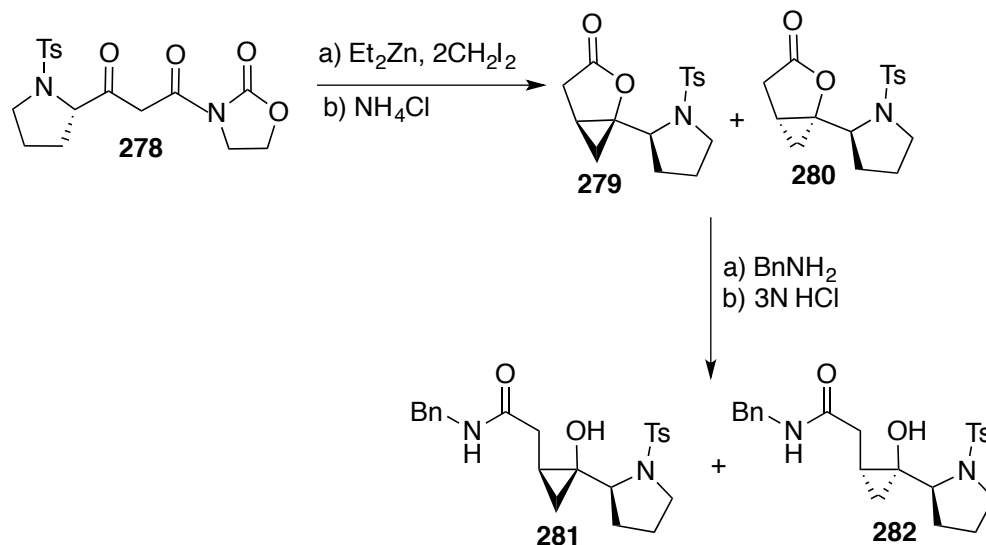
Scheme 74. Hydrogenolysis of bicyclic lactone **271**

The Cbz-protected proline-derived lactone **273** was also subjected to benzyl amine opening followed by hydrogenolysis to afford the cyclopropanol **274** (**Scheme 74**). Acylation and intramolecular cyclization of **276** using triphosgene was expected to afford the rigid tricyclic **277**, which would allow for NOE studies. However, cyclization using triphosgene was unsuccessful and resulted in the apparent decomposition of **276**.



Scheme 75. Attempt at rigid structure **277** for NOE studies

Due to the failure of the above attempted methods and the challenges imposed by carbamate rotamers, Taschner studied tosyl-protected proline-derived lactones **279** and **280**. The products were synthesized and subjected to benzyl amine opening (**Scheme 75**). Taschner attempted to grow an X-ray quality crystal of the minor diastereomer yielded from benzyl amine opening. Although this material was a solid, the effort was unsuccessful.



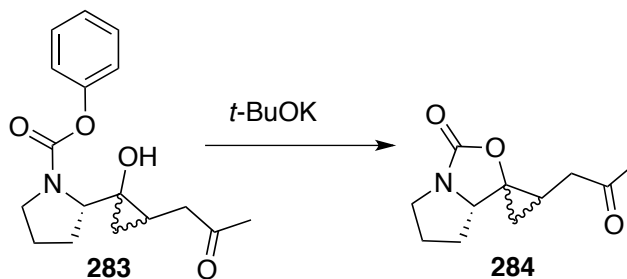
Scheme 76. Formation of bicyclic lactones followed by ring opening

Current work

Taschner's efforts to probe the stereochemistry of the major diastereomer of the bicyclic lactone resulting from the HCRL reaction were unsuccessful. However, the elucidation of the relative stereochemistry was believed to be crucial to potential application of the method. Hence the current work continued our efforts to probe the diastereoselectivity of the HCRL reaction and to confirm the stereochemistry of the major bicyclic lactone. Proline-derived substrates were employed for the current investigation. The study reported below focused on exploring the roles of the amino acid stereocenter, chiral auxiliary and the proline's protecting group in controlling the diastereoselectivity of the HCRL reaction.

Peter Moran, a previous graduate student in the Zercher group, in an attempt to understand the stereoselectivity of the homologation-cyclopropanation reaction of β -ketones, converted phenyl carbamate-protected proline cyclopropanol **283** to tricyclic species **284** by treatment with potassium *tert*-butoxide.³³ The rigidity of the tricyclic species **284**, facilitated NOE studies for the determination of cyclopropane stereochemistry (**Scheme 76**). Adaptation of

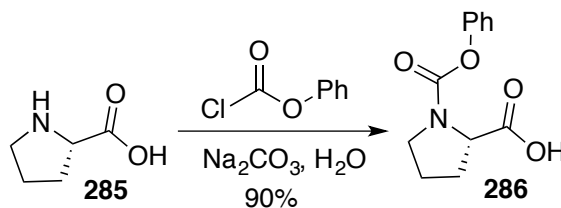
this strategy to study the stereochemistry of the major bicyclic lactone resulting from the HCRL reaction was proposed.



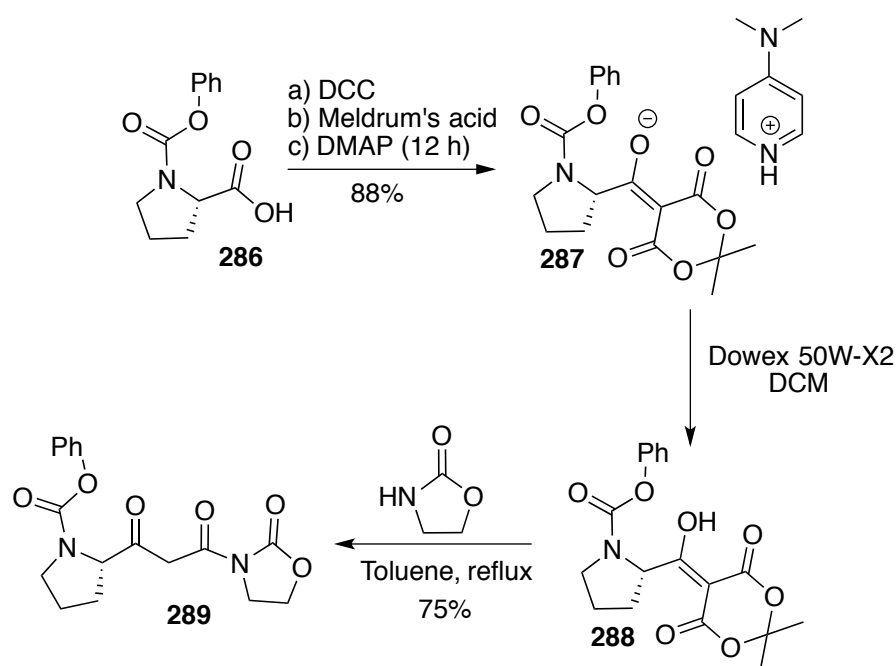
Scheme 77. Potassium *tert*-butoxide mediated cyclization of **60**

Synthesis of β -keto imide of phenyl carbamate protected proline

Preparation of β -keto imide **289** started with phenyl-carbamate protected proline (**Scheme 77**). While there are other methods available for the preparation of β -keto imides,^{45, 121} the mild DCC coupling method reported by Raillard and co-workers gave the best results.⁹¹ The route was initiated by reacting Meldrum's acid with **286** in the presence of DCC and DMAP. A conventional aqueous work-up of the Meldrum's acid adduct **287** results in decomposition of the product; however, the DMAP salt of the Meldrum's acid adduct **287** has high stability. The DMAP salt was treated with DOWEX 50W-X2, an acidic polymeric residue, to generate the free Meldrum's acid adduct, which was refluxed in toluene with the desired oxazolidinone to afford the corresponding β -keto imide. Following the above procedure β -keto imide **289** was synthesized in moderate yield. (**Scheme 78**).



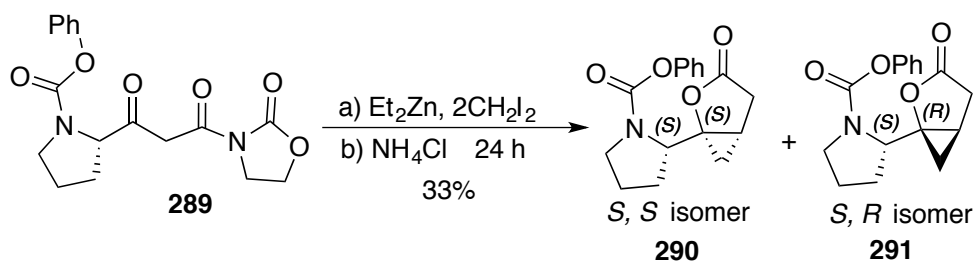
Scheme 78. Phenyl carbamate protection of proline



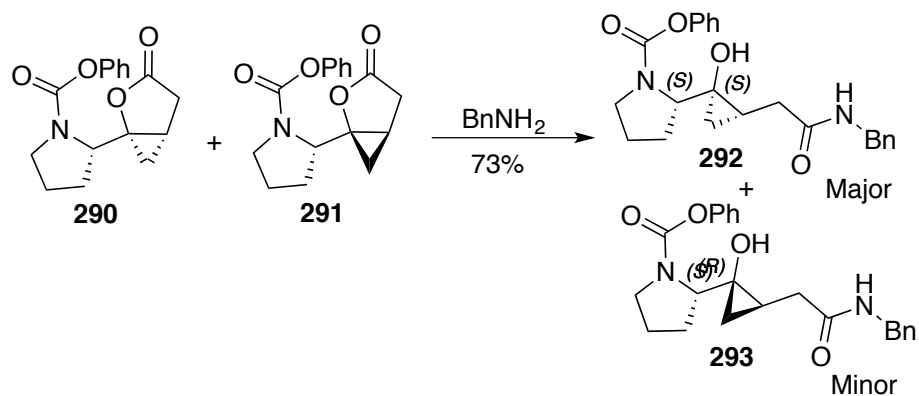
Scheme 79. DCC coupling route towards the synthesis of β -keto imide **289**

The β -keto imide **289** was subjected to the HCRL reaction using five equivalents of the bis(iodomethyl)zinc to afford the bicyclic lactones **290** (*S, S* isomer) and **291** (*S, R* isomer) (**Scheme 79**) in a diastereomeric ratio of 2.6:1 as determined by ^1H NMR, analysis of the crude reaction mixture. Mestrenova line fitting programme was used to establish the dr. The two diastereomers **290** and **291** co-eluted on flash column chromatography. Benzyl amine opening of the mixture of **290** and **291** resulted in the two cyclopropanols **292** and **293**, which were separated by preparative thin layer chromatography (**Scheme 80**). The major diastereomer of the benzyl amine opening was subjected to a pentane diffusion chamber and a single crystal was grown and analyzed by X-ray diffraction (**Figure 26**). The product was dissolved in ethyl acetate and stored in a diffusion chamber filled with *n*-pentane to grow an X-ray quality crystal. The major diastereomer as determined by X-ray crystallographic analysis was the cyclopropanol **292**

(*S, S* isomer). Benzyl amine opening of the bicyclic lactones **290** and **291** is a high yielding reaction; therefore, the major cyclopropanol **292** is assumed to be derived from the major bicyclic lactone **290**.



Scheme 80. HCRL reaction of β -keto imide **289**



Scheme 81. Benzyl amine opening of bicyclic lactones **290** and **291**

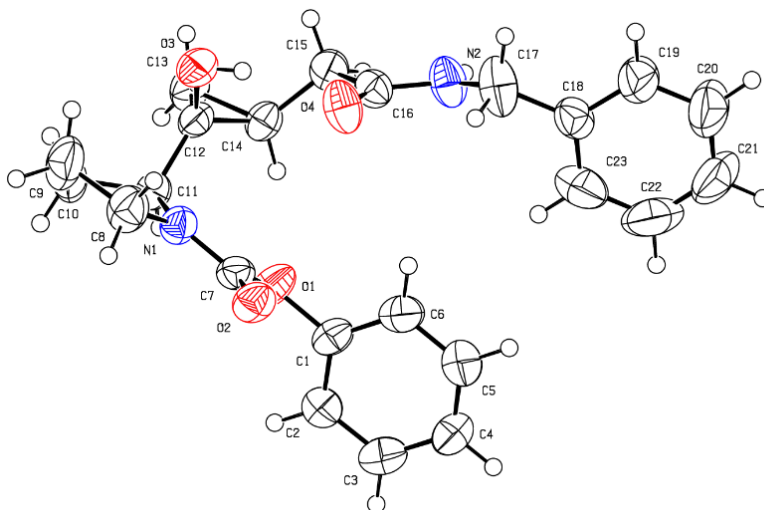
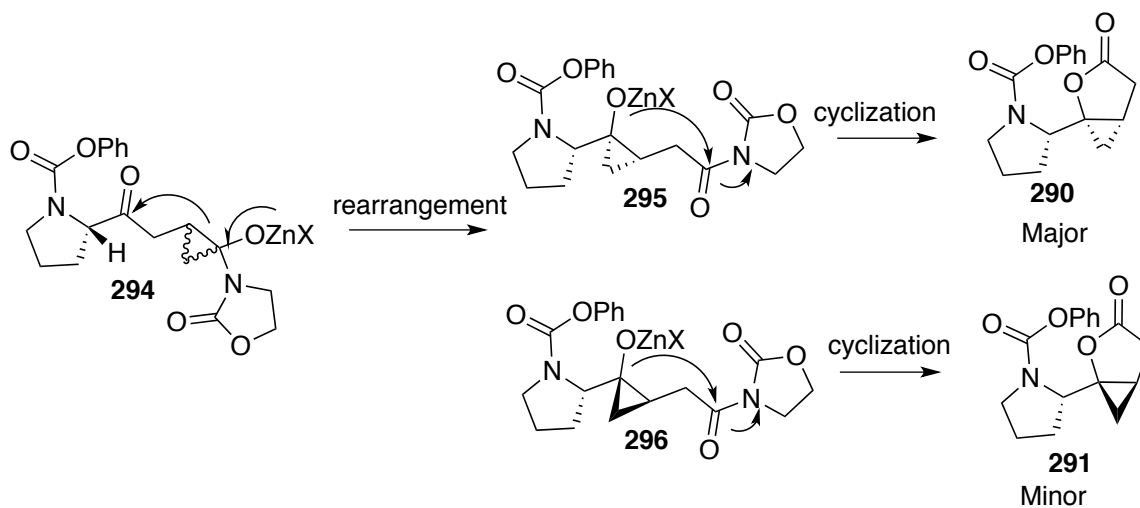


Figure 26. X-ray crystal structure depicting the absolute stereochemistry of cyclopropane of cyclopropanol **292**

Chelation Model vs Felkin-Anh Model



Scheme 82. Rearrangement of zinc cyclopropanoxide to bicyclic lactones

The crystal structure of the major bicyclic lactone **290** confirmed the absolute stereochemistry of the major bicyclic lactone of the HCRL reaction. Lactones are believed to result from the initial rearrangement of cyclopropanoxide **294** to the cyclopropanoxide **295** followed by intramolecular acylation involving the imide carbonyl. The initial

cyclopropanoxides (**294**) are expected to be formed in very similar amounts due to the achiral oxazolidinone. However, the stereochemistry of the cyclopropanoxide rearrangement product (**294**) determines the stereochemistry of the bicyclic lactones **290** and **291**, which are formed in different amounts. Hence, the stereochemistry of the cyclopropanol of the bicyclic lactone is determined in the rearrangement step. The stereochemistry of the major bicyclic lactone (*s,s*)-**290**, can be rationalized by a chelation model (**Figure 27**), in which chelation of the carbamate and the ketone serves to influence facial selectivity of the ketone in the rearrangement. The zinc cyclopropanoxide attacks the carbonyl from the least hindered face. As suggested in **Figure 27**, both of the cyclopropanols A or B rearrange to the major bicyclic lactone **290**. The Felkin-Anh model, assigns the protected nitrogen as the large group, predicts the formation of the other diastereomer **291** as the major bicyclic lactone (**Figure 28**).¹²²

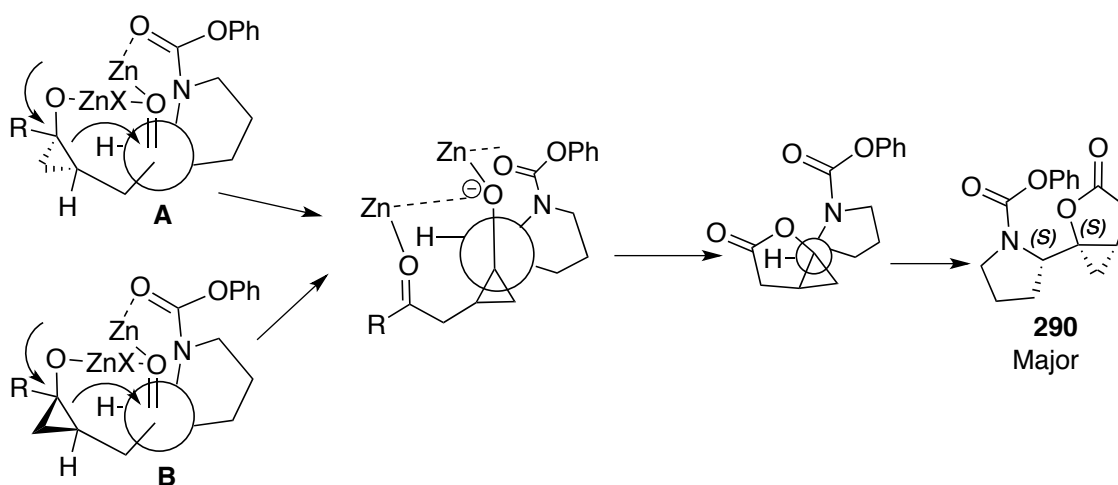


Figure 27. Chelation model predicting the stereochemistry of major bicyclic lactone

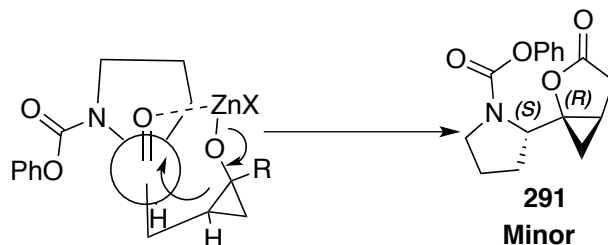
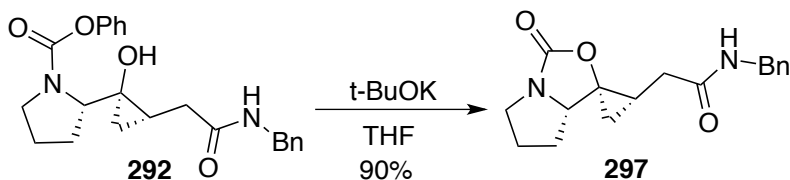


Figure 28. Felkin-Anh model would predict potential formation of the minor diastereomer

NOE studies to determine the stereochemistry of major bicyclic lactone

The major diastereomer **292** was subjected to cyclization to form the tricyclic compound **297** using potassium *tert*-butoxide (**Scheme 82**). The stereochemistry of the tricyclic compound **297** was then analyzed by NOE studies. All the protons of the tricyclic compound **297** are identified and characterized by gCOSY and gHSQC. Using the NOE experiment, the proline methane (**1, Figure 29**) was irradiated and the cyclopropane methine proton (**2, Figure 29**) was observed and vice-versa (**Figure 29** and **30**). The distance between protons 1 and 2 (**Figure 29**) is 2.596 Å (obtained from optimized structure on Spartan using Semi-empirical PM3 level of theory), which gives good opportunity for NOE observance (NOE observed for distances less than 3.5 Å). Both the NOE study and the crystal structure confirm that the major diastereomer of benzyl amine opening is **292**. The stereochemistry of the major diastereomer of the benzyl amine opening can be attributed to the major bicyclic lactone resulting from the HCRL reaction. The major diastereomer of the HCRL reaction is bicyclic lactone **290 (S, S isomer)** (**Scheme 79**).



Scheme 83. Potassium *tert*-butoxide mediated cyclization

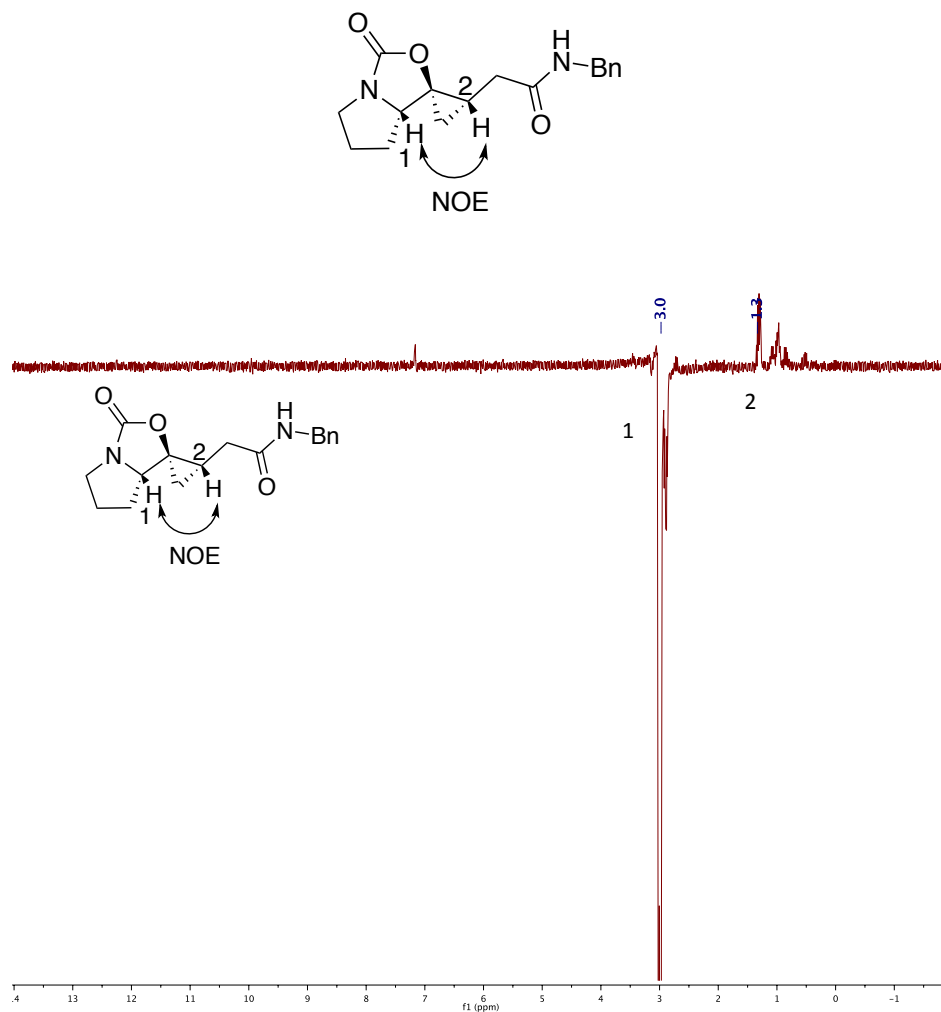


Figure 29. NOE of the tricyclic compound **297**
(proline methine **1** was irradiated and methine on cyclopropane **2** was observed)

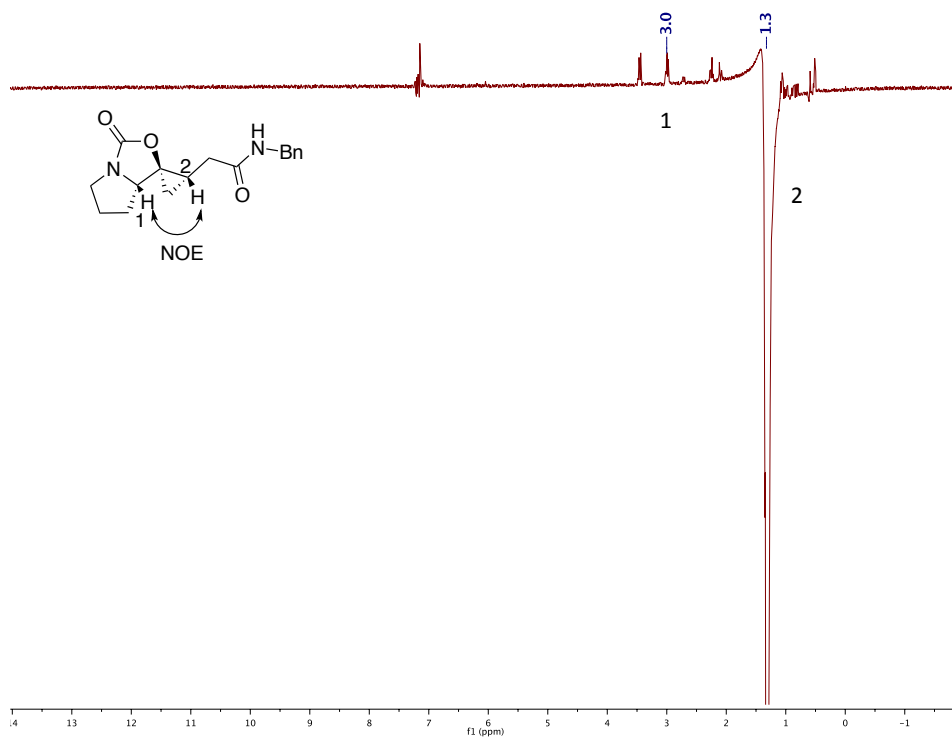
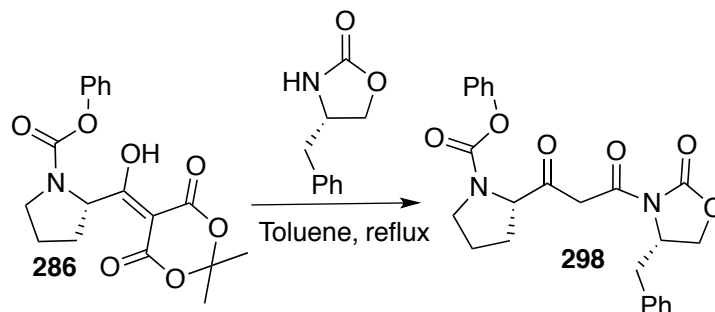
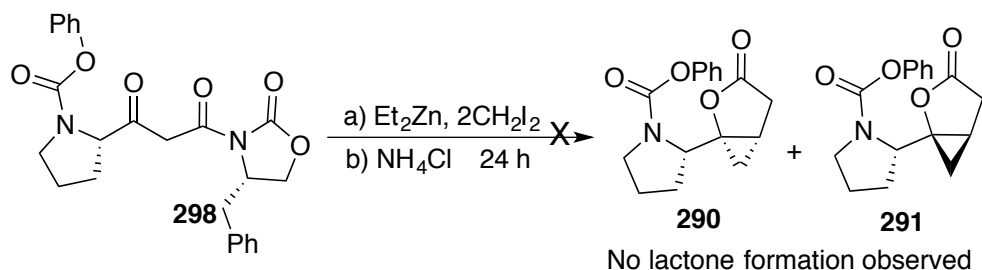


Figure 30. NOE of the tricyclic compound **297**
(methine on cyclopropane **2** was irradiated and observed proline methine proton **1**)

The bicyclic lactones **290** and **291** were obtained in a diastereomeric ratio of 2.6:1 from the β -keto imide **289** derived from the achiral oxazolidinone. A study to understand the influence of a chiral oxazolidinone on the diastereomeric ratio of the bicyclic lactones formed in the HCRL reaction was undertaken. Hence, β -keto imide **298** was synthesized by reacting the chiral oxazolidinone derived from L-phenylalanine with the Meldrum's acid adduct (**Scheme 83**). However, the HCRL reaction of the β -keto imide **298** resulted in a complex reaction mixture and the ^1H NMR of the crude reaction mixture did not show resonances of the bicyclic lactones (**Scheme 84**). The experiment was repeated; however, no formation of bicyclic lactones was observed.



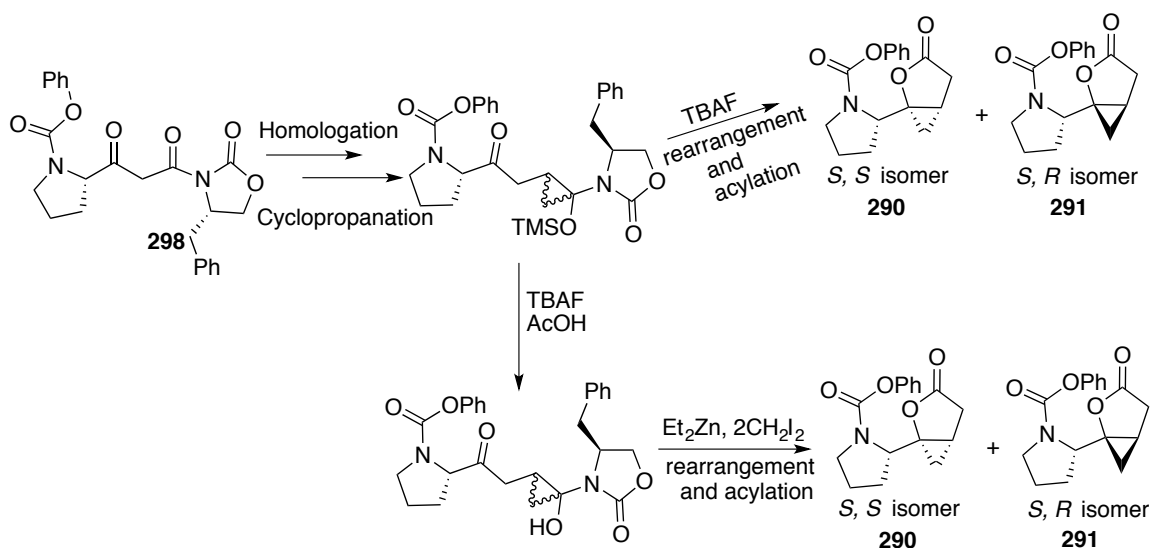
Scheme 84. Synthesis of β -keto imide **298**



Scheme 85. HCRL reaction of β -keto imide **298**

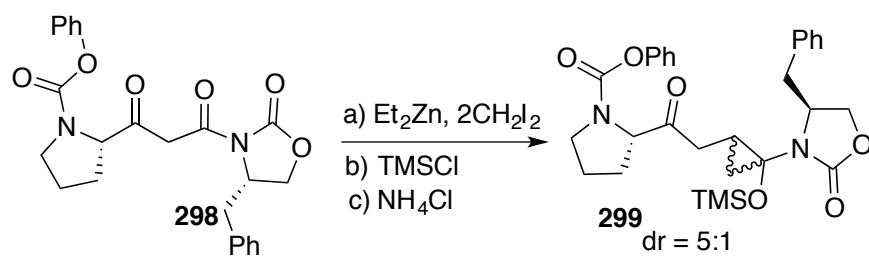
Synthesis of bicyclic lactone from TMS cyclopropanol

An alternative strategy was employed to trap the initial cyclopropanol, which would be further manipulated to encourage rearrangement to the bicyclic lactones (**Scheme 85**). Based on a report of Taschner, we believed that the cyclopropanol resulting from the initial homologation-cyclopropanation reaction could be trapped with TMSCl to afford the TMS ether (**Scheme 9**). Treatment with tetra-*n*-butylammonium fluoride (TBAF) would release the cyclopropanoxide and facilitate the rearrangement to afford the bicyclic lactones. Alternatively, as reported by Moran, the TMS ether could be deprotected with TBAF in the presence of acetic acid to afford the corresponding cyclopropanol, which upon exposure to carbenoid could afford the bicyclic lactones via rearrangement and acylation (**Scheme 85**). The ability to trap the initial cyclopropanol as a TMS ether and then facilitate rearrangement to afford the bicyclic lactones provides support for the proposed mechanism of the HCRL reaction.



Scheme 86. Synthesis of bicyclic lactones from the rearrangement of TMS ether

Application of homologation-cyclopropanation conditions to **298** in the presence of TMSCl afforded the TMS ether as a mixture of diastereomers in a ratio of 5:1 (**Scheme 86**). The stereochemistry of the major diastereomer was controlled by the chiral auxiliary and explained later in the chapter. The two diastereomers could not be separated by chromatography. Hence the mixture of the two diastereomers, obtained from the purification of crude reaction mixture by preparative thin layer chromatography, was analyzed by NMR variable temperature (VT) experiment to differentiate the two diastereomers from their rotameric forms due to the carbamate protecting group (**Figure 31**).



Scheme 87. Synthesis of TMS ether **299** from β -keto imide **298**

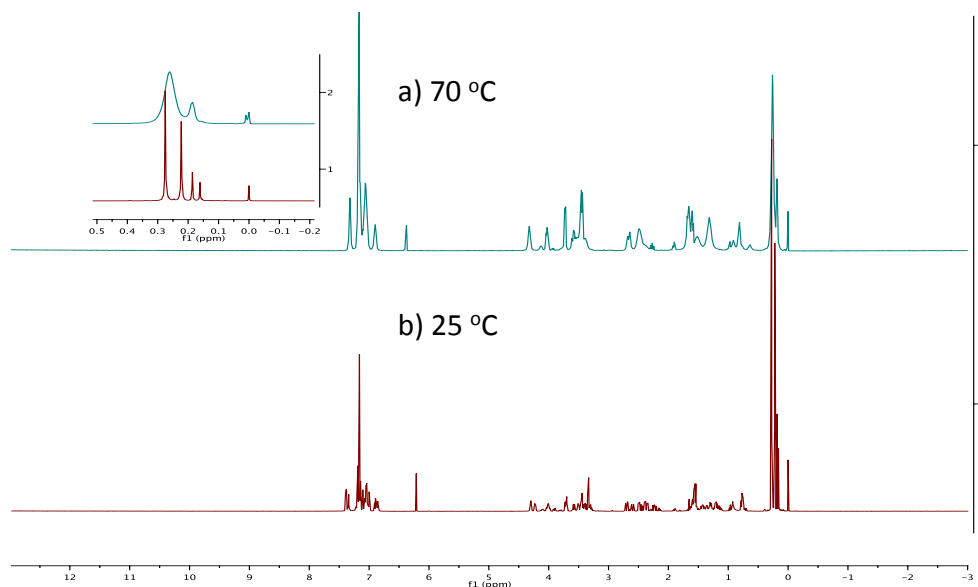


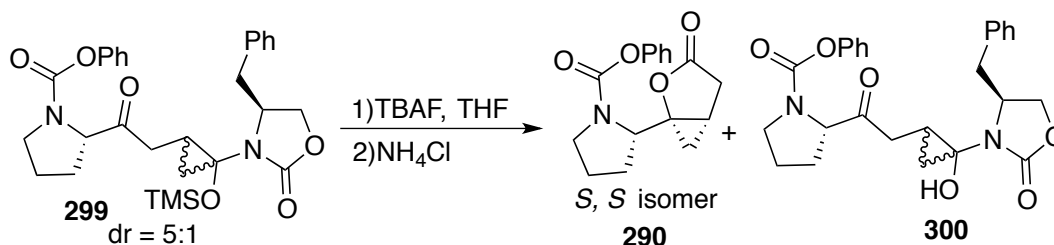
Figure 31. ¹H NMR of TMS cyclopropanol **299** at a) 70 °C b) 25 °C

VT Experiment of TMS cyclopropanol **299**

A variable temperature (VT) experiment was performed on the TMS-protected cyclopropanol **299** at 25 °C and 70 °C to distinguish the two diastereomers from their rotameric forms. In the ¹H NMR at 25 °C (**Figure 31b**), the protons of the trimethylsilyl group on the major diastereomer and its rotamer showed singlets at 0.27 and 0.22 ppm. Both the singlets coalesced as a broad singlet at 0.25 ppm at high temperature (**Figure 31a**). Similarly the minor diastereomer and its rotamer showed singlets at 0.18 and 0.16 ppm (**Figure 31b**). At 70 °C, both the singlets coalesced into a broad singlet at 0.17 ppm (**Figure 31a**). VT experiment provided good support to distinguish the major and minor diastereomers of the TMS cyclopropanol **299**.

On the basis of ^1H NMR analysis, the diastereomeric ratio was determined to be 5:1.

The TMS cyclopropanol **299** was then subjected to TBAF in anhydrous conditions to facilitate the rearrangement to bicyclic lactones. If the stereochemistry of the cyclopropanol **299** exerts an influence on the facial selectivity in the addition to the ketone, the diastereomeric ratio of the bicyclic lactones was expected to be 5:1. In contrast to the expected results, TBAF-mediated rearrangement of TMS cyclopropanol afforded only the bicyclic lactone **290** (*S, S* isomer) and minor amounts of cyclopropanol **300** (Scheme 87). Since no chelation is possible in a TBAF mediated reaction, unlike the carbenoid mediated HCRL reaction, direct comparison to the diastereoselectivity of the HCRL reaction is not possible.

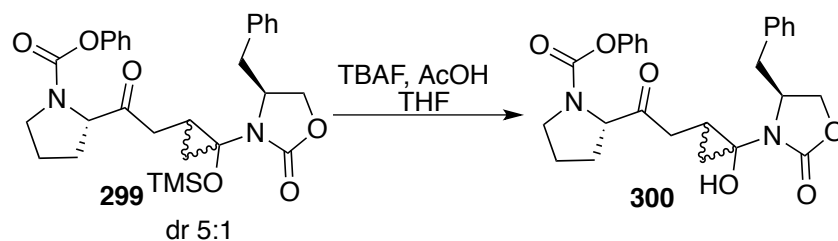


Scheme 88. TBAF rearrangement of TMS cyclopropanol **299**

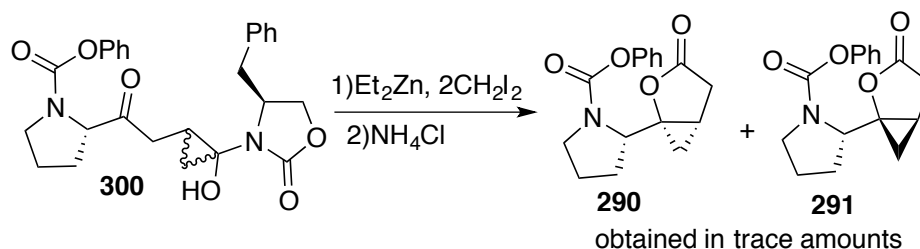
The mixture of TMS cyclopropanol (**299**) was deprotected using TBAF and acetic acid to provide **300** (Scheme 88). The diastereomeric mixture of TMS cyclopropanols could not be separated by chromatography. The mixture of two diastereomers of cyclopropanol was subjected to carbenoid to facilitate the rearrangement (Scheme 89). The cyclopropanols, when subjected to carbenoid, gave a complex reaction mixture similar to the HCRL reaction of the β -keto imide **298**. Trace amounts of bicyclic lactones **290** and **291** co-eluting with an unknown compound was observed. This study confirms that cyclopropanoxide rearrangement-lactonization sequence is inefficient when using chiral oxazolidinone starting material.

Homologation-cyclopropanation of the β -keto imide derived from chiral oxazolidinone in the presence of TMSCl, followed by TBAF initiated rearrangement is a more efficient route for formation of bicyclic lactone.

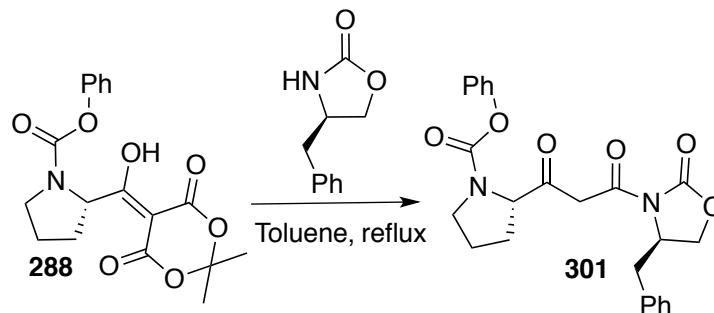
Since the TBAF rearrangement of the TMS ethers **299** yielded only bicyclic lactone **290**, our next attempts focused on the synthesis and reaction of β -keto imide **301**, which incorporated the chiral oxazolidinone produced from D-phenylalanine (**Scheme 90**). Compound **301** was generated by the Meldrum's acid route as described earlier for the synthesis of **298**.



Scheme 89. Deprotection of TMS cyclopropanol **299** to cyclopropanol **300**

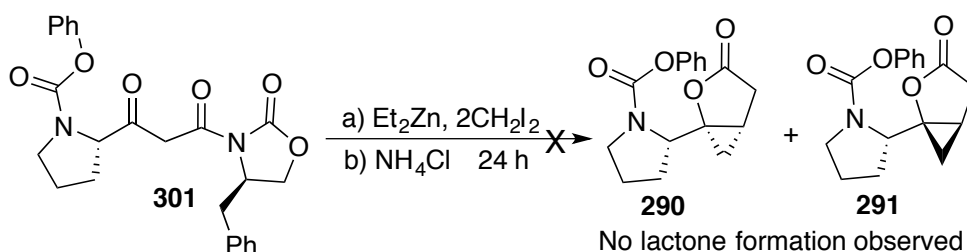


Scheme 90. Carbenoid facilitated rearrangement of cyclopropanol **300**



Scheme 91. Synthesis of β -keto imide **301**

The β -keto imide **301** was subjected to standard HCRL reaction conditions which utilized bis(iodomethyl)zinc(Scheme 91). The reaction was attempted using different numbers of equivalents of carbenoid to probe the feasibility of the reaction; However, β -keto imide **301**, which contains the chiral oxazolidinone, gave a complex reaction mixture with each variation of the HCRL reaction. Therefore, the β -keto imide **301** was subjected to homologation-cyclopropanation conditions in the presence of TMSCl to produce the TMS ether **302** (Scheme 92).



Scheme 92. HCRL reaction of β -keto imide **301**



Scheme 93. Synthesis of TMS cyclopropanol **302**

A VT ^1H NMR experiment was again performed on TMS ether **302** at 25 $^\circ\text{C}$, 55 $^\circ\text{C}$ and 70 $^\circ\text{C}$ to differentiate the diastereomers from their rotameric forms (Figure 32). Overlapping resonances of the protons on the trimethylsilyl group of both the diastereomers made it challenging to accurately determine the diastereomeric ratio. Hence a MestReNova line fit simulation program was applied to determine the diastereomeric ratio. The protons on the

trimethyl group of the major and minor diastereomers at 0.25 and 0.19 ppm (70 °C) respectively were used to establish the diastereomeric ratio. A line fit was applied to each singlet of the two diastereomers, which established the area under the curve. The diastereomeric ratio of the TMS cyclopropanols **302** was 7:1 (**Figure 33**). Based on the facial selectivity in similar system observed by Lai and Taschner, the major diastereomer was assigned as **314**.

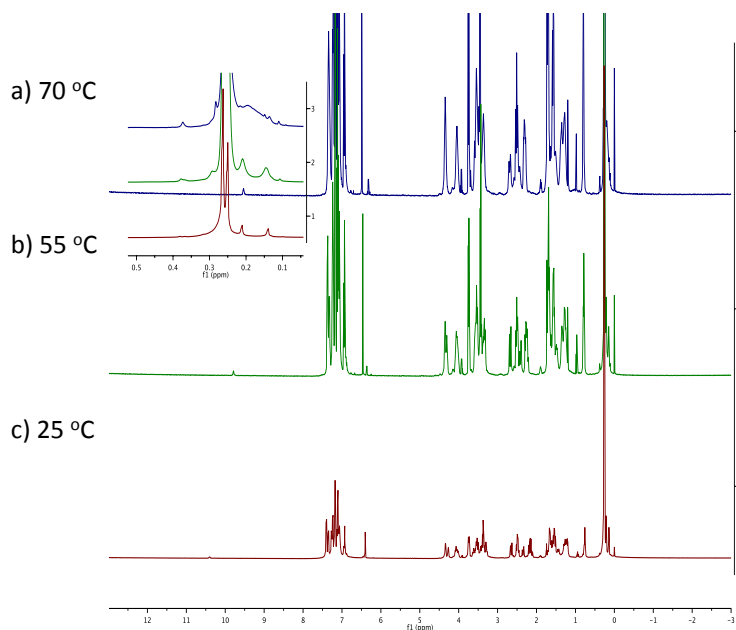


Figure 32. VT ¹H NMR (500 MHz) experiment of TMS cyclopropanol **302** a) 70 °C b) 55 °C c) 25 °C

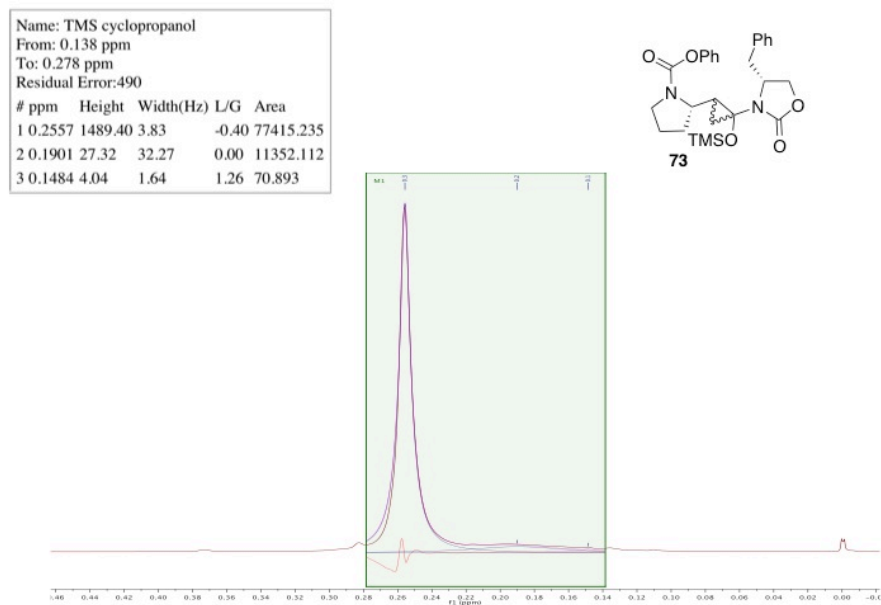
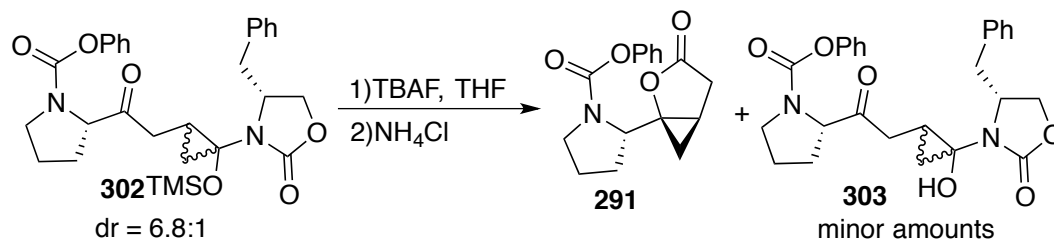


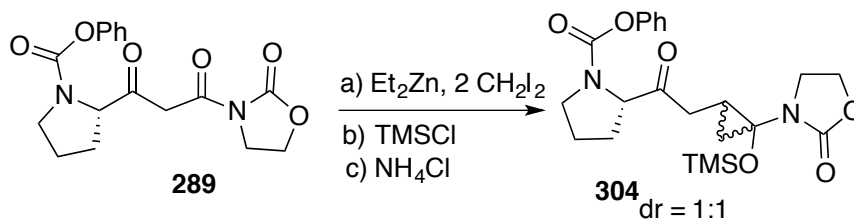
Figure 33. Determination of diastereomeric ratio of TMS cyclopropanol **302** using MestReNova line fitting

The mixture of diastereomers of TMS ether **302** was treated with TBAF under anhydrous conditions to facilitate the rearrangement. Bicyclic lactone **291** (*S, R isomer*) and minor amounts of cyclopropanol **303** were produced from the TBAF-mediated rearrangement of TMS ether **302** (Scheme 93).

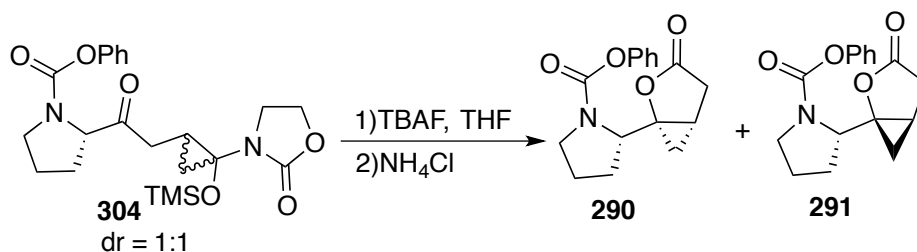
Similar to the β -keto imides derived from chiral oxazolidinone, β -keto imide derived from achiral oxazolidinone **289** was also treated with TMSCl in the presence of homologation-cyclopropanation conditions to yield the TMS cyclopropanol **304** (Scheme 94). As expected the TMS cyclopropanol **304** was obtained in a diastereomeric ratio of 1:1 due to the lack of stereocontrol from achiral oxazolidinone. Tetra-*n*-butylammonium fluoride (TBAF)-mediated rearrangement of TMS cyclopropanol **304** yielded both diastereomers of bicyclic lactones **290** and **291** (Scheme 94).



Scheme 94. TBAF rearrangement of TMS cyclopropanol **302**



Scheme 95. Synthesis of TMS ether **304** from β -keto imide **289**

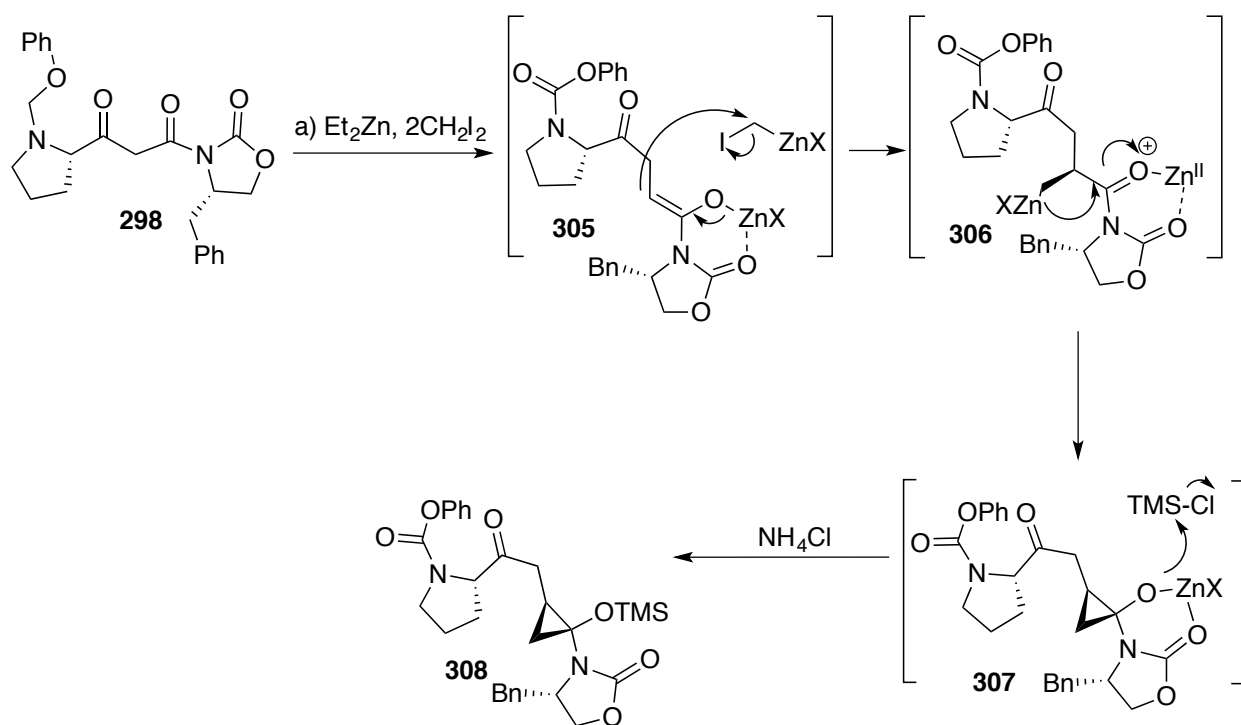


Scheme 96. TBAF rearrangement of β -keto imide to bicyclic lactones

Effect of Evans auxiliary on the diastereoselectivity of formation of bicyclic lactones **290** and **291**

Rearrangement of cyclopropane is believed to play an important role in the HCRL reaction, influencing the diastereoselectivity of the reaction. The chiral oxazolidinone employed in the β -keto imide is expected to influence the enolate facial selectivity in the formation of the homoenolate and cyclization into the ketone. Hence trapping of the initial cyclopropoxide with TMSCl, followed by TBAF mediated rearrangement and acylation to provide the bicyclic lactone, provided some insight into the diastereoselectivity of the HCRL reaction.

The starting chiral β -keto imide **298** was subjected to homologation using bis(iodomethyl)zinc. Based on the previous studies by Lai and Lin, the *Z*-enolate of the imide **305** would be predicted to be formed due to the 1,3-allylic strain of the *E*-enolate. The formation of homoenolate **306** would be directed by the chirality of the imide functionality. Based on the enolate facial selectivity reported by Lin and Lai, the alkylation of the *Z*-enolate with the carbenoid occurs on the opposite face compared to the substituent of the imide functionality resulting in the formation **307** (**Scheme 96**). The cyclopropoxide **307** then *O*-silylates with TMSCl to yield the TMS-protected cyclopropanol **308**. However, there is crystallographic evidence to confirm the absolute stereochemistry of TMS cyclopropanol **308**. The proposed structure of **308** is consistent with the facial selectivity reported by Taschner, who provided X-ray crystallographic analysis data of TMS cyclopropanol **256** (**Figure 68**), in support of his assignment.



Scheme 97. Proposed diastereoselective mechanism for the formation of **308**

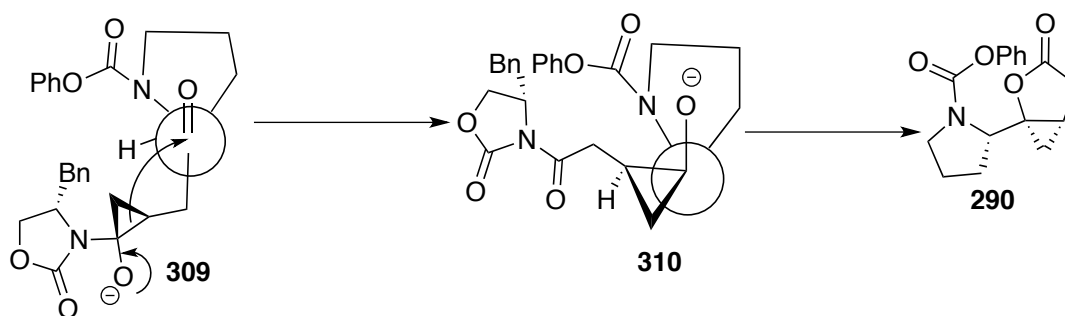
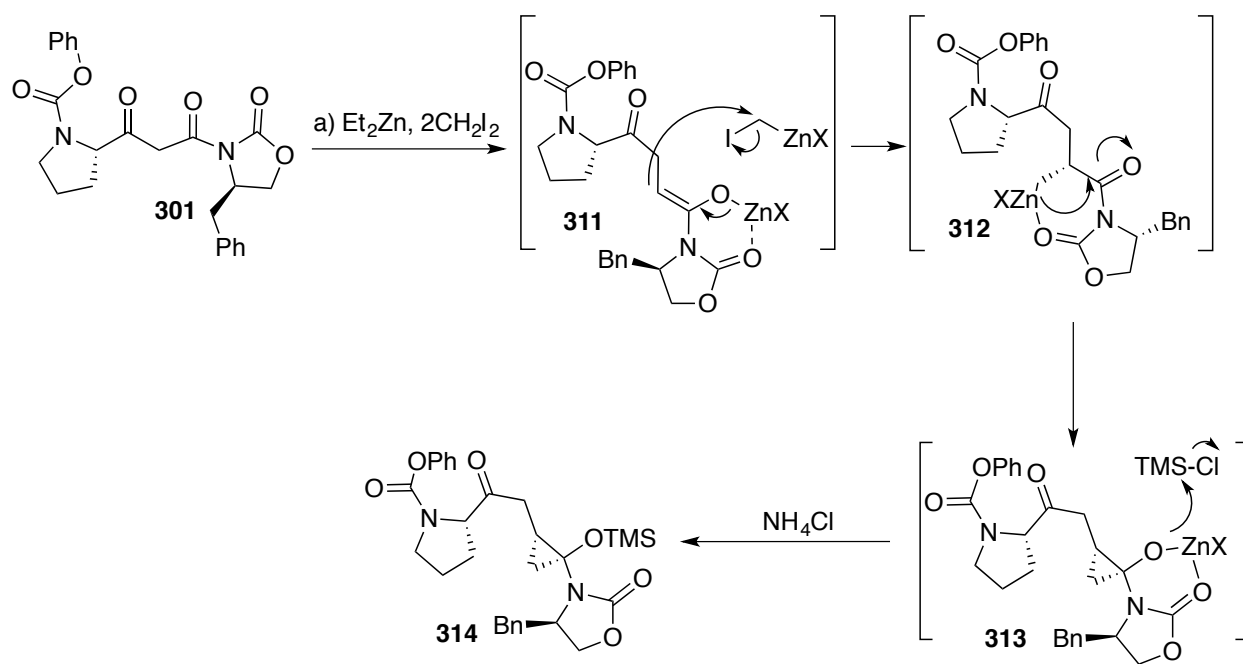


Figure 34. Model of TBAF mediated rearrangement of TMS protected cyclopropanol

Tetra-*n*-butylammonium fluoride (TBAF) mediated rearrangement followed by acylation of the diastereomeric mixture of **308** yielded only the bicyclic lactone **290**. The model as depicted in **Figure 34** is presented to account for this selectivity. The chiral auxiliary plays role in the initial facial selectivity of the enolate to form the TMS cyclopropanol and the established stereocenters of the cyclopropanol directs the diastereoselectivity of the rearrangement. From the

model it was observed that both the established stereocenters from initial cyclopropanation and also the bulky phenyl carbamate-protecting group on the proline residue determines the diastereoselectivity of the cyclopropanoxide rearrangement. Similarly diastereoselectivity for the formation of the major diastereomer of TMS cyclopropanol from β -keto imide **301** and subsequent TBAF-mediated rearrangement of TMS cyclopropanol **302** followed by acylation to bicyclic lactone **291** was depicted in **Scheme 97** and **Figure 35**.



Scheme 98. Proposed diastereoselective mechanism for the formation of **314**

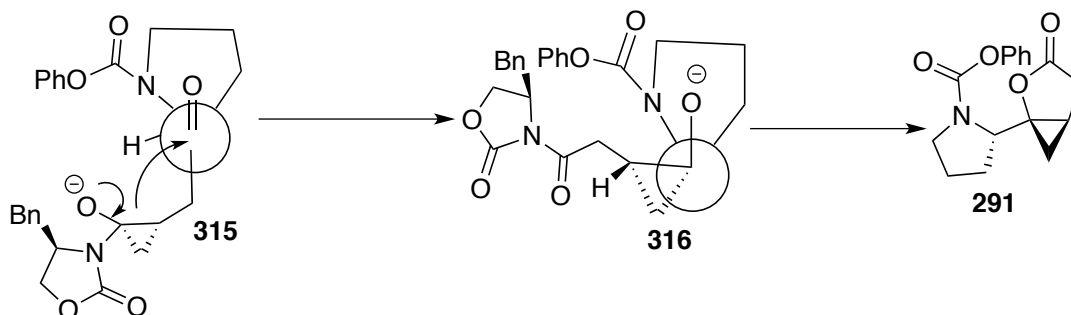
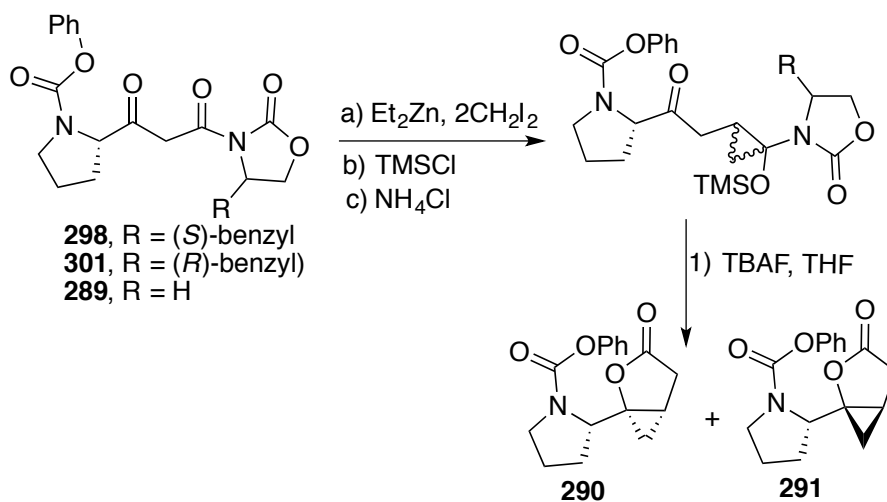


Figure 35. Model of TBAF mediated rearrangement of TMS protected cyclopropanol

Summary of TBAF mediated rearrangement of TMS cyclopropanols

The TMS cyclopropanol **299** was prepared in a 5:1 dr from β -keto imide **298**, which incorporated the oxazolidinone produced from L-phenylalanine. Rearrangement was initiated by TBAF and yielded the bicyclic lactone (*S,S* isomer) **290**. The TMS cyclopropanol **302** was prepared in a 7:1 dr from β -keto imide **301**, which incorporated the oxazolidinone produced from D-phenylalanine. Rearrangement initiated by treatment with TBAF yielded the bicyclic lactone (*S,R* isomer) **291** (**Table 9**). The TMS cyclopropanol **304** derived from achiral oxazolidinone was obtained in a diastereomeric ratio of 1:1 and afforded both diastereomers of bicyclic lactones **290** and **291** on TBAF rearrangement (**Table 9**). These reactions provide good evidence to confirm the role of chiral auxiliary in controlling the diastereoselectivity of the cyclopropanoxide rearrangement.

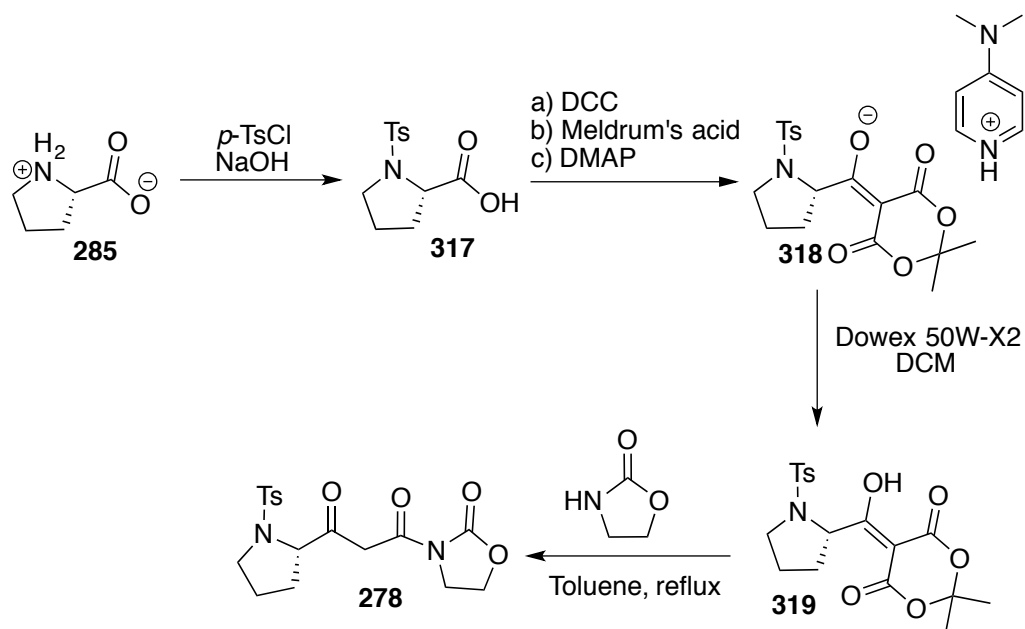


R (β - keto imide)	TMS cyclopropanol (dr)	Bicyclic lactones
298	299 5:1	290
301	302 7:1	291
289	304 1:1	290 and 291

Table 9. Summary of TBAF mediated rearrangement of TMS cyclopropanol

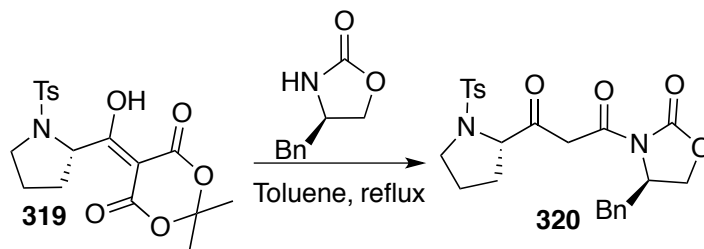
Tosyl Protected Proline derived β -keto imides

Studies were focused on the role of proline's protecting group in controlling the diastereoselectivity of the HCRL reaction. Sulfonamide protection of L-proline was achieved by treatment of L-proline with *p*-toluenesulfonyl chloride in aqueous sodium hydroxide (**Scheme 98**). Tosyl-protected proline (**317**) was subjected to DCC coupling reaction to form an acylated Meldrum's acid adduct as the DMAP salt (**318**).²⁹ The DMAP salt of the Meldrum's acid adduct was treated with DOWEX 50W-X2, to generate the free Meldrum's acid adduct **319**, which was refluxed in toluene with achiral oxazolidinone to afford the corresponding β -keto imide **278**. β -Keto imide **278** was then subjected to the HCRL reactions to obtain bicyclic lactones **279** and **280** (**Scheme 75**). The bicyclic lactones **279** and **280** co-eluted together off the column similar to the results reported by Taschner.²⁹ The spectral data of bicyclic lactones **279** and **280** was consistent with the spectral data reported by Taschner.

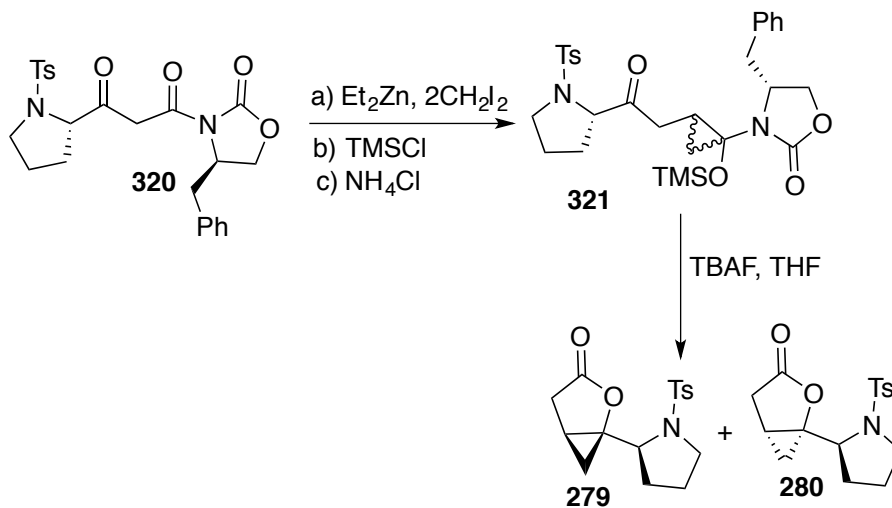


Scheme 99. Formation of sulfonamide-derived β -keto imide **278**

Chiral β -keto imide **320**, derived from D-phenylalanine was synthesized by refluxing free acid **319** with chiral oxazolidinone in toluene (**Scheme 99**). Chiral β -keto imide **320** was subjected to homologation cyclopropanation in the presence of TMSCl. The TMS cyclopropanol **321** was purified by preparative thin layer chromatography. However, the purified TMS cyclopropanol **321** contained an unknown impurity. The impurity was predicted as the other possible TMS ether, however, more analysis is needed to confirm the identity of the unknown impurity. Mower observed some decomposition products when tosyl-protected proline systems were subjected to the carbenoid conditions.³² The TMS cyclopropanol **321** along with the impurity was subjected to TBAF rearrangement (**Scheme 100**). Tetra-n-butylammonium fluoride (TBAF)-mediated rearrangement of the TMS cyclopropanol **321** afforded only one isomer of the bicyclic lactone as a white solid. Based on ¹H NMR analysis, this compound was identical to the minor bicyclic lactone obtained by Taschner in the HCRL reaction of β -keto imide **278** (**Scheme 100 and Figure 36**). Since the relative stereochemistry of the major and minor bicyclic lactones derived from HCRL reaction of **321** are unknown, an X-ray crystal structure of bicyclic lactone obtained from TBAF rearrangement of TMS cyclopropanol **321** would be of great value. Efforts to grow the crystal structure of the bicyclic lactone obtained from **321** are underway. Since the TMS cyclopropanol **321** is impure, interpretation of the selectivity in the formation of the bicyclic lactone via the TBAF rearrangement will be difficult. More work is needed to understand the selectivity of the HCRL reaction of tosyl-protecting-proline substrate.



Scheme 100. Synthesis of chiral β -keto imide **320**



only one isomer among bicyclic lactones **279** and **280** obtained

Scheme 101. Synthesis and TBAF mediated rearrangement of TMS cyclopropanol **119**

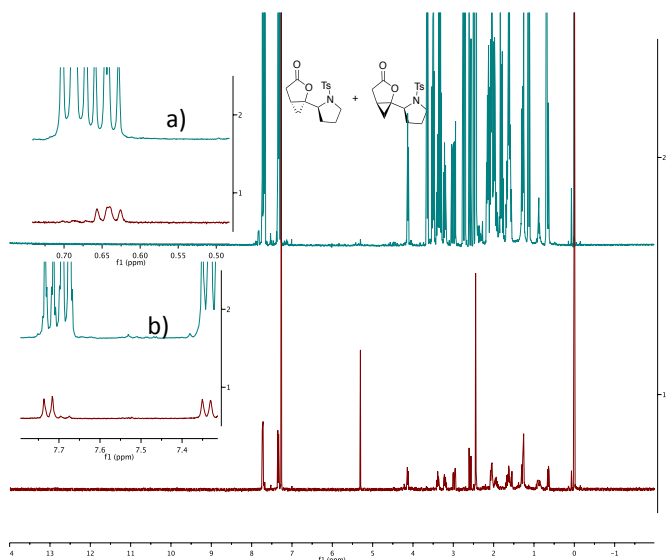


Figure 36. ^1H NMR of a) mixture of bicyclic lactones b) bicyclic lactone obtained from the TBAF rearrangement.

Conclusions and Future Work

A novel cyclopropanol peptide isostere possessing H-bonding capability has been designed in the Zercher group. Sequential homologation-cyclopropanation-rearrangement-lactonization reactions (HCRL) have been utilized to form bicyclic lactones, which upon opening with amines provide products that contain a cyclopropanol moiety and are proposed to serve as peptide isostere. A HCRL reaction of β -keto imide, which incorporated a achiral oxazolidinone, was followed by treatment with benzyl amine, which resulted in the formation of the cyclopropanol containing peptide isostere. The structure of the major product was determined by X-ray analysis, which allowed the assignment of the relative stereochemistry of the cyclopropane of the major diastereomer resulting from the HCRL reaction. Bis-carbenoid-mediated HCRL

reaction of β -keto imides that incorporated chiral oxazolidinones did not afford bicyclic lactones. Therefore, an alternative approach that involved intermediate formation of a TMS cyclopropanol was employed. Tetra-*n*-butylammonium fluoride (TBAF)-mediated rearrangement of TMS cyclopropanol provided good evidence for the role of chiral auxiliary in controlling the diastereoselectivity of the bicyclic lactone formation.

With the ability to open the bicyclic lactones, various amine residues can be used to establish a library of peptide isosteres. The α -carbon of bicyclic lactones can be functionalized to incorporate substituents that would mimic amino acid side chains in the peptide isosteres.

CHAPTER IV

EXPERIMENTALS

GENERAL EXPERIMENTAL SECTION

Solvents

Anhydrous solvents dichloromethane (DCM), methanol, tetrahydrofuran (THF), toluene, dimethylformamide (DMF) are obtained from EMD Millipore OmniSolv and dispensed the solvent from Innovative Technology Inc. solvent delivery system and stored over 3 Å and 4 Å molecular sieves. Methanol was stored over 3 Å molecular sieves.

Reagents and Reactions

All reagents are obtained from commercial sources and were used as received unless specified in detail. Reaction glassware and magnetic stir bars were stored in an oven at 200 °C. Sigma-Aldrich rubber septa and Teflon-coated magnetic stir bars were used unless specified differently. Nitrogen gas was introduced into the reaction vessel through a Tygon® tube with glass inlet adapter or a needle. Henke Sass Wolf Norm-Ject® plastic syringes and oven dried needles were used for volumetric addition of reagents.

Chromatography

Flash column chromatography was performed with Silica-P Flash Silica Gel with 40-63 µm particle size. Thin Layer Chromatography (TLC) analysis was performed on Whatman glass-

backed Silica Gel 60 Å 250- μ m thickness with fluorescent indicators for UV detection. Anisaldehyde and phosphomolybdic acid stains were used in certain cases for TLC analysis. Preparative Thin Layer chromatography was accomplished with the use of Analtech Uniplate Silica gel GF 1000 microns with UV 254 glass-backed plates.

Spectroscopy

Nuclear Magnetic Resonance (NMR) spectroscopy was achieved using a Varian Mercury spectrometer operating at 400 or 500 MHz for ^1H and 100 or 126 MHz for ^{13}C spectroscopy. All carbon spectra were proton-decoupled. All ^1H spectra were referenced relative to TMS (δ 0 ppm) unless otherwise specified. All ^{13}C resonances were referenced to CDCl_3 (δ 77.16 ppm) or TMS (δ 0 ppm). The ^1H and ^{13}C NMR run in C_6D_6 are referenced relative to TMS. Infrared spectroscopy (IR) was conducted using a Thermo Nicolet iS10 FTIR using a diamond ATR probe. Diastereomeric ratios were calculated from integrations obtained by applying a MestReNova line fit simulation in the ^1H spectra.

DETAILED EXPERIMENTAL SECTION

(R)-5-Methyldihydrofuran-2(3H)-one (181)

An oven-dried 500-mL three-necked round-bottomed flask equipped with a magnetic stir bar, nitrogen gas adaptor, reflux condenser and a rubber septum was charged with anhydrous methanol (115 mL). Freshly cut sodium metal (100 mmol, 2.29 g), rinsed in hexanes was added slowly in small portions to the methanol. The solution was then cooled to 0 °C using an ice-water bath and then freshly distilled dimethyl malonate (100 mmol, 11.5 mL) dissolved in anhydrous methanol (12 mL) was added dropwise to the reaction mixture while stirring and was heated to reflux for 0.5 h. The solution was then cooled back to room temperature at which time *R*-propylene oxide (20 mmol, 1.4 mL) dissolved in anhydrous methanol (7 mL) was added via syringe in one portion to the stirred solution of the anion of dimethyl malonate. The reaction mixture was then stirred for 20 h at room temperature. The reaction was then heated at 50 °C using an oil bath for 8 h and then heated to reflux for 20 h, at which time the reaction mixture turned yellow. The reaction was then quenched with acetic acid (6 mL) and then stirred for 20 min. The reaction mixture was then concentrated in vacuo to yield a yellow residue, which was then dissolved in water (31 mL) and extracted with diethyl ether (3 x 20 mL). The combined organic extracts were dried over sodium sulfate (*ca.* 5 g) gravity filtered and concentrated via rotary evaporation (10 mmHg, 21 °C) to afford yellow oil, which contained both the lactone ester and excess dimethyl malonate. The major portion of the dimethyl malonate was removed by fractional distillation and the remaining reaction mixture containing lactone ester was refluxed for 10 h in DMSO: H₂O (96/4, v/v, 25 mL) containing lithium chloride (3.98 g, 94 mmol). The

reaction was monitored by TLC ($R_f = 0.51$, 1:1 EtOAc - hexane). The cooled reaction mixture was diluted with brine (25 mL) and then extracted with dichloromethane (2 x 50 mL). The combined organic extracts were washed with brine (50 mL), dried over sodium sulfate (*ca.* 10 g), gravity filtered and concentrated by rotary evaporation (10 mmHg, 21 °C) to afford the crude product as brown oil. The crude product was purified by flash column chromatography on silica, eluting with a gradient mobile phase of 2%,4%,6%,8%,10%,15%,20%,25%,30% diethyl ether and hexane. The pure (*R*)- γ -valerolactone was obtained as a colorless oil (0.80 g, 40%). ^1H NMR (400 MHz, CDCl_3) δ 4.65 (m, 1H), 2.38 (m, 2H), 1.84 (m, 1H), 1.90 - 1.78 (m, 1H), 1.42 (d, $J = 6.3$ Hz, 3H). ^{13}C NMR (101 MHz, CDCl_3) δ 177.5, 77.4, 29.8, 29.2, 21.2.

(*R*)-*tert*-Butyldimethylsilyl 4-((*tert*-butyldimethylsilyloxy)pentanoate (190)

An oven-dried 100-mL round-bottomed flask equipped with a magnetic stir bar and rubber septum was charged with (*R*)-(+)- γ -valerolactone (0.74 g, 7.4 mmol) in a mixture of water (4 mL) and dioxane (4 mL). Sodium hydroxide (0.30 g, 7.4 mmol) was added to the reaction mixture, which was stirred at room temperature for 30 min. The reaction mixture was concentrated on a rotary evaporator until a white solid was formed. The white solid was then dried on high vacuum pump for 3 h. The dried white solid was suspended in distilled dimethyl formamide to which *tert*-butyldimethylsilylchloride (3.36 g, 22.3 mmol), imidazole (2.02 g, 29.7 mmol) and dimethylaminopyridine (0.45 g, 3.72 mmol) were added. The reaction mixture was stirred overnight at room temperature and then at 50 °C for 1 h. The reaction was quenched with water (4.5 mL) and extracted with diethyl ether (3 x 10 mL). The combined ether extracts were washed with 10% citric acid (10 mL), brine (10 mL) and then dried over anhydrous magnesium sulfate, vacuum filtered and concentrated by rotary evaporation to afford the crude product as

yellow oil. The crude product was purified by flash column chromatography on silica, eluting with 2 : 1 (hex : EtoAc, $R_f = 0.61$) (2.42 g, 94%). ^1H NMR (500 MHz, CDCl_3) δ 3.83 (sex, $J = 6.0$ Hz, 1H), 2.43 - 2.30 (m, 2H), 1.78 – 1.62 (m, 2H) 1.11 (d, $J = 6.2$ Hz, 3H), 0.87 (s, 9H), 0.85 (s, 9H), 0.05 (s, 6H), 0.02 (s, 3H), 0.01 (s, 3H). ^{13}C NMR (126 MHz, CDCl_3) δ 184.0, 72.3, 39.0, 35.0, 30.7, 30.5, 28.4, 22.8, 22.8, 1.2, 0.4, 0.0. IR (neat) ν 2955, 2857, 1710, 1472, 1361, 1253, 1136, 1089 cm^{-1} .

(R)-4-((*tert*-Butyldimethylsilyl)oxy)pentanoic acid (191)

An oven-dried 250-mL round-bottomed flask equipped with a magnetic stir bar was charged with methanol (90.2 mL) and cooled to 0 °C in an ice-water bath. Bis-TBDMS derivative **190** (3.14 g, 9.03 mmol) dissolved in methanol (10 mL) was added via an oven-dried needle in one portion. Potassium carbonate (3.12 g, 22.6 mmol) dissolved in water (27 mL) was added to the above reaction mixture and the reaction mixture stirred at room temperature for 4 h. The solvent was removed via rotary evaporation (10 mmHg, 45 °C) to afford a yellow residue. The crude residue was then dissolved in water (45 mL), cooled in an ice-water bath and acidified to pH 4 with 10% aqueous citric acid (*ca.* 40 mL) and extracted with ethyl acetate (4 x 40 mL). The organic layers were combined, dried over sodium sulfate (*ca.* 30 g), gravity filtered and concentrated *in vacuo* to yield the crude acid as yellow oil (1.57 g, 75 %). ^1H NMR (400 MHz, CDCl_3) δ 3.88 (m, 1H), 2.51 – 2.36 (m, 2H), 1.84 – 1.65 (m, 2H), 1.15 (d, $J = 6.3$ Hz, 3H), 0.89 (s, 9H), 0.06 (s, 3H), 0.05 (s, 3H); ^{13}C NMR (101 MHz, CDCl_3) δ , 184.4, 72.3, 38.8, 35.0, 30.6, 28.4, 22.9, 0.4, 0.0. IR (neat) ν 1563, 1356, 1004, 828 cm^{-1} .

4-(Dimethylamino)pyridin-1-ium (*R*)-4-((*tert*-butyldimethylsilyl)oxy)-1-(2,2-dimethyl-4,6-dioxo-1,3-dioxan-5-ylidene)pentan-1-olate DMAP salt (192)

An oven-dried 250-mL round-bottomed flask equipped with a magnetic stir bar and nitrogen gas inlet was charged with acid **191** (1.57 g, 6.75 mmol) in dry dichloromethane (12 mL) and cooled to 0 °C in an ice-water bath. Dicyclohexylcarbodiimide (1.39 g, 6.75 mmol) was then added to the above reaction mixture and stirred at 0 °C for 30 min. Meldrums acid (0.97 g, 6.75 mmol) and 4-(dimethylamino)pyridine (0.82 g, 6.75 mmol) were added to the solution as solids in one portion and the reaction was allowed to warm to room temperature and stir for 12 h at which time dicyclohexylurea was removed by vacuum filtration as a white solid. The filtrate was concentrated *in vacuo* and dried on a high vacuum pump (1 mmHg, 21 °C) to yield the crude DMAP salt as a yellowish green solid ($R_f = 0.25$, 1:1 EtOAc – hexane). The crude DMAP salt was proceeded to the next step without any purification. ^1H NMR (500 MHz, CDCl_3) δ 8.34 - 8.31 (m, 2H), 6.65 - 6.60 (m, 2H), 3.90 (h, $J = 6.1$ Hz, 1H), 3.17 (s, 6H), 3.00 (m, 2H), 1.86 - 1.71 (m, 2H), 1.67 (s, 6H), 1.17 (d, $J = 6.0$ Hz, 3H), 0.89 (s, 9H), 0.08 (s, 3H), 0.06 (s, 3H). ^{13}C NMR (126 MHz, CDCl_3) δ 203.6, 170.8, 160.9, 147.8, 110.9, 73.4, 44.3, 42.8, 40.1, 38.5, 32.2, 30.9, 30.5, 28.3, 22.8, 4.5. IR (CH_2Cl_2) ν 2927, 1641, 1598, 1555, 1442, 1372, 1262, 1209, 1019 cm^{-1} .

(*R*)-4-((*tert*-Butyldimethylsilyl)oxy)-1-(2,2-dimethyl-4,6-dioxo-1,3-dioxan-5-ylidene)pentan-1-olate (193)

An oven-dried 100-mL round-bottomed flask equipped with a magnetic stir bar and nitrogen gas inlet was charged with anhydrous dichloromethane (50 mL), DMAP salt (3.24 g, 6.75 mmol) and anhydrous DOWEX 50WX2 ion exchange resin (10.1 g, 1.5 g for 1 mmol of DMAP salt). The solution was stirred at room temperature for 1 h. The resin was removed by

filtration and the filtrate was concentrated *in vacuo* to afford the free acid as a greenish yellow oil ($R_f = 0.12$, 1:1 EtOAc-hexane), which was carried on to the next step without purification. ^1H NMR (400 MHz, CDCl_3) δ 3.92 (sextet, 1H), 3.21-3.06 (m, 2H), 1.87-1.75 (m, 2H), 1.73 (s, 6H), 1.19 (d, $J = 6.1$ Hz, 3H), 0.89 (s, 9H), 0.07 (s, 3H), 0.06 (s, 3H)

(*R*)-1-((*S*)-4-Benzyl-2-oxooxazolidin-3-yl)-6-((*tert*-butyldimethyl silyl)oxy) heptane 1,3-dione (194)

An oven-dried 250-mL round-bottomed flask, equipped with a magnetic stir bar, reflux condenser and nitrogen gas adaptor was charged with free acid **193** (3.4 mmol, 1.205 g) in anhydrous toluene (60 mL). Chiral oxazolidinone **161** (4.0 mmol, 0.71 g) was added in one portion as a solid to the reaction mixture and was heated to reflux for 4 h. The reaction was monitored by TLC (hexane:EtOAc 1:1, $R_f = 0.57$). The reaction mixture was cooled and then washed with water (30 mL) and brine (30 mL). The organic layer was concentrated *in vacuo* to yield crude product as yellow oil. The crude product was purified by flash column chromatography on silica, eluting with a gradient mobile phase of 2%,4%,6%,8%,10%,12%,14%,16%,18%,20%,25%,30% diethyl ether and hexane. The titled compound **194** was obtained as light yellow colored solid containing both keto-enol forms (0.70 g, 48%). ^1H NMR keto form (400 MHz, CDCl_3) δ 7.38 - 7.20 (m, 5H), 4.76 - 4.68 (m, 1H), 4.26 - 4.14 (m, 2H), 4.14 - 4.00 (AB, 2H), 3.85 (sextet, $J = 6.2$ Hz, 1H), 3.39 (dd, $J = 13.6, 3.4$ Hz, 1H), 2.79 (dd, $J = 13.5, 9.8$ Hz, 1H), 2.72 - 2.54 (m, 2H), 1.84 - 1.62 (m, 2H), 1.13 (d, $J = 6.1$ Hz, 3H), 0.89 (s, 9H), 0.05 (s, 3H), 0.01 (s, 3H). ^{13}C NMR (101 MHz, CDCl_3) δ 208.1, 171.3, 158.4, 139.9, 134.2, 133.7, 132.1, 72.2, 71.1, 59.8, 55.4, 43.7, 42.4, 37.5, 30.6, 28.4, 22.8, 0.40, 0.00. IR (neat) ν 2955, 2852, 1761, 1690, 1396, 1089, 990, 834 cm^{-1} . The enol form is identified through the presence of the proton resonances at 6.53 and 13.6 ppm.

(4S)-4-Benzyl-3-((2R,3R)-5-((R)-3-((tert-butyldimethylsilyl)oxy)butyl)-2-(3-((tert-butyldiphenylsilyl)oxy)propyl)-5-hydroxytetrahydrofuran-3-carbonyl)oxazolidin-2-one
(210, 211)

An oven-dried 100-mL round-bottomed flask equipped with a magnetic stir bar and nitrogen gas inlet was charged with dry dichloromethane (14 mL) and cooled to 0 °C in an ice-water bath. Neat diethylzinc (0.37 mL, 3.6 mmol) was added in one portion via an oven-dried needle followed by dropwise addition of diiodomethane (0.29 mL, 3.6 mmol) over the course of 5 min. The reaction was allowed to stir at 0 °C for 10 min at which time a milky white suspension was formed. *tert*-Butyldiphenylsilyl protected aldehyde **209** (0.43 g, 1.3 mmol) in dry dichloromethane (2 mL) was added via syringe in one portion to the carbenoid at 0 °C. β -Keto imide **194** (0.52 g, 1.2 mmol) in dry dichloromethane (3 mL) was added by syringe to the reaction mixture in one portion at 0 °C and stirred at the same temperature for 1 h. The reaction mixture was stirred at room temperature for 1 h. The reaction mixture was quenched with saturated ammonium chloride (*ca.* 6 mL) and extracted with dichloromethane (3 x 15 mL). The organic layers were pooled, dried with sodium sulfate (*ca.* 10 g), gravity filtered and concentrated *invacuo* to afford a viscous brown oil. The crude mixture was purified by flash column chromatography on silica, eluting with a gradient mobile phase of 2%,5%,7%,8%,10%,12%,15%,20%,25%,30%,35%,40%,45%,50%,55%,60%,65%,70%,75%,80% diethyl ether and hexane (hexane:EtOAc 1:1, R_f = 0.64) to afford the title compound XX as a mixture of open-hemiacetal isomers as a yellow oil (0.41 g, 44%). ^1H NMR (400 MHz, CDCl_3) δ 7.69 - 7.57 (m, 4H), 7.43 - 7.07 (m, 11H), 4.73 - 4.54 (m, 2H), 4.44 - 4.31 (m, 1H), 4.30 - 4.00 (m, 4H), 3.89 - 3.73 (m, 2H), 3.73 - 3.57 (m, 2H), 3.35 - 3.05 (m, 3H), 2.82 - 2.61 (m, 2H), 2.60 - 2.39 (m, 2H), 2.28 (ddd, J = 10.2, 3.3, 10.4 Hz, 1H), 1.97 - 1.42 (m, 8H), 1.15 - 1.04 (m, 3H),

1.01 (s, 9H), 0.85 (s, 9H), 0.04 (s, 3H), 0.02 (s, 3H). ^{13}C NMR (101 MHz, CDCl_3) δ ^{13}C NMR (101 MHz, CDCl_3) δ 215.3, 214.6, 181.2, 179.2, 175.8, 162.3, 158.5, 157.7, 141.2, 140.3, 139.6, 138.7, 138.3, 134.4, 134.3, 134.2, 134.1, 133.7, 133.6, 133.5, 132.4, 132.3, 131.6, 130.2, 111.6, 111.1, 76.1, 73.3, 72.3, 71.4, 71.1, 70.6, 69.4, 68.7, 68.4, 65.1, 62.2, 60.1, 51.9, 48.5, 45.7, 45.07, 44.4, 44.0, 43.7, 42.5, 41.1, 40.5, 39.1, 39.0, 37.9, 36.7, 36.4, 35.0, 33.8, 33.6, 31.6, 30.65, 28.5, 26.8, 25.8, 24.3, 24.0, 22.8, 20.0, 18.9, 0.3, 0.1. IR (CH_2Cl_2) ν 1780, 1698, 1386, 1251, 1095, 833, 773 cm^{-1} .

Spirocyclization

An oven-dried 100-mL round-bottomed flask equipped with a magnetic stir bar and nitrogen gas inlet was charged with aldol product **210** (0.87 g, 1.12 mmol) in dry dichloromethane (10 mL). Camphorsulfonic acid (0.28 g, 1.2 mmol) was added as a solid in one portion to the reaction mixture and stirred at room temperature for 18 h. The crude reaction mixture was filtered through a plug of celite and the dichloromethane was removed by rotary evaporation to yield a yellow oil. The crude reaction mixture was purified by flash column chromatography on silica, eluting with a gradient mobile phase of 2%, 4%, 6%, 8%, 10%, 12%, 15%, 20%, 25%, 27%, 30%, 40% and 45% ethyl acetate and hexane. Spiroketal (**214**) eluted with 30% ethyl acetate and hexane ($R_f = 0.63$, 1:1 EtOAc - hexane) followed by spiroketal (**215**) with 35% ethyl acetate and hexane ($R_f = 0.57$, 1:1 EtOAc - hexane). Spiroketal (**212**) eluted with 40% ethyl acetate ($R_f = 0.51$, 1:1 EtOAc - hexane) and hexane followed by spiroketal (**213**) with 45% ethyl acetate and hexane ($R_f = 0.42$, 1:1 EtOAc - hexane) (overall 30% yield, 90 mg of spiroketal 3, 28 mg spiroketal 4).

(S)-4-Benzyl-3-((2R,3R,5R,7R)-2-(3-((tert-butyl)diphenylsilyloxy)propyl)-7-methyl-1,6-dioxaspiro[4.4]nonane-3-carbonyl)oxazolidin-2-one (212)

^1H NMR (500 MHz, CDCl_3) ^1H NMR (400 MHz, CDCl_3) δ 7.74 - 7.63 (m, 4H), 7.50 - 7.11 (m, 11H), 4.72 - 4.62 (m, 1H), 4.41 - 4.05 (m, 6H), 3.76 - 3.64 (m, 2H), 3.24 (dd, $J = 13.3, 3.4$ Hz, 1H), 2.72 (dd, $J = 13.4, 9.6$ Hz, 1H), 2.50 - 2.30 (m, 2H), 2.17 - 2.05 (m, 2H), 1.89 - 1.71 (m, 3H), 1.70 - 1.55 (m, 1H), 1.49 - 1.36 (m, 1H), 1.18 (d, $J = 6.2$ Hz, 3H), 1.04 (s, 9H). ^{13}C NMR (101 MHz, CDCl_3) δ 174.0, 153.2, 135.8, 135.3, 134.3, 129.7, 129.6, 129.2, 127.8, 127.6, 115.3, 82.8, 74.4, 66.3, 64.1, 55.5, 48.5, 40.3, 38.1, 35.7, 32.9, 32.0, 29.7, 27.1, 21.5, 19.4. DEPT-135 (101 MHz, CDCl_3) δ 135.8, 129.7, 129.6, 129.2, 127.8, 127.6, 82.9, 74.5, -66.3, -64.1, 55.6, 48.5, -40.4, -38.2, -35.8, -33.0, -32.0, -29.7, 27.1, 21.5, 19.5. IR (CH_2Cl_2) ν 2928, 1779, 1697, 1384, 1165, 1104, 822 cm^{-1}

(S)-4-Benzyl-3-((2R,3R,5S,7R)-2-(3-((tert-butyl)diphenylsilyloxy)propyl)-7-methyl-1,6-dioxaspiro[4.4]nonane-3-carbonyl)oxazolidin-2-one (213)

^1H NMR (400 MHz, CDCl_3) ^1H NMR (400 MHz, CDCl_3) δ 7.69 - 7.64 (m, 4H), 7.43 - 7.15 (m, 11H), 4.68 (ddt, $J = 10.4, 6.9, 3.5$ Hz, 1H), 4.62 - 4.56 (m, 1H), 4.33 - 4.06 (m, 4H), 3.80 (ddd, $J = 11.1, 8.3, 6.9$ Hz, 1H), 3.73 - 3.64 (m, 2H), 3.29 (dd, $J = 13.3, 3.4$ Hz, 1H), 2.69 (dd, $J = 13.3, 9.8$ Hz, 1H), 2.57 (dd, $J = 13.3, 11.1$ Hz, 1H), 2.15 (dd, $J = 13.4, 6.9$ Hz, 1H), 2.12 - 2.00 (m, 2H), 1.96 - 1.86 (m, 1H), 1.83 - 1.56 (m, 4H), 1.28 (d, $J = 6.2$, 3H), 1.03 (s, 9H). ^{13}C NMR (101 MHz, CDCl_3) δ 173.1, 153.3, 135.7, 135.4, 134.2, 129.7, 129.6, 129.1, 127.8, 127.5, 113.7, 79.1, 76.4, 66.4, 63.9, 55.6, 48.1, 40.6, 38.1, 37.1, 32.5, 30.9, 29.5, 27.1, 23.5, 19.4. IR (CH_2Cl_2) ν 2931, 1776, 1687, 1384, 1165, 1104, 815 cm^{-1}

(2*R*,3*R*,5*R*,7*R*)-2-(3-((*tert*-Butyldiphenylsilyl)oxy)propyl)-7-methyl-1,6-dioxaspiro[4.4]nonane-3-carboxylic acid (216)

An oven-dried 100-mL round-bottomed flask equipped with a magnetic stir was charged with 0.05 M solution of spiroketal **212** (90 mg, 0.14 mmol) in THF : H₂O (3 : 1) mixture (5 mL) and cooled to 0 °C in an ice-water bath. Hydrogen peroxide (30 % by weight in water) (0.07 mL, 0.56 mmol) was added to the reaction mixture at 0 °C via syringe over a 5 min period. Anhydrous lithium hydroxide (7 mg, 0.28 mmol) was added as a white solid in one portion to the above reaction mixture at 0 °C. The reaction mixture was then warmed to room temperature and stirred for 12 h. The reaction mixture was quenched with 1M sodium sulfite (5 mL) and stirred for 20 min. The bulk of the THF was removed via rotary evaporation (1 mmHg, 30 °C). The resulting mixture was basified with 10% sodium bicarbonate to pH 12 and extracted with dichloromethane (3 x 10 mL) to remove the oxazolidinone. The aqueous layer was acidified to pH 1 with 6 M hydrochloric acid and extracted with ethyl acetate (3 x 5 mL), concentrated in vacuo to recover the carboxylic acid. However the NMR of the crude reaction mixture showed the presence of both oxazolidinone and carboxylic acid **216** in dichloromethane extracts and only traces of acid in the ethyl acetate layer. The dichloromethane extracts were combined, concentrated in vacuo and was purified by flash column chromatography on silica, eluting with a gradient mobile phase of 5%, 10%, 20%, 30% methyl *tert* butyl ether (MTBE) and hexane ($R_f = 0.13$, 2 : 1 hexane - MTBE) (0.051 g, 76% yield). The carboxylic acid XX was eluted with 30 % MTBE : hexane. ¹H NMR (400 MHz, CDCl₃) δ 7.73 - 7.63 (m, 4H), 7.56 - 7.33 (m, 6H), 4.27 - 4.13 (m, 2H), 3.72 - 3.64 (m, 1H), 3.12 - 3.04 (q, $J = 8.8$ Hz, 1H), 2.37 - 2.28 (m, 2H), 2.16 - 1.97 (m, 2H), 1.83 - 1.56 (m, 3H), 1.50 - 1.29 (m, 5H), 1.18 (d, $J = 6.2$ Hz, 3H), 1.04 (s, 9H). IR (CH₂Cl₂) ν 3100, 1707, 1434, 1412, 1278, 1110, 928 cm⁻¹

(2R,3R,5S,7R)-2-(3-((*tert*-Butyldiphenylsilyl)oxy)propyl)-7-methyl-1,6-dioxaspiro[4.4]nonane-3-carboxylic acid (217**)**

An oven-dried 100-mL round-bottomed flask equipped with a magnetic stir was charged with 0.05 M solution of spiroketal **213** (28 mg, 0.04 mmol) in THF : H₂O (3 : 1) mixture (2 mL) and cooled to 0 °C in an ice-water bath. Hydrogen peroxide (30 % by weight in water) (1.6 μL, 0.16 mmol) was added to the reaction mixture at 0 °C via syringe over a five minute period. Anhydrous lithium hydroxide (2 mg, 0.08 mmol) was added as a white solid in one portion to the above reaction mixture at 0 °C. The reaction mixture was warmed to room temperature and stirred for 12 h. The reaction mixture was quenched with 1M sodium sulfate (2 mL) and stirred for 20 min. The bulk of the THF was removed via rotary evaporation (1 mmHg, 30 °C). The resulting mixture was basified with 10% sodium bicarbonate to pH 12 and extracted with dichloromethane (3 x 5 mL) to remove the oxazolidinone. The aqueous layer was acidified to pH 1 with 6 M hydrochloric acid and extracted with ethyl acetate (3 x 5 mL) to recover the carboxylic acid. However, NMR showed the presence of both oxazolidinone and carboxylic acid in dichloromethane extracts and only traces of acid in the ethyl acetate layer. The carboxylic acid **217** was purified by flash column chromatography on silica, eluting with a gradient mobile phase of 5%, 10%, 20%, 30% methyl *tert*-butyl ether (MTBE) and hexane ($R_f = 0.13$, 2 : 1 hexane - MTBE) (0.020 g, 90% yield). The carboxylic acid **217** was eluted with 30 % MTBE : hexane. The spectra showed minor impurities. ¹H NMR (400 MHz, CDCl₃) δ 7.73 - 7.62 (m, 4H), 7.55 - 7.32 (m, 6H), 4.34 - 4.11 (m, 3H), 3.71 - 3.64 (m, 2H), 2.80 (ddd, $J = 10.2, 6.1, 3.9$ Hz, 1H), 2.37 - 2.19 (m, 2H), 2.16 - 1.94 (m, 3H), 1.85 - 1.55 (m, 5H), 1.30 (d, $J = 6.2$, 3H), 1.04 (s, 9H). ¹³C NMR (101 MHz, CDCl₃) δ 175.9, 135.7, 134.1, 129.7, 127.8, 114.4, 80.5, 63.8, 49.5, 38.4, 35.4,

32.6, 31.9, 29.9, 28.7, 27.1, 23.0, 19.4. IR (CH₂Cl₂) ν 3109, 1705, 1434, 1412, 1278, 1110, 928 cm⁻¹

Barton decarboxylation of carboxylic acid of spiroketal 3

An oven-dried 100-mL round-bottomed flask, equipped with a magnetic stir bar and nitrogen gas inlet was charged with carboxylic acid XX (0.051 g, 0.11 mmol) in anhydrous dichloromethane (3 mL). Oxalyl chloride (0.033 mL, 0.38 mmol) was slowly added to the reaction mixture and stirred at room temperature for 50 min. The solvent and excess oxalyl chloride was removed using a rotary evaporator and the residual oil was dried on high vacuum line (1.0 torr) for 10 min.

Decarboxylation

Commercially available chloroform (ACS grade) was washed with water, dried over potassium carbonate and distilled over P₂O₅ under nitrogen and then stored in 3Å MS in dark until used. 1-Hydroxypyridine-2(1H)-thione sodium salt was dried on high vacuum pump.

An oven-dried 50-mL two-necked round-bottomed flask, equipped with a magnetic stir bar, nitrogen gas inlet and a reflux condenser, was charged with 1-hydroxypyridine-2(1H)-thione sodium salt (0.02 g, 0.13 mmol) and DMAP (4 mg, 0.003 mmol) in distilled chloroform (2 mL). The resulting white suspension was refluxed. The acid chloride prepared above was dissolved in distilled chloroform (4 mL) and added dropwise via syringe with concomitant irradiation from halogen lamp (200 W) over a 20 min period. The reaction mixture turned from white suspension to light yellow colored clear solution on addition of the acid chloride. The mixture was refluxed for 150 min and monitored by TLC. The reaction mixture was cooled to room temperature, quenched with 1M hydrochloric acid (5 mL) and extracted with dichloromethane (3 x 5 mL).

The organic layers were combined, washed with brine (5 mL), dried over sodium sulfate, filtered and concentrated in vacuo. The crude reaction mixture was purified by preparative thin layer chromatography, eluting with a mobile phase of 20% EtOAc – hexane to afford the desired spiroketals 92 ($R_f = 0.56$, 3 : 1 hexane – ethyl acetate) (19 mg, 40% yield) and 93 ($R_f = 0.53$, 3 : 1 hexane – ethyl acetate) (17 mg, 35% yield) as yellow oils.

***tert*-Butyl(3-((2R,5R,7R)-7-methyl-1,6-dioxaspiro[4.4]nonan-2-yl)propoxy)diphenylsilane
(206)**

^1H NMR (500 MHz, CDCl_3) δ 7.68 - 7.64 (m, 4H), 7.44 - 7.34 (m, 6H), 4.20 (sextet, $J = 6.3$ Hz, 1H), 4.00 - 3.97 (m, 1H), 3.67 (t, $J = 6.3$ Hz, 2H), 2.16 - 1.88 (m, 6H), 1.80 - 1.53 (m, 6H), 1.20 (d, $J = 6.2$ Hz, 3H), 1.04 (s, 9H). ^{13}C NMR (126 MHz, CDCl_3) δ 135.5, 134.1, 129.5, 127.6, 114.4, 79.7, 73.7, 64.00, 36.3, 35.5, 33.7, 31.8, 30.8, 29.3, 26.9, 21.3, 19.2. DEPT-135 (101 MHz, CDCl_3) δ 135.6, 134.1, 29.5, 127.5, 114.4, 79.7, 73.7, -64.0, -36.3, -35.1, -33.7, -31.8, -30.8, -29.3, 26.9, 21.3, 19.2.

***tert*-Butyl(3-((2R,5S,7R)-7-methyl-1,6-dioxaspiro[4.4]nonan-2-yl)propoxy)diphenylsilane
(207)**

^1H NMR (400 MHz, CDCl_3) δ 7.69 - 7.63 (m, 4H), 7.45 - 7.33 (m, 6H), 4.22 - 4.06 (m, 2H), 3.72 - 3.62 (m, 2H), 2.16 - 1.86 (m, 6H), 1.77 - 1.42 (m, 6H), 1.26 (d, $J = 6.2$ Hz, 3H), 1.04 (s, 9H). ^{13}C NMR (101 MHz, CDCl_3) δ 135.6, 134.1, 129.5, 127.6, 114.5, 77.7, 75.7, 63.9, 36.7, 35.1, 32.6, 32.0, 30.0, 29.0, 26.9, 22.8, 19.2.

Barton decarboxylation of carboxylic acid of spiroketal 4

An oven-dried 100-mL round-bottomed flask, equipped with a magnetic stir bar and nitrogen gas inlet was charged with carboxylic acid XX (0.020 g, 0.04 mmol) in anhydrous dichloromethane (2 mL). Oxalyl chloride (0.012 mL, 0.14 mmol) was slowly added to the reaction mixture and stirred at room temperature for 50 min. The solvent and excess oxalyl chloride were removed using a rotary evaporator and the residual oil was dried on high vacuum line (1.0 torr) for 10 min.

Decarboxylation

Commercially available chloroform (ACS grade) was washed with water, dried over potassium carbonate and distilled over P₂O₅ under nitrogen and then stored in 3A MS in dark until used. 1-Hydroxypyridine-2(1H)-thione sodium salt was dried on high vacuum pump.

An oven-dried 50-mL two-necked round-bottomed flask, equipped with a magnetic stir bar, nitrogen gas inlet and a reflux condenser was charged with 1-hydroxypyridine-2(1H)-thione sodium salt (7 mg, 0.05 mmol) and DMAP (2 mg, 0.001 mmol) in distilled chloroform (2 mL). The resulting white suspension was refluxed. The acid chloride prepared above was dissolved in distilled chloroform (2 mL) was added dropwise via syringe with concomitant irradiation from halogen lamp (200 W) over a 20 min period. The reaction mixture turned from white suspension to light yellow colored clear solution on addition of the acid chloride. The mixture was refluxed for 2.5 h and monitored by TLC. The reaction mixture was cooled to room temperature, quenched with 1M hydrochloric acid (3 mL) and extracted with dichloromethane (3 x 3 mL). The organic layers were combined, washed with brine, dried over sodium sulfate, filtered and concentrated in vacuo. The crude reaction mixture was purified by preparative thin layer chromatography, eluting with a mobile phase of 20% EtOAc – hexane to afford the desired

spiroketals **206** and **207** as a yellow oil. The spectral data and yields of spiroketals **206** and **207** were identical to the ones reported earlier.

4-((*tert*-Butyldimethylsilyl)oxy)butan-1-ol (180**)**

An oven-dried 100-mL round-bottomed flask equipped with a magnetic stir bar and nitrogen gas inlet was charged with anhydrous THF (24 mL). Sodium hydride (11.2 mmol, 0.45 g, 60% wt in mineral oil) was washed with hexane under the bed of nitrogen and added to the reaction flask in one portion as a solid. A solution of 1,4-butanediol **180** (1 mL, 10 mmol) in THF (3 mL) was added to the stirred suspension of sodium hydride in THF. *tert*-Butyldimethylsilyl chloride (1.69 g, 11.2 mmol) dissolved in THF (3 mL) was added to the resulting suspension of sodium hydride and stirred at room temperature overnight. The reaction mixture turned light yellow after stirring for overnight. The reaction mixture was quenched with saturated potassium carbonate (12 mL) and extracted with diethyl ether (3 x 10 mL). The combine organic extracts were washed with brine (15 mL), dried over sodium sulfate, filtered and concentrated in vacuo to afford the crude product as yellow oil. The crude product was purified by flash column chromatography on silica, eluting with a mobile phase of 15% EtOAc – hexane (2.04 g, 60% yield). ¹H NMR (400 MHz, CDCl₃) δ 3.67 - 3.52 (m, 4H), 2.85 (bs, OH) 1.70 – 1.60 (m, 4H), 0.90 (s, 9H), 0.07 (s, 6H).

4-((*tert*-Butyldimethylsilyl)oxy)butanal (176**)**

A 250-mL oven-dried round-bottomed flask equipped with a magnetic stir bar and nitrogen inlet and powdered molecular sieves was charged with anhydrous dichloromethane (75 mL). Pyridinium chlorochromate (1.94 g, 9.0 mmol) and sodium acetate (0.15 g, 1.8 mmol) were added to the reaction flask. To the above resulting suspension was added monoprotected 1,4-butanediol (**180**) (1.23 g, 6.00 mmol) in dichloromethane (75 mL) and stirred at room

temperature for 36 h. Diethyl ether (30 mL) was added and the mixture was passed through a short pad of florisil to remove any unreacted pyridinium chlorochromate. The filtrate was then dried over sodium sulfate, filtered and concentrated in vacuo. The crude reaction mixture was purified by flash column chromatography on silica, eluting with a mobile phase of 7:3 hexane - diethyl ether to afford the aldehyde **176** as a colorless oil (0.76 g, 63 %). ¹H NMR (400 MHz, CDCl₃) δ 9.79 (t, *J* = 1.7 Hz, 1H), 3.65 (t, *J* = 6.0 Hz, 2H), 2.51 (td, *J* = 7.1, 1.7 Hz, 2H), 1.86 (quintet, *J* = 7.0 Hz, 2H), 0.89 (s, 9H), 0.04 (s, 6H).

4-((*tert*-Butyldiphenylsilyl)oxy)butan-1-ol (208)

An oven-dried 100-mL round-bottomed flask equipped with a magnetic stir bar and nitrogen gas inlet was charged with 1,4-butanediol (**179**) (1.35 g, 15 mmol) and *N,N*-diisopropylethylamine (2.72 mL, 15.6 mmol) in anhydrous dichloromethane (5 mL). *tert*-Butyldiphenylsilyl chloride (1.3 mL, 4.95 mmol) was added dropwise to the reaction mixture and stirred at room temperature overnight. The crude reaction mixture was concentrated in vacuo to afford yellow oil. The crude product was purified by flash column chromatography on silica, eluting with a mobile phase of 20% EtOAc – hexane to afford the monoprotected diol **208** as a clear oil (1.54 g, 95% yield). ¹H NMR (400 MHz, CDCl₃) δ 7.71 -7.63 (m, 4H), 7.47 - 7.34 (m, 6H), 3.75 - 3.62 (m, 4H), 2.01 (bs, OH), 1.73 - 1.60 (m, 4H), 1.05 (s, 9H).

4-((*tert*-Butyldiphenylsilyl)oxy)butanal (209)

An oven-dried 250-mL round-bottomed flask equipped with a magnetic stir bar and nitrogen gas inlet was charged with anhydrous dichloromethane (20 mL) and cooled to -78 °C in a dry ice-acetone bath. Oxalyl chloride (0.67 mL, 7.81 mmol) followed by a solution of dimethyl sulfoxide (1.15 mL, 16.1 mmol) in dichloromethane (4 mL) was added to the cooled reaction mixture. The reaction mixture was stirred for 5 min and a solution of *tert*-butyldiphenylsilyl

chloride protected butanol XX (2.44 g, 7.44 mmol) in dichloromethane (8 mL) was added via syringe to the reaction mixture and the resulting suspension was stirred for 50 min at -78 °C. Triethylamine (5.06 mL, 36.3 mmol) was added dropwise followed by the stirring at -78 °C for additional 10 min. The reaction mixture was allowed to warm to room temperature and stirred for 3 h at room temperature. The reaction mixture was then diluted with dichloromethane, washed successively with 3% hydrochloric acid, water, saturated aqueous sodium bicarbonate and water. The organic layer was dried over sodium sulfate, filtered and concentrated in vacuo to yield the crude product as brown oil. The crude product was purified by flash column chromatography on silica, eluting with a mobile phase of 20% EtOAc – hexane to afford the aldehyde **209** as a colorless oil (2.30 g, 95% yield) ¹H NMR (400 MHz, CDCl₃) δ 9.78 (t, *J* = 1.7 Hz, 1H), 7.67 - 7.62 (m, 4H), 7.45 - 7.34 (m, 6H), 3.69 (t, *J* = 6.1 Hz, 2H), 2.54 (td, *J* = 7.2, 1.7 Hz, 2H), 1.93 – 1.84 (m, 2H), 1.05 (s, 9H).

5-(1-hydroxyethylidene)-2,2-dimethyl-1,3-dioxane-4,6-dione (166)

An oven-dried 100-mL round-bottomed flask equipped with a magnetic stir bar and nitrogen gas inlet was charged with Meldrums Acid (3.60 g, 25 mmol) in anhydrous dichloromethane (10 mL). The flask and its contents were cooled to 0 °C in an ice-water bath and pyridine (4.8 mL, 60 mmol) was added with stirring over a 10 min period. To the resulting clear solution, was added a solution of acetyl chloride (1.78 ml, 25 mmol) in dichloromethane (8 mL) over a 20 min period at 0 °C. After the addition was complete the resulting orange reaction mixture was warmed to room temperature and stirred overnight. The reaction mixture was then diluted with dichloromethane (10 mL) and then poured into 2N hydrochloric acid (15 mL) containing crushed ice. The organic layer was separated and the aqueous layer was extracted with dichloromethane (2 x 10 mL). The organic layers were combined and washed with 2N

hydrochloric acid (10 mL), brine (10 mL), dried over sodium sulfate, filtered and concentrated in vacuo to yield acetylated Meldrum's Acid **166** as a pale yellow solid (3.6 g, 79% yield). ¹H NMR (500 MHz, CDCl₃) δ 2.68 (s, 3H), 1.74 (s, 6H). ¹³C NMR (126 MHz, CDCl₃) δ 194.6, 170.2, 160.5, 104.9, 91.8, 26.8, 23.5.

(S)-1-(4-Benzyl-2-oxooxazolidin-3-yl)butane-1,3-dione (167)

An oven-dried 100 mL round-bottomed flask equipped with a magnetic stir bar, water condenser and nitrogen gas inlet was charged with acetylated Meldrum's Acid **166** (1.82 g, 10 mmol), chiral oxazolidinone **161** (1.77 g, 10 mmol) in anhydrous toluene (40 mL) and refluxed for 5 h. The organic layer was washed with brine (20 mL), water (20 mL) and dried over sodium sulfate, filtered and concentrated in vacuo to afford the crude product. The crude product was purified by flash column chromatography on silica, eluting with a mobile phase of 1:3 EtOAc – hexane to yield the β-keto imide **167** as white solid (0.83 g, 32% yield) (R_f = 0.5 in 1:1 EtOAc – hexane). ¹H NMR (400 MHz, CDCl₃) δ 7.37 - 7.27 (m, 3H), 7.26 - 7.21 (m, 2H), 4.76 - 4.68 (m, 1H), 4.26 - 4.16 (m, 2H), 4.07 (AB, *J* = 2.3 Hz, 2H), 3.38 (dd, *J* = 13.5, 3.5 Hz, 1H), 2.80 (dd, *J* = 13.5, 9.6 Hz, 1H), 2.30 (s, 3H). ¹³C NMR (101 MHz, CDCl₃) δ 201.2, 166.6, 153.9, 135.3, 129.7, 129.2, 127.6, 66.6, 55.2, 51.6, 37.9, 30.4.

(S)-3-Acetyl-4-benzyloxazolidin-2-one (169)

An oven-dried 25 mL round-bottomed flask equipped with a magnetic stir bar, water condenser and nitrogen gas inlet was charged with chiral oxazolidinone (0.89 g, 5 mmol) and acetyl chloride (1.05 mL, 15 mmol). Pyridine (0.40 mL, 5 mmol) was added dropwise to the

reaction mixture and refluxed for 10 h. The reaction mixture was cooled and dichloromethane (50 mL) was added. The organic layer was washed with 5% hydrochloric acid (20 mL), saturated sodium bicarbonate (20 mL), water (20 mL) and brine (20 mL). The organic layer was dried over magnesium sulfate, filtered and concentrated in vacuo to yield the crude product. The crude product was filtered by column chromatography on silica, eluting with 1:3 EtOAc – hexane to afford the acylated chiral oxazolidinone **169** as a orange solid (0.42 g, 65% yield). ¹H NMR (400 MHz, CDCl₃) δ 7.38 - 7.27 (m, 3H), 7.25 - 7.19 (m, 2H), 4.68 (m, 1H), 4.24 - 4.15 (m, 2H), 3.31 (dd, *J* = 13.4, 3.4 Hz, 1H), 2.78 (dd, *J* = 13.4, 9.6 Hz, 1H), 2.56 (s, 3H). ¹³C NMR (101 MHz, CDCl₃) δ 170.5, 153.8, 135.4, 129.6, 129.2, 127.6, 66.3, 55.2, 38.0, 24.1.

(S)-2-Amino-3-phenylpropan-1-ol (163)

An oven-dried 500-mL three-necked round-bottomed flask equipped with a mechanical stirrer, water condenser and nitrogen gas inlet was charged with anhydrous tetrahydrofuran (250 mL) and cooled to 0 °C in an ice-water bath. Lithium aluminum hydride (5.92 g, 156 mmol) was added in portion to the flask followed by slow addition of *S*-phenyl alanine (16.5 g, 100 mmol). The reaction mixture was heated to reflux for 3 h and cooled to room temperature. The excess lithium aluminum hydride was quenched with slow addition of potassium hydroxide (2.8 g) in water (15 mL). After the addition of aqueous potassium hydroxide, the reaction mixture was heated to reflux for 20 min. The reaction mixture was cooled and then vacuum filtered. The aluminum salts were washed with boiling tetrahydrofuran (2 x 50 mL). The combined filtrate (THF) was dried over anhydrous sodium sulfate, filtered and concentrated in vacuo to yield amino alcohol as a light yellow colored solid (12.3 g, 82% yield). The product was carried on without further purification. ¹H NMR (400 MHz, CDCl₃) δ 7.25 - 7.07 (m, 5H), 6.28 (bs, OH),

3.84 - 3.45 (m, 2H), 3.13 (dd, $J = 13.6, 5.2$ Hz, 1H), 3.02 - 2.61 (m, 2H). ^{13}C NMR (101 MHz, CDCl_3) δ 135.8, 129.5, 129.0, 127.3, 61.1, 55.2, 35.9.

(S)-Ethyl (1-hydroxy-3-phenylpropan-2-yl)carbamate (164)

An oven-dried 250-mL round-bottomed flask equipped with a magnetic stir bar was charged with amino alcohol **163** (12.3 g, 80.8 mmol), water (61 mL), sodium bicarbonate (34 g, 404 mmol) and ethyl chloroformate (8 mL, 84.8 mmol). The reaction mixture was stirred at room temperature for 4 h and then extracted with ethyl acetate (4 x 40 mL). The organic extracts were washed with water (50 mL), brine (50 mL), dried over magnesium sulfate, filtered and concentrated on a rotary evaporator to yield ethyl carbamate **164** as light yellow colored solid (14.2 g, 78.6% yield). The product was carried on without further purification. ^1H NMR (400 MHz, CDCl_3) δ 7.34 - 7.17 (m, 5H), 5.09 (bs, 1H), 4.07 (q, $J = 7.1$ Hz, 2H), 3.91 (bs, 1H), 3.64 (dd, $J = 11.1, 3.9$ Hz, 1H), 3.54 (dd, $J = 11, 5.1$ Hz, 1H) 2.99 - 2.78 (m, 3H), 1.20 (t, $J = 7.1$ Hz, 3H). ^{13}C NMR (101 MHz, CDCl_3) δ 157.1, 137.9, 129.5, 128.7, 126.7, 64.1, 61.2, 54.2, 37.6, 14.7.

(S)-4-benzyloxazolidin-2-one (161)

An oven-dried 100-mL round-bottomed flask was equipped with a magnetic stir bar and short path distillation head. The flask was charged with ethyl carbamate (5.60 g, 25 mmol) and potassium carbonate (0.14 g, 1.01 mmol). The reaction was heated to 125-130 °C under reduced pressure (ca. 40 mmHg) until gas evolution has stopped. The reaction mixture was allowed to cool to room temperature to afford a brown oily solid. The crude product was recrystallized from 1:2 EtOAc – hexanes to yield the chiral oxazolidinone as a light orange colored solid (1.86 g, 52% yield). ^1H NMR (400 MHz, CDCl_3) δ 7.38 - 7.27 (m, 3H), 7.21 - 7.16 (m, 2H), 5.16 (bs,

1H), 4.48 (dd, $J = 8.6, 8.0$ Hz, 1H), 4.16 (dd, $J = 8.6, 5.5$ Hz, 1H), 4.13 – 4.03 (m, 1H), 2.94 - 2.81 (m, 2H). ^{13}C NMR (126 MHz, CDCl_3) δ 159.7, 136.0, 129.1, 128.9, 127.2, 69.5, 53.8, 41.3.

(4S)-4-benzyl-3-((2R,3R)-5-((R)-3-((tert-butyldimethylsilyloxy)butyl)-2-(3-((tert-butyldimethylsilyloxy)propyl)-5-hydroxytetrahydrofuran-3-carbonyl)oxazolidin-2-one
(177)

An oven-dried 100-mL round-bottomed flask equipped with a magnetic stir bar and nitrogen gas inlet was charged with anhydrous dichloromethane (9 mL) and cooled to 0 °C in an ice-water bath. Neat diethylzinc (0.16 mL, 1.50 mmol) was added via syringe in one portion followed by dropwise addition of diiodomethane (0.12 mL, 1.50 mmol) over 5 min. The reaction mixture was allowed to stir for 10 min at 0 °C during which time a milky white suspension was formed. At this time β -keto imide **175** (0.22 g, 0.50 mmol) dissolved in dichloromethane (3 mL), was added via syringe in one portion and allowed to stir at 0 °C for 30 min. *tert*-Butyldimethylsilyl-protected aldehyde **176** (0.12 g, 0.6 mmol) was added via syringe in one portion to the reaction flask and stirred at 0 °C for 40 min. The reaction mixture was quenched with saturated ammonium chloride (6 mL) and the organic layer was separated. The aqueous layer was extracted with dichloromethane (3 x 5 mL). The combined organic extracts were washed with brine, dried over sodium sulfate, filtered and concentrated on a rotary evaporator to yield the crude product as a yellow oil. The crude mixture was purified by flash column chromatography on silica, eluting with a gradient mobile phase of 2%,5%,7%,8%,10%,12%,15%,20%,25%,30%,35%,40% ethyl acetate in hexane to afford the title compound **177** as a mixture of open-hemiacetal isomers as a yellow oil (0.23 g, 70%). It was not possible to identify the specific ^1H NMR resonances that resulted from the ketone and

hemiacetal form, although the relative integration of the Ph, *t*Bu, Si-Me and Me resonances were consistent with the chain extension aldol product. ¹H NMR (400 MHz, CDCl₃) δ 7.37 - 7.17 (m, 5H), 4.76 - 4.61 (m, 2H), 4.51 - 4.36 (m, 1H), 4.36 - 4.09 (m, 3H), 4.05 (ddd, *J* = 10.3, 5.2, 3.5 Hz, 1H), 3.99 - 3.75 (m, 2H), 3.72 - 3.57 (m, 2H), 3.40 (dd, 1H), 3.30 - 3.10 (m, 2H) 2.84 - 2.69 (m, 2H), 2.63 - 2.43 (m, 2H), 2.36 (dd, *J* = 13.6, 10.2 Hz, 1H), 2.26 (dd, *J* = 13.6, 9.2 Hz, 1H), 2.17 - 2.10 (m, 1H), 1.95 - 1.50 (m, 8H), 1.43 (s, OH), 1.16 (d, *J* = 6.2 Hz, 1.5 H) 1.15 (d, *J* = 6.1 Hz, 1.5 H), 1.11 (d, *J* = 6.1 Hz, 3H) 0.89 (s, 9H), 0.88 (s, 3H), 0.87 (s, 2 H), 0.06 (s, 6H), 0.05 (s, 2H), 0.04 (s, 2H). ¹³C NMR (101 MHz, CDCl₃) 215.3, 214.9, 181.8, 181.2, 179.8, 179.7, 159.0, 158.8, 158.3, 141.1, 140.7, 140.2, 140.2, 134.8, 134.4, 134.3, 132.6, 132.6, 132.5, 112.3, 111.7, 87.2, 86.3, 76.6, 74.0, 73.8, 73.0, 72.8, 71.7, 71.5, 71.3, 68.7, 68.6, 68.3, 61.1, 60.7, 53.2, 52.8, 52.5, 49.5 49.3, 46.3, 45.5, 45.3, 45.0, 44.2, 44.0, 43.7, 43.1, 42.6, 41.8, 41.2, 39.7, 39.2, 38.5, 37.6, 37.3, 37.2, 35.7, 34.8, 34.6, 34.4, 31.3, 31.3, 29.2, 29.1, 28.6. Evidence of hemiacetal in the ¹³C resonances at 112.3 and 111.7 ppm and evidence of ketone isomer at peaks 215.3 and 214.9 ppm.

(*S*)-1-(Phenoxy carbonyl) pyrrolidine-2-carboxylic acid (286)

An oven-dried 100-mL round-bottomed flask equipped with a rubber septum, magnetic stir bar was charged with L-proline (2.9 g, 25 mmol) in aqueous sodium carbonate (0.75 M, 6.9 g in 87 mL water). The reaction flask was cooled to 0 °C in an ice-water bath to which the phenyl chloroformate (3.14 mL, 25 mmol) was added in a dropwise fashion over 3 min via syringe. The reaction mixture was warmed to room temperature and stirred overnight. The reaction mixture was then washed with ethyl acetate (2 x 50 mL) and the aqueous layer was acidified to pH 1 using concentrated HCl (*ca.* 15 mL). The acidified aqueous layer was extracted with ethyl acetate (4 x 75 mL). The organic layers were combined, dried over sodium sulfate and

concentrated *in vacuo* to yield the crude product as an yellow oily residue. Diethyl ether (3 x 25 mL) was added to the crude oily residue, sonicated and then removed on the rotary evaporator to yield the **286** as a white crystalline solid (5.26 g, 89.6%) (m.p. 93.4 – 95.5 °C) ($R_f = 0.26$; 1:1 hexane: ethyl acetate); ^1H NMR (400 MHz, CDCl_3) δ 10.89 (s, 1H), 7.40 – 7.05 (m, 5H) 4.47 (dd, $J = 8.5, 3.8$ Hz, 1H), 3.82 - 3.47 (m, 2H), 2.42 - 1.89 (m, 4H). ^{13}C NMR (101 MHz, CDCl_3) mixture of rotameric forms δ 177.75, 176.82, 153.55, 152.58, 150.71, 128.93, 125.16, 121.33, 59.05, 58.73, 46.77, 30.63, 29.33, 24.06, 23.13. IR (neat) ν 2972, 2668, 1657, 1411, 1196, 1162 cm^{-1} .

4-(Dimethylamino)pyridin-1-ium(S)-(2,2-dimethyl-4,6-dioxo-1,3-dioxan-5-ylidene)(1-(phenoxycarbonyl)pyrrolidin-2-yl)methanolate (287)

An oven-dried 250-mL round-bottomed flask equipped with a rubber septum, magnetic stir bar and nitrogen gas inlet was charged with anhydrous dichloromethane (15 mL) and cooled to 0 °C in an ice-water bath. Phenyl carbamate protected L-proline **286** (1.90 g, 8 mmol) dissolved in dry dichloromethane (10 mL) was added to the reaction flask. Dicyclohexylcarbodiimide (1.65 g, 8 mmol), Meldrums acid (1.15 g, 8 mmol) and *N,N'*-dimethylaminopyridine (0.98 g, 8 mmol) were added in the indicated order as solids in one portion to the reaction mixture at 0 °C. The reaction mixture turned yellow on the addition of *N,N'*-dimethylaminopyridine. The reaction mixture was allowed to stir at room temperature for 12 h at which time the reaction mixture was filtered to remove *N,N'*-dicyclohexylurea byproduct and then concentrated on a rotary evaporator to yield an foamy yellow solid. The crude solid was dissolved in minimal amount of ethyl acetate, diluted with diethyl ether and concentrated *in vacuo* three times to afford the title compound **287** as an fluffy yellow solid (3.61 g, 88%) (m.p. 66 – 70 °C). The product was carried on without further purification. ^1H NMR (500 MHz,

CDCl₃) mixture of rotameric forms δ 8.23 (d, $J = 7.5$ Hz, 2H), 7.34 - 6.92 (m, 5H), 6.56 (d, $J = 7.5$ Hz, 2H), 5.75 (dd, $J = 8.8, 3.4$ Hz, 1H), 3.87 - 3.53 (m, 2H), 3.14 (s, 6H), 2.60 - 2.48 (m, 1H), 2.09 - 1.97 (m, 1H), 1.96 - 1.84 (m, 2H), 1.77 (s, 1H), 1.65 (s, 6H). ¹³C NMR (126 MHz, CDCl₃) mixture of rotameric forms δ 196.05, 194.90, 166.32, 156.92, 153.75, 153.09, 151.58, 140.94, 128.99, 128.89, 128.75, 124.67, 124.43, 121.91, 121.61, 106.32, 101.14, 100.97, 87.24, 65.02, 47.93, 39.86, 31.60, 31.03, 27.50, 26.28, 23.79, 23.04. IR (neat) ν 2953, 1715, 1640, 1598, 1556, 1492, 1442, 1378, 1318, 1261, 1198, 1160 cm⁻¹.

(S)-phenyl 2-(3-oxo-3-(2-oxooxazolidin-3-yl)propanoyl)pyrrolidine-1-carboxylate (289)

An oven-dried 250-mL round-bottomed flask equipped with a rubber septum, magnetic stir bar and nitrogen gas inlet was charged with DMAP salt XX (3.86 g, 8 mmol) and DOWEX 50W-X2 ion exchange resin (12 g, 1.5 g of DOWEX for 1 mmol of DMAP salt) in anhydrous dichloromethane (20 mL) and stirred at room temperature for 3 h. The resin was removed by filtration and filtrate concentrated on a rotary evaporator to afford the crude free acid **288** (2.41 g, 6.67 mmol) as a yellowish gummy solid, which was then dried on high vacuum line overnight.

An oven-dried 250-mL round-bottomed flask equipped with a rubber septum, magnetic stir bar and nitrogen gas inlet was charged with free acid **288** (2.41 g, 6.67 mmol) and 2-oxazolidone (0.64 g, 7.33 mmol) in anhydrous toluene (150 mL). The reaction mixture was refluxed for 5 h and monitored by TLC. The reaction mixture was then cooled to room temperature and then washed with water (50 mL) and brine (50 mL). The organic layer was then dried over sodium sulfate, filtered and concentrated on a rotary evaporator to yield the crude title compound **289** as a yellow viscous oil. The crude product was purified by flash column chromatography on silica, eluting with 50% ethyl acetate in hexane ($R_f = 0.1, 1:1$

hexane:ethylacetate) to afford the title compound as a white crystalline solid (1.73 g, 75%) (m.p. 52.4 – 53.8 °C), as a mixture of carbamate rotamers and also keto-enol isomers.

¹H NMR (400 MHz, CDCl₃) *major keto tautomer* δ 7.40 – 7.30 (m, 2H), 7.22 – 7.07 (m, 3H), 4.65 (dd, *J* = 8.0, 5.1 Hz, 1H), 4.46 – 4.38 (m, 2H), 4.25 (AB, 2H), 4.12 - 4.01 (m, 2H), 3.80 - 3.59 (m, 2H), 2.40 - 1.90 (m, 4H). ¹³C NMR (101 MHz, CDCl₃) mixture of keto-enol and rotameric forms δ 202.83, 202.53, 166.50, 166.38, 153.89, 152.91, 151.34, 151.11, 129.50, 125.72, 125.63, 121.84, 65.60, 65.42, 62.50, 48.54, 47.70, 47.57, 42.48, 29.84, 28.67, 24.68, 23.73. IR (neat) ν 3340, 2980, 1773, 1696, 1593, 1570, 1492, 1476, 1455, 1385, 1364, 1338, 1303, 1196, 1162, 1119 cm⁻¹.

**(*S*)-phenyl 2-((1*S*,5*S*)-3-oxo-2-oxabicyclo[3.1.0]hexan-1-yl)pyrrolidine-1-carboxylate (290)
and (*S*)-phenyl 2-((1*R*,5*R*)-3-oxo-2-oxabicyclo[3.1.0]hexan-1-yl)pyrrolidine-1-carboxylate
(291)**

An oven-dried 100-mL round bottomed flask equipped with a magnetic stir bar and nitrogen gas inlet was charged with anhydrous dichloromethane (30 mL) and cooled to 0 °C in an ice-water bath. Diethylzinc (0.60 mL, 5.77 mmol) was added to the reaction mixture via syringe at 0 °C and allowed to stir for 5 min. Diiodomethane (0.92 mL, 11.5 mmol) was added to the solution dropwise via syringe over a 5 min period and the reaction mixture was stirred at 0 °C for 15 min. β-keto imide **289** (0.4 g, 1.15 mmol) dissolved in anhydrous dichloromethane (10 mL) was added to the milky white suspension via syringe and then allowed the reaction mixture to stir at room temperature for 3 h. The progress of the reaction was monitored by thin layer chromatography. The reaction was then quenched with saturated ammonium chloride (15 mL). The organic layer was separated, washed with water (15 mL), brine (15 mL), dried over anhydrous sodium sulfate and concentrated via rotary evaporation to afford a 2.5 : 1 mixture of

diastereomers as a yellow oil. The crude residue was purified by flash column chromatography on silica, eluting with a gradient mobile phase of 2%, 4%, 6%, 8%, 10%, 12%, 14%, 16%, 18%, 20%, 22%, 24%, 26%, 28%, 30%, 32%, 34%, 36%, 38%, 40% ethyl acetate in hexane ($R_f = 0.42$ 1:1 Hexane : ethyl acetate) to afford the title compound **290**, the major diastereomer, as a mixture of carbamate rotamers, as an yellow oil (0.108 g, 33% yield).

^1H NMR (400 MHz, C_6D_6) **Major diastereomer (290)** δ 7.29 - 6.87 (m, 5H), 3.49 - 3.19 (m, 3H), 2.53 (dd, $J = 18.6, 6.9$ Hz, 1H), 1.94 (d, $J = 18.5$ Hz, 1H), 1.88 – 1.73 (m, 2H), 1.54 – 1.44 (m, 1H), 1.40 - 1.18 (m, 2H), 0.31 (t, $J = 7.9$ Hz, 1H), 0.03 (t, $J = 6.2$ Hz, 1H). ^{13}C NMR (101 MHz, C_6D_6) δ 175.3, 153.3, 152.1, 129.3, 125.2, 122.1, 68.6, 60.3, 47.9, 33.4, 29.5, 24.0, 17.4, 17.2. IR (neat) ν 2360, 2341, 2159, 1977, 1772, 1493, 1455, 11359, 1200, 1165, 1100, 1059. **Minor diastereomer (291)** ($R_f = 0.38$, 1:1 Hexane: ethylacetate) ^1H NMR (400 MHz, C_6D_6) δ 7.25 – 6.90 (m, 5H), 3.80 (d, $J = 8.6$ Hz, 1H), 3.37 - 3.31 (m, 1H), 3.30 - 3.20 (m, 1H), 2.18 (dd, $J = 18.6, 6.8$ Hz, 1H), 1.87 (d, $J = 18.7$ Hz, 1H), 1.82 – 1.70 (m, 1H), 1.66 - 1.56 (m, 2H), 1.50 – 1.39 (m, 1H), 1.17 (t, $J = 8.9$ Hz, 1H), 0.69 (t, $J = 7.9$ Hz, 1H), 0.26 (t, $J = 6.1$ Hz, 1H). ^{13}C NMR (101 MHz, C_6D_6) δ 174.8, 157.0, 153.5, 129.3, 125.2, 122.0, 68.7, 59.5, 47.3, 33.2, 28.5, 24.1, 19.5, 13.5.

(S)-phenyl-2-((1S,2S)-2-(2-(benzylamino)-2-oxoethyl)-1-hydroxycyclopropyl)pyrrolidine-1-carboxylate (292) and (S)-phenyl 2-((1R,2R)-2-(2-(benzylamino)-2-oxoethyl)-1-hydroxycyclopropyl)pyrrolidine-1-carboxylate (293)

An oven-dried 10 mL round-bottomed flask equipped with a magnetic stir bar and nitrogen gas inlet was charged with lactones containing mostly major diastereomer **290** and some minor diastereomer **291** (86 mg, 0.30 mmol) in benzylamine (200 μL , 1.5 mmol). The reaction

mixture was stirred at room temperature overnight. Ethyl acetate (3 mL) was added and washed with 2 N HCl (3 x 5 mL). The ethyl acetate layer was separated, dried over sodium sulfate, filtered and concentrated on a rotary evaporator to yield the crude reaction mixture containing both major and minor diastereomers as a yellow oil. The crude reaction mixture was purified by preparative thin layer chromatography, eluting four times with 30% methyl *tert*-butyl ether in hexane (140 mL) by adding 10 mL of methanol each time to the above eluting solvent containing 30% MTBE in hexane ($R_f = 0.19$, 1:1 hexane:ethyl acetate) to afford the title compound **292**, the major diastereomer containing carbamate rotamers as a white solid (0.086 g, 73% overall yield). ^1H NMR (400 MHz, C_6D_6) δ 7.37 - 7.28 (m, 2H), 7.14 - 6.85 (m, 8H), 5.95 (s, NH), 4.39 (dd, $J = 14.6, 6.3$ Hz, 1H), 3.97 (dd, $J = 14.6, 5.4$ Hz, 1H), 3.71 - 3.63 (m, 1H), 3.58 - 3.45 (m, 1H), 3.33 (dd, $J = 8.8, 3.5$ Hz, 1H), 2.23 (d, $J = 4.5$ Hz, 1H), 2.19 - 2.02 (m, 3H), 1.72 - 1.50 (m, 2H), 1.46 - 1.33 (m, 2H), 0.57 - 0.48 (m, 2H). ^{13}C NMR (126 MHz, C_6D_6) δ 173.5, 153.9, 152.5, 139.0, 129.1, 128.6, 128.5, 127.3, 124.9, 122.6, 65.5, 59.6, 48.3, 43.7, 36.8, 29.2, 24.5, 23.1, 18.1. IR (neat) ν 3330, 2972, 1780, 1715, 1647, 1594, 1538, 1454, 1383, 1160, 1061, 1024.

(S)-Phenyl2-((1R,2R)-2-(2-(benzylamino)-2-oxoethyl)-1-hydroxycyclopropyl)pyrrolidine-1-carboxylate

The minor diastereomer existing of its carbamate rotamers was obtained as a white solid ($R_f = 0.21$, 1:1 hexane:ethyl acetate). ^1H NMR (400 MHz, C_6D_6) δ 7.37-7.17 (m, 2H), 7.14 - 6.85 (m, 8H), 5.75 (t, $J = 6.1$ Hz, NH), 4.46 - 4.17 (m, 2H), 3.94 - 3.79 (m, 1H), 3.46 - 3.37 (m, 1H), 3.22 - 3.04 (m, 1H), 2.27 - 2.15 (tt, $J = 9.2, 4.5$ Hz, 0H), 1.48 - 1.25 (m, 6H), 1.15 - 0.88 (m, 4H), 0.80 - 0.70 (m, 1H). ^{13}C NMR (101 MHz, C_6D_6) δ 176.17, 155.50, 152.02, 139.82, 129.51, 128.72, 128.62, 127.28, 125.55, 122.31, 65.27, 60.07, 48.42, 43.41, 40.06, 28.85, 24.51, 24.06, 18.54, 18.12.

N-Benzyl-2-((1S,2S,7a'S)-3'-oxotetrahydro-3'H-spiro[cyclopropane-1,1'-pyrrolo[1,2-c]oxazol]-2-yl)acetamide (297)

An oven-dried 10 mL round-bottomed flask equipped with a magnetic stir bar and nitrogen gas inlet was charged with cyclopropanol amide **290** (34 mg, 0.08 mmol) in anhydrous tetrahydrofuran (3 mL) and cooled to 0 °C in an ice-water bath. Potassium t-butoxide (24 mg, 0.21 mmol) was added as a solid in portions to the reaction mixture, upon which the solution turned yellow. The reaction mixture was stirred at 0 °C for 50 min. Water (2 mL) was added and the reaction mixture was extracted with ethyl acetate (3 x 5 mL), organic layers were combined, dried over sodium sulphate, gravity filtered and concentrated *in vacuo* to yield the crude reaction mixture as an oil. The crude reaction mixture was purified by preparative thin layer chromatography, eluting with 50 % ethyl acetate in hexane ($R_f = 0.11$, 1 : 1 hexane : ethyl acetate) and obtained as a white solid (22 mg, 90% yield). ^1H NMR (500 MHz, C_6D_6) δ 7.20 - 7.03 (m, 5H), , 6.15 (bs, NH), 4.30 (AB, $J = 14.9, 5.9$ Hz, 2H), 3.45 (dt, $J = 11.3, 7.9$ Hz, 1H), 2.99 (dd, $J = 9.8, 5.8$ Hz, 1H), 2.72 (ddd, $J = 11.2, 9.3, 3.9$ Hz, 1H), 2.28 - 2.04 (m, 2H), 1.38 - 1.24 (m, 2H), 1.13 - 1.03 (m, 1H), 1.01 - 0.95 (m, 1H), 0.92 - 0.80 (m, 1H) 0.59 (t, $J = 7.1$ Hz, 1H), 0.52 (dd, $J = 10.1, 7.1$ Hz, 1H). ^{13}C NMR (126 MHz, C_6D_6) δ 171.6, 160.7, 129.8, 128.7, 128.6, 127.3, 66.5, 64.7, 46.4, 43.7, 34.8, 29.0, 25.2, 20.1, 12.8. IR neat ν 3316, 2916, 1722, 1672, 1540, 1496, 1420, 1363, 1211, 1076.

(S)-phenyl 2-(3-((S)-4-benzyl-2-oxooxazolidin-3-yl)-3-oxopropanoyl)pyrrolidine-1-carboxylate (298)

An oven-dried 250-mL round-bottomed flask equipped with a rubber septum, magnetic stir bar and nitrogen gas inlet was charged with free acid **286** (1.30 g, 3.61 mmol) and chiral oxazolidinone (0.70 g, 3.97 mmol) in anhydrous toluene (150 mL). The reaction mixture was

refluxed for 5 h and monitored by TLC. The reaction mixture was then cooled to room temperature and then washed with water (50 mL) and brine (50 mL). The organic layer was dried over sodium sulfate, filtered and concentrated on a rotary evaporator to yield the crude title compound **298** as yellow viscous oil. The crude product was purified by flash column chromatography on silica, eluting with 25% ethyl acetate in hexane ($R_f = 0.1$, 1:1 hexane:ethylacetate) to afford the title compound **298** as a white crystalline solid (1.18 g, 75% yield) (m.p. 131.2 – 133.1 °C), as a mixture of carbamate rotamers and also keto-enol isomers. ^1H NMR (500 MHz, CDCl_3) δ 7.40 - 7.26 (m, 5H), 7.24 - 7.09 (m, 5H), 4.76 - 4.64 (m, 2H), 4.35 (dd, $J = 16.9, 4.5$ Hz, 1H), 4.23 - 4.13 (m, 3H), 3.78 - 3.58 (m, 2H), 3.40 – 3.32 (m, 1H), 2.84 – 2.72 (m, 1H), 2.38 – 2.26 (m, 1H), 2.23 - 2.13 (m, 1H), 2.02 - 1.92 (m, 2H). ^{13}C NMR (126 MHz, CDCl_3) δ 202.6, 202.4, 166.3, 166.2, 153.8, 153.7, 152.8, 151.2, 151.0, 135.2, 135.1, 129.5, 129.5, 129.3, 129.3, 129.3, 129.0, 129.0, 127.4, 127.4, 125.5, 125.5, 66.5, 66.1, 65.5, 65.3, 55.1, 48.7, 47.9, 47.5, 47.4, 37.7, 30.4, 29.6, 28.4, 24.5, 23.5.

(S)-phenyl2-(2-((1R,2S)-2-((S)-4-benzyl-2-oxooxazolidin-3-yl)-2-((trimethylsilyl)oxy)cyclopropyl)acetyl)pyrrolidine-1-carboxylate (299)

An oven-dried 100-mL round bottomed flask equipped with a magnetic stir bar and nitrogen gas inlet was charged with anhydrous dichloromethane (20 mL) and cooled to 0 °C in an ice-water bath. Neat diethylzinc (0.14 mL, 1.40 mmol) was added in one portion via an oven-dried needle followed by dropwise addition of diiodomethane (0.23 mL, 2.80 mmol) over the course of 5 min. The reaction was allowed to stir at 0 °C for 10 min at which time a milky white suspension was formed. Trimethylsilyl chloride (0.04 mL, 0.31 mmol) followed by β -keto imide **298** (0.12 g, 0.28 mmol) dissolved in dichloromethane (6 mL) was added to the reaction mixture.

The reaction mixture was allowed to stir at 0 °C for 30 min and then allowed to warm to room temperature. The reaction mixture was allowed to stir at room temperature for 5 h. The crude reaction mixture was quenched with saturated ammonium chloride (10 mL). The layers were separated and the aqueous layer was extracted with dichloromethane (3 X 15 mL). All the organic layers were combined and washed with brine, dried over sodium sulfate, filtered and concentrated in vacuo. The crude reaction mixture was purified by preparative thin layer chromatography where the plate was first eluted with 10% ethyl acetate in hexane (180 mL). Additional amount of ethyl acetate (35 mL) was added to the above eluting solvent to increase the polarity and the plate was eluted again to afford **299** (0.09 g, 62% yield) (R_f = 0.42; 1:1 EtoAc: Hexane) as a mixture of diastereomers in a diastereomeric ratio of 5:1. **Major diastereomer and its rotamer** ¹H NMR (500 MHz, C₆D₆) δ 7.42 - 7.33 (m, 3H), 7.23 - 7.17 (m, 3H), 7.16 - 6.83 (m, 10H), 4.30 (dd, *J* = 8.5, 5.5 Hz, 1H), 4.25 - 4.20 (m, 1H), 4.05 - 3.96 (m, 2H), 3.71 (dt, *J* = 8.8, 3.9 Hz, 1H), 3.58 (dd, *J* = 12.9, 3.7 Hz, 1H), 3.53 - 3.48 (m, 1H), 3.48 - 3.37 (m, 3H), 3.37 - 3.26 (m, 3H), 2.70 (dd, *J* = 18.4, 3.3 Hz, 1H), 2.63 - 2.57 (m, 1H), 2.52 - 2.42 (m, 1H), 2.42 - 2.33 (m, 2H), 2.27 - 2.20 (m, 1H), 1.64 - 1.49 (m, 4H), 1.48 - 1.34 (m, 3H), 1.33 - 1.26 (m, 2H), 1.24 - 1.09 (m, 3H), 0.99 - 0.89 (m, 1H), 0.80 - 0.74 (m, 2H), 0.28 (s, 9H), 0.22 (s, 6H). ¹³C NMR (126 MHz, C₆D₆) δ 209.0, 208.8, 156.0, 155.9, 153.2, 152.5, 152.0, 151.80, 137.5, 137.1, 130.1, 129.9, 129.4, 129.3, 129.0, 128.9, 127.1, 126.9, 125.3, 121.8, 121.8, 66.6, 66.5, 66.4, 66.1, 66.1, 58.0, 47.7, 47.3, 40.7, 40.7, 37.5, 37.1, 30.2, 28.9, 24.5, 23.6, 22.3, 22.1, 18.9, 18.7, 1.07, 1.00.

TBAF rearrangement of TMS cyclopropanol (299)

An oven-dried 100 mL round bottomed flask equipped with a magnetic stir bar and nitrogen gas inlet was charged with TMS cyclopropanol **299** (25.4 mg, 0.05 mmol) in anhydrous

THF (5 mL). Tetra-*n*-butylammonium fluoride (1M in THF) (0.05 mL, 0.05 mmol) was added to the reaction mixture and stirred at room temperature overnight. The reaction mixture was quenched with saturated ammonium chloride and the layers were separated. The aqueous layer was extracted with diethyl ether (3 X 5 mL). The ether extracts were combined, dried over sodium sulfate, filtered and concentrated in vacuo. The crude reaction mixture was purified using preparative thin layer chromatography. The plate was eluted with 20% ethyl acetate in hexane to yield the bicyclic lactone **290**. δ 7.29 - 6.87 (m, 5H), 3.49 - 3.19 (m, 3H), 2.53 (dd, J = 18.6, 6.9 Hz, 1H), 1.94 (d, J = 18.5 Hz, 1H), 1.88 – 1.73 (m, 2H), 1.54 – 1.44 (m, 1H), 1.40 - 1.18 (m, 2H), 0.31 (t, J = 7.9 Hz, 1H), 0.03 (t, J = 6.2 Hz, 1H). ^{13}C NMR (101 MHz, C_6D_6) δ 175.3, 153.3, 152.1, 129.3, 125.2, 122.1, 68.6, 60.3, 47.9, 33.4, 29.5, 24.0, 17.4, 17.2.

(*S*)-phenyl 2-(3-((*R*)-4-benzyl-2-oxooxazolidin-3-yl)-3-oxopropanoyl)pyrrolidine-1-carboxylate (301**)**

An oven-dried 250-mL round bottomed flask equipped with a rubber septum, magnetic stir bar and nitrogen gas inlet was charged with free acid **288** (2.91 g, 8.05 mmol) and chiral oxazolidinone derived from *R*-phenylalanine (1.57 g, 8.86 mmol) in anhydrous toluene (150 mL). The reaction mixture was refluxed for 5 h and monitored by TLC. The reaction mixture was then cooled to room temperature and then washed with water (50 mL) and brine (50 mL). The organic layer was then dried over sodium sulfate, filtered and concentrated on a rotary evaporator to yield the crude title compound **301** as yellow viscous oil. The crude product was purified by flash column chromatography on silica, eluting with 50% ethyl acetate in hexane (R_f = 0.1, 1:1 hexane:ethylacetate) to afford the title compound **301** as a white crystalline solid (m.p. 132.5 – 134.8 °C), as a mixture of carbamate rotamers and also keto-enol isomers. ^1H NMR (400

MHz, CDCl₃) δ 7.39 - 7.26 (m, 5H), 7.25 - 7.09 (m, 5H), 4.76 - 4.64 (m, 2H), 4.35 (dd, $J = 16.8$, 11.5 Hz, 1H), 4.25 - 4.14 (m, 3H), 3.85 - 3.61 (m, 2H), 3.41 (ddd, $J = 13.0, 9.0, 3.4$ Hz, 1H), 2.86 - 2.72 (m, 1H), 2.42 - 1.91 (m, 4H). ¹³C NMR (101 MHz, CDCl₃) mixture of rotamers δ 203, 202.7, 166.3, 154.0, 152.9, 151.3, 151.1, 135.5, 135.3, 129.6, 129.5, 129.2, 127.6, 127.5, 125.7, 125.6, 121.8, 88.3, 88.2, 66.6, 66.2, 65.6, 65.4, 60.6, 60.5, 55.3, 48.9, 48.1, 47.7, 47.5, 37.8, 30.9, 29.8, 28.7, 24.7, 24.3, 23.7.

(*S*)-phenyl2-(2-((1*S*,2*R*)-2-((*R*)-4-benzyl-2-oxooxazolidin-3-yl)-2-((trimethylsilyloxy)cyclopropyl)acetyl)pyrrolidine-1-carboxylate (302)

An oven-dried 100-mL round bottomed flask equipped with a magnetic stir bar and nitrogen gas inlet was charged with anhydrous dichloromethane (20 mL) and cooled to 0 °C in an ice-water bath. Neat diethylzinc (0.24 mL, 2.30 mmol) was added in one portion via an oven-dried needle followed by dropwise addition of diiodomethane (0.37 mL, 4.60 mmol) over the course of 5 min. The reaction was allowed to stir at 0 °C for 10 min at which time a milky white suspension was formed. Trimethylsilyl chloride (0.05 mL, 0.51 mmol) followed by β -keto imide **301** (0.20 g, 0.46 mmol) dissolved in dichloromethane (15 mL) was added to the reaction mixture. The reaction mixture was allowed to stir at 0 °C for 30 min and then allowed to warm to room temperature. The reaction mixture was allowed to stir at room temperature for 5 h. The crude reaction mixture was quenched with saturated ammonium chloride (20 mL). The layers were separated and the aqueous layer was extracted with dichloromethane (3 X 20 mL). All the organic layers were combined and washed with brine, dried over sodium sulfate, filtered and concentrated in vacuo. The crude reaction mixture was purified by preparative thin layer chromatography where the plate was first eluted with 10% ethyl acetate in hexane (180 mL). Additional amount of ethyl acetate (35 mL) was added to the above eluting solvent to increase

the polarity and the plate was eluted again to afford the TMS cyclopropanol **302** as a mixture of diastereomers in a diastereomeric ratio of 5:1. *Major diastereomer and its rotamer* ^1H NMR (500 MHz, C_6D_6) δ 7.42 - 7.38 (m, 2H), 7.37 - 7.33 (m, 1H), 7.25 (m, 3H), 7.20 - 7.15 (m, 6H), 7.14 - 7.02 (m, 5H), 6.95 - 6.90 (m, 2H), 4.33 (dd, $J = 8.3, 3.9$ Hz, 1H), 4.26 (dd, $J = 8.0, 4.6$ Hz, 1H), 4.10 - 3.98 (m, 2H), 3.76 - 3.71 (m, 2H), 3.65 - 3.53 (m, 2H), 3.53 - 3.48 (m, 1H), 3.42 (dd, $J = 12.8, 3.5$ Hz, 1H), 3.39 - 3.33 (m, 2H), 3.29 (dt, $J = 10.2, 7.4$ Hz, 1H), 2.64 (dd, $J = 18.7, 3.2$ Hz, 1H), 2.48 (dd, $J = 12.8, 11.0$ Hz, 2H), 2.32 (dd, $J = 18.7, 3.2$ Hz, 1H), 2.20 - 2.07 (m, 2H), 1.70 - 1.50 (m, 6H), 1.49 - 1.40 (m, 1H), 1.32 - 1.16 (m, 4H), 0.75 (td, $J = 6.8, 2.3$ Hz, 2H), 0.26 (s, 9H), 0.25 (s, 6H). ^{13}C NMR (126 MHz, C_6D_6) δ 208.5, 208.4, 156.0, 156.0, 153.2, 152.5, 152.2, 152.1, 137.2, 137.0, 130.0, 130.0, 129.4, 129.3, 129.0, 129.0, 128.3, 127.1, 127.0, 77.8, 66.5, 66.1, 66.0, 64.8, 58.0, 58.0, 55.6, 47.5, 47.2, 40.8, 40.7, 39.3, 38.5, 29.7, 28.7, 24.2, 23.1, 22.1, 22.1, 18.8, 18.8, 1.07, 1.05, 0.83, 0.74.

TBAF rearrangement of TMS cyclopropanol (302)

An oven-dried 100 mL round bottomed flask equipped with a magnetic stir bar and nitrogen gas inlet was charged with TMS cyclopropanol **302** (25.4 mg, 0.05 mmol) in anhydrous THF (5 mL). Tetra-*n*-butylammonium fluoride (1M in THF) (0.05 mL, 0.05 mmol) was added to the reaction mixture and stirred at room temperature overnight. The reaction mixture was quenched with saturated ammonium chloride and the layers were separated. The aqueous layer was extracted with diethyl ether (3 X 5 mL). The ether extracts were combined, dried over sodium sulfate, filtered and concentrated in vacuo. The crude reaction mixture was purified using preparative thin layer chromatography. The plate was eluted with 20% ethyl acetate in hexane to yield the bicyclic lactone **291**. ^1H NMR (400 MHz, C_6D_6) δ 7.25 - 6.90 (m, 5H), 3.80 (d, $J = 8.6$ Hz, 1H), 3.37 - 3.31 (m, 1H), 3.30 - 3.20 (m, 1H), 2.18 (dd, $J = 18.6, 6.8$ Hz, 1H), 1.87 (d, $J =$

18.7 Hz, 1H), 1.82 – 1.70 (m, 1H), 1.66 - 1.56 (m, 2H), 1.50 – 1.39 (m, 1H), 1.17 (t, $J = 8.9$ Hz, 1H), 0.69 (t, $J = 7.9$ Hz, 1H), 0.26 (t, $J = 6.1$ Hz, 1H). ^{13}C NMR (101 MHz, C_6D_6) δ 174.8, 157.0, 153.5, 129.3, 125.2, 122.0, 68.7, 59.5, 47.3, 33.2, 28.5, 24.1, 19.5, 13.5.

(2*S*)-phenyl-2-(2-(2-(2-oxooxazolidin-3-yl)-2-((trimethylsilyl)oxy)cyclopropyl)acetyl)pyrrolidine-1-carboxylate (320)

An oven-dried 250-mL round bottomed flask equipped with a rubber septum, magnetic stir bar and nitrogen gas inlet was charged with free acid **319** (0.50 g, 1.26 mmol) and chiral oxazolidinone derived from *R*-phenylalanine (0.23 g, 1.33 mmol) in anhydrous toluene (25 mL). The reaction mixture was refluxed for 5 h and monitored by TLC. The reaction mixture was then cooled to room temperature and then washed with water (15 mL) and brine (15 mL). The organic layer was then dried over sodium sulfate, filtered and concentrated on a rotary evaporator to yield the crude title compound XX as yellow viscous oil. The crude product was purified by flash column chromatography on silica, eluting with 20% ethyl acetate in hexane ($R_f = 0.1$, 1:1 hexane:ethylacetate) to afford the title compound **320** as a cream colored solid (0.26 g, 45% yield) (m.p. = 68.2 – 69.7 °C) ^1H NMR (500 MHz, CDCl_3) δ 7.75 – 7.71 (m, 2H), 7.41 - 7.21 (m, 7H), 4.80 – 4.72 (m, 1H), 4.52 (AB, 2H), 4.26 (td, $J = 8.5, 2.4$ Hz, 1H), 4.22 – 4.16 (m, 2H), 3.60 – 3.50 (m, 1H), 3.42 – 3.33 (m, 1H), 3.30 – 3.20 (m, 1H), 2.82 (ddd, $J = 12.6, 9.5, 2.5$ Hz, 1H), 2.45 (s, 3H), 2.29 - 2.20 (m, 1H), 1.92 – 1.82 (m, 1H), 1.68 - 1.49 (m, 2H). ^{13}C NMR (126 MHz, CDCl_3) δ 204.0, 166.8, 153.7, 144.2, 135.2, 133.5, 129.9, 129.5, 129.0, 127.8, 127.3, 67.3, 66.4, 55.1, 49.5, 48.5, 37.7, 28.7, 24.6, 21.6.

References

1. Dotz, K. H. Carbene Complexes in Organic-Synthesis. *Angew. Chem. Int. Ed.* **1984**, *23*, 587-608.
2. Cardin, D. J.; Cetinkay.B; Lappert, M. F. Transition Metal-Carbene Complexes. *Chem. Rev.* **1972**, *72*, 545.
3. Marek, I. Sp(3) organozinc carbenoid homologation in organic synthesis. *Tetrahedron* **2002**, *58*, 9463-9475.
4. Emschwiller, G. Effect of the zinc-copper couple on methylene iodide. *C. R. Hebd. Acad. Sci.* **1929**, *188*, 1555-1557.
5. Simmons, H. E.; Smith, R. D. A New Synthesis of Cyclopropanes from Olefins. *J. Am. Chem. Soc.* **1958**, *80*, 5322-5324.
6. Simmons, H. E.; Smith, R. D. A New Synthesis of Cyclopropanes. *J. Am. Chem. Soc.* **1959**, *81*, 4256-4264.
7. Voituriez, A.; Zimmer, L. E.; Charette, A. B. Preparation of a Storable Zinc Carbenoid Species and Its Application in Cyclopropanation, Chain Extension, and [2,3]-Sigmatropic Rearrangement Reactions. *J. Org. Chem.* **2010**, *75*, 1244-1250.
8. Furukawa, J.; Kawabata, N.; Nishimur.J. A Novel Route to Cyclopropanes from Olefins. *Tetrahedron Lett.* **1966**, 3353.
9. Furukawa, J.; Kawabata, N.; Nishimur.J. Synthesis of Cyclopropanes by Reaction of Olefins with Dialkylzinc and Methylene Iodide. *Tetrahedron* **1968**, *24*, 53.
10. Furukawa, J.; Kawabata, N.; Nishimura, J. A Stereospecific Synthesis of Cyclopropane Derivatives from Olefins. *Tetrahedron Lett.* **1968**, 3495.
11. Brogan, J. B.; Zercher, C. K. Zinc-mediated conversion of beta-keto esters to gamma-keto esters. *J. Org. Chem.* **1997**, *62*, 6444-6446.
12. Bierauge.H; Akkerman, J. M.; Armande, J. C. L.; Pandit, U. K. Specific Insertion of Carbenes into Carbon-Carbon Bonds. *Tetrahedron Lett.* **1974**, 2817-2820.
13. Grimm, E. L.; Reissig, H. U. 2-Siloxy-Substituted Methyl Cyclopropanecarboxylates as Building-Blocks in Synthesis - Efficient One-Pot Conversion to Gamma-Butyrolactones. *J. Org. Chem.* **1985**, *50*, 242-244.
14. Dowd, P.; Choi, S. C. Novel Free-Radical Ring-Expansion Reactions. *Tetrahedron* **1989**, *45*, 77-90.
15. Dowd, P.; Choi, S. C. A New Tri-Normal-Butyltin Hydride Based Rearrangement of Bromomethyl Beta-Keto-Esters - a Synthetically Useful Ring Expansion to Gamma-Keto Esters. *J. Am. Chem. Soc.* **1987**, *109*, 3493-3494.
16. Saigo, K.; Kurihara, H.; Miura, H.; Hongu, A.; Kubota, N.; Nohira, H.; Hasegawa, M. Conversion of 1,3-Dicarbonyls to 1,4-Dicarbonyls. *Synth. Commun.* **1984**, *14*, 787-796.
17. Bhogadhi, Y. N. D. Z., C. K. Formation of gamma-keto esters from beta-keto esters. *Org. Synth.* **2014**, *91*, 248-259.
18. Verbicky, C. A.; Zercher, C. K. Zinc-mediated chain extension of beta-keto phosphonates. *J. Org. Chem.* **2000**, *65*, 5615-5622.

19. Karanewsky, D. S.; Badia, M. C.; Cushman, D. W.; DeForrest, J. M.; Dejneka, T.; Loots, M. J.; Perri, M. G.; Petrillo, E. W., Jr.; Powell, J. R. (Phosphinyloxy)acyl amino acid inhibitors of angiotensin converting enzyme (ACE). 1. Discovery of (S)-1-[6-amino-2-[[hydroxy(4-phenylbutyl)phosphinyl]oxy]-1-oxohexyl]-L-proline a novel orally active inhibitor of ACE. *J. Med. Chem.* **1988**, *31*, 204-12.
20. Hilgenkamp, R.; Zercher, C. K. Zinc carbenoid-mediated chain extension of beta-keto amides. *Tetrahedron* **2001**, *57*, 8793-8800.
21. Lai, S.; Zercher, C. K.; Jasinski, J. P.; Reid, S. N.; Staples, R. J. Tandem chain extension-aldol reaction: Syn selectivity with a zinc enolate. *Org. Lett.* **2001**, *3*, 4169-4171.
22. Csakai, A. The tandem chain extension aldol reaction of B-keto imides. B.S. Thesis, University of New Hampshire, 2006.
23. Lin, W. I. Peptide isosteric replacement preparation using zinc-mediated chain extension-aldol reactions. II. Formal synthesis of (+)-Brefeldin A. III. Zinc-mediated chain extension reactions with substituted carbenoids. Ph.D. Dissertation, University of New Hampshire, 2006.
24. Henderson, T. J. M.S. Thesis, University of New Hampshire, 2009.
25. Sadlowski, C. B.S. Thesis, University of New Hampshire, 2008.
26. Eger, W. A.; Zercher, C. K.; Williams, C. M. A Mechanistic Investigation into the Zinc Carbenoid-Mediated Homologation Reaction by DFT Methods: Is a Classical Donor-Acceptor Cyclopropane Intermediate Involved? *J. Org. Chem.* **2010**, *75*, 7322-7331.
27. Aiken, K. S. The Tandem Chain Extension-Aldol reaction of α -keto esters. Ph.D. Dissertation, University of New Hampshire, 2005.
28. Pu, Q. M.S. Thesis, University of New Hampshire, 2007.
29. Taschner, I. S. I. Ph.D. Dissertation, University of New Hampshire, 2011.
30. Xue, S.; Li, L. Z.; Liu, Y. K.; Guo, Q. X. Zinc-mediated chain extension reaction of 1,3-diketones to 1,4-diketones and diastereoselective synthesis of trans-1,2-disubstituted cyclopropanols. *J. Org. Chem.* **2006**, *71*, 215-218.
31. Heathcock, C. H. D., H. Reversal of stereochemistry in the aldol reactions of a chiral boron enolate. *J. Org. Chem.* **1990**, *55*, 173-181.
32. Mower, M. P. B.S. Thesis, University of New Hampshire, 2012.
33. Moran, P. F. M.S. Thesis, University of New Hampshire, 2013.
34. Bala, K. Unpublished results. University of New Hampshire, **2015**.
35. Lin, W. M.; McGinness, R. J.; Wilson, E. C.; Zercher, C. K., Formation of beta-substituted gamma-keto esters via zinc carbenoid mediated chain extension. *Synthesis-Stuttgart* **2007**, 2404-2408.
36. Neuman, R. C.; Rahm, M. L. Synthesis and Nuclear Magnetic Resonance Spectra of Some 1-Halo-1-Iodoalkanes. *J. Org. Chem.* **1966**, *31*, 1857.
37. Bull, J. A.; Charette, A. B. Improved procedure for the synthesis of gem-diiodoalkanes by the alkylation of diiodomethane. Scope and limitations. *J. Org. Chem.* **2008**, *73*, 8097-8100.
38. Letsinger, R. L.; Kammeyer, C. W. The Preparation of Ethylidene Iodide. *J. Am. Chem. Soc.* **1951**, *73*, 4476-4476.
39. Friedrich, E. C.; Falling, S. N.; Lyons, D. E., Convenient Synthesis of Ethylidene Iodide. *Synth. Commun.* **1975**, *5*, 33-36.

40. Jung, M. E.; Mossman, A. B.; Lyster, M. A. Direct Synthesis of Dibenzocyclooctadienes Via Double Ortho Friedel-Crafts Alkylation by Use of Aldehyde-Trimethylsilyl Iodide Adducts. *J. Org. Chem.* **1978**, *43*, 3698-3701.
41. Charette, A. B.; Lemay, J. Diastereo- and enantioselective synthesis of 1,2,3-substituted cyclopropanes with zinc carbenoids. *Angew. Chem. Int. Ed.* **1997**, *36*, 1090-1092.
42. Starosci, Ja; Rickborn, B. Conformational Aspects of Directive Effect of Homoallylic Hydroxyl Group in Simmons-Smith Reaction. *J. Org. Chem.* **1972**, *37*, 738-&.
43. Kawabata, N.; Nakagawa, T.; Nakao, T.; Yamashita, S. Stereochemistry of Cycloaddition Reaction of Methylcarbenoid of Zinc to Cyclic Allylic Alcohols. *J. Org. Chem.* **1977**, *42*, 3031-3035.
44. Mazzone, J. R. Ph.D. Dissertation, University of New Hampshire, 2011.
45. Jacobine, A. M. Ph.D. Dissertation, University of New Hampshire, 2010.
46. Jacobine, A. M.; Puchlopek, A. L. A.; Zercher, C. K.; Briggs, J. B.; Jasinski, J. P.; Butcher, R. J. Tandem chain extension-Mannich reaction: an approach to beta-proline derivatives. *Tetrahedron* **2012**, *68*, 7799-7805.
47. Hilgenkamp, R.; Zercher, C. K. Tandem chain extension-homoenolate formation: The formation of alpha-methylated-gamma-keto esters. *Org. Lett.* **2001**, *3*, 3037-3040.
48. Ronsheim, M. D.; Zercher, C. K. Zinc carbenoid-mediated chain extension: Preparation of alpha,beta-unsaturated-gamma-keto esters and amides. *J. Org. Chem.* **2003**, *68*, 4535-4538.
49. Spencer, C. M. Ph.D. Dissertation, University of New Hampshire, 2013.
50. Dekker, J.; Budzelaar, P. H. M.; Boersma, J.; Vanderkerk, G. J. M.; Spek, A. L. The Nature of the Reformatsky Reagent - Crystal-Structure of (BrzncH2coo-Tert-Bu.Thf)2. *Organometallics* **1984**, *3*, 1403-1407.
51. Dekker, J.; Boersma, J.; Vanderkerk, G. J. M. The Structure of the Reformatsky Reagent. *J. Chem. Soc. Chem. Comm.* **1983**, 553-555.
52. Dewar, M. J. S.; Merz, K. M. The Reformatsky Reaction. *J. Am. Chem. Soc.* **1987**, *109*, 6553-6554.
53. Zimmerman, H. E.; Traxler, M. D. The Stereochemistry of the Ivanov and Reformatsky Reactions. *J. Am. Chem. Soc.* **1957**, *79*, 1920-1923.
54. Aiken, K. S.; Eger, W. A.; Williams, C. M.; Spencer, C. M.; Zercher, C. K. A Combined DFT and NMR Investigation of the Zinc Organometallic Intermediate Proposed in the Syn-Selective Tandem Chain Extension-Aldol Reaction of beta-Keto Esters. *J. Org. Chem.* **2012**, *77*, 5942-5955.
55. Lai, S. M.S. Thesis, University of New Hampshire, 2001.
56. Danda, H.; Hansen, M. M.; Heathcock, C. H. Acyclic Stereoselection Reversal of Stereochemistry in the Aldol Reactions of a Chiral Boron Enolate. *J. Org. Chem.* **1990**, *55*, 173-181.
57. Evans, D. A.; Takacs, J. M.; Mcgee, L. R.; Ennis, M. D.; Mathre, D. J.; Bartroli, J. Chiral Enolate Design. *Pure Appl. Chem.* **1981**, *53*, 1109-1127.
58. Jacobine, A. M.; Lin, W. M.; Walls, B.; Zercher, C. K. Formation of gamma-lactones through CAN-mediated oxidative cleavage of hemiketals. *J. Org. Chem.* **2008**, *73*, 7409-7412.

59. Ronsheim, M. D.; Zercher, C. K. Ring expansions of beta-keto lactones with zinc carbenoids: Syntheses of (+)-patulolide A and (+/-)-patulolide B. *J. Org. Chem.* **2003**, *68*, 1878-1885.
60. Drew, K. L. B.S. Thesis, University of New Hampshire, 2012.
61. Su, F. B.S. Thesis, University of New Hampshire, 2003.
62. Minetto, G.; Raveglia, L. F.; Sega, A.; Taddei, M. Microwave-assisted Paal-Knorr reaction - Three-step regiocontrolled synthesis of polysubstituted furans, pyrroles and thiophenes. *Eur. J. Org. Chem.* **2005**, 5277-5288.
63. Perron, F.; Albizati, K. F. Chemistry of Spiroketal. *Chem. Rev.* **1989**, *89*, 1617-1661.
64. Mazzone, J. R.; Zercher, C. K. Syntheses of Papyracillic Acids: Application of the Tandem Chain Extension-Acylation Reaction. *J. Org. Chem.* **2012**, *77*, 9171-9178.
65. Edwards, P. J.; Ley, S. V. Dispiroketal in Synthesis .18. Regioselective and Enantioselective Protection of Symmetrical Polyol Substrates Using an Enantiopure (2s,2's)-Dimethyl-Bis-Dihydropyran. *Synlett* **1995**, 1196-1196.
66. Downham, R.; Edwards, P. J.; Entwistle, D. A.; Hughes, A. B.; Kim, K. S.; Ley, S. V. Dispiroketal in Synthesis .19. Dispiroketal as Enantioselective and Regioselective Protective Agents for Symmetrical Cyclic and Acyclic Polyols. *Tetrahedron: Asymmetry* **1995**, *6*, 2403-2440.
67. Mead, K. T.; Brewer, B. N. Strategies in spiroketal synthesis revisited: Recent applications and advances. *Curr. Org. Chem.* **2003**, *7*, 227-256.
68. Kluge, A. F. Synthesis of 1,7-Dioxaspiro[5.5]Undecanes. *Heterocycles* **1986**, *24*, 1699-1740.
69. Boivin, T. L. B. Synthetic Routes to Tetrahydrofuran, Tetrahydropyran, and Spiroketal Units of Polyether Antibiotics and a Survey of Spiroketal of Other Natural-Products. *Tetrahedron* **1987**, *43*, 3309-3362.
70. Deslongchamps, P. *Stereoelectronic effects in organic chemistry*. 1st ed.; Pergamon Press: Oxford Oxfordshire ; New York, 1983; p xi, 375.
71. Wolfe, S.; Whangbo, M. H.; Mitchell, D. J. Molecular-Orbitals from Group Orbitals .7. Magnitudes and Origins of the Anomeric Effects, Exo-Anomeric Effects, Reverse Anomeric Effects, and C-X and C-Y Bond Lengths in Xch2yh Molecules. *Carbohydr. Res.* **1979**, *69*, 1-26.
72. Deslongchamps, P.; Rowan, D. D.; Pothier, N.; Saunders, J. K. 1,7-Dithia and 1-Oxa-7-Thiaspiro[5.5]Undecanes - Excellent Systems for the Study of Stereoelectronic Effects (Anomeric and Exo-Anomeric Effects) in the Monothio and the Dithioacetal Functions. *Can. J. Chem.* **1981**, *59*, 1122-1131.
73. Dekker, K. A.; Inagaki, T.; Gootz, T. D.; Kaneda, K.; Nomura, E.; Sakakibara, T.; Sakemi, S.; Sugie, Y.; Yamauchi, Y.; Yoshikawa, N.; Kojima, N. CJ-12,954 and its congeners, new anti-Helicobacter pylori compounds produced by Phanerochaete velutina: Fermentation, isolation, structural elucidation and biological activities. *J. Antibiot.* **1997**, *50*, 833-839.
74. Montecucco, C.; de Bernard, M. Molecular and cellular mechanisms of action of the vacuolating cytotoxin (VacA) and neutrophil-activating protein (HP-NAP) virulence factors of Helicobacter pylori. *Microbes and infection Institut Pasteur* **2003**, *5*, 715-21.

75. Parente, F.; Cucino, C.; Anderloni, A.; Grandinetti, G.; Porro, G. B. Treatment of helicobacter pylori infection using a novel antiadhesion compound (3' sialyllactose sodium salt). A double blind, placebo-controlled clinical. *Helicobacter* **2003**, *8*, 252-256.
76. Parente, F.; Cucino, C.; Porro, G. B. Treatment options for patients with Helicobacter pylori infection resistant to one or more eradication attempts. *Digest. Liver. Dis.* **2003**, *35*, 523-528.
77. Arnone, A.; Assante, G.; Nasini, G.; Depava, O. V. Secondary Mold Metabolites Spirolaxine and Sporotricale - 2 Long-Chain Phthalides Produced by Sporotrichum-Laxum. *Phytochemistry* **1990**, *29*, 613-616.
78. Mondal, M.; Argade, N. P. Synthesis of a new microbial secondary metabolite: anti-Helicobacter pylori CJ-13,015. *Tetrahedron Lett.* **2004**, *45*, 5693-5695.
79. Brimble, M. A.; Flowers, C. L.; Hutchinson, J. K.; Robinson, J. E.; Sidford, M. Synthesis of the phthalide-containing anti-Helicobacter pylori agents CJ-13,015, CJ-13,102, CJ-13,103, CJ-13,104 and CJ-13,108. *Tetrahedron* **2005**, *61*, 10036-10047.
80. Radcliff, F. J.; Fraser, J. D.; Wilson, Z. E.; Heapy, A. M.; Robinson, J. E.; Bryant, C. J.; Flowers, C. L.; Brimble, M. A. Anti-Helicobacter pylori activity of derivatives of the phthalide-containing antibacterial agents spiroloxine methyl ether, CJ-12,954, CJ-13,013, CJ-13,102, CJ-13,104, CJ-13,108 and CJ-13,015. *Bioorg. Med. Chem.* **2008**, *16*, 6179-6185.
81. Brimble, M. A.; Bryant, C. J. Synthesis of the spiroacetal-containing anti-Helicobacter pylori agents CJ-12,954 and CJ-13,014. *Chem. Commun.* **2006**, 4506-4508.
82. Brimble, M. A.; Bryant, C. J. Synthesis and assignment of the absolute configuration of the anti-Helicobacter pylori agents CJ-12,954 and CJ-13,014. *Org. Biomol. Chem.* **2007**, *5*, 2858-2866.
83. Evans, D. A.; Bartroli, J.; Shih, T. L. Enantioselective Aldol Condensations .2. Erythro-Selective Chiral Alol Condensations Via Boron Enolates. *J. Am. Chem. Soc.* **1981**, *103*, 2127-2129.
84. Ager, D. J.; Prakash, I.; Schaad, D. R. 1,2-amino alcohols and their heterocyclic derivatives as chiral auxiliaries in asymmetric synthesis. *Chem. Rev.* **1996**, *96*, 835-875.
85. Evans, D. A.; Kim, A. S.; Metternich, R.; Novack, V. J. General strategies toward the syntheses of macrolide antibiotics. The total syntheses of 6-deoxyerythronolide B and oleandolide. *J. Am. Chem. Soc.* **1998**, *120*, 5921-5942.
86. Evans, D. A.; Gage, J. R.; Leighton, J. L. Total Synthesis of (+)-Calyculin-A. *J. Am. Chem. Soc.* **1992**, *114*, 9434-9453.
87. Crimmins, M. T.; Choy, A. L. An asymmetric aldol-ring-closing metathesis strategy for the enantioselective construction of oxygen heterocycles: An efficient approach to the enantioselective synthesis of (+)-laurencin. *J. Am. Chem. Soc.* **1999**, *121*, 5653-5660.
88. Wu, Y. K.; Shen, X. A high-yielding low-cost facile synthesis of 2-oxazolidinones chiral auxiliaries. *Tetrahedron: Asymmetry* **2000**, *11*, 4359-4363.

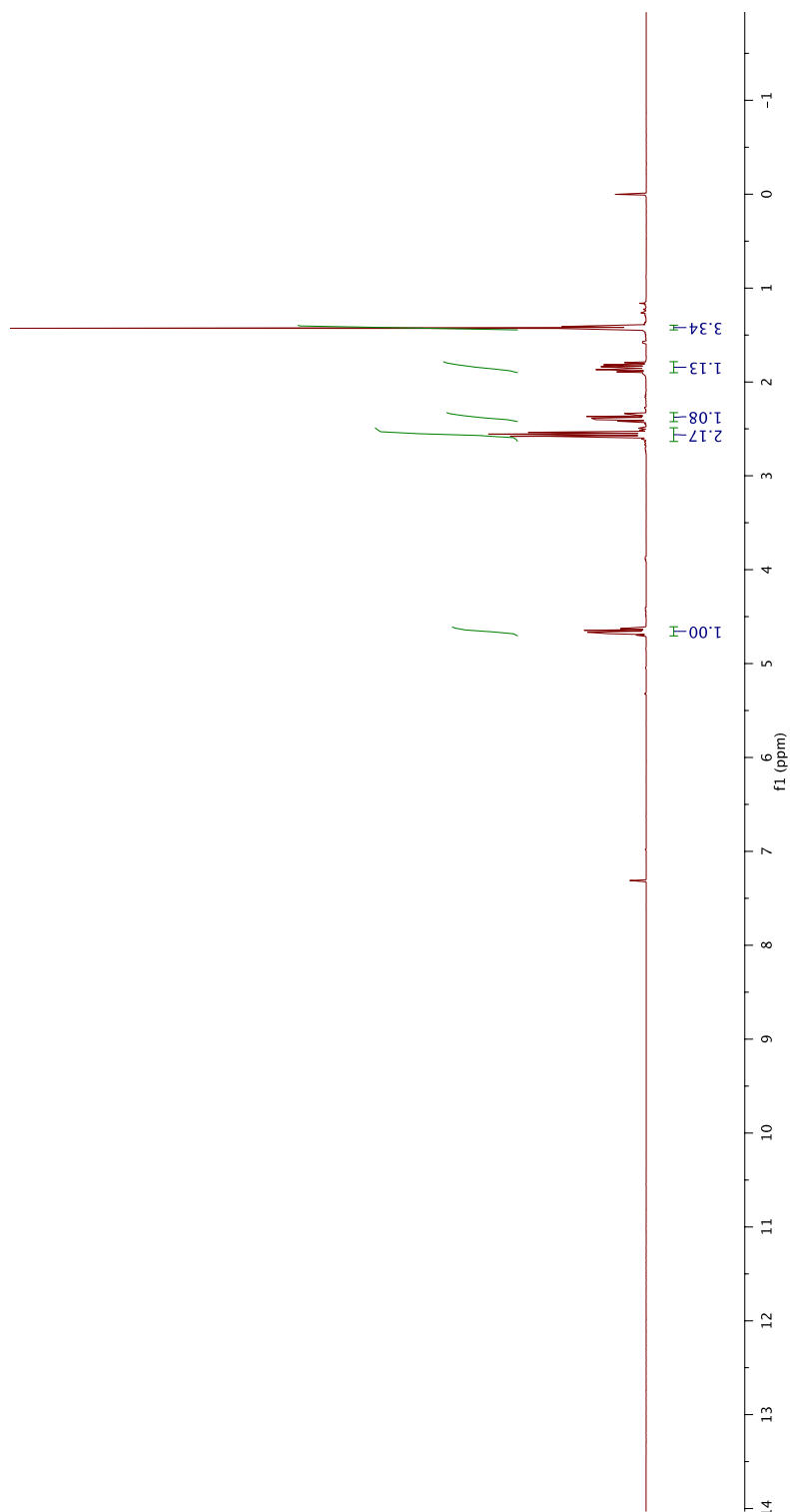
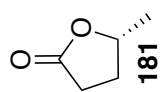
89. Jayasundera, K. P.; Brodie, S. J.; Taylor, C. M. Synthesis of a transition-state analog for the hydrolysis of the zearalenone lactone. *Tetrahedron* **2007**, *63*, 10077-10082.
90. Hamada, Y.; Kondo, Y.; Shibata, M.; Shioiri, T. Efficient Total Synthesis of Didemnins a and B. *J. Am. Chem. Soc.* **1989**, *111*, 669-673.
91. Raillard, S. P.; Chen, W. W.; Sullivan, E.; Bajjalieh, W.; Bhandari, A.; Baer, T. A. Preparation and improved stability of N-Boc-alpha-amino-5-acyl Meldrum's acids, a versatile class of building blocks for combinatorial chemistry. *J. Comb. Chem.* **2002**, *4*, 470-474.
92. Lee, A. H. F.; Chan, A. S. C.; Li, T. H. Synthesis of 5-(7-hydroxyhept-3-enyl)-1,2-dithiolan-3-one 1-oxide, a core functionality of antibiotic leinamycin. *Tetrahedron* **2003**, *59*, 833-839.
93. Bonini, C.; Checconi, M.; Righi, G.; Rossi, L. Enantio and Stereoselective Synthesis of (5r,6s)-6-Acetoxyhexadecanolide, a Mosquito Oviposition Attractant Pheromone. *Tetrahedron* **1995**, *51*, 4111-4116.
94. Brown, H. C.; Joshi, N. N. Hydroboration of Terpenes .9. A Simple Improved Procedure for Upgrading the Optical Purity of Commercially Available Alpha-Pinenes and Beta-Pinenes - Conversion of (+)-Alpha-Pinene to (+)-Beta-Pinene Via Hydroboration Isomerization. *J. Org. Chem.* **1988**, *53*, 4059-4062.
95. Ramachandran, P. V.; Pitre, S.; Brown, H. C. Selective reductions. Effective intramolecular asymmetric reductions of alpha-, beta- and gamma-keto acids with diisopinocampheylborane and intermolecular asymmetric reductions of the corresponding esters with B-chlorodiisopinocampheylborane. *J. Org. Chem.* **2002**, *67*, 5315-5319.
96. Hedenstrom, E.; Hogberg, H. E.; Wassgren, A. B.; Bergstrom, G.; Lofqvist, J.; Hansson, B.; Anderbrant, O. Sex-Pheromone of Pine Sawflies - Chiral Syntheses of Some Active Minor Components Isolated from Neodiprion-Sertifer and of Some Chiral Analogs of Diprionyl Acetate. *Tetrahedron* **1992**, *48*, 3139-3146.
97. Freeman, F.; Kim, D. S. H. L.; Rodriguez, E. Preparation of 1,4-Diketones and Their Reactions with Bis(Trialkyltin) or Bis(Triphenyltin) Sulfide Boron-Trichloride. *J. Org. Chem.* **1992**, *57*, 1722-1727.
98. Zimmerman, H. E.; Nesterov, E. E. Quantitative cavities and reactivity in stages of crystal lattices: Mechanistic and exploratory organic photochemistry. *J. Am. Chem. Soc.* **2002**, *124*, 2818-2830.
99. Mazzone, J. R. I. Ph.D. Dissertation, University of New Hampshire, 2011.
100. Evans, D. A.; Britton, T. C.; Ellman, J. A. Contrasteric Carboximide Hydrolysis with Lithium Hydroperoxide. *Tetrahedron Lett.* **1987**, *28*, 6141-6144.
101. Barton, D. H. R.; Crich, D.; Motherwell, W. B. The Invention of New Radical Chain Reactions .8. Radical Chemistry of Thiohydroxamic Esters - a New Method for the Generation of Carbon Radicals from Carboxylic-Acids. *Tetrahedron* **1985**, *41*, 3901-3924.
102. Sadeghi-Khomami, A.; Blake, A. J.; Wilson, C.; Thomas, N. R. Synthesis of a carbasugar analogue of a putative intermediate in the UDP-Galp-mutase catalyzed isomerization. *Org. Lett.* **2005**, *7*, 4891-4894.

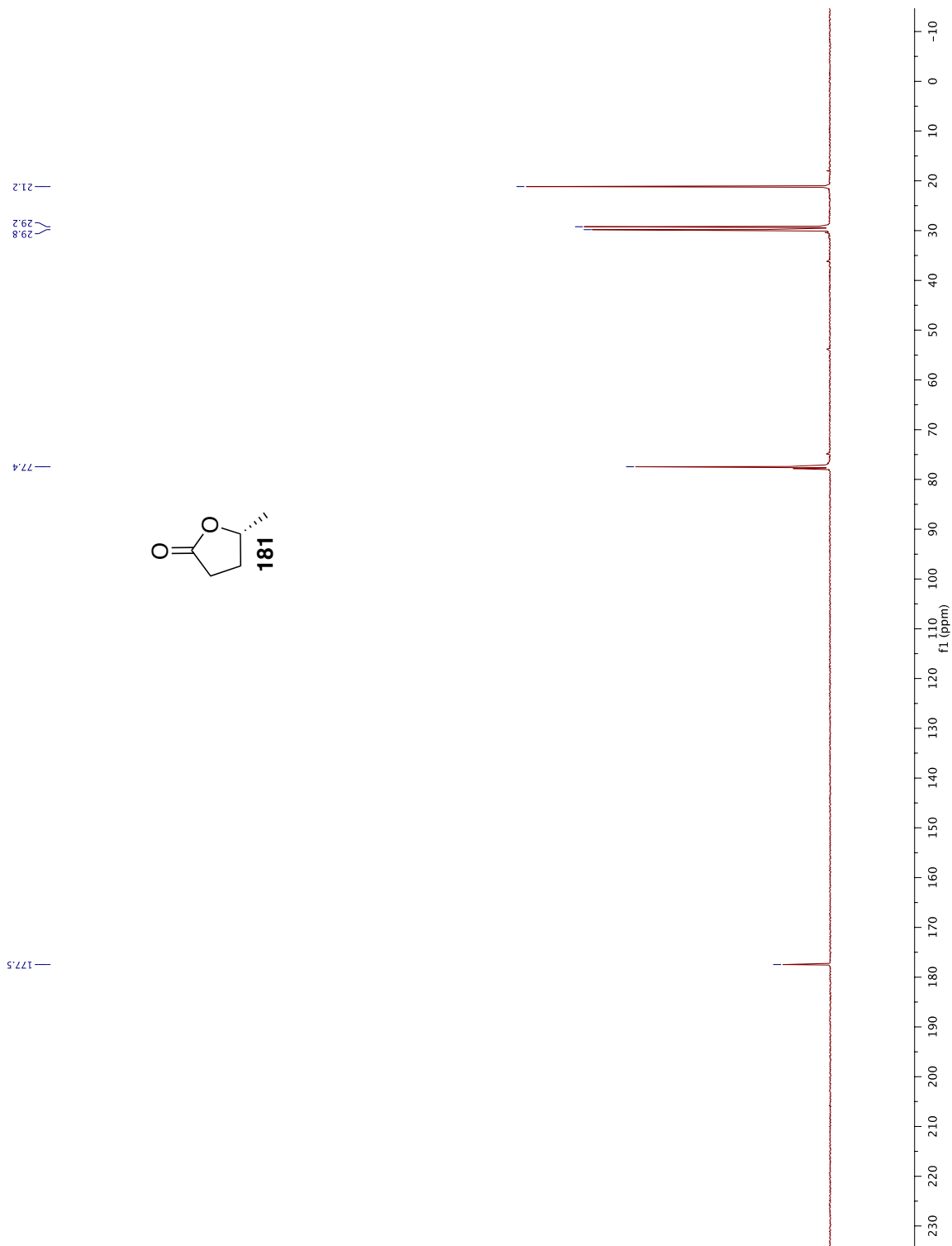
103. Ko, E. J.; Savage, G. P.; Williams, C. M.; Tsanaktsidis, J. Reducing the Cost, Smell, and Toxicity of the Barton Reductive Decarboxylation: Chloroform as the Hydrogen Atom Source. *Org. Lett.* **2011**, *13*, 1944-1947.
104. Langmuir, I. The Structure of Atoms and the Octet Theory of Valence. *Proc.Natl. Acad. Sci. USA.* **1919**, *5*, 252-9.
105. Kath, J. C.; DiRico, A. P.; Gladue, R. P.; Martin, W. H.; McElroy, E. B.; Stock, I. A.; Tylaska, L. A.; Zheng, D. The discovery of structurally novel CCR1 antagonists derived from a hydroxyethylene peptide isostere template. *Bioorg. Med. Chem. Lett.* **2004**, *14*, 2163-7.
106. Martin, S. F.; Dorsey, G. O.; Gane, T.; Hillier, M. C.; Kessler, H.; Baur, M.; Matha, B.; Erickson, J. W.; Bhat, T. N.; Munshi, S.; Gulnik, S. V.; Topol, I. A. Cyclopropane-derived peptidomimetics. Design, synthesis, evaluation, and structure of novel HIV-1 protease inhibitors. *J. Med. Chem.* **1998**, *41*, 1581-97.
107. Mastrolorenzo, A.; Rusconi, S.; Scozzafava, A.; Barbaro, G.; Supuran, C. T. Inhibitors of HIV-1 protease: current state of the art 10 years after their introduction. From antiretroviral drugs to antifungal, antibacterial and antitumor agents based on aspartic protease inhibitors. *Curr. Med. Chem.* **2007**, *14*, 2734-48.
108. Clavel, F.; Mammano, F. Role of Gag in HIV Resistance to Protease Inhibitors. *Viruses* **2010**, *2*, 1411-26.
109. Wipf, P.; Henninger, T. C.; Geib, S. J. Methyl- and (Trifluoromethyl)alkene Peptide Isosteres: Synthesis and Evaluation of Their Potential as beta-Turn Promoters and Peptide Mimetics. *J. Org. Chem.* **1998**, *63*, 6088-6089.
110. Kim, J.; Sieburth, S. M. A silanediol inhibitor of the metalloprotease thermolysin: synthesis and comparison with a phosphinic acid inhibitor. *J. Org. Chem.* **2004**, *69*, 3008-14.
111. Benedetti, F.; Magnan, M.; Miertus, S.; Norbedo, S.; Parat, D.; Tossi, A. Stereoselective synthesis of non symmetric dihydroxyethylene dipeptide isosteres via epoxy alcohols derived from alpha-amino acids. *Bioorg. Med. Chem. Lett.* **1999**, *9*, 3027-30.
112. Vabeno, J.; Nielsen, C. U.; Ingebrigtsen, T.; Lejon, T.; Steffansen, B.; Luthman, K. Dipeptidomimetic ketomethylene isosteres as pro-moieties for drug transport via the human intestinal di-/tripeptide transporter hPEPT1: design, synthesis, stability, and biological investigations. *J. Med. Chem.* **2004**, *47*, 4755-65.
113. Harbeson, S. L.; Rich, D. H., Inhibition of aminopeptidases by peptides containing ketomethylene and hydroxyethylene amide bond replacements. *J. Med. Chem.* **1989**, *32*, 1378-92.
114. Engstrom, K.; Henry, R.; Hollis, L. S.; Kotecki, B.; Marsden, I.; Pu, Y. M.; Wagaw, S.; Wang, W. An efficient, stereoselective synthesis of the hydroxyethylene dipeptide isostere core for the HIV protease inhibitor A-792611. *J. Org. Chem.* **2006**, *71*, 5369-72.
115. Niu, Y.; Wang, Y.; Zou, X.; Yang, X.; Ma, C.; Lu, Y.; Zhou, B.; Yuan, Y.; Du, G.; Xu, P. Synthesis and preliminary evaluation of peptidomimetic inhibitors of human beta-secretase. *Eur. J. Med. Chem.* **2010**, *45*, 2089-94.

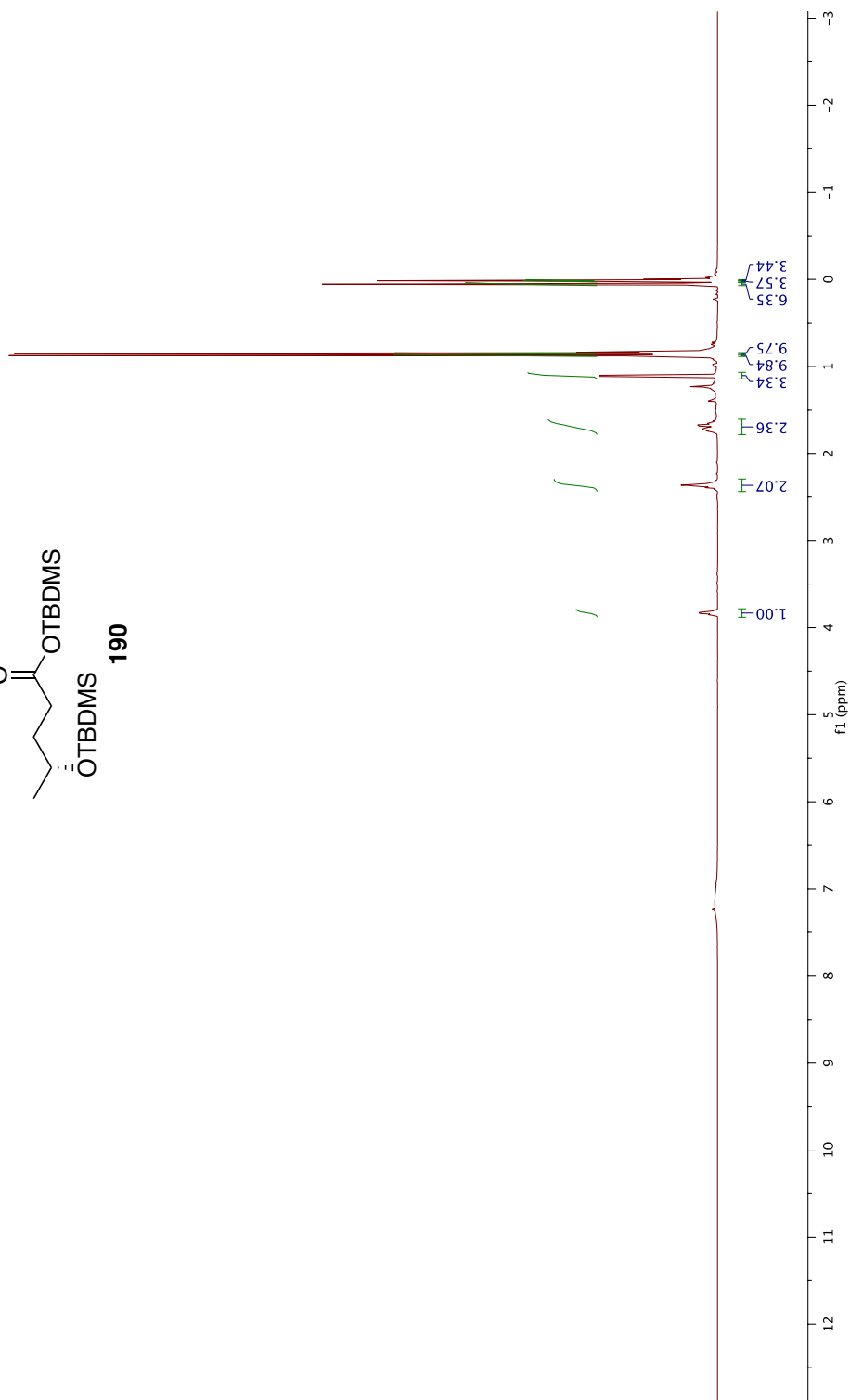
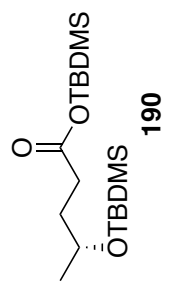
116. Theberge, C. R.; Zercher, C. K. Chain extension of amino acid skeletons: preparation of ketomethylene isosteres. *Tetrahedron* **2003**, *59*, 1521-1527.
117. Lin, W.; Tryder, N.; Su, F.; Zercher, C. K.; Jasinski, J. P.; Butcher, R. J. Stereocontrolled formation of ketomethylene isosteres through tandem chain extension reactions. *J. Org. Chem.* **2006**, *71*, 8140-5.
118. Lin, W.; Theberge, C. R.; Henderson, T. J.; Zercher, C. K.; Jasinski, J.; Butcher, R. J. Stereoselective formation of a functionalized dipeptide isostere by zinc carbenoid-mediated chain extension. *J. Org. Chem.* **2009**, *74*, 645-51.
119. Wipf, P.; Xiao, J. Convergent approach to (E)-alkene and cyclopropane peptide isosteres. *Org. Lett.* **2005**, *7*, 103-6.
120. Hilgenkamp, R. K. M.S. Thesis, University of New Hampshire, 2000.
121. Schobert, R. Domino syntheses of bioactive tetronic and tetramic acids. *Die Naturwissenschaften* **2007**, *94*, 1-11.
122. Anh, N. T. E., O.; Lefour, J-M.; Dau, M-E. *J. Am. Chem. Soc.* **1973**, *95*.

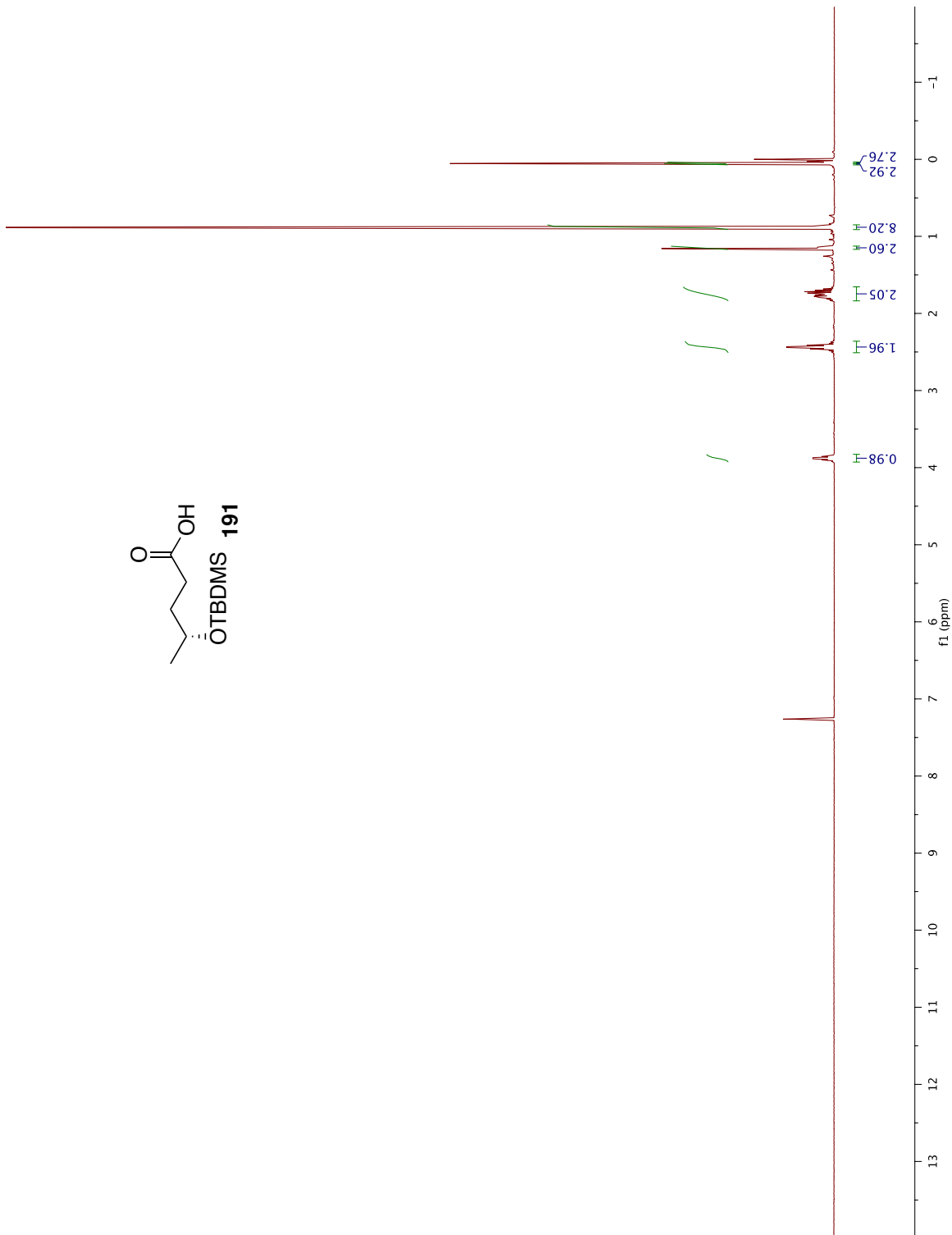
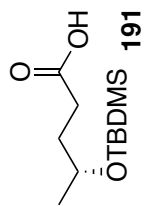
APPENDIX A

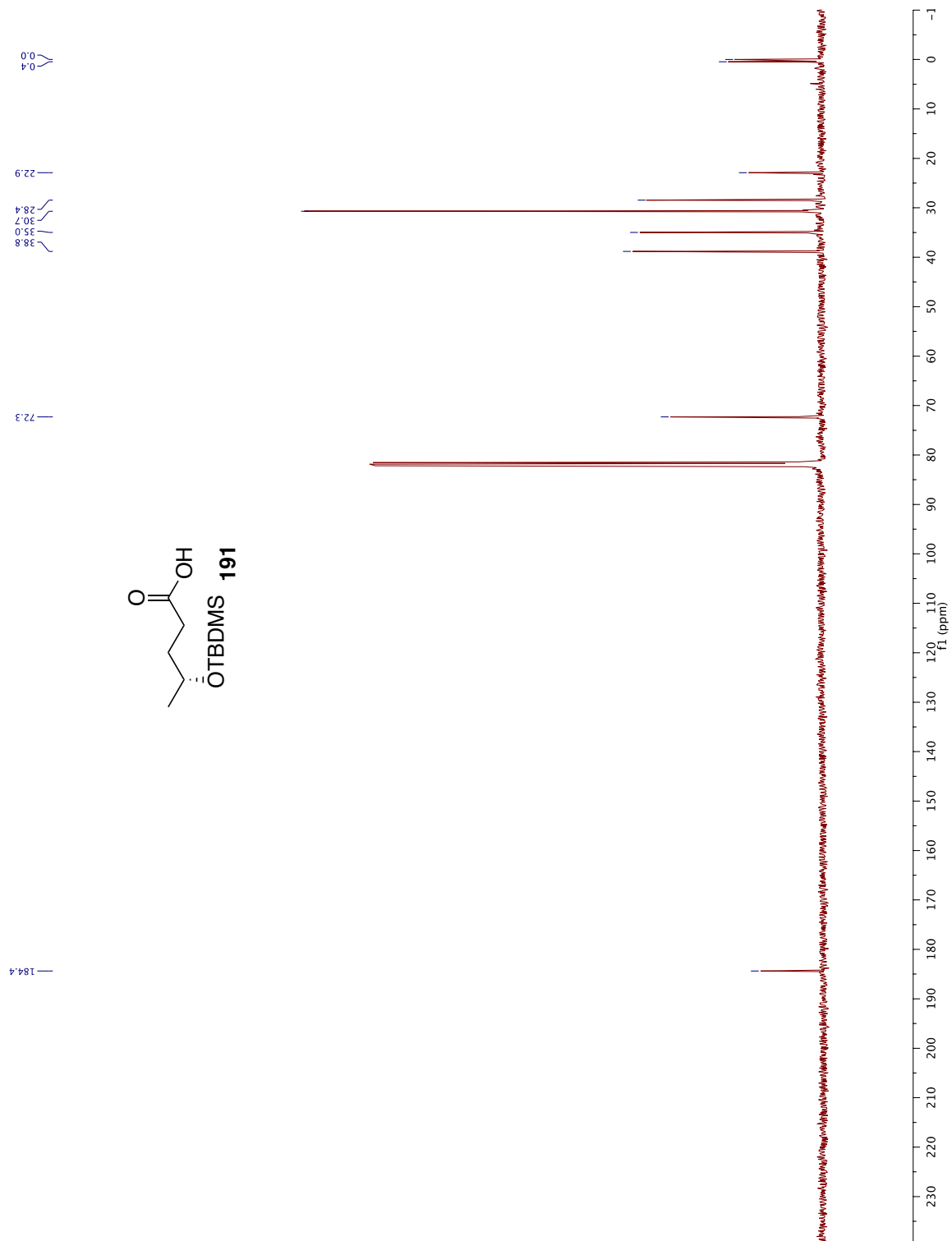
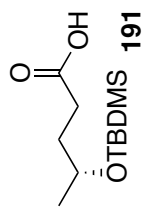
Spectra

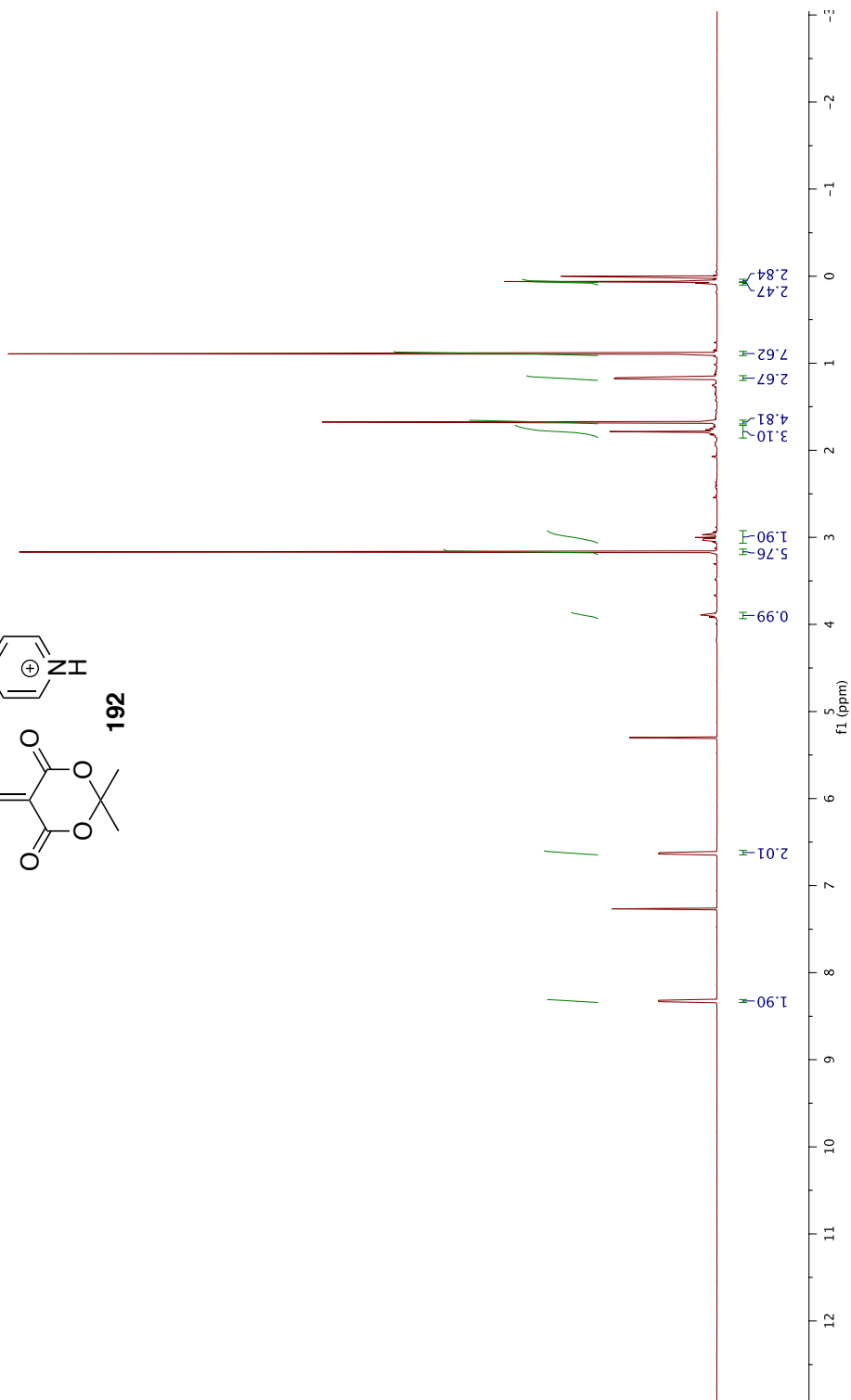
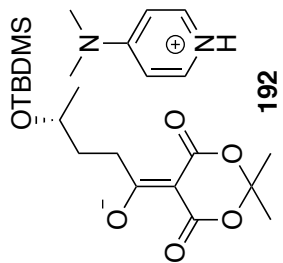


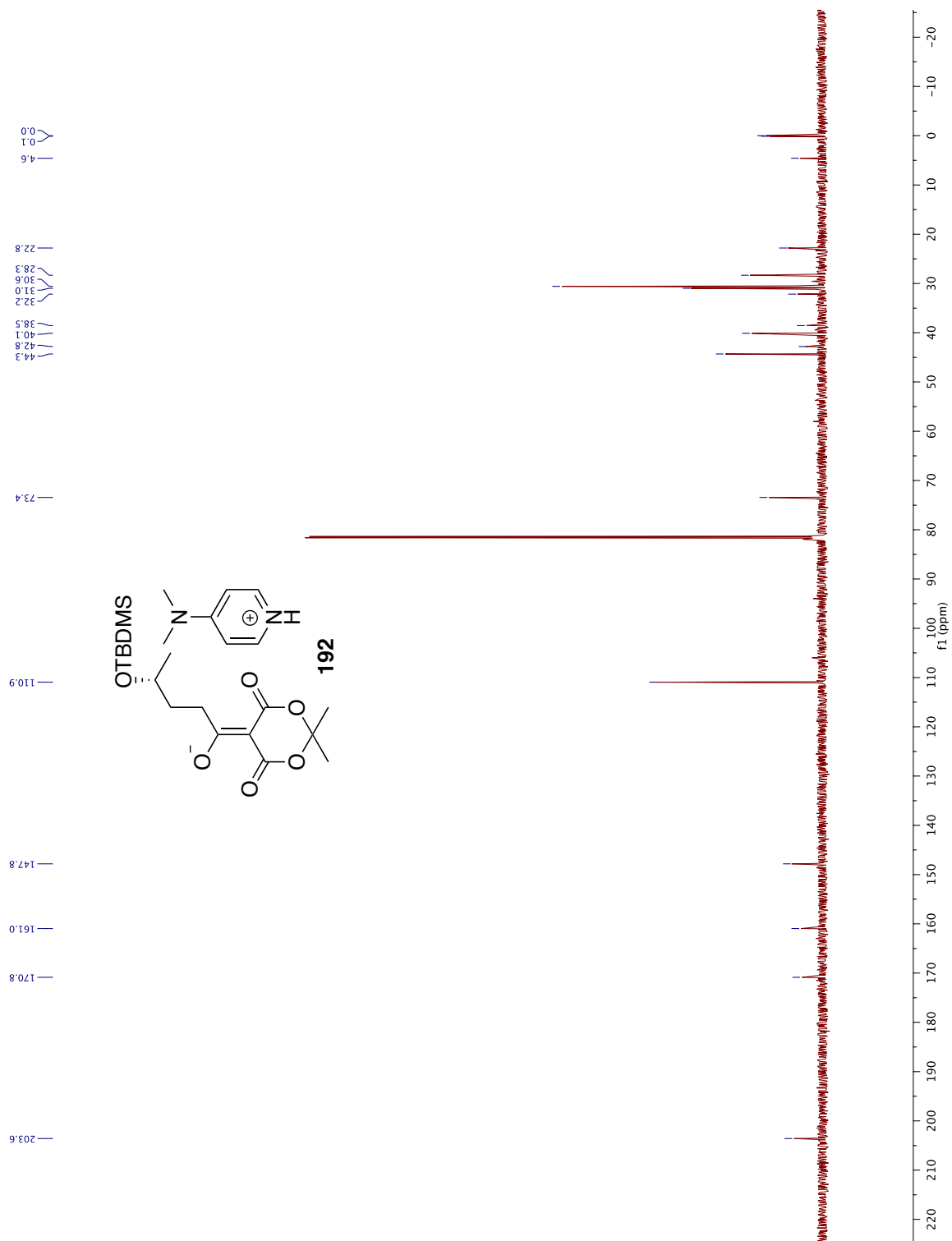


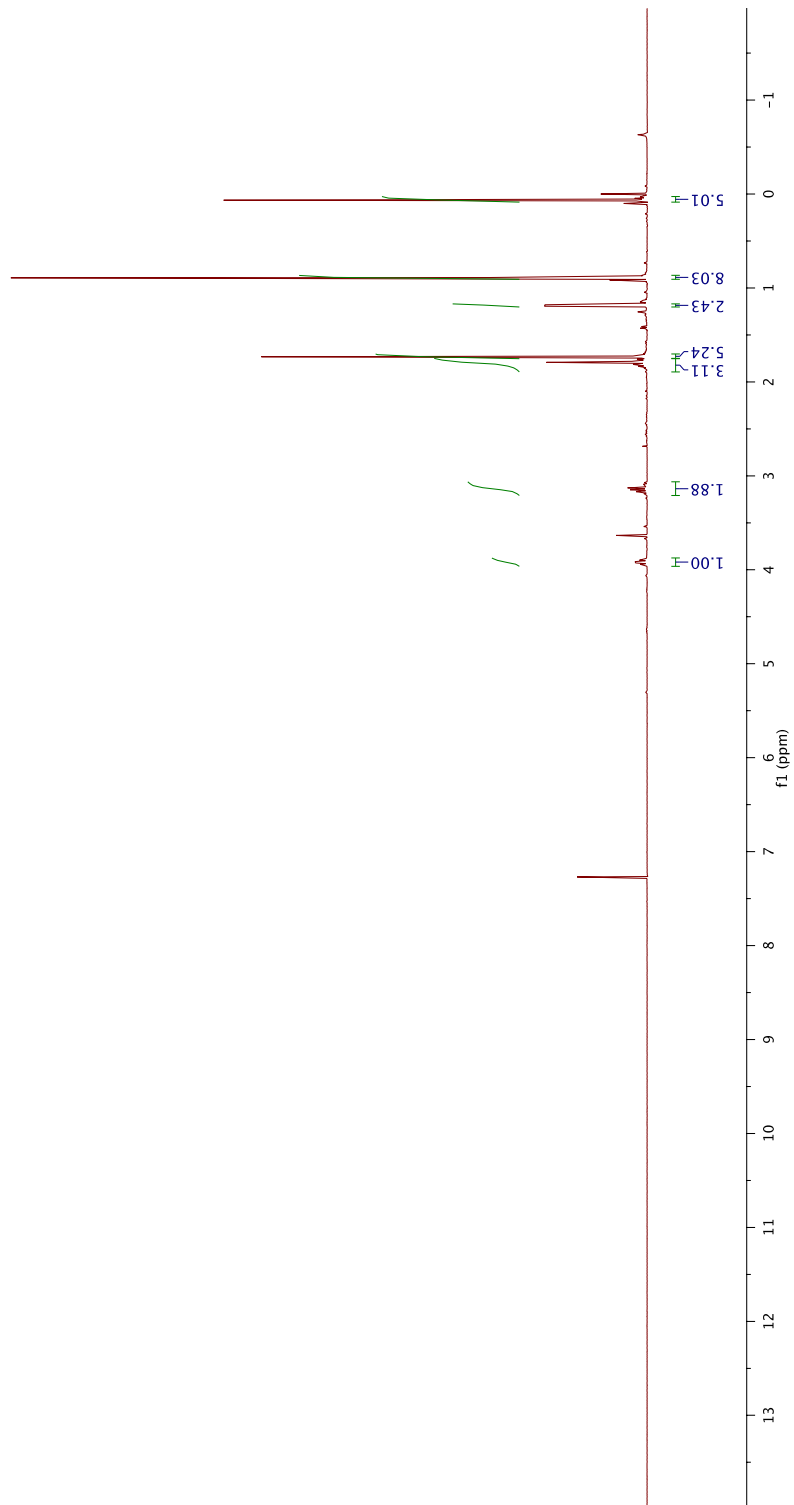
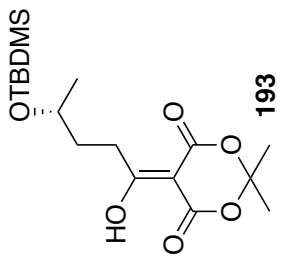


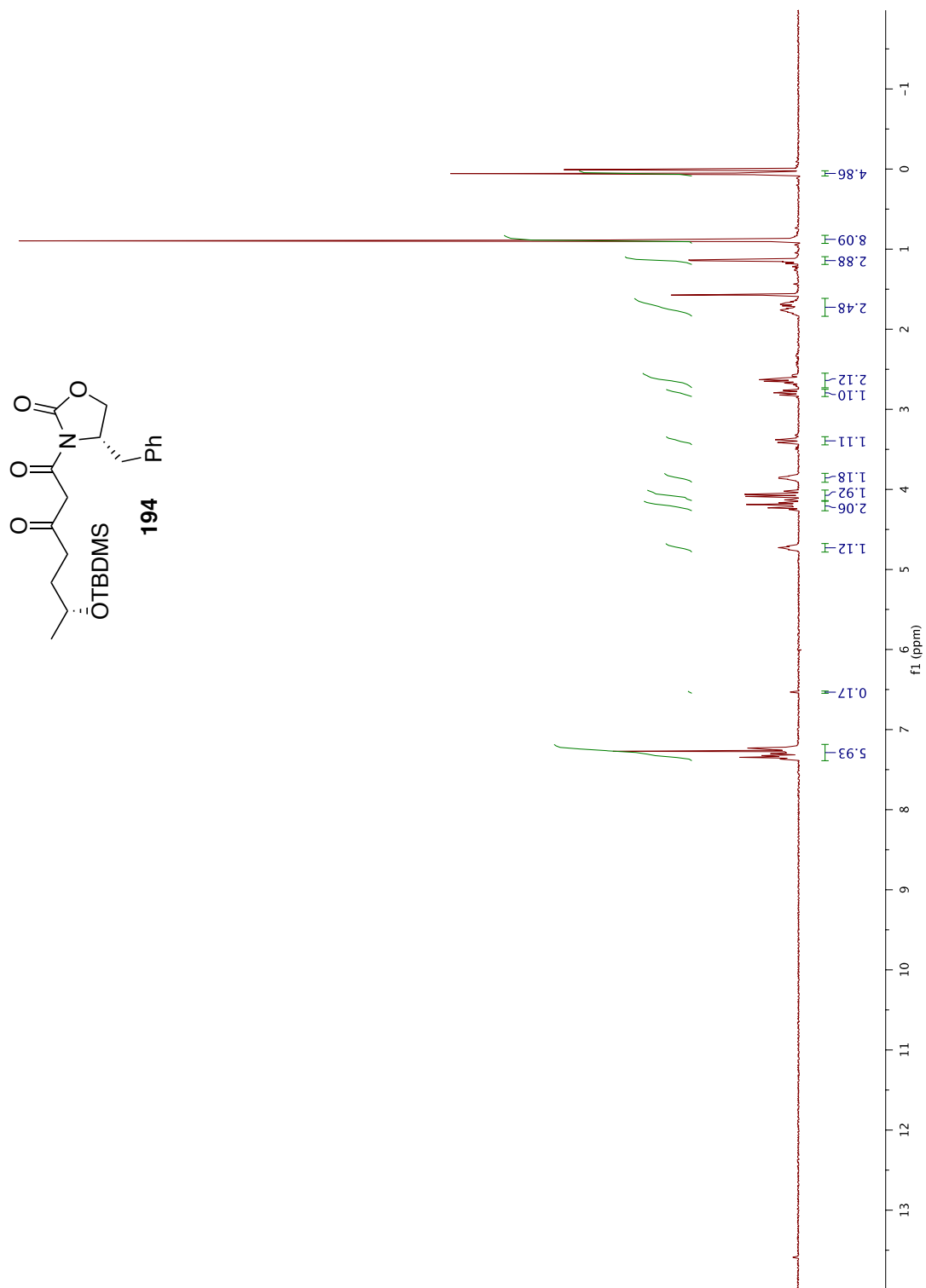


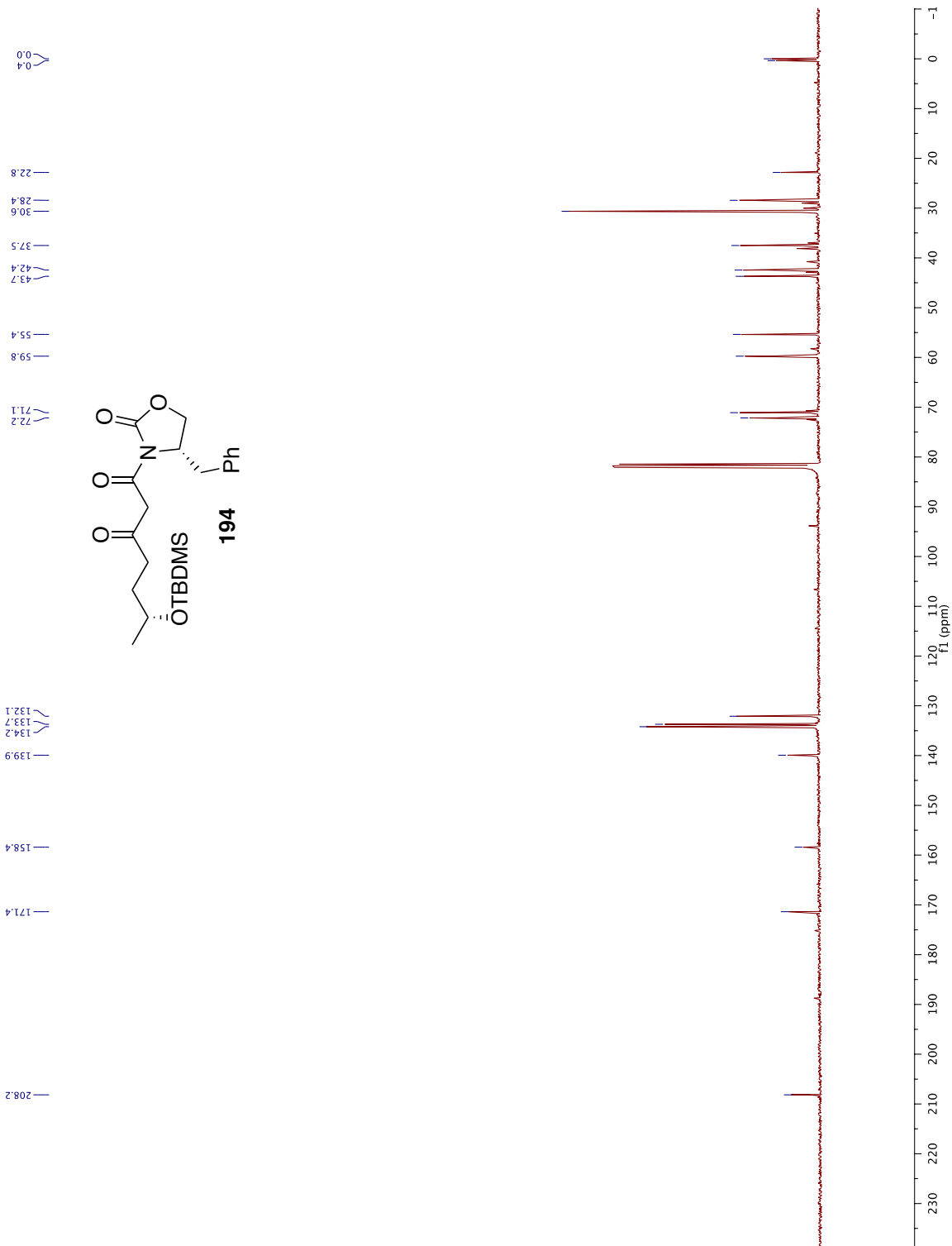


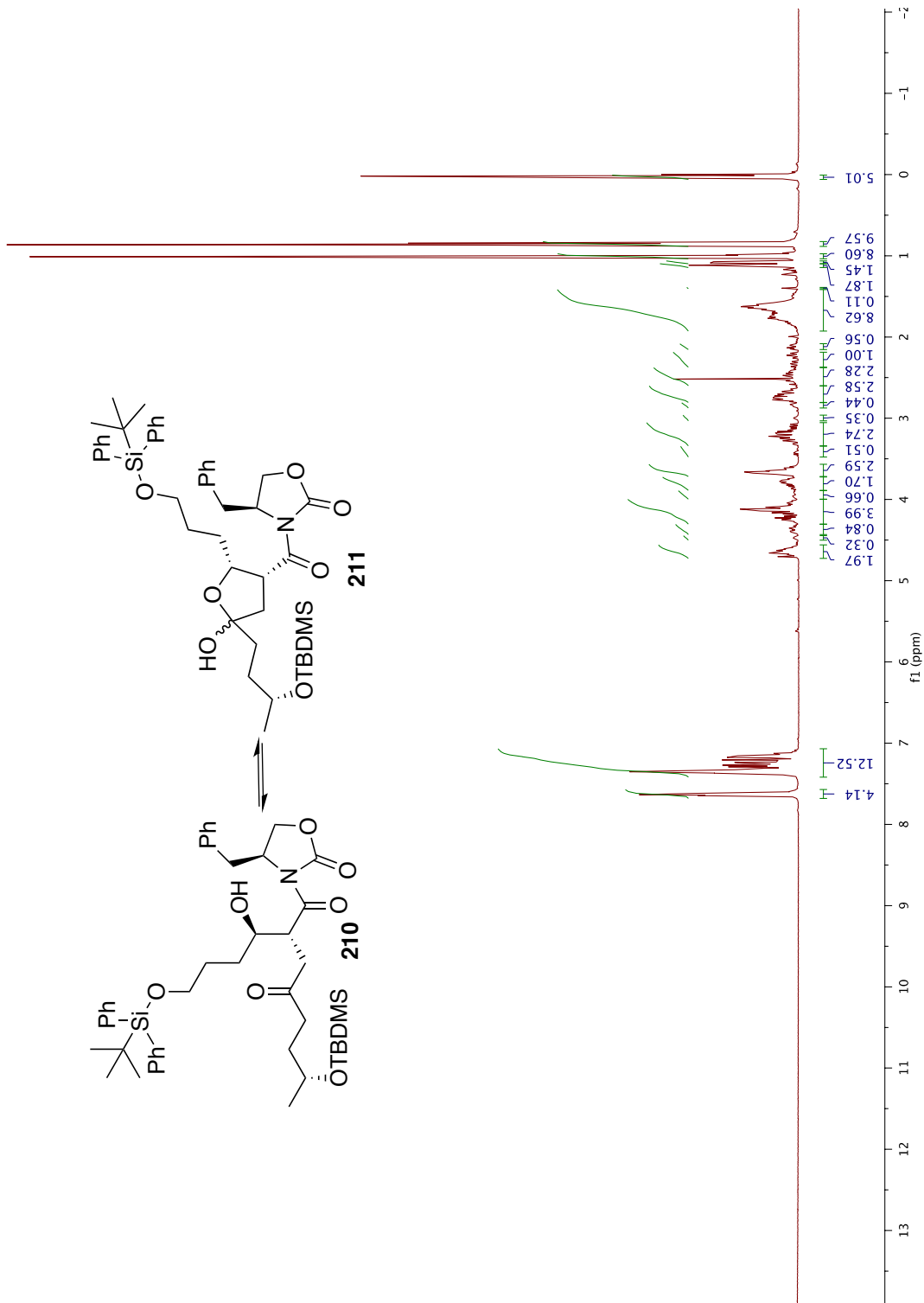
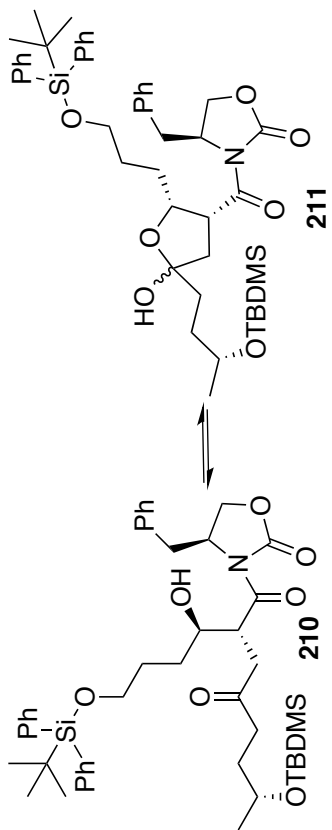


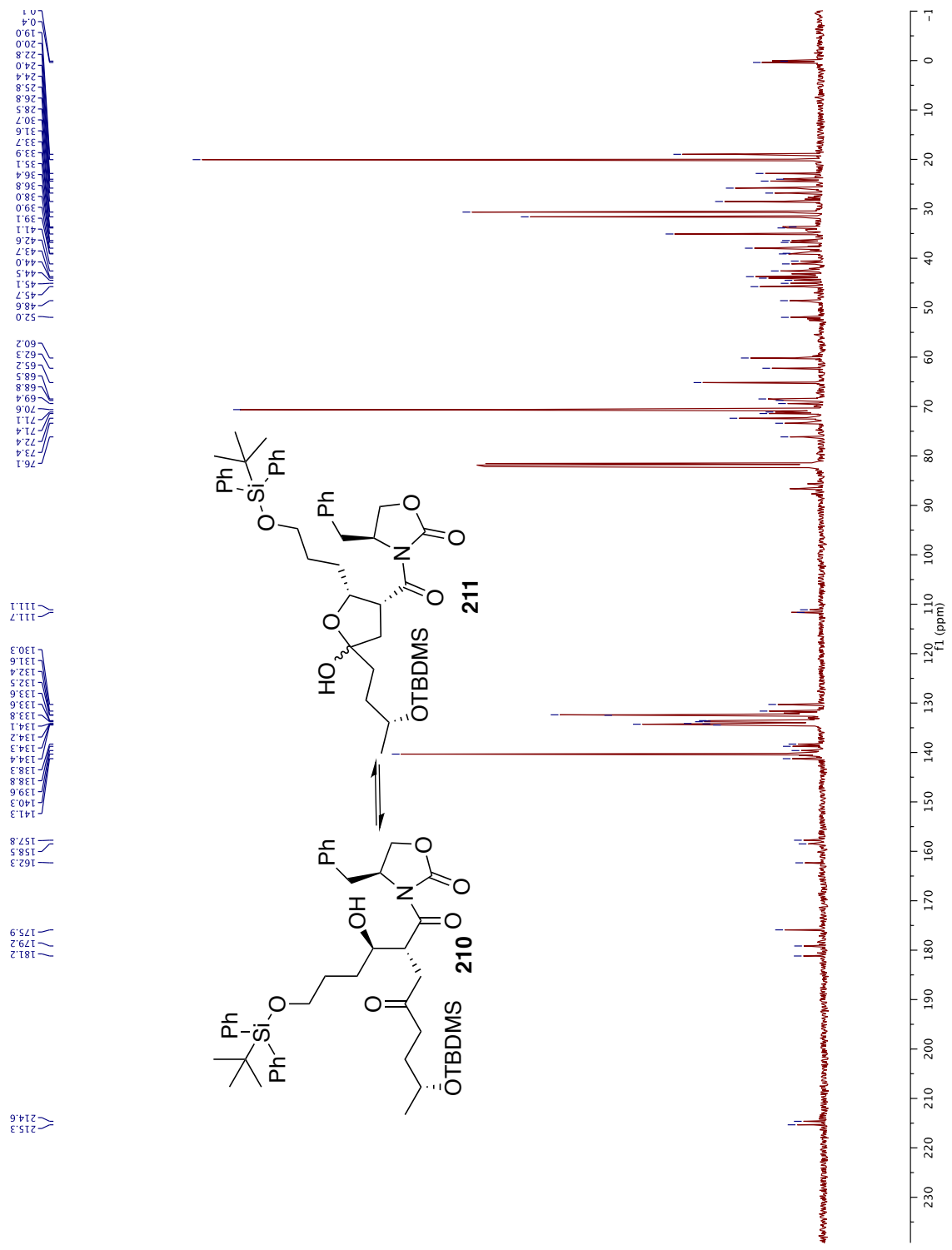


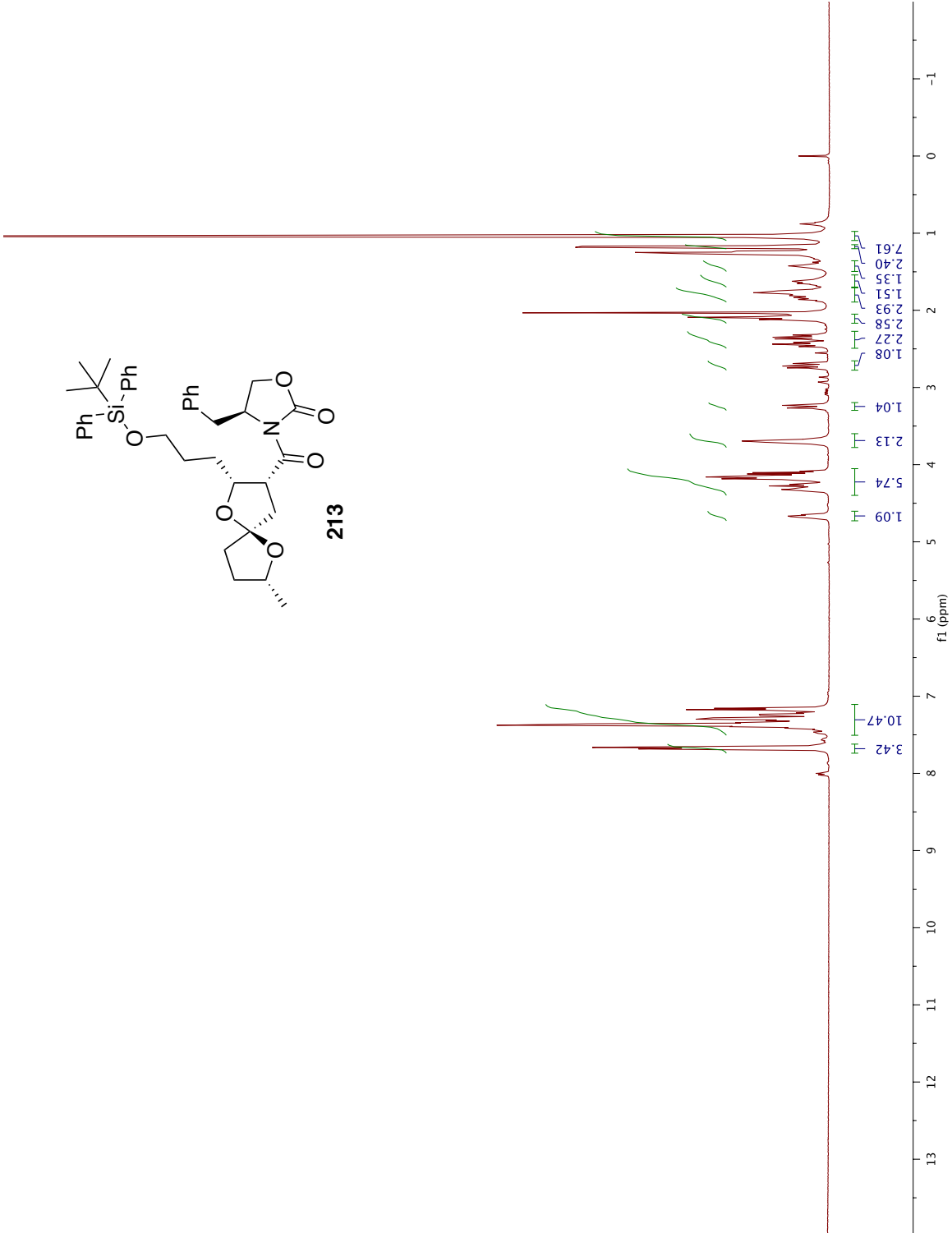


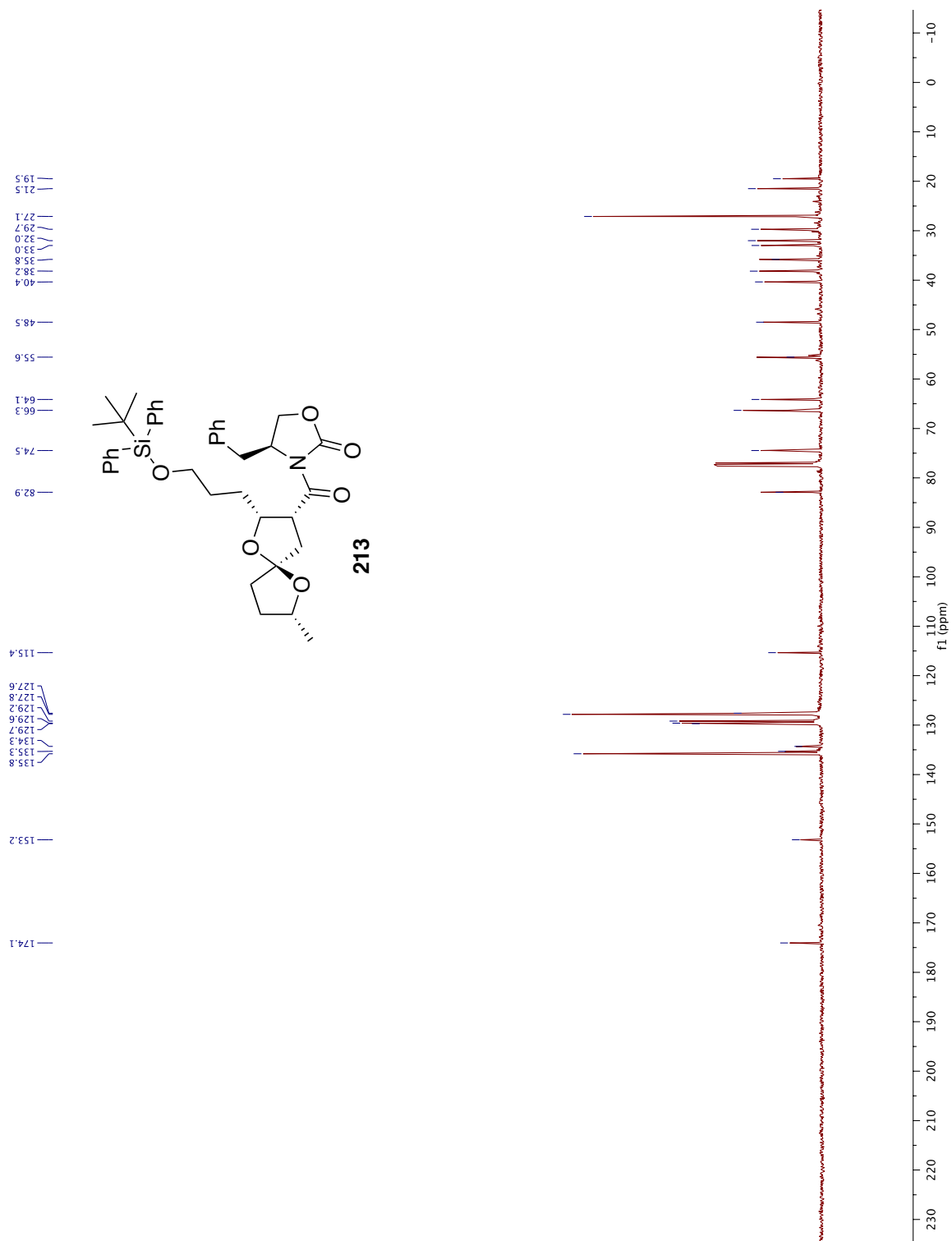


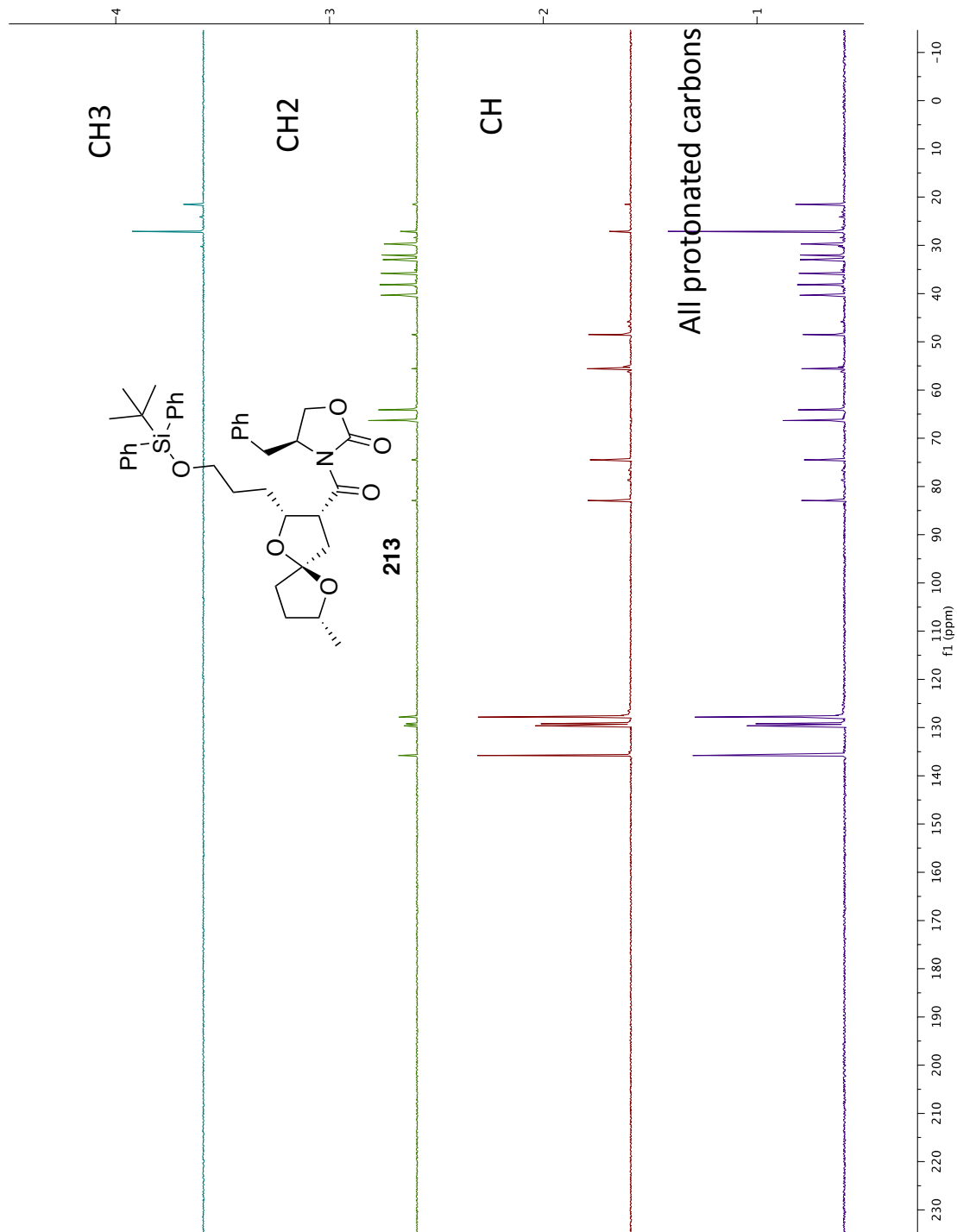


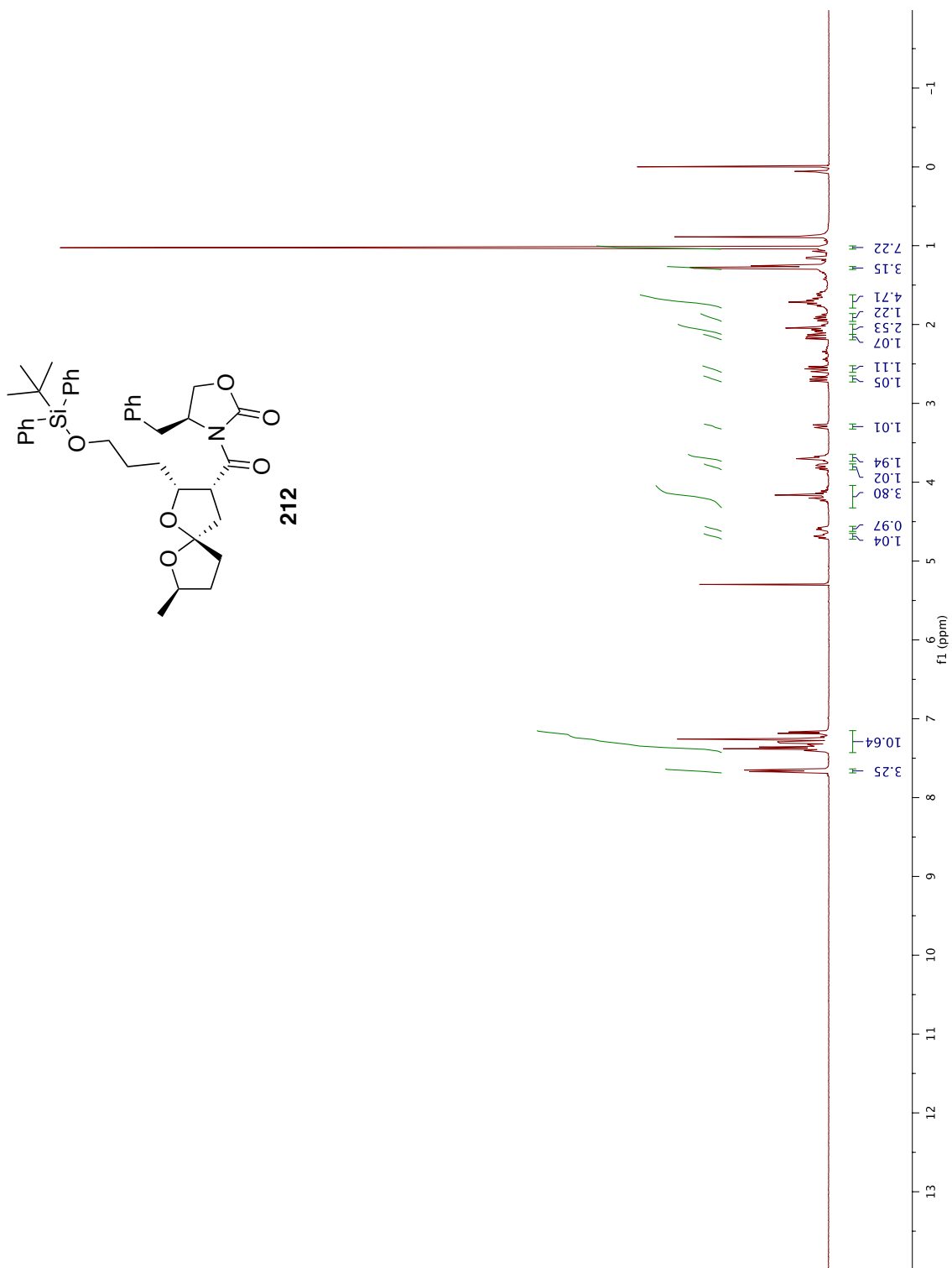


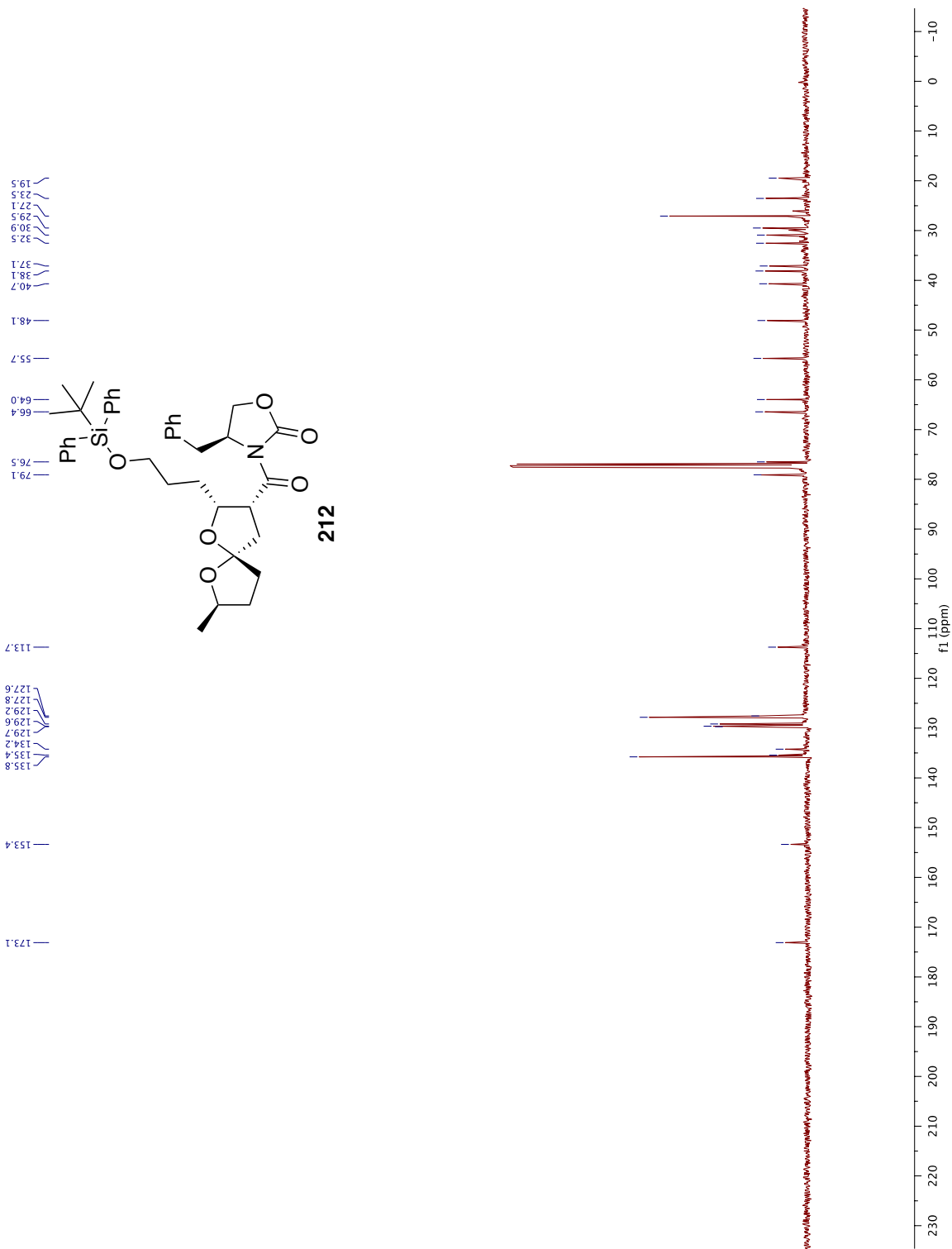


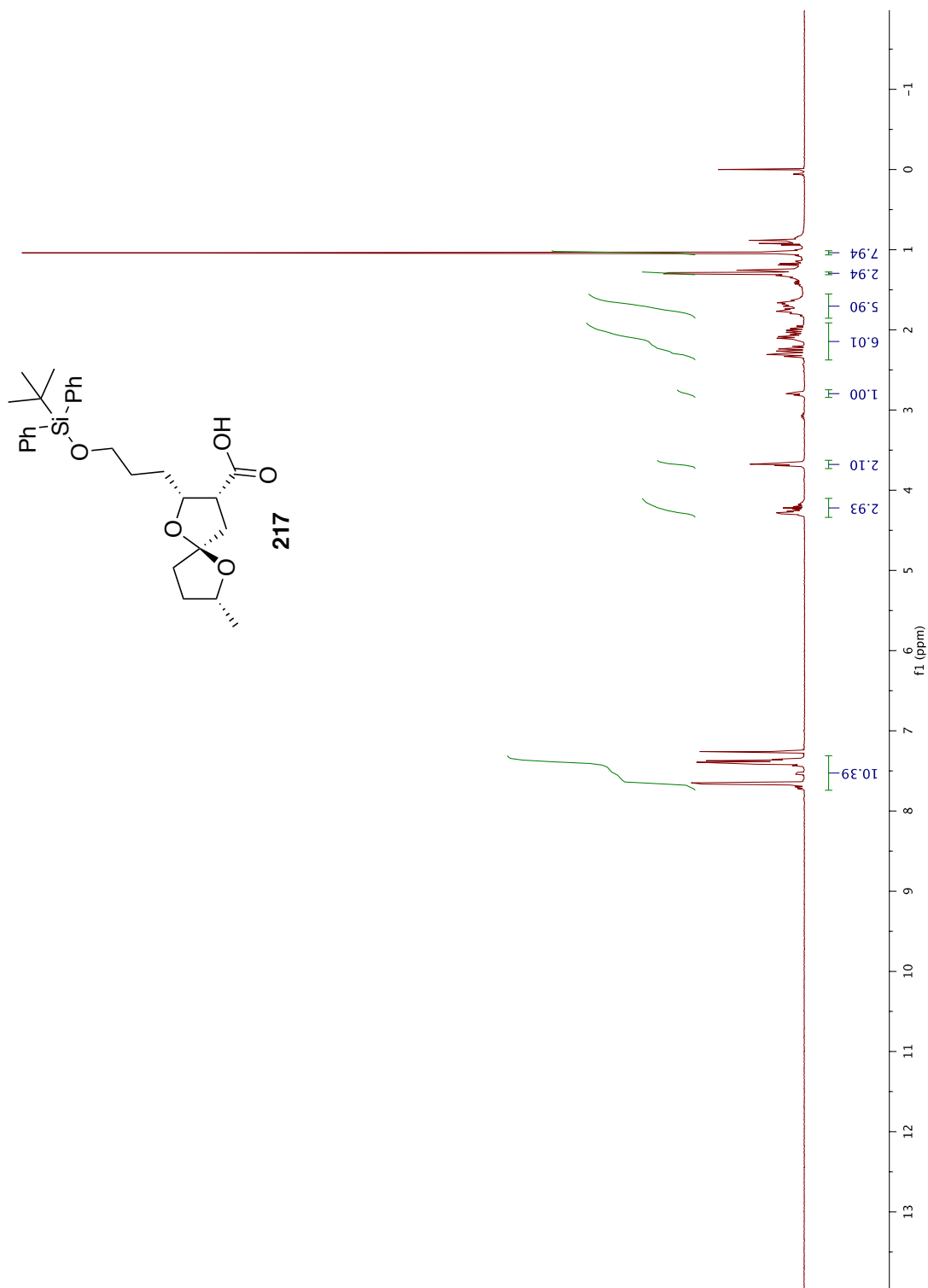


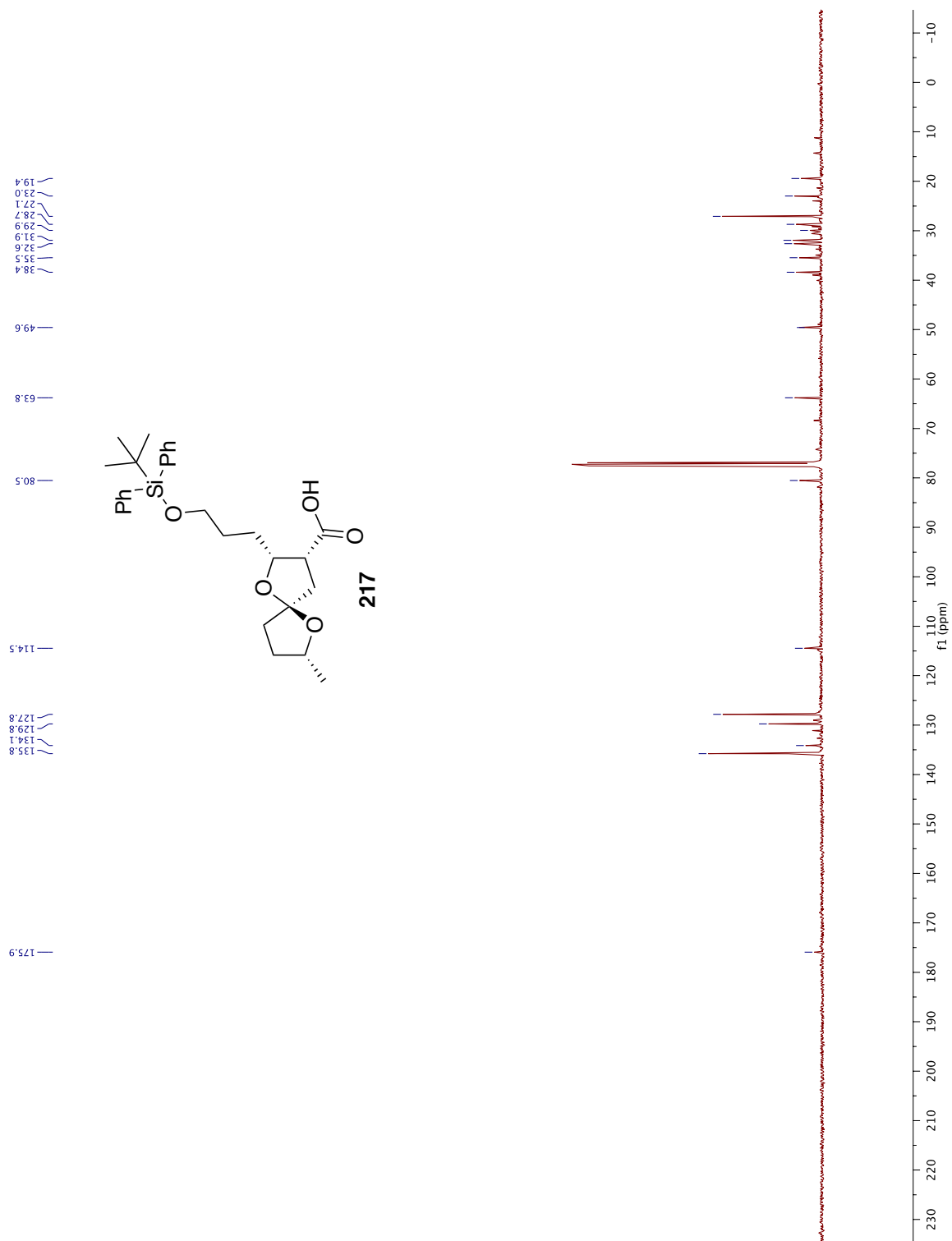


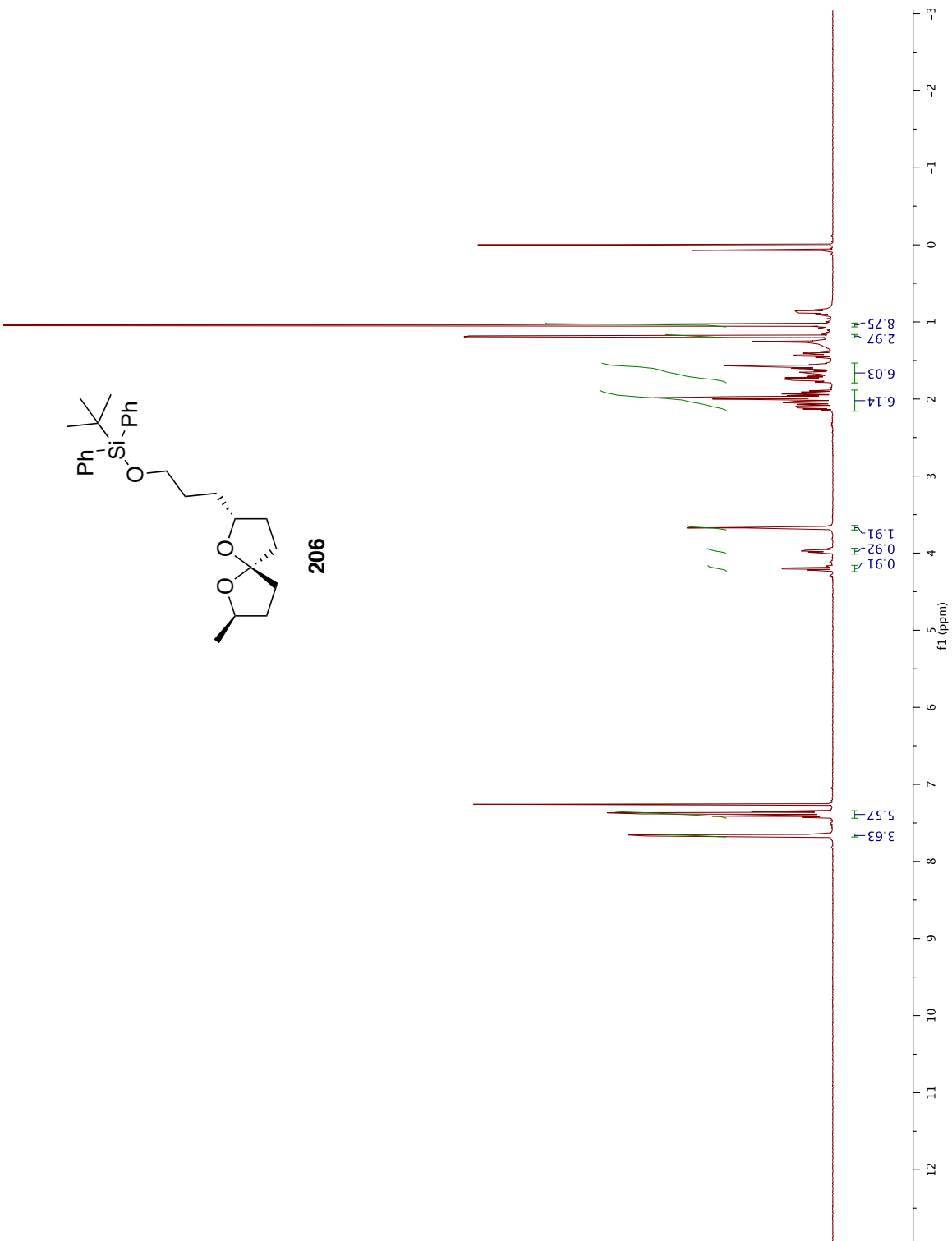


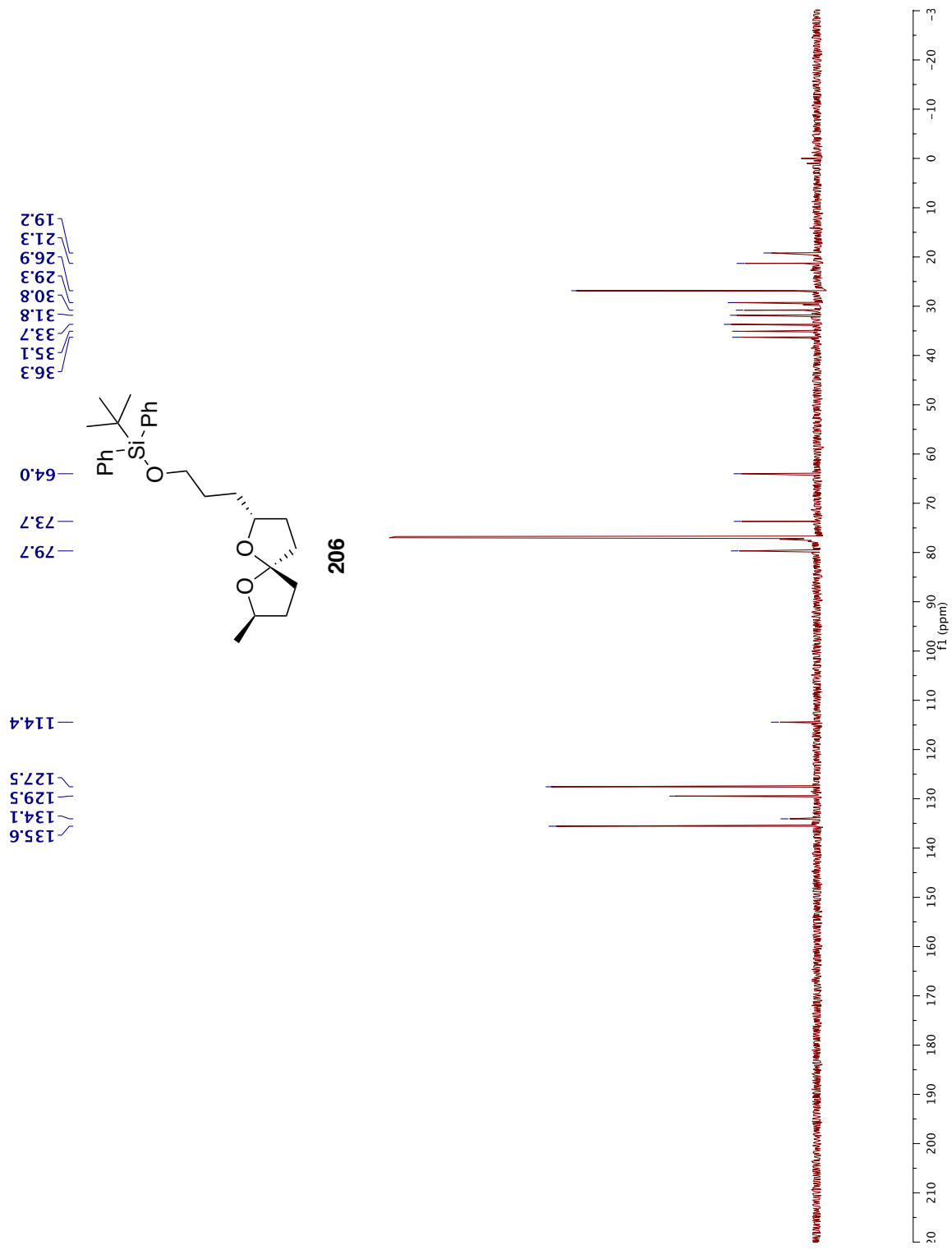


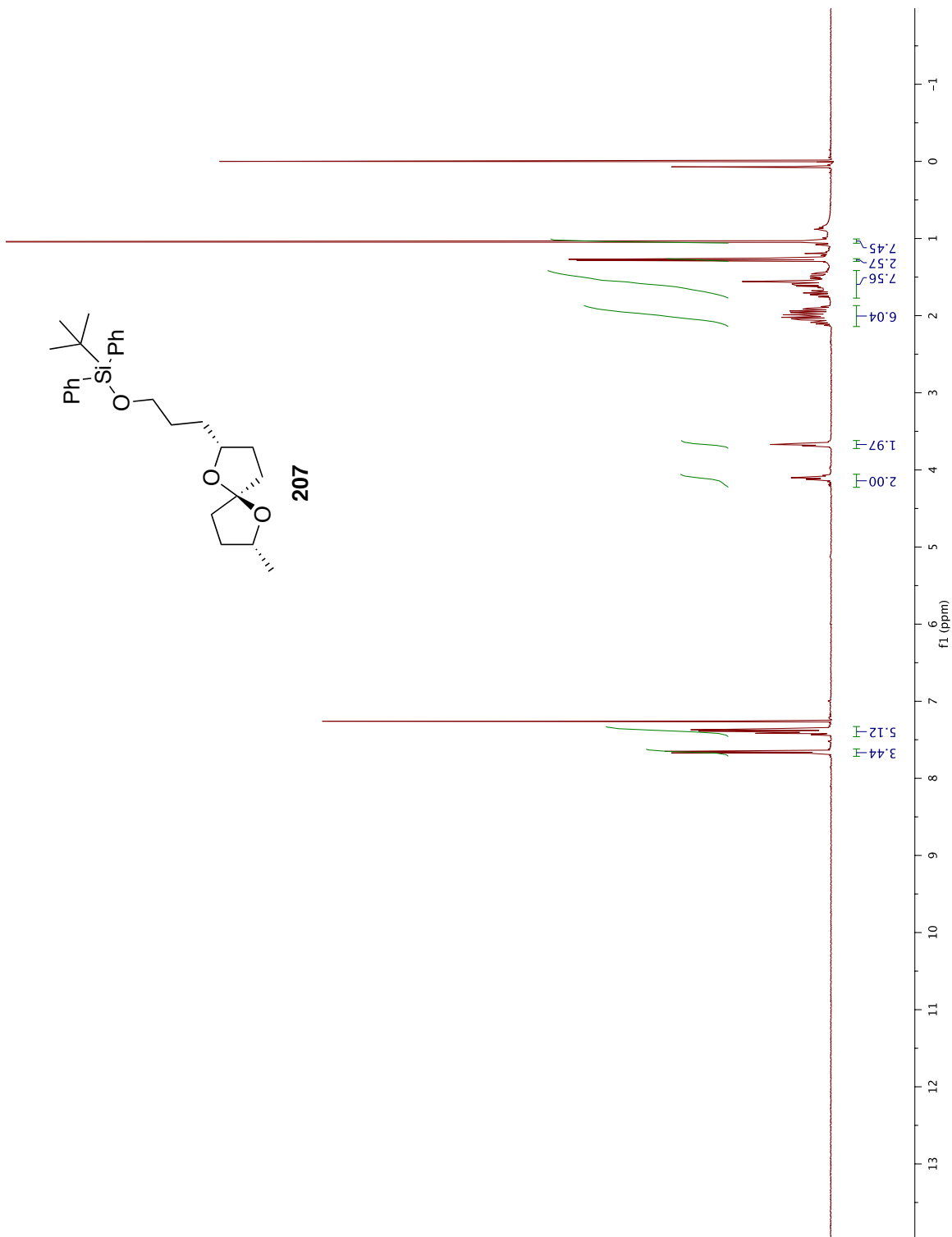


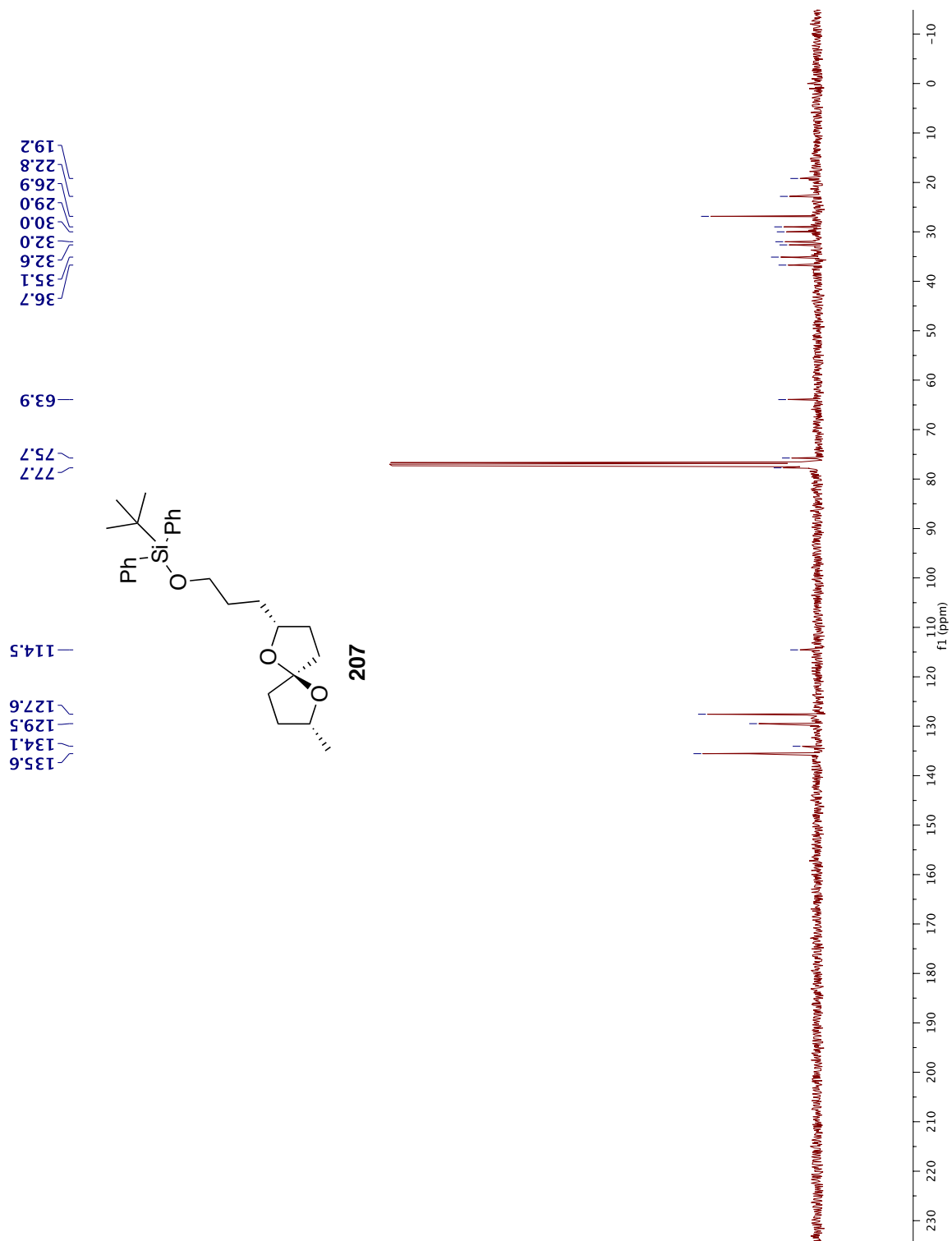


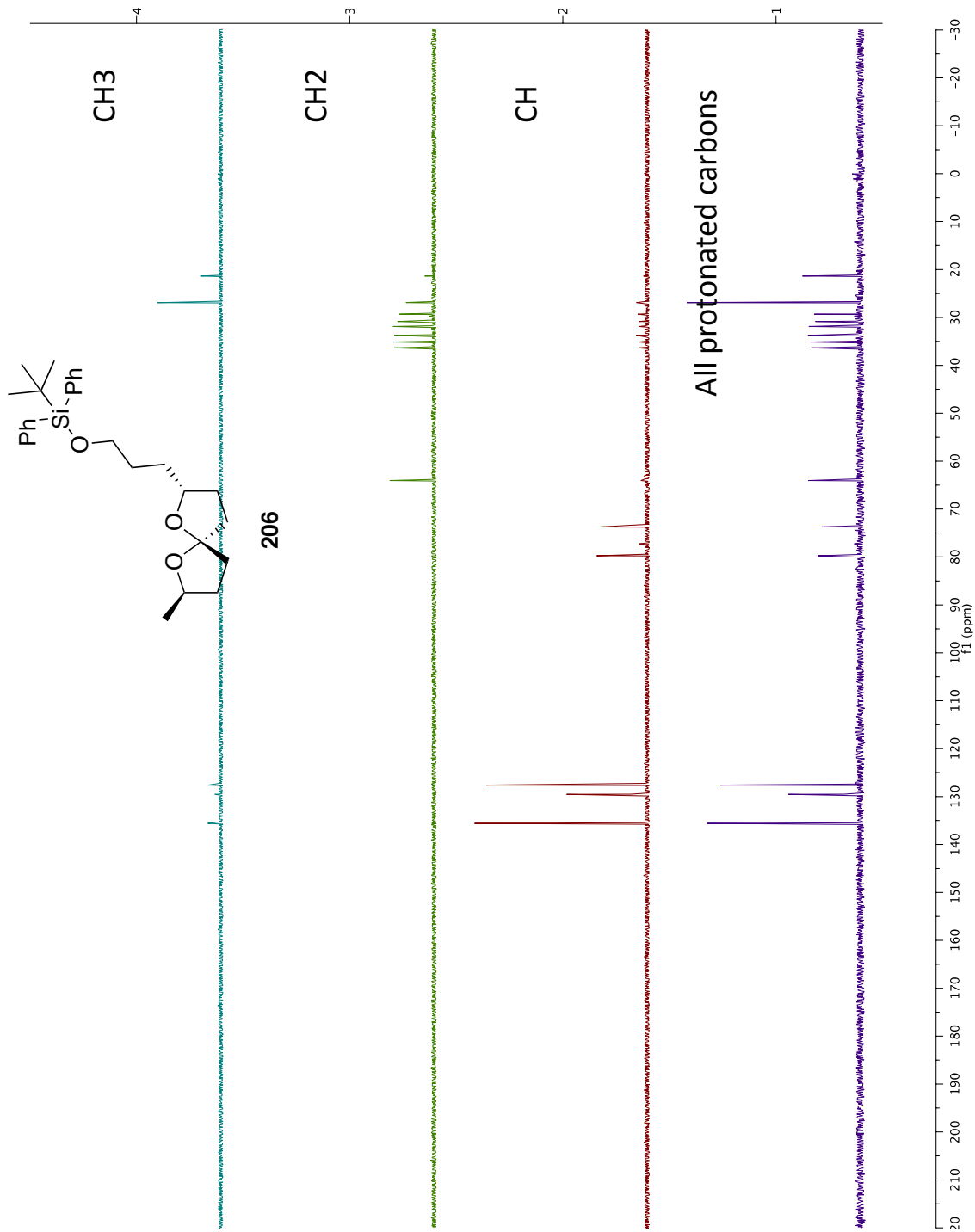


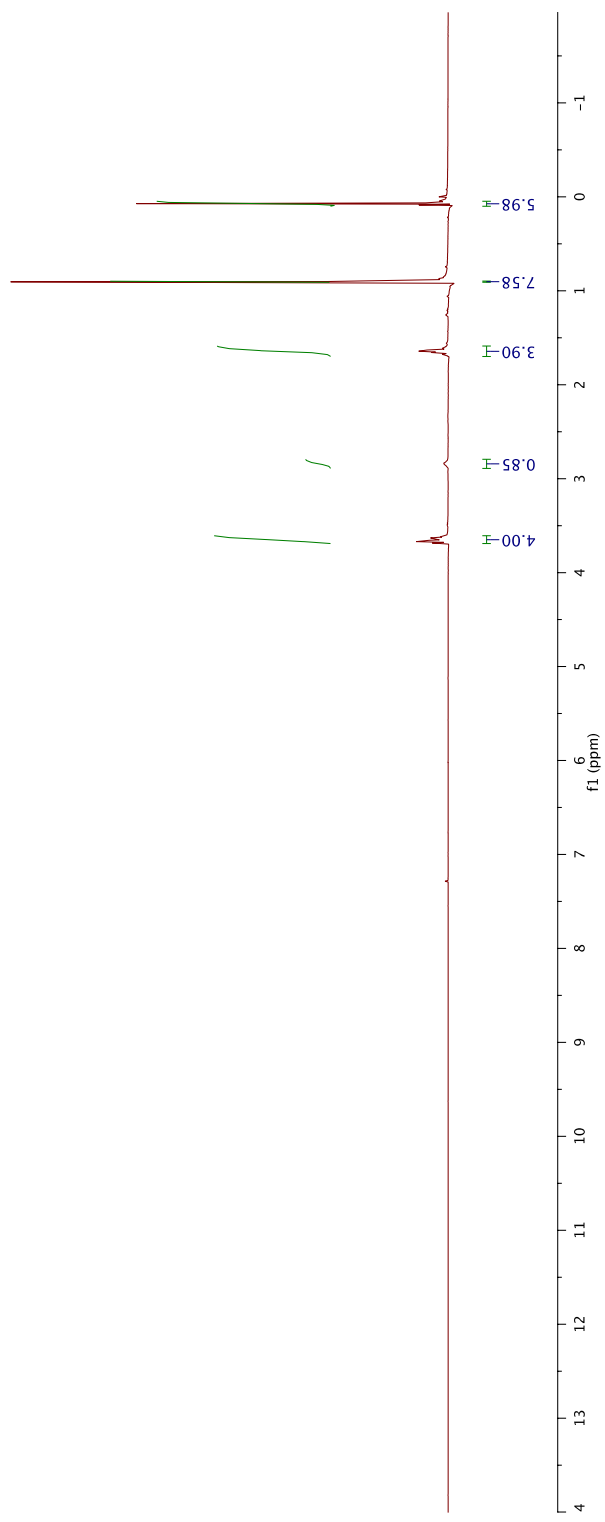
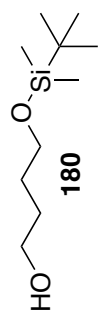


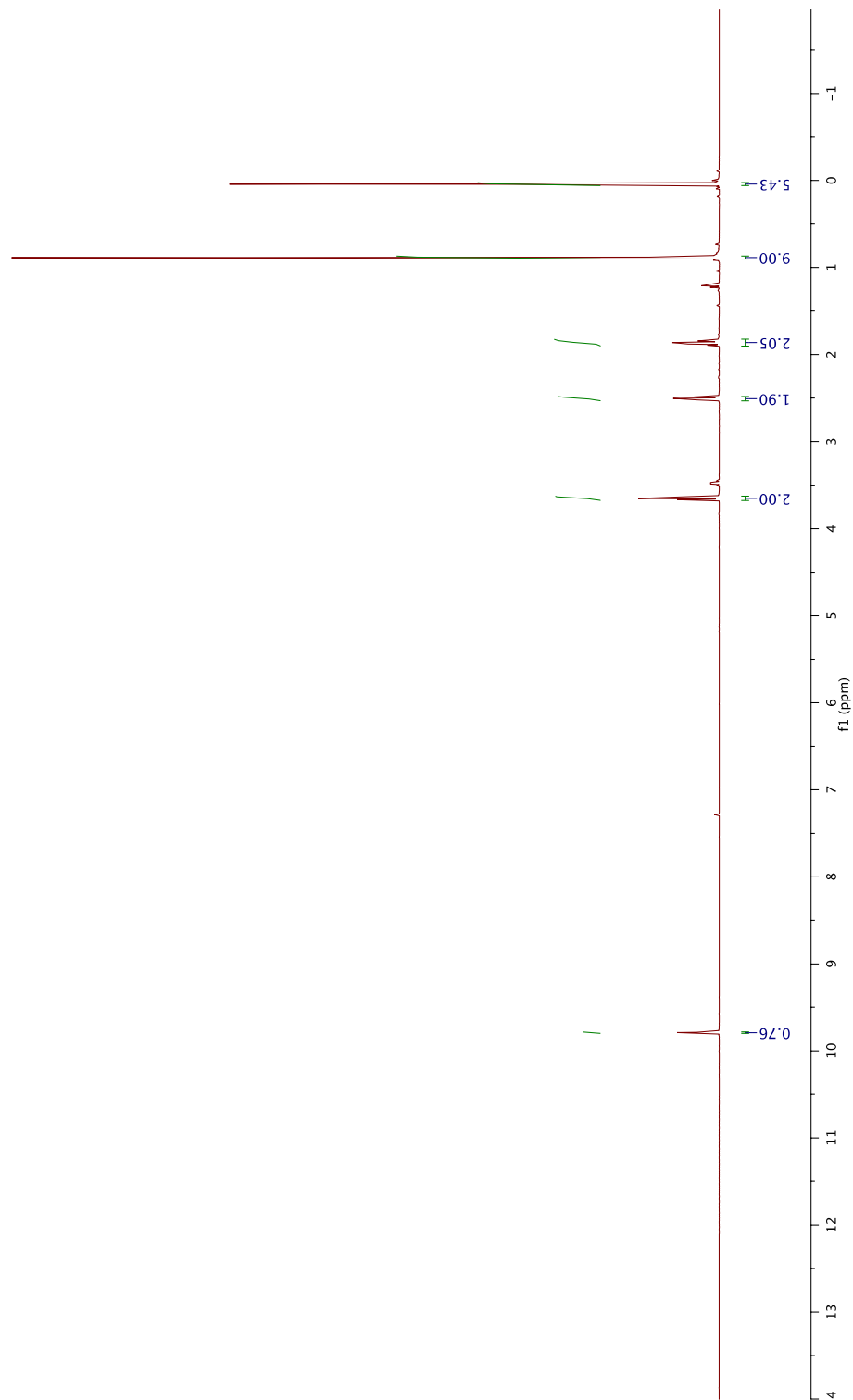
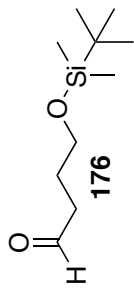


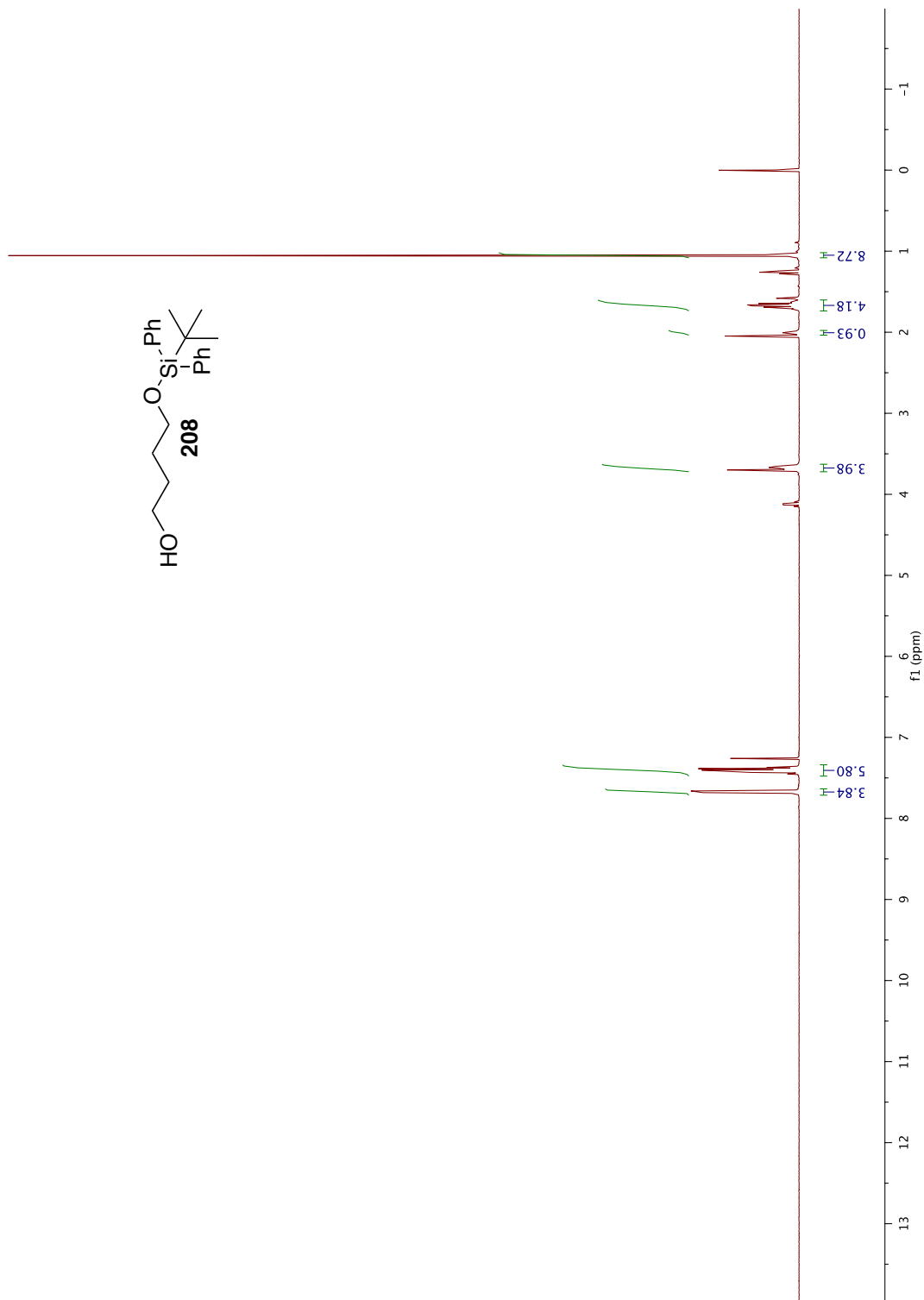
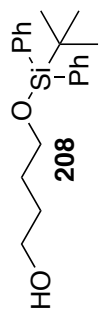


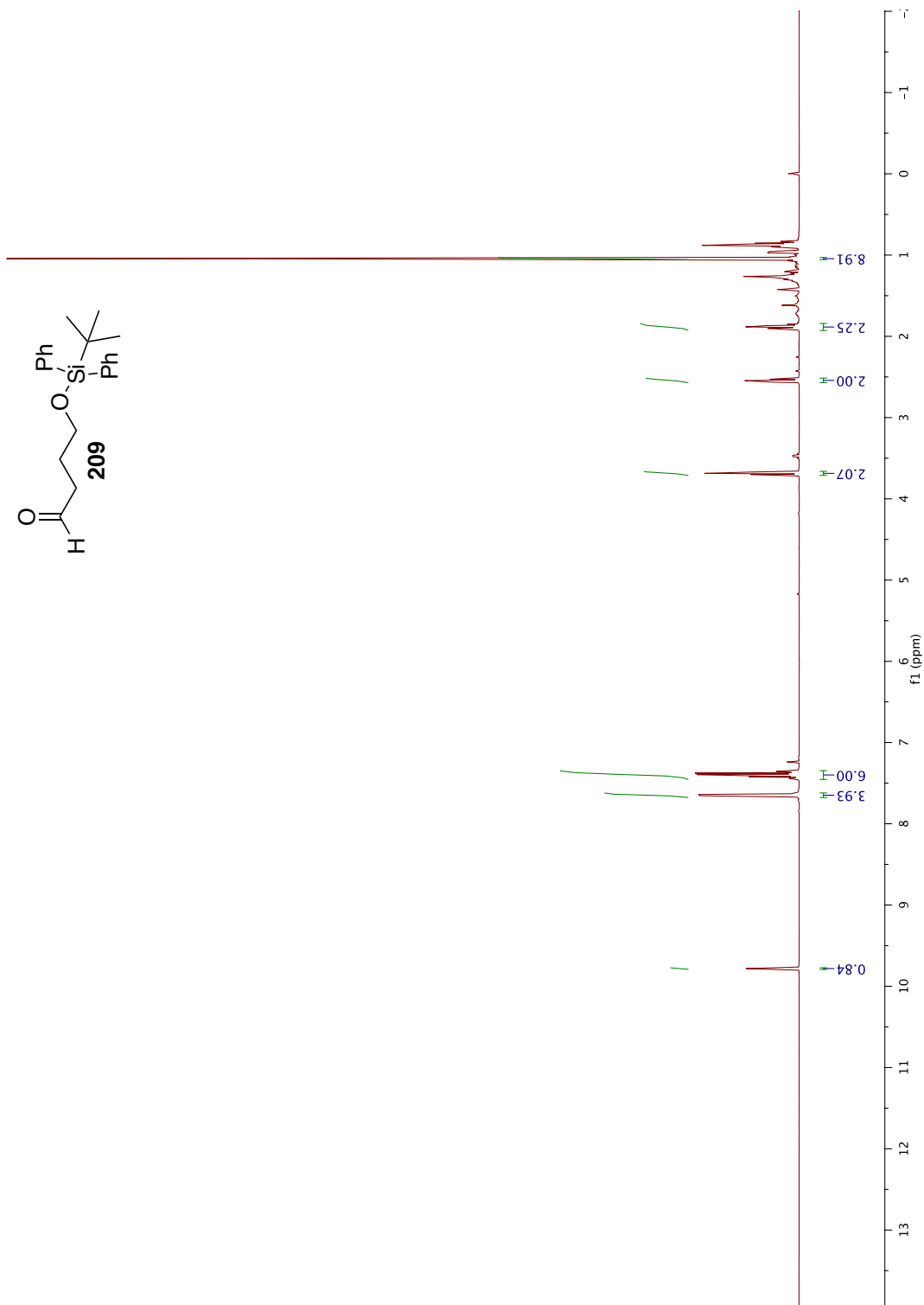
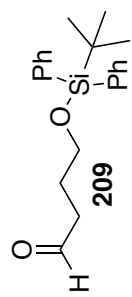


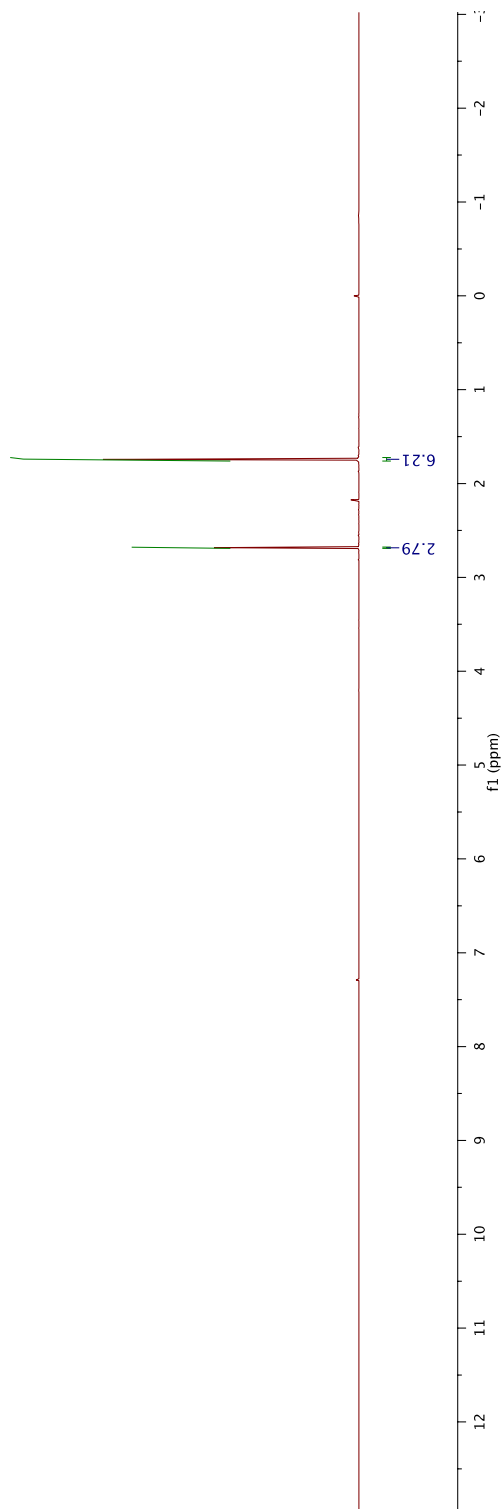
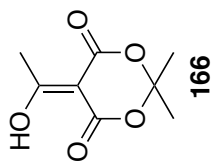


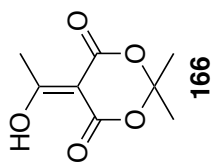












26.9
23.5

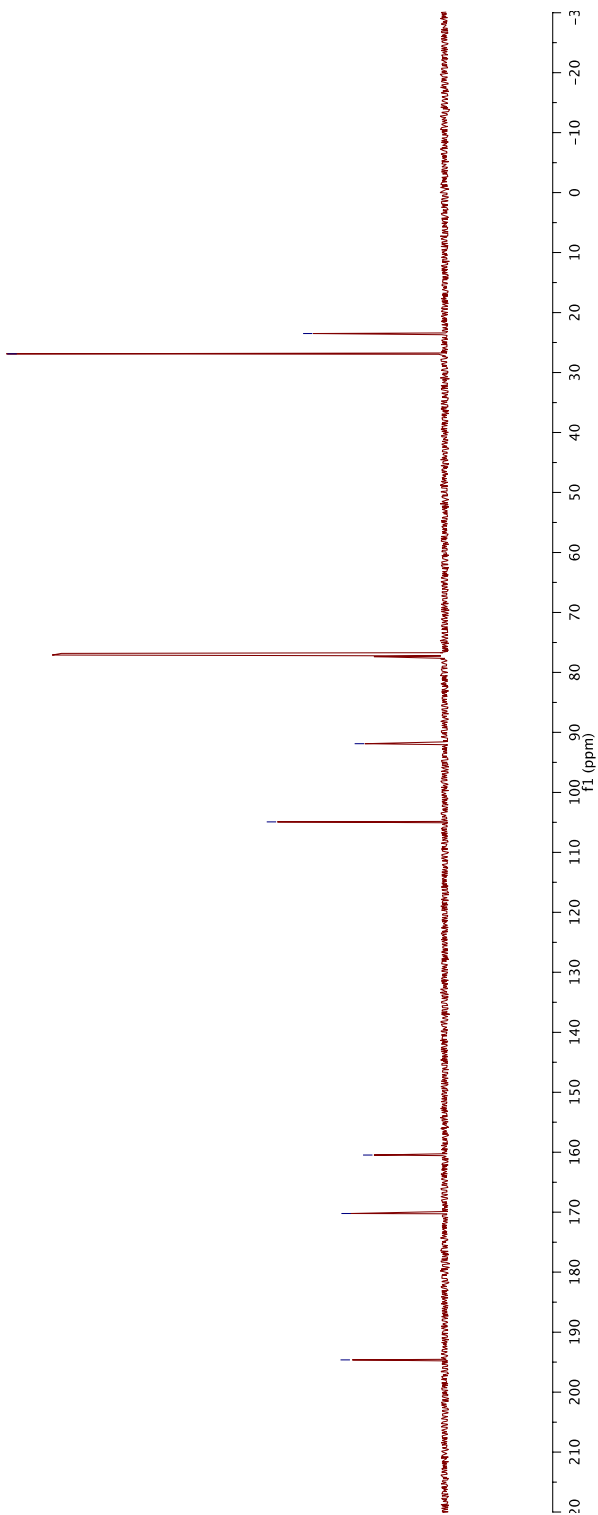
91.9

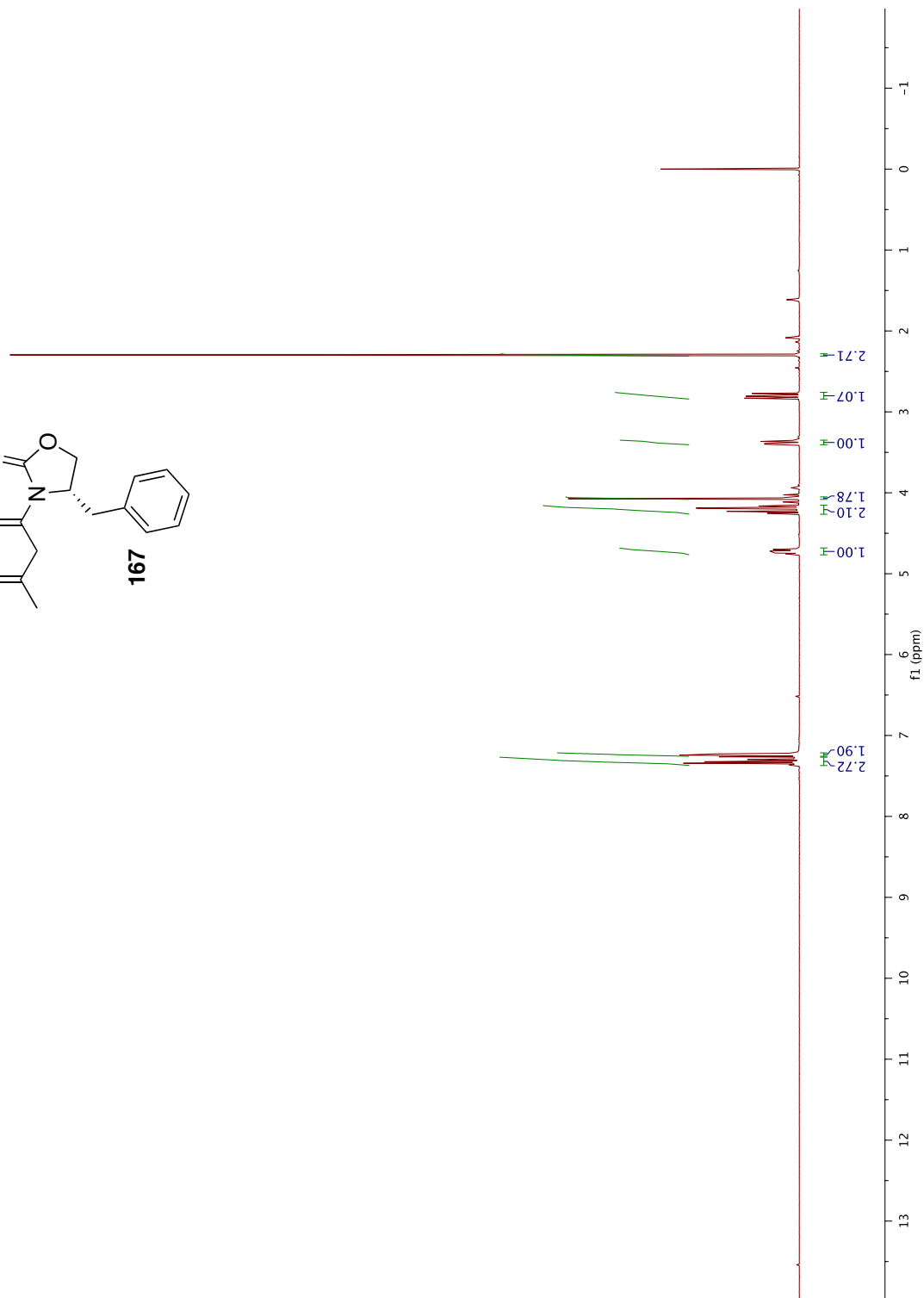
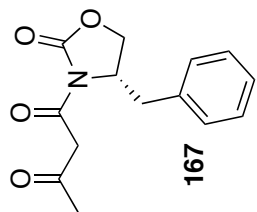
104.9

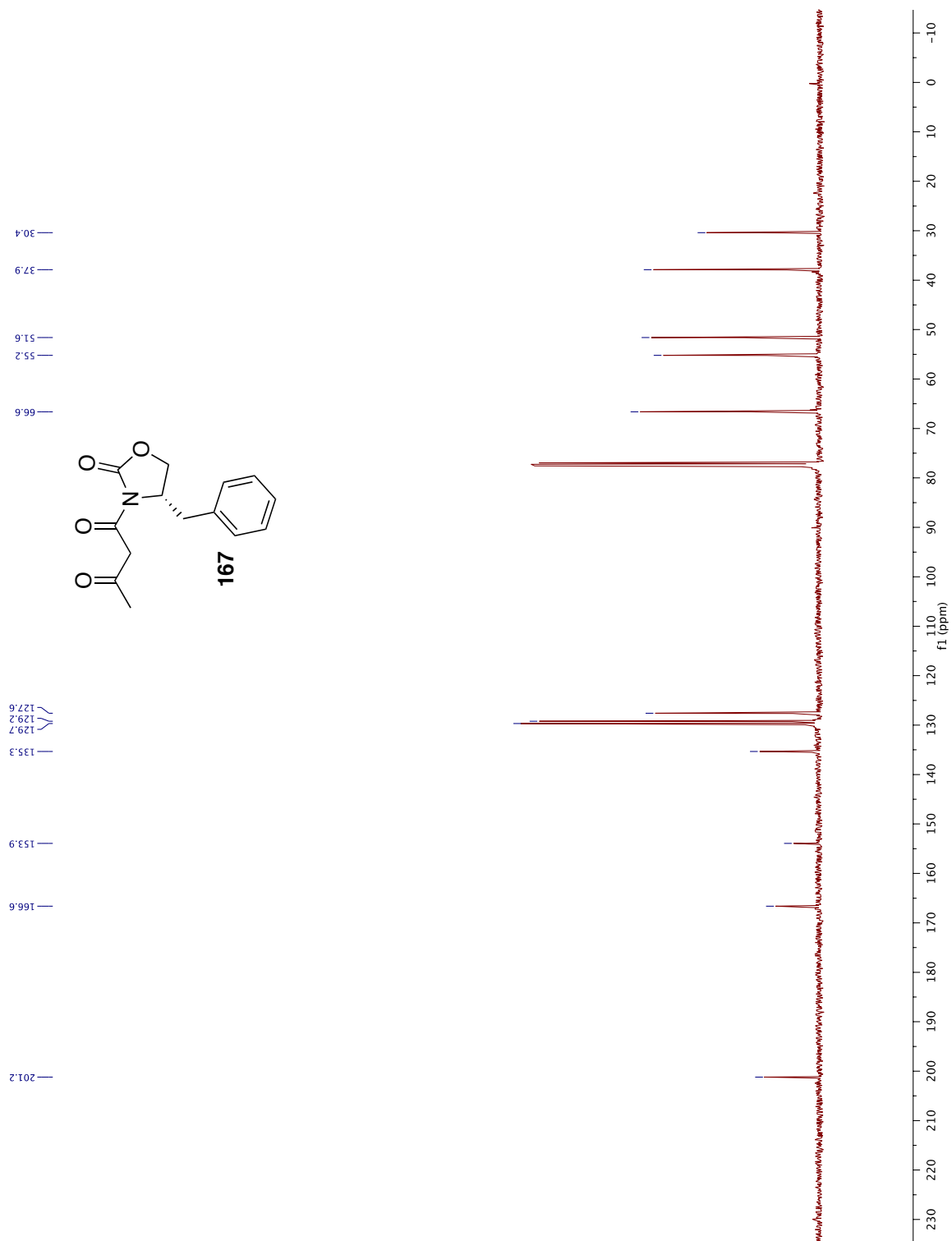
160.5

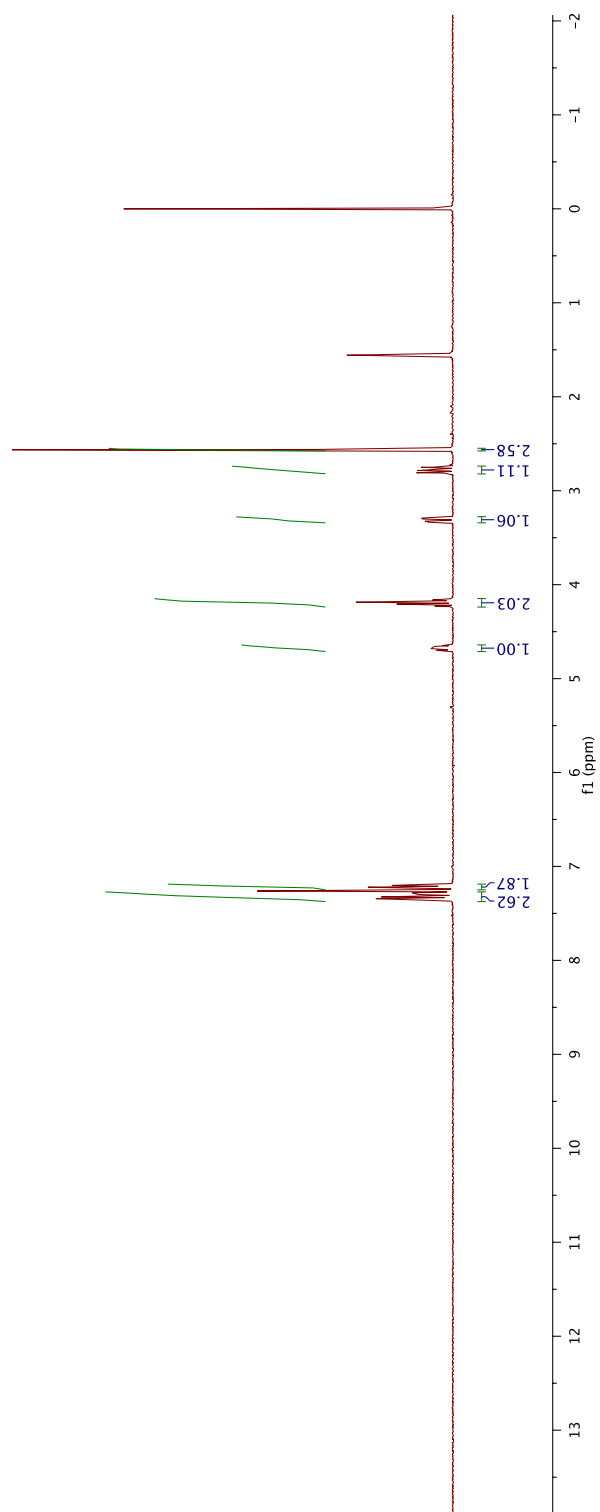
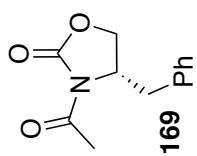
170.2

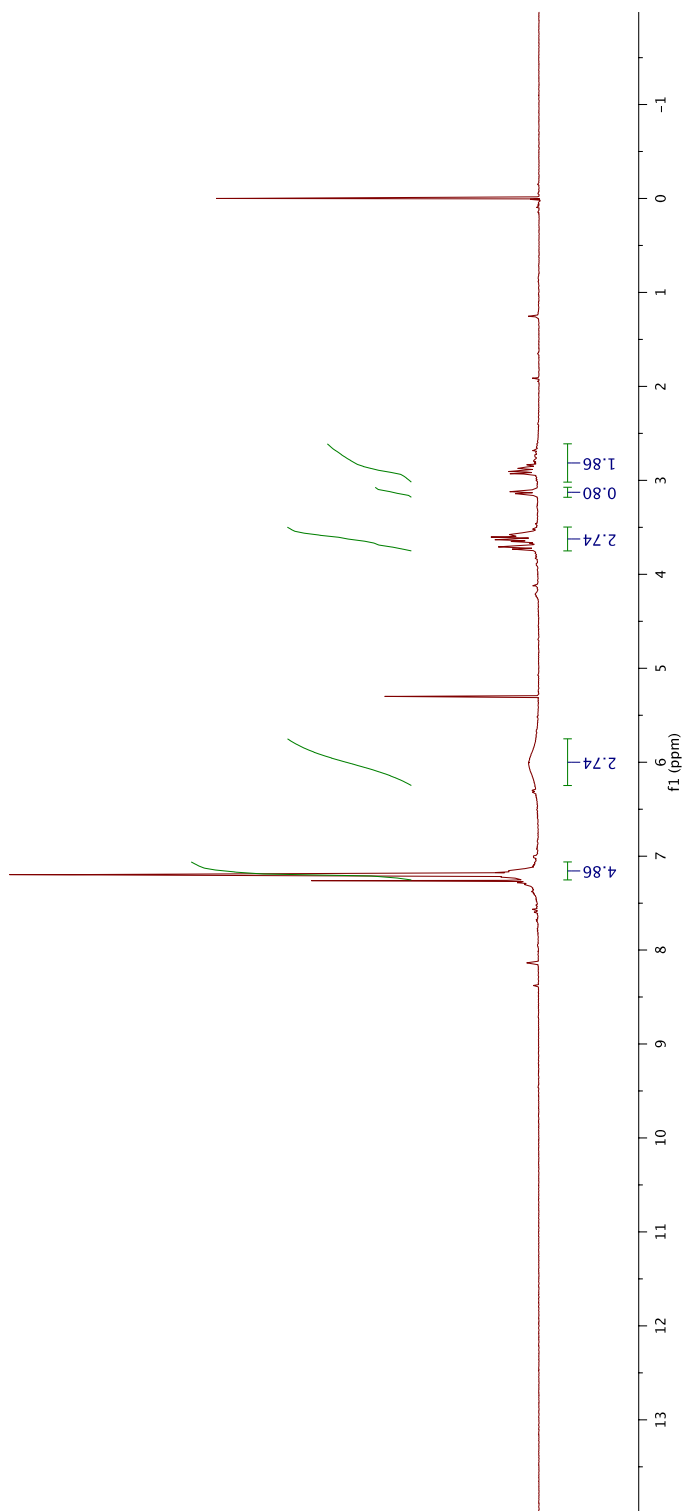
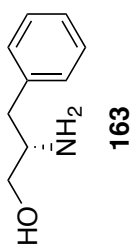
194.6

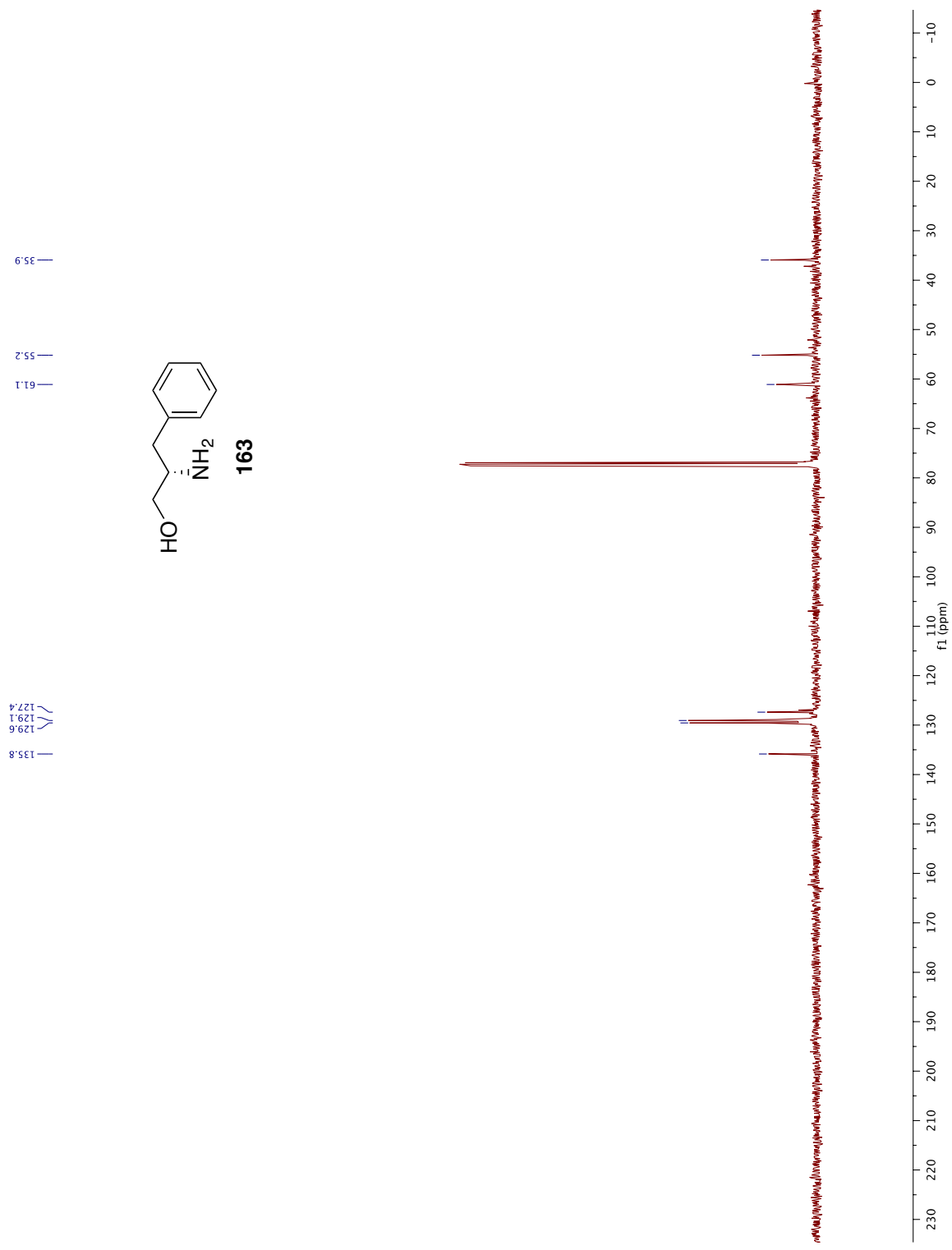


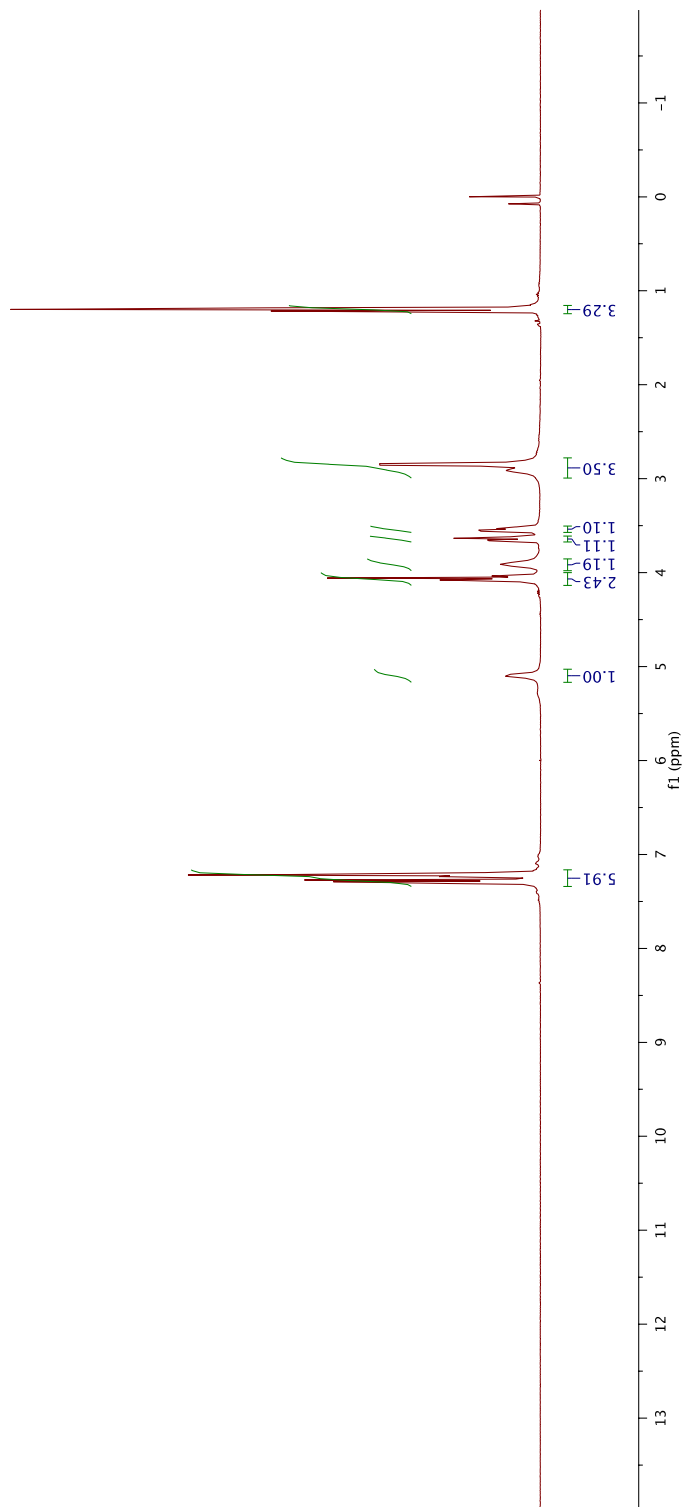
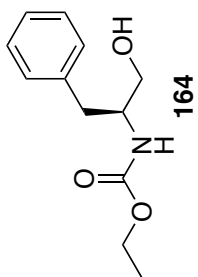


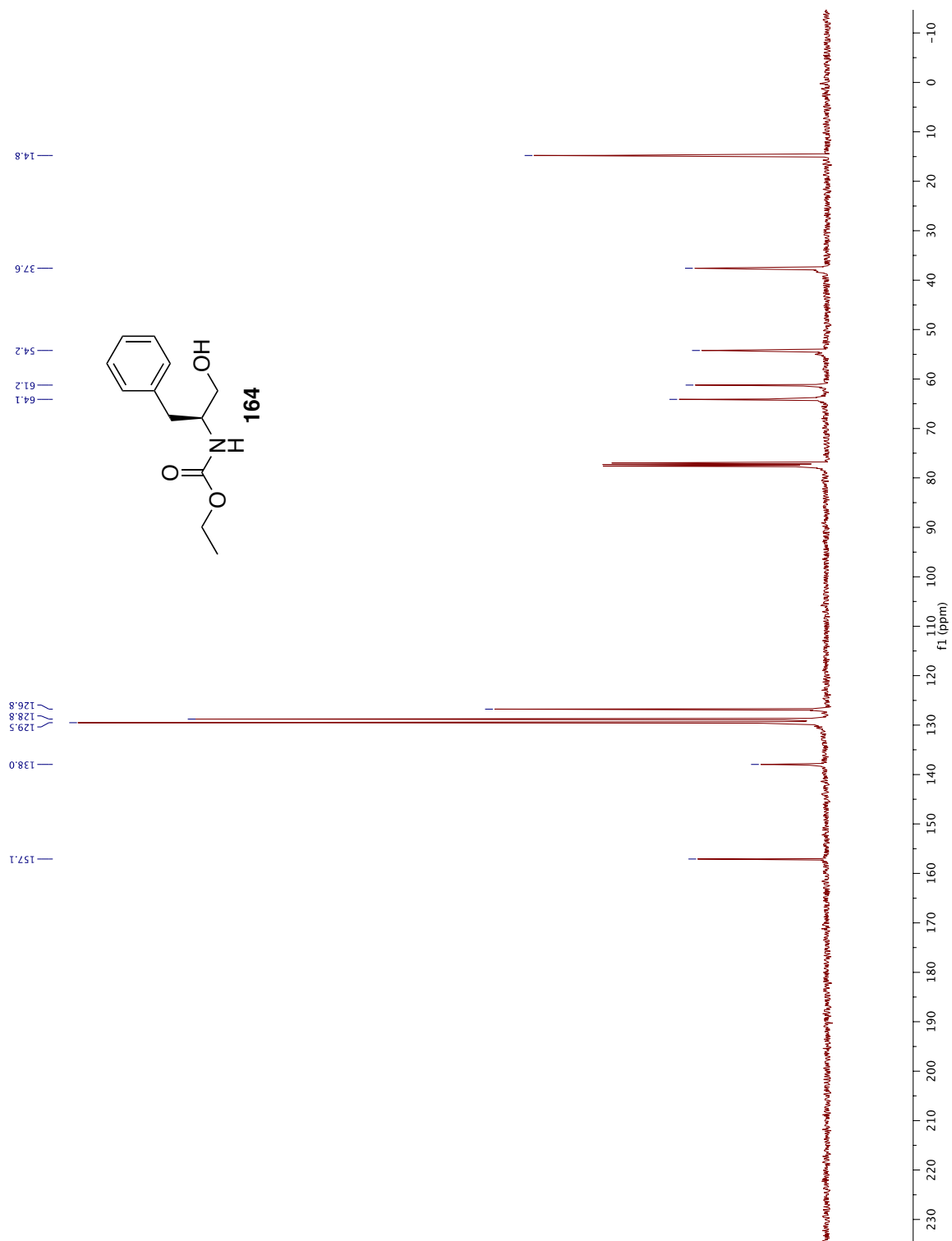


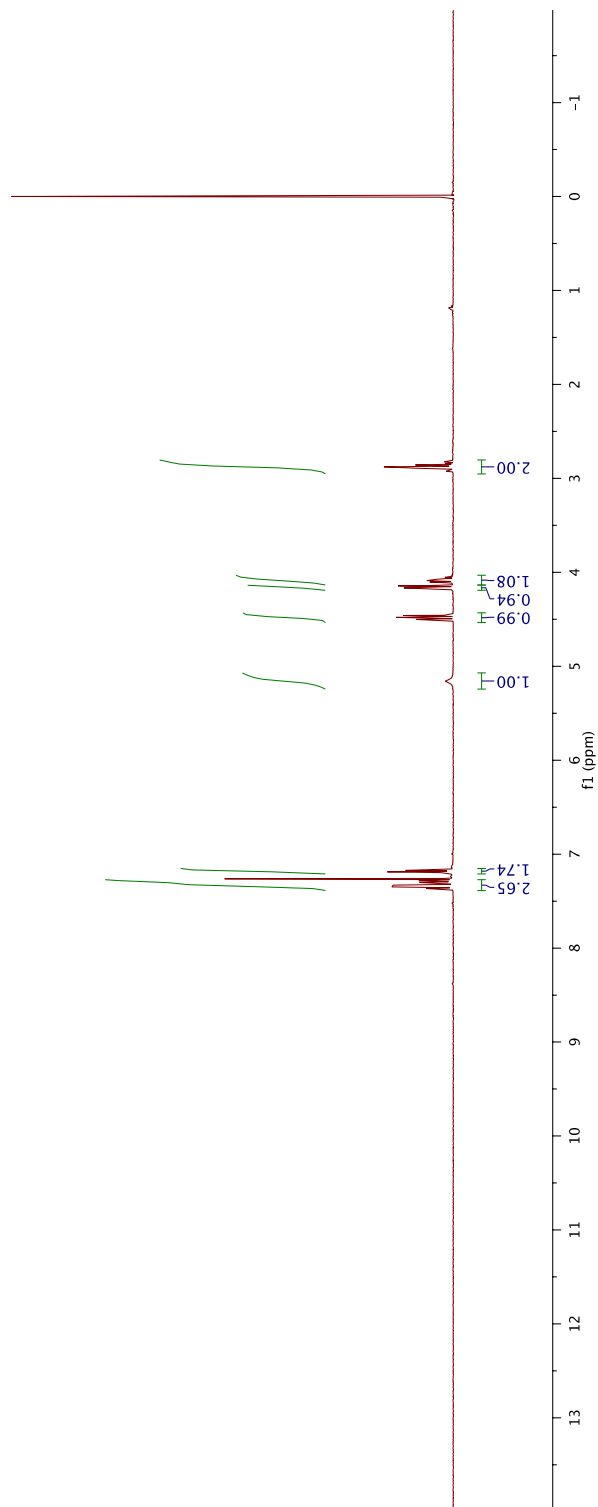
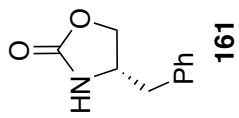


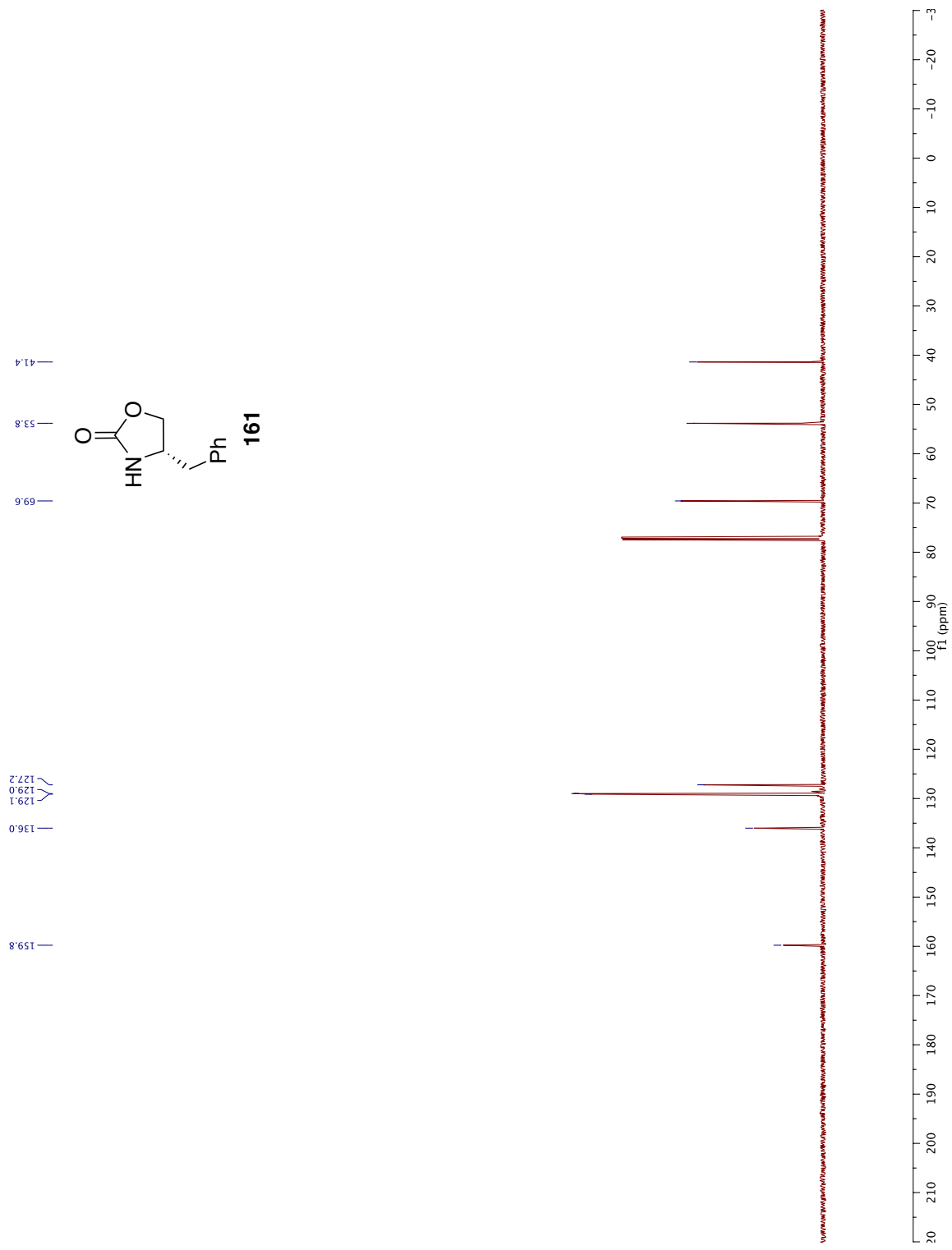


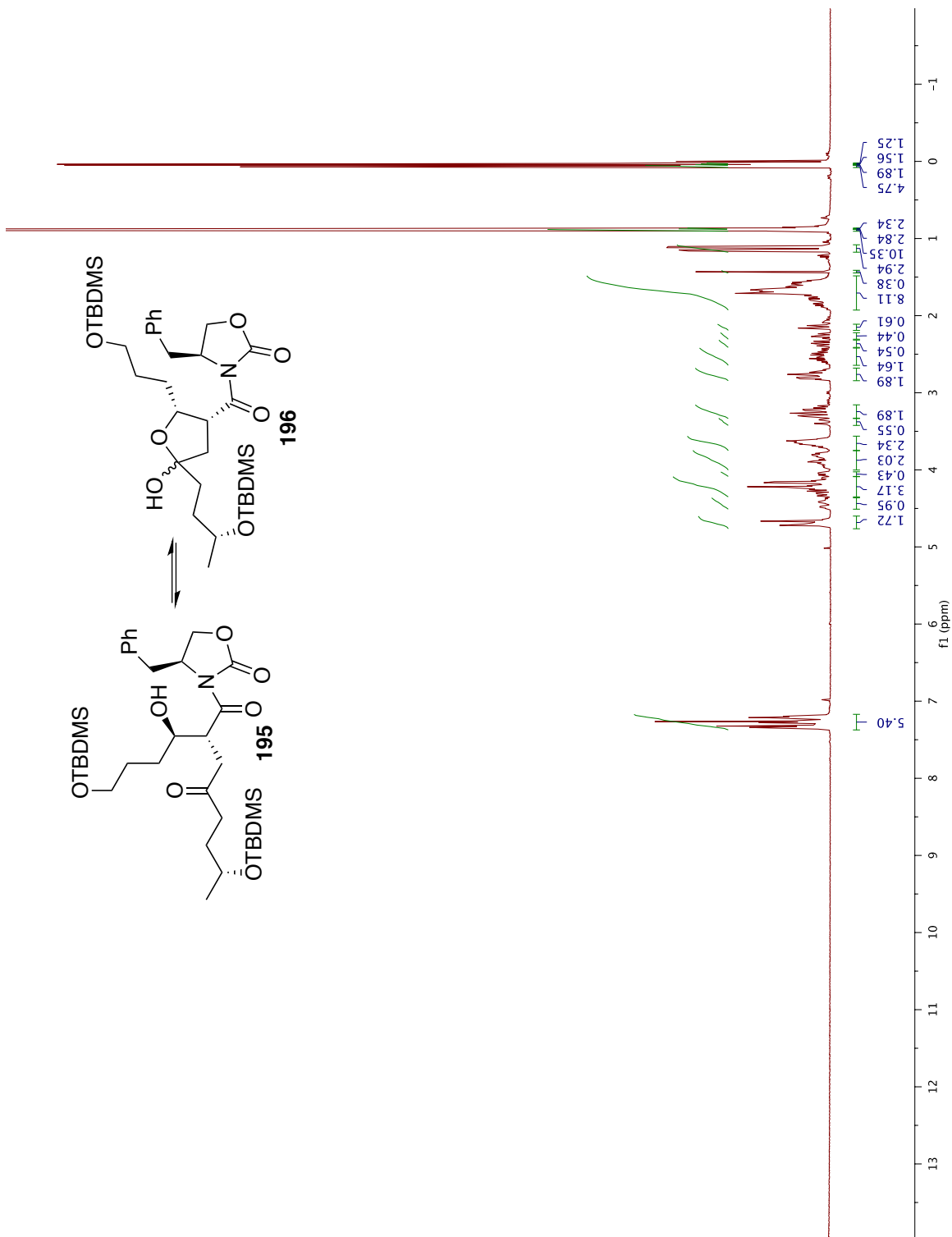


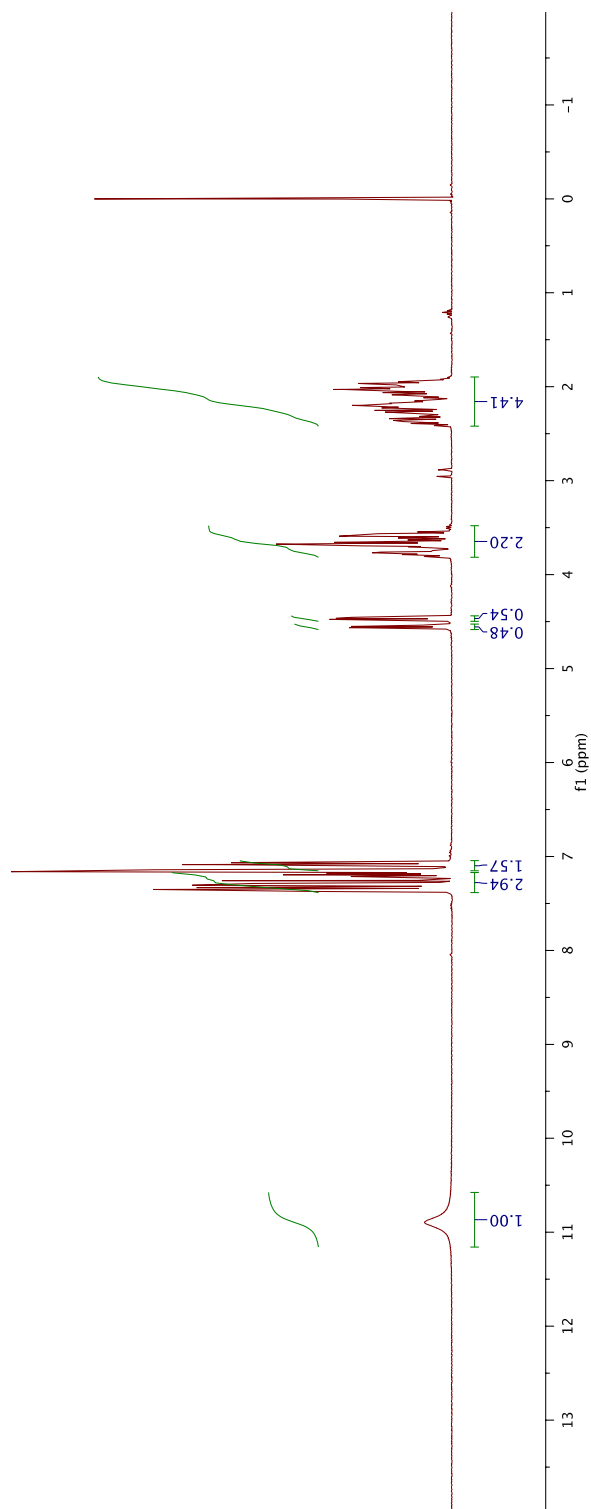
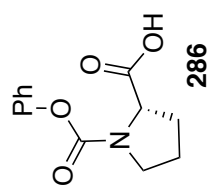


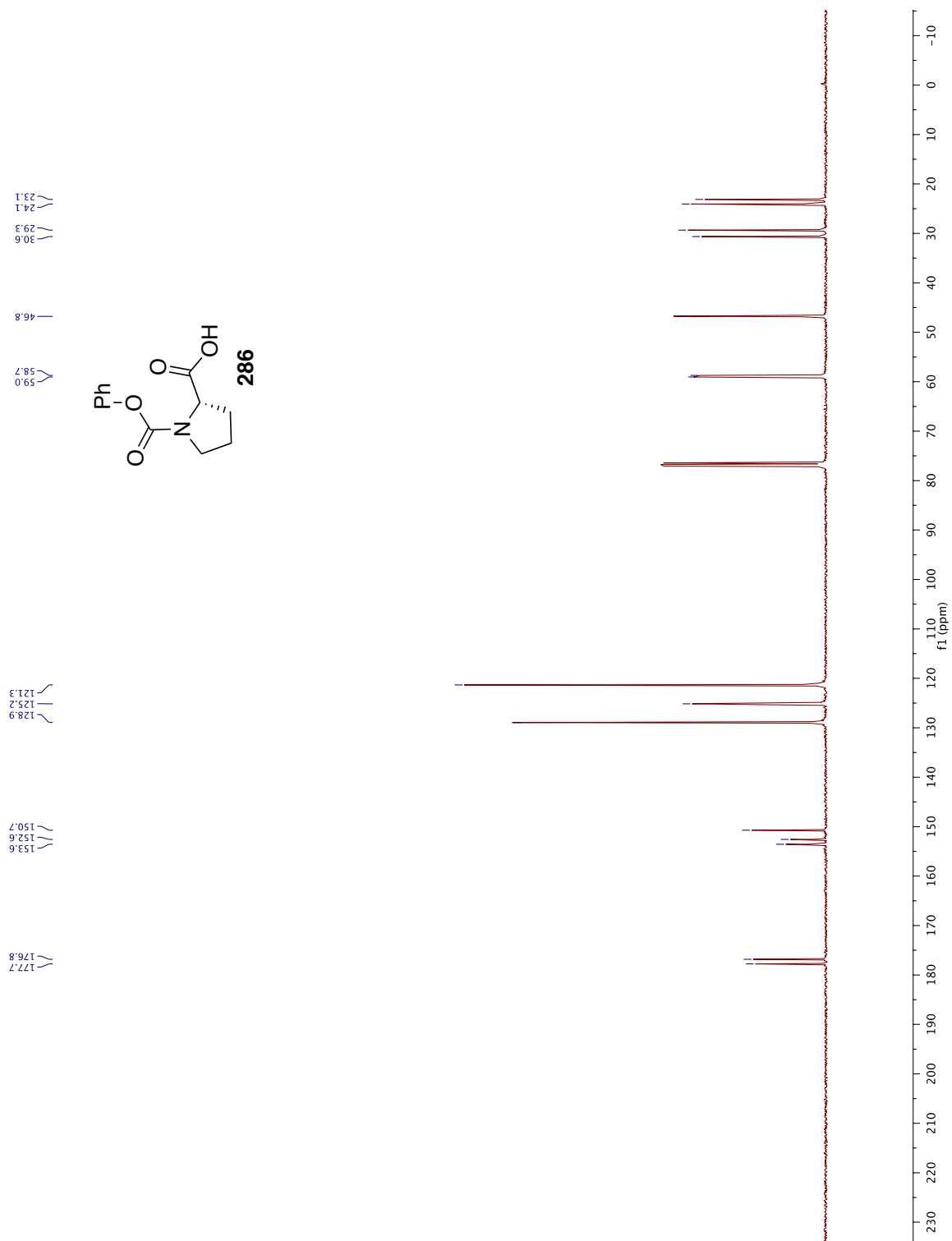


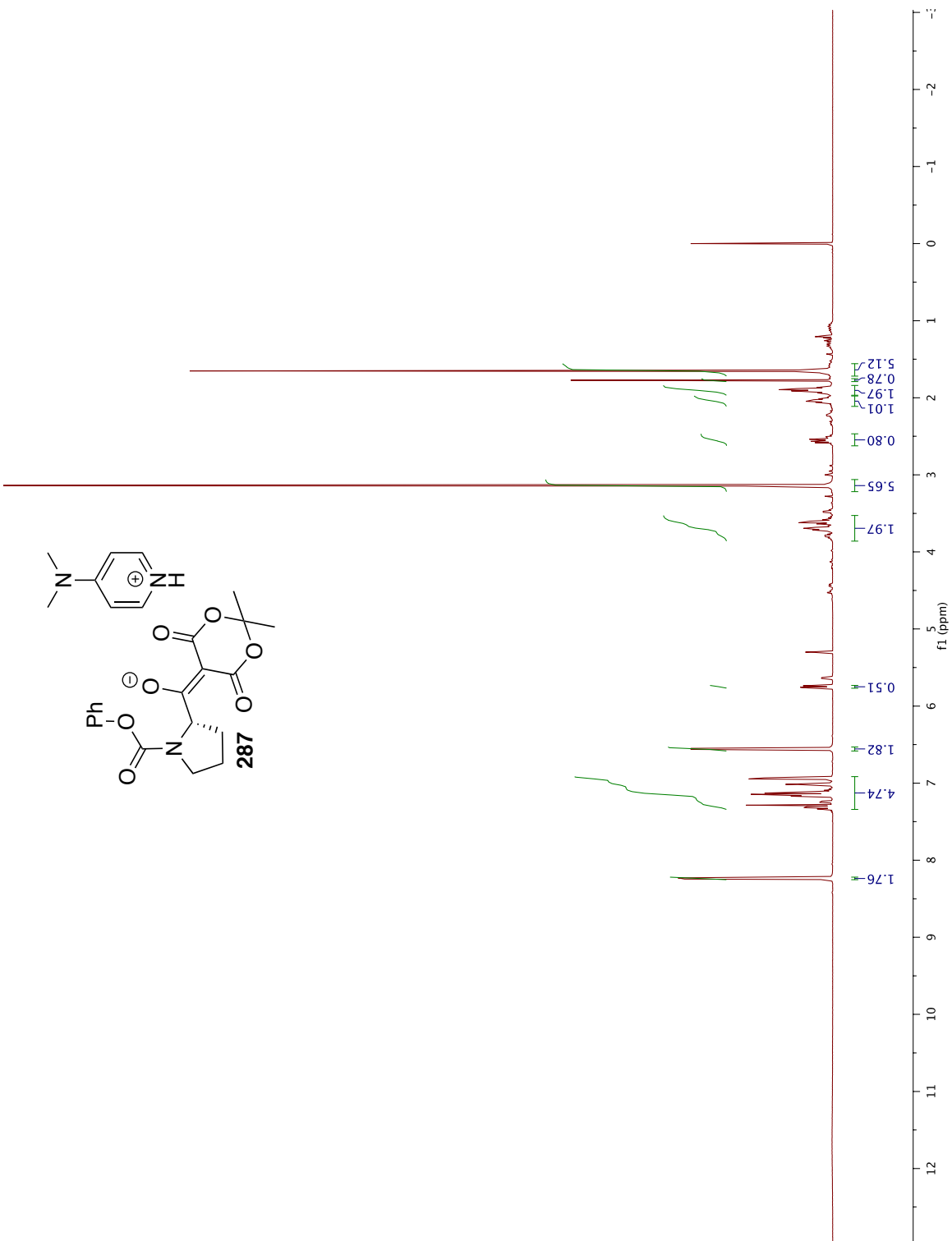


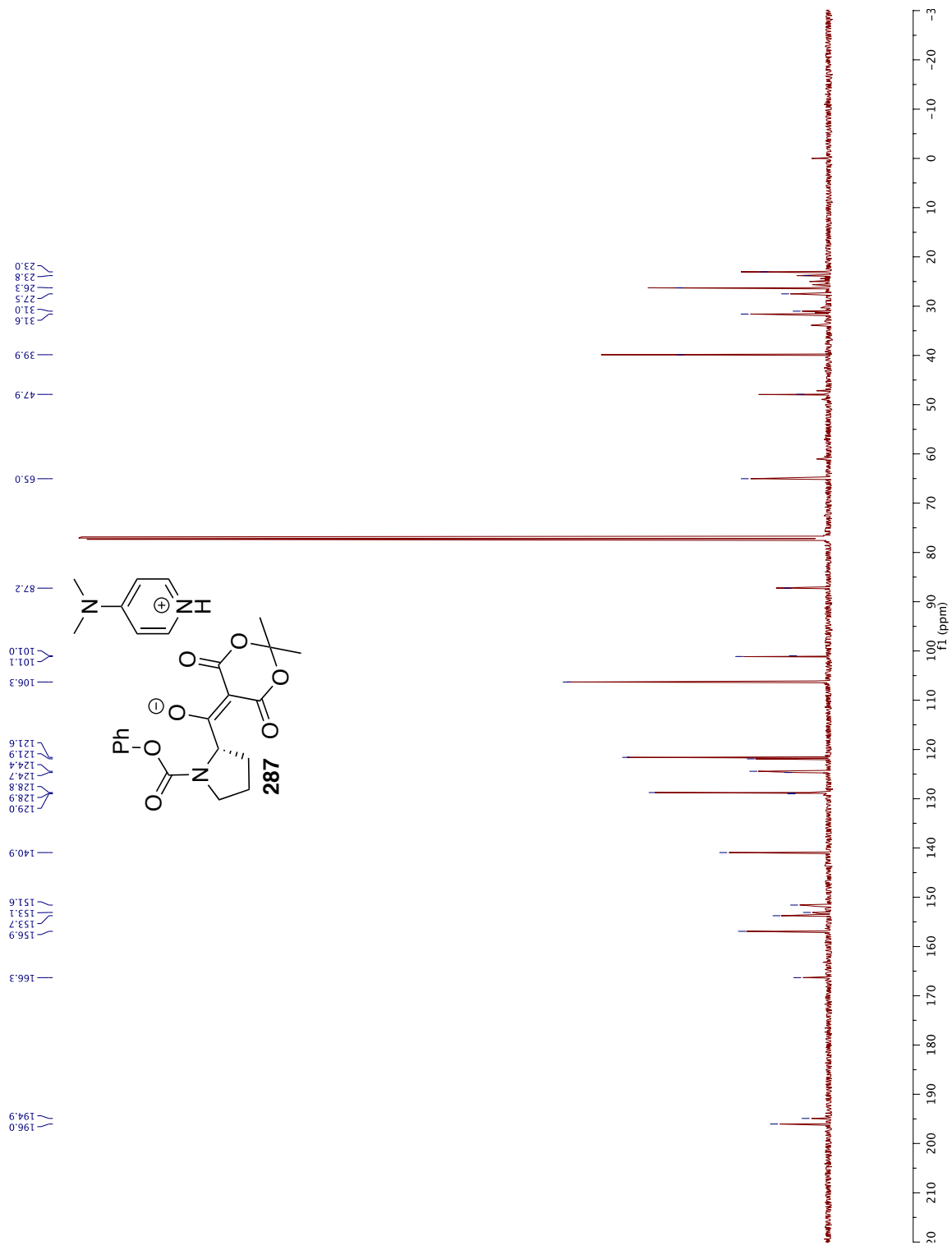


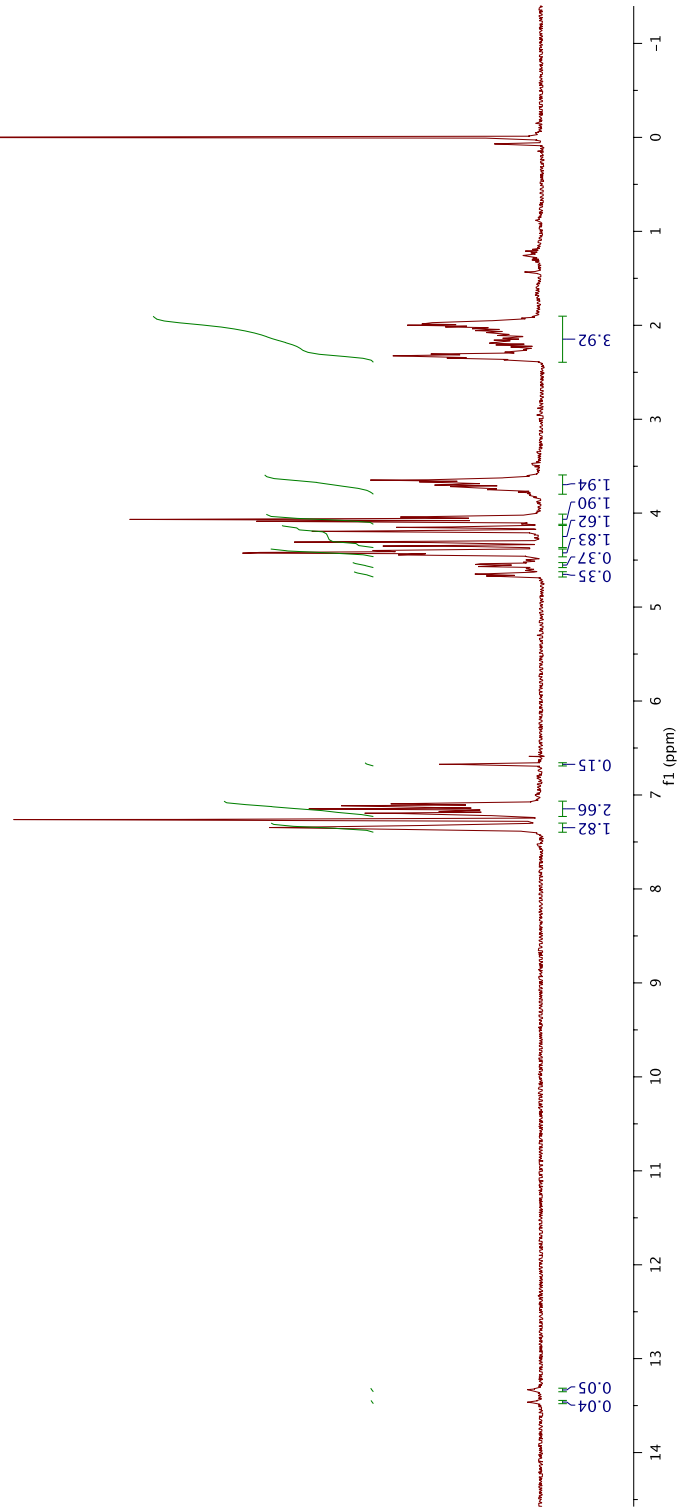
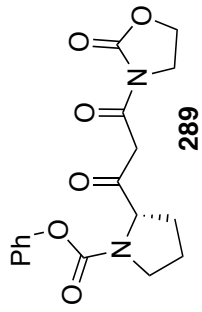


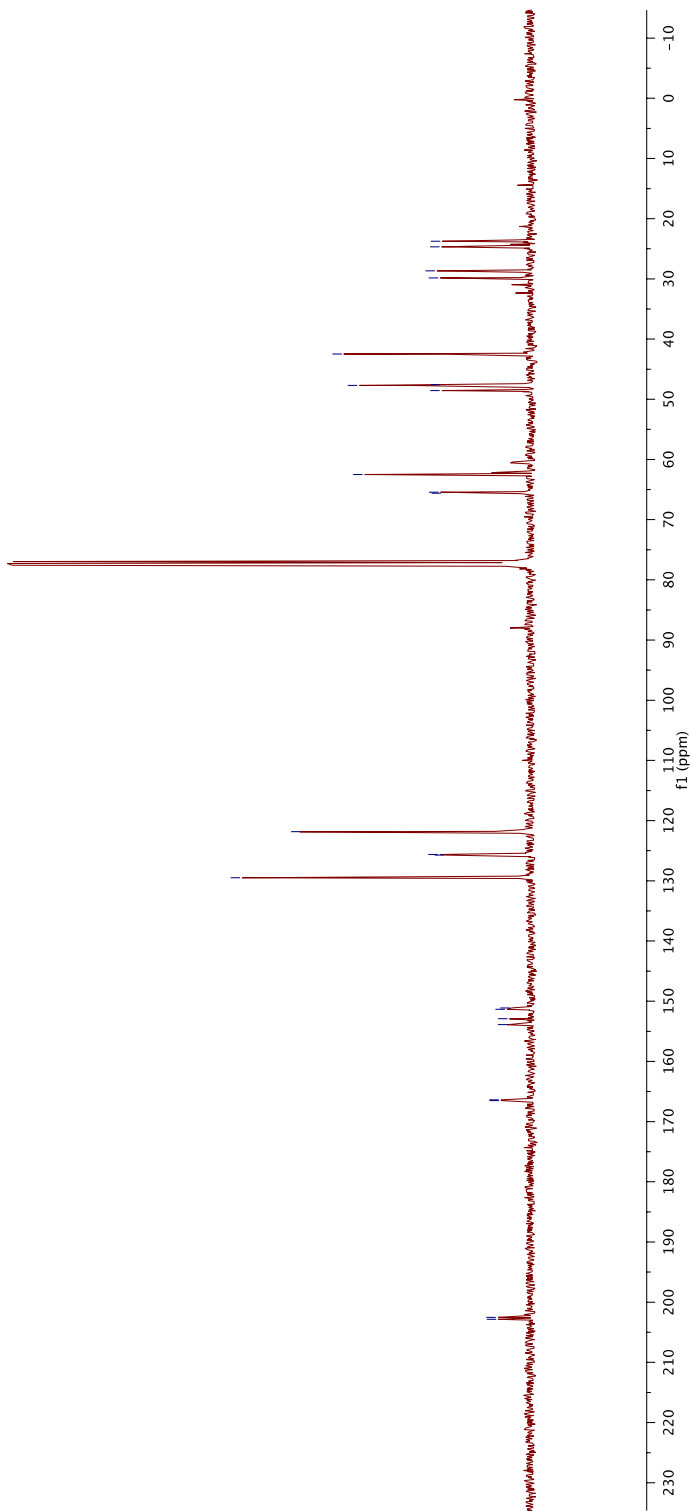
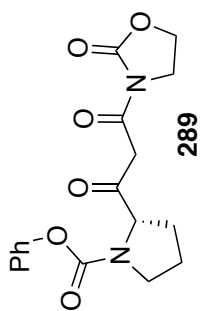


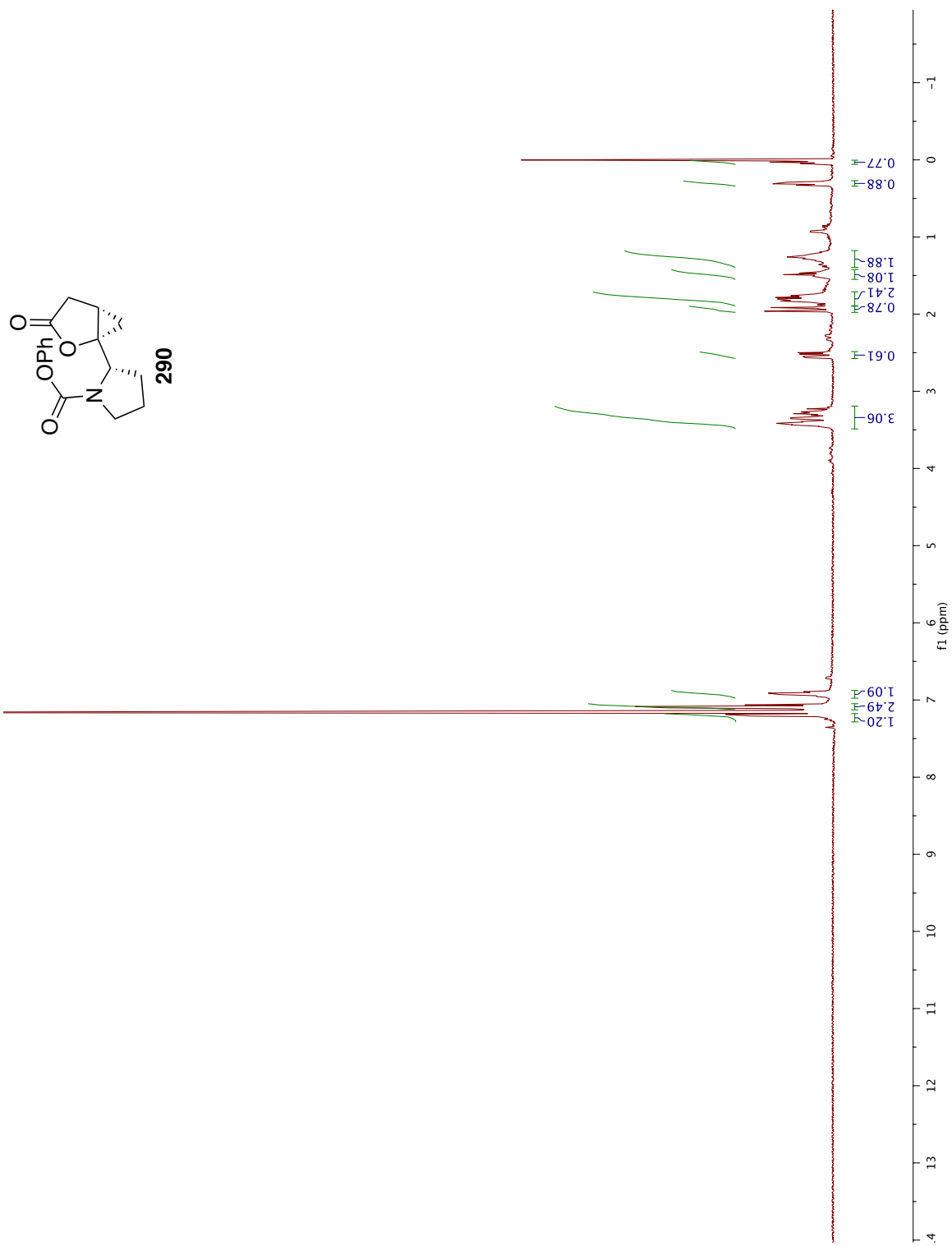


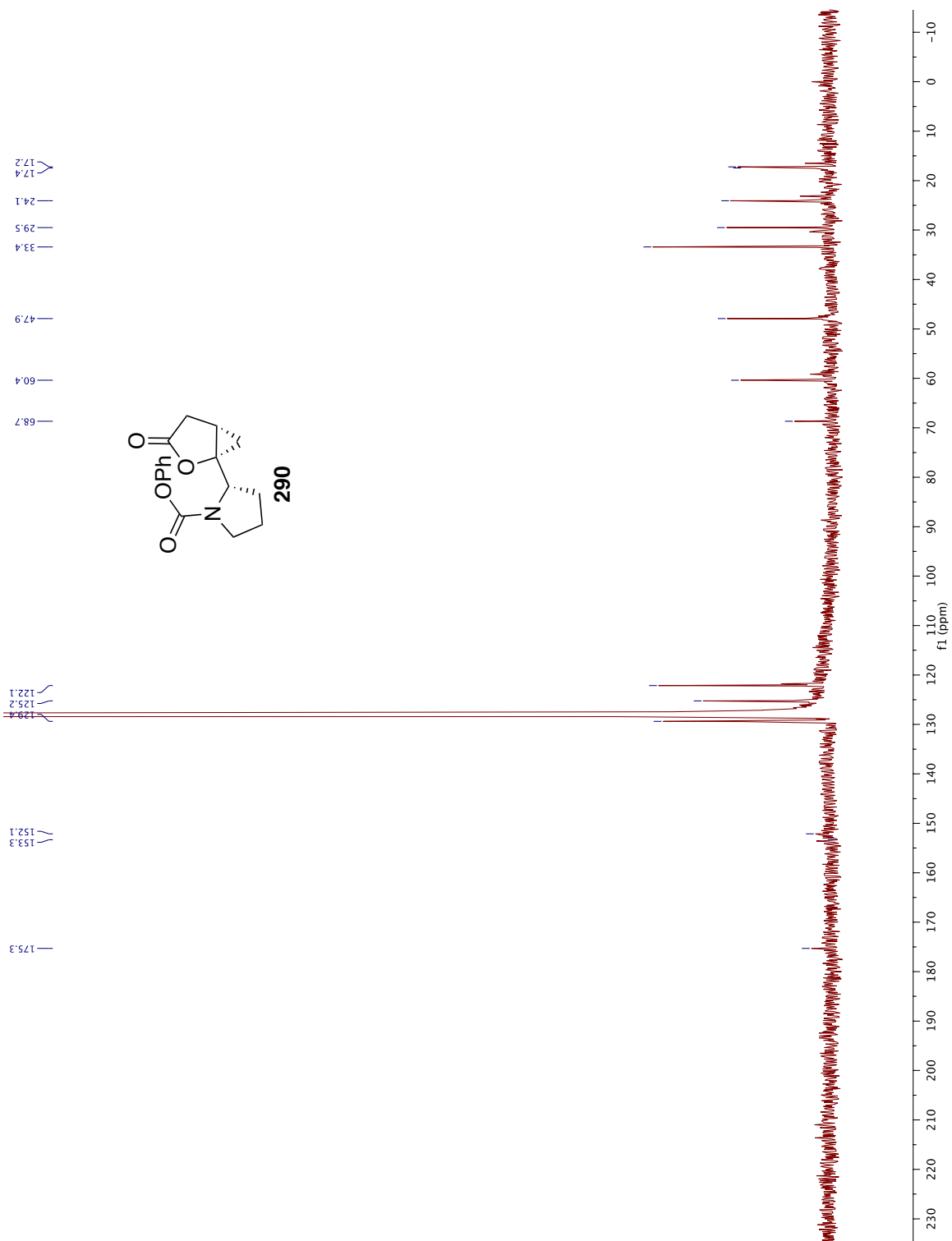


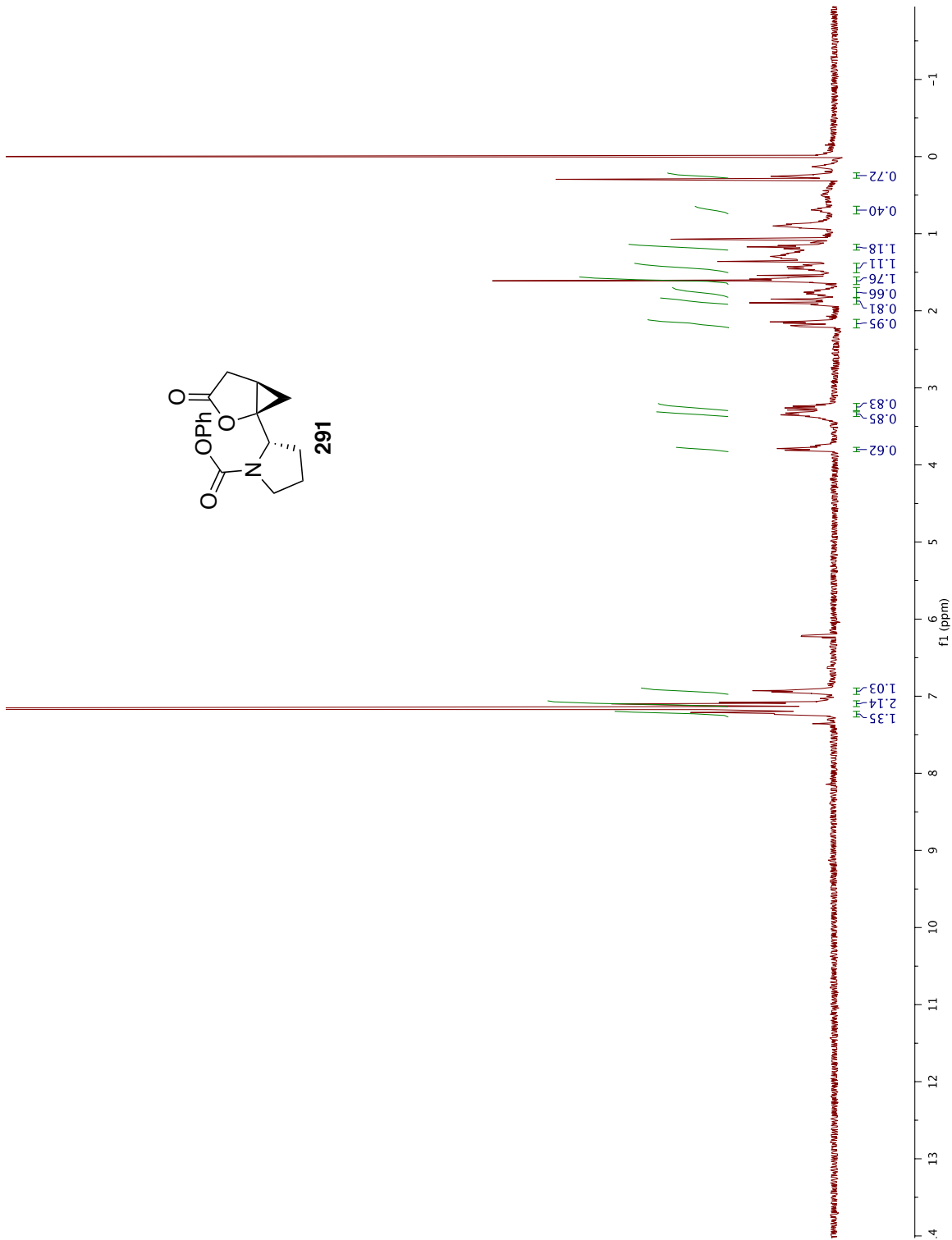
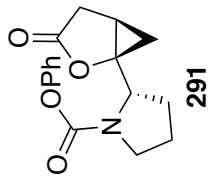


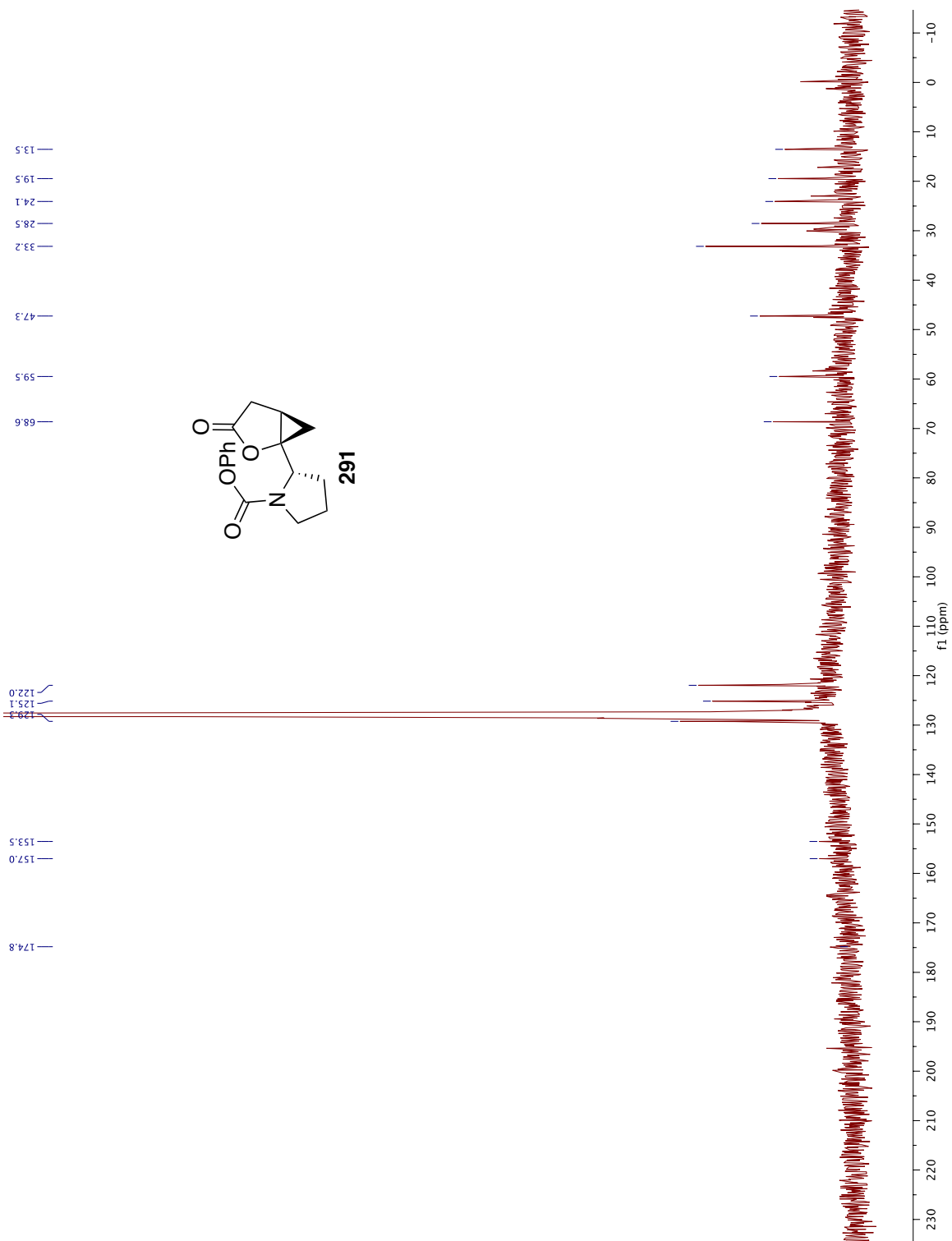


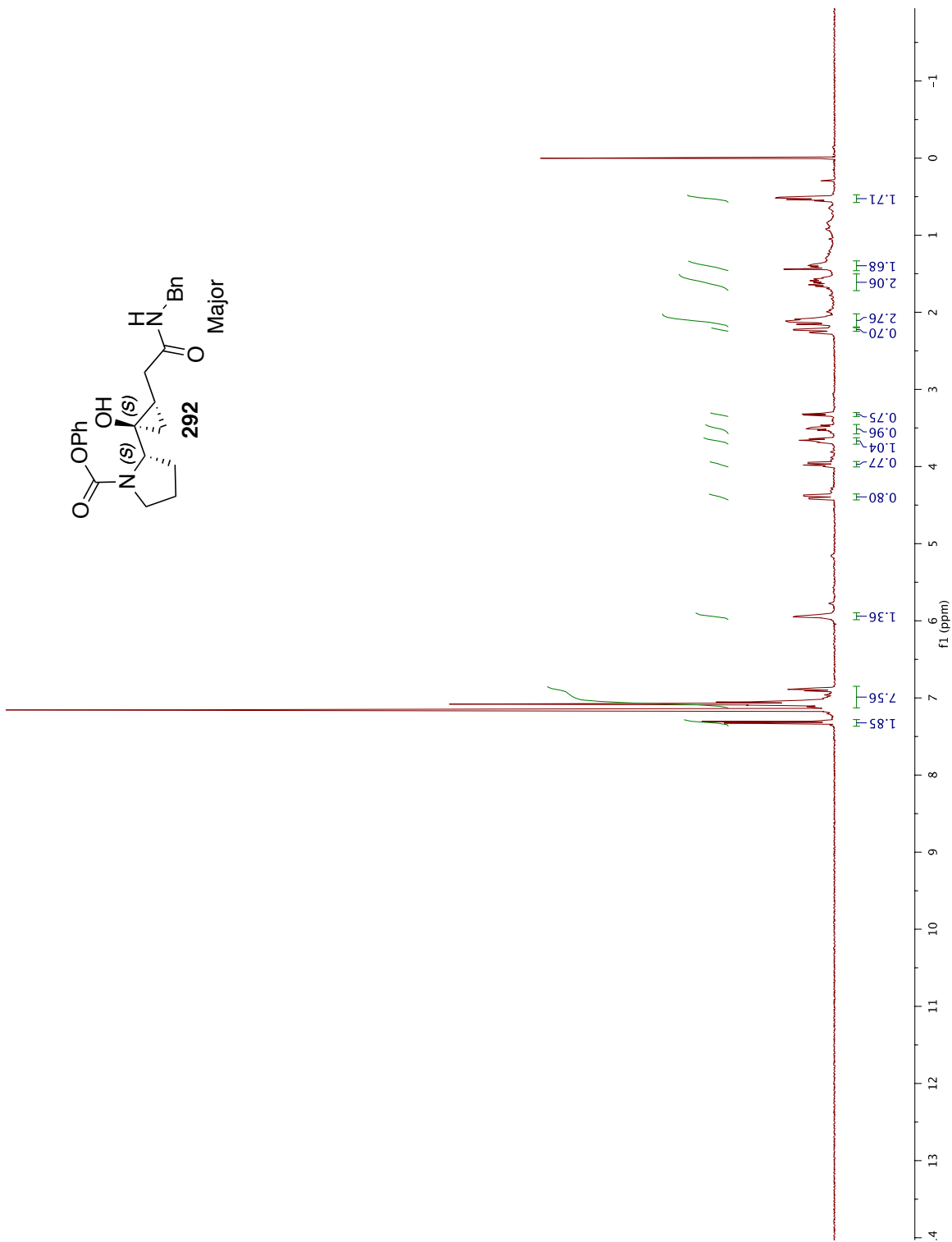


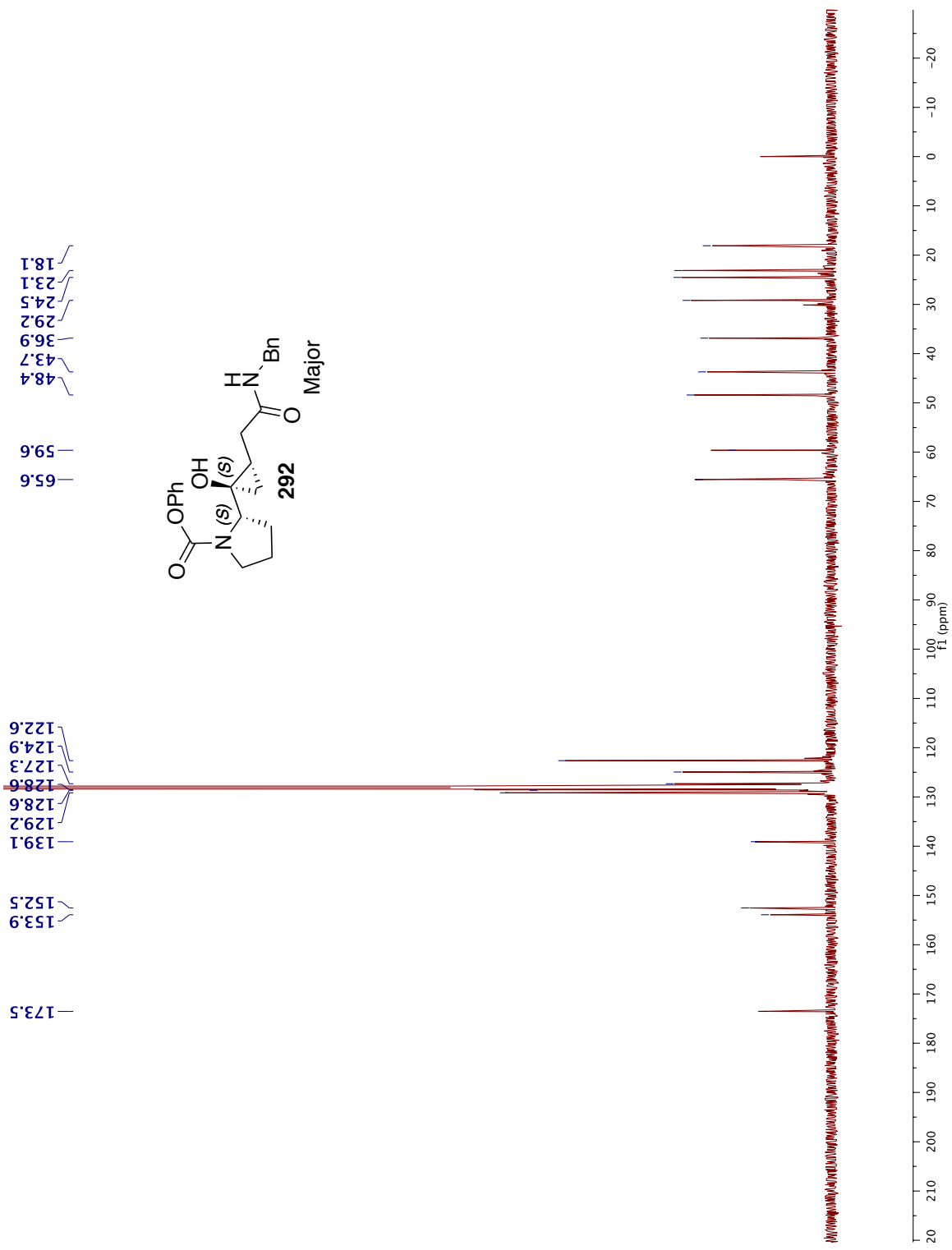


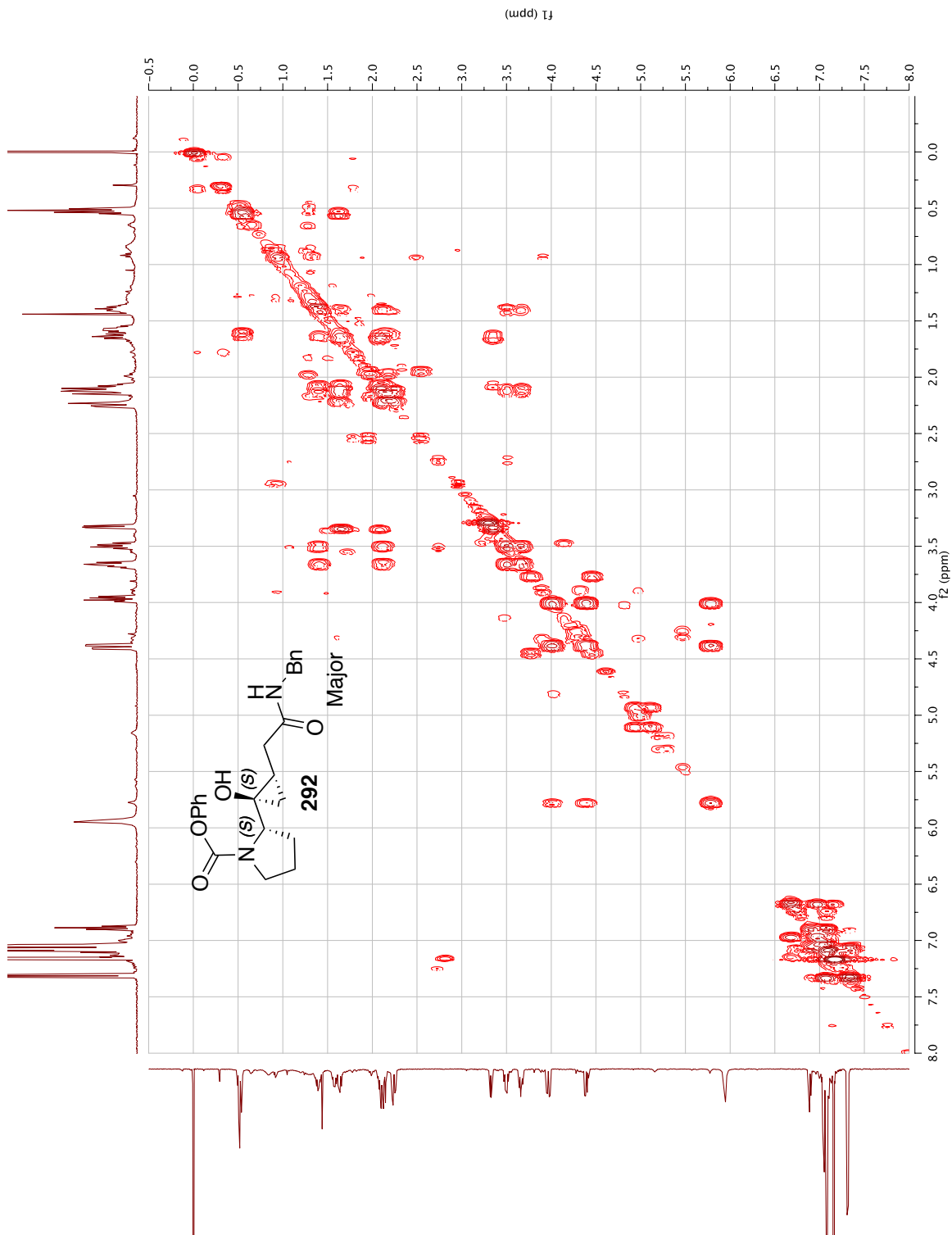


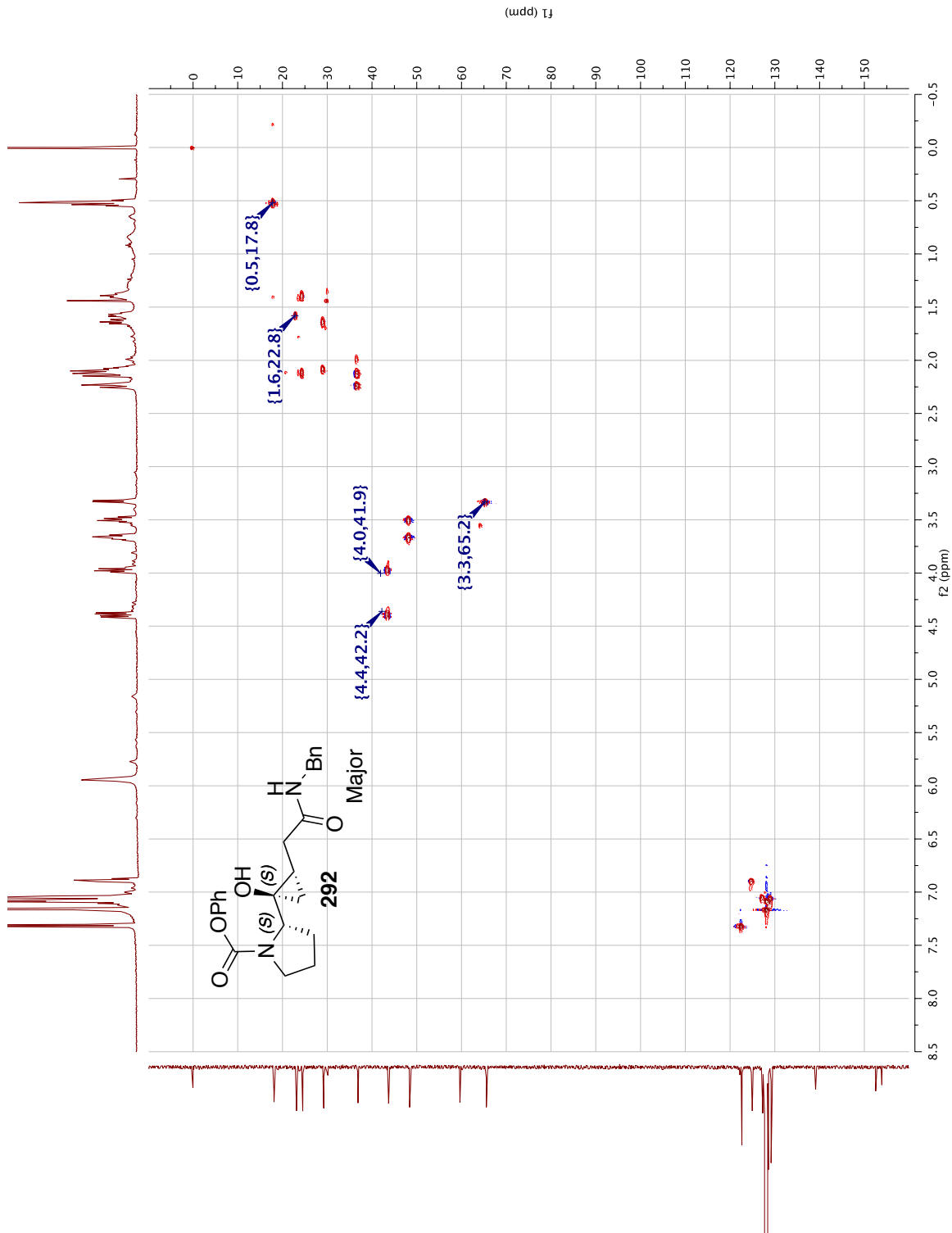


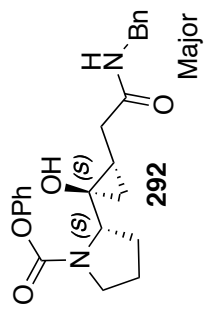










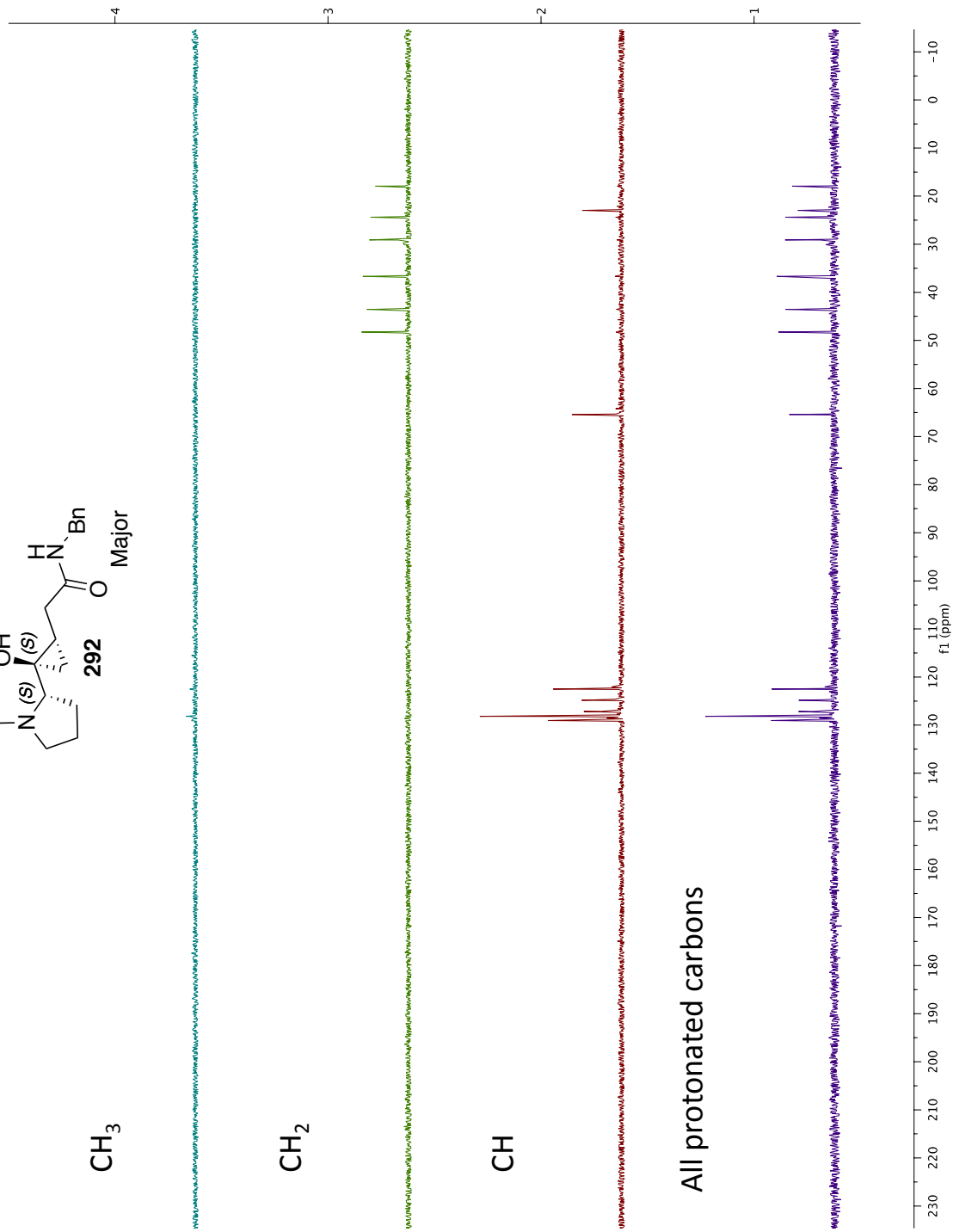


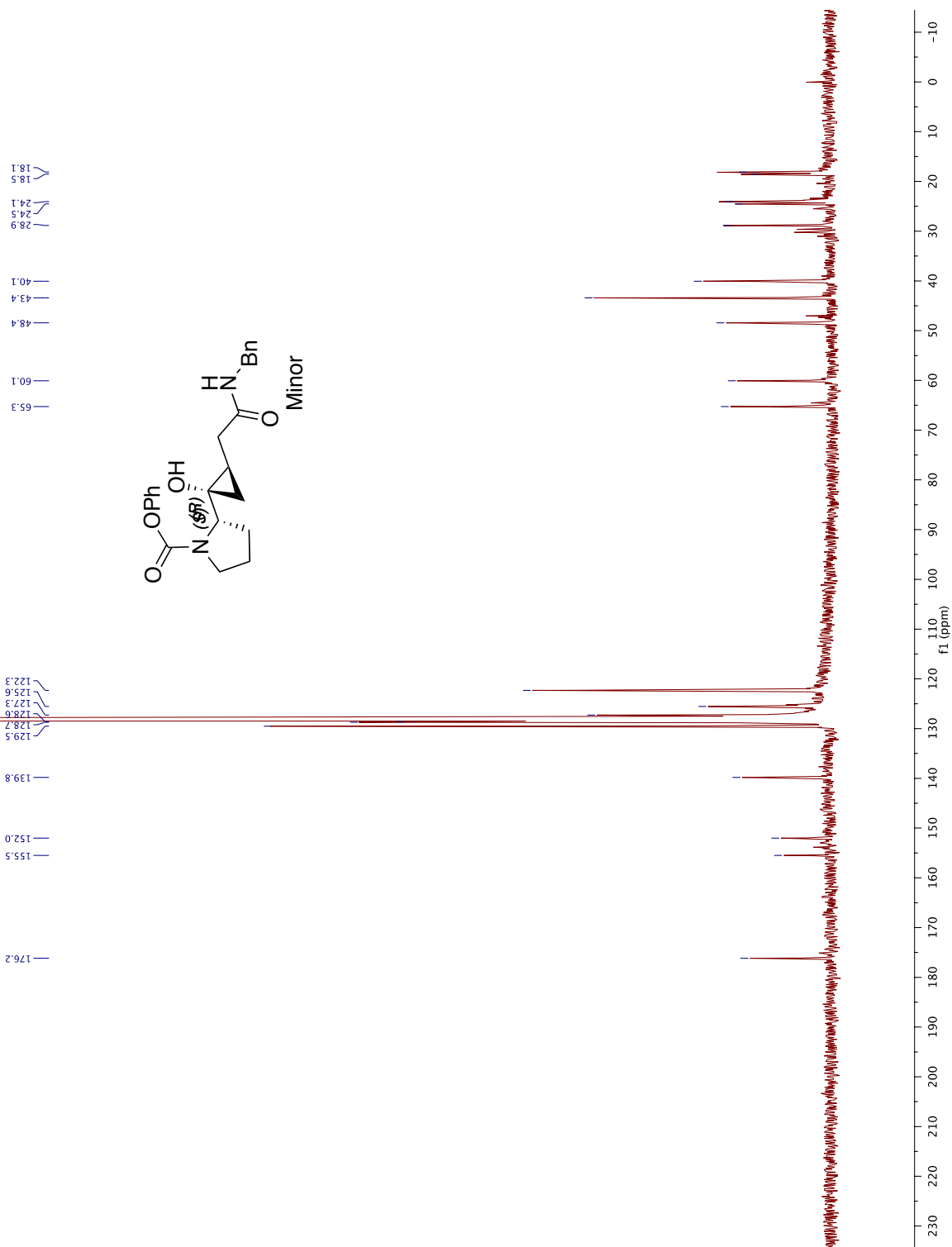
CH₃

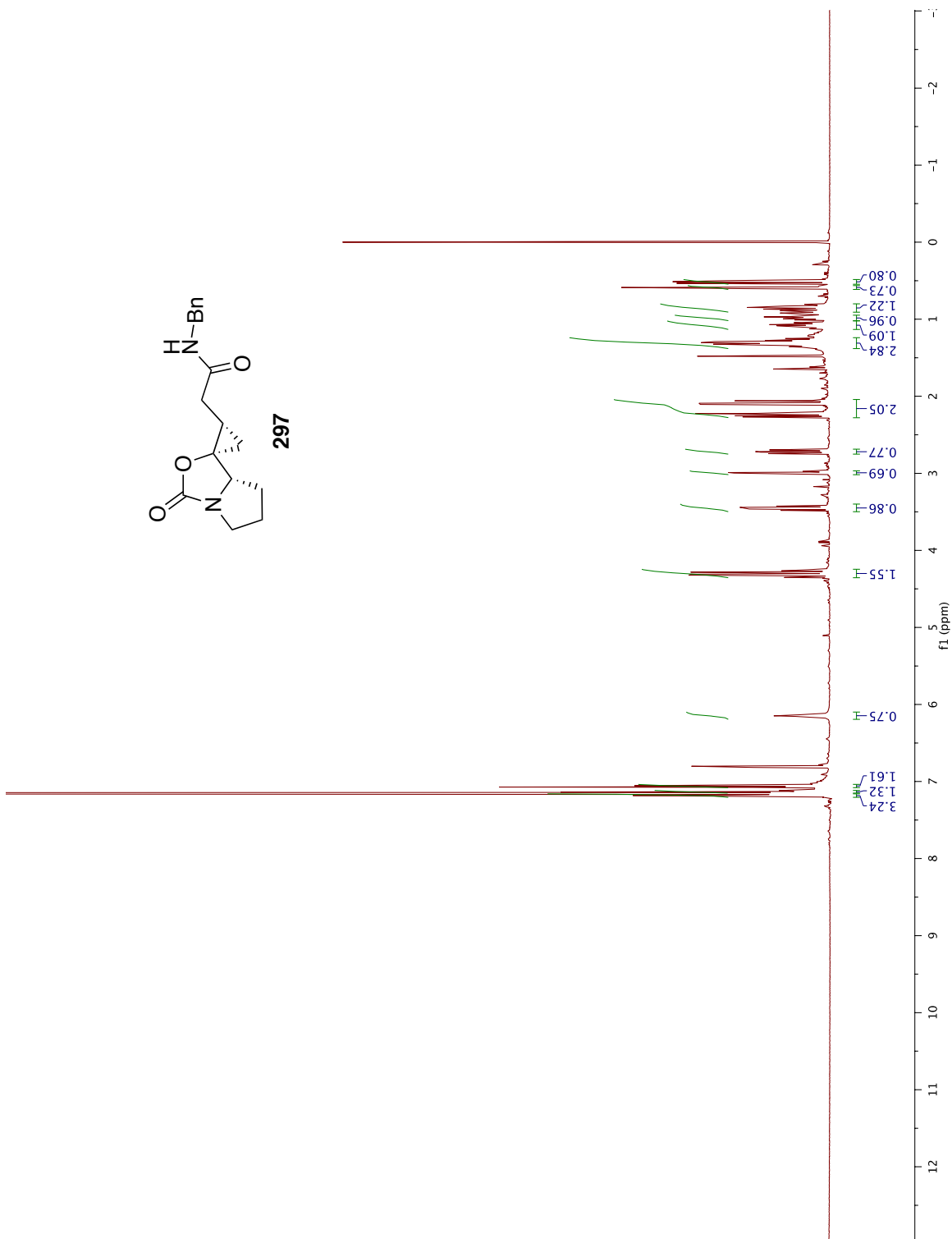
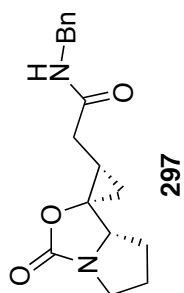
CH₂

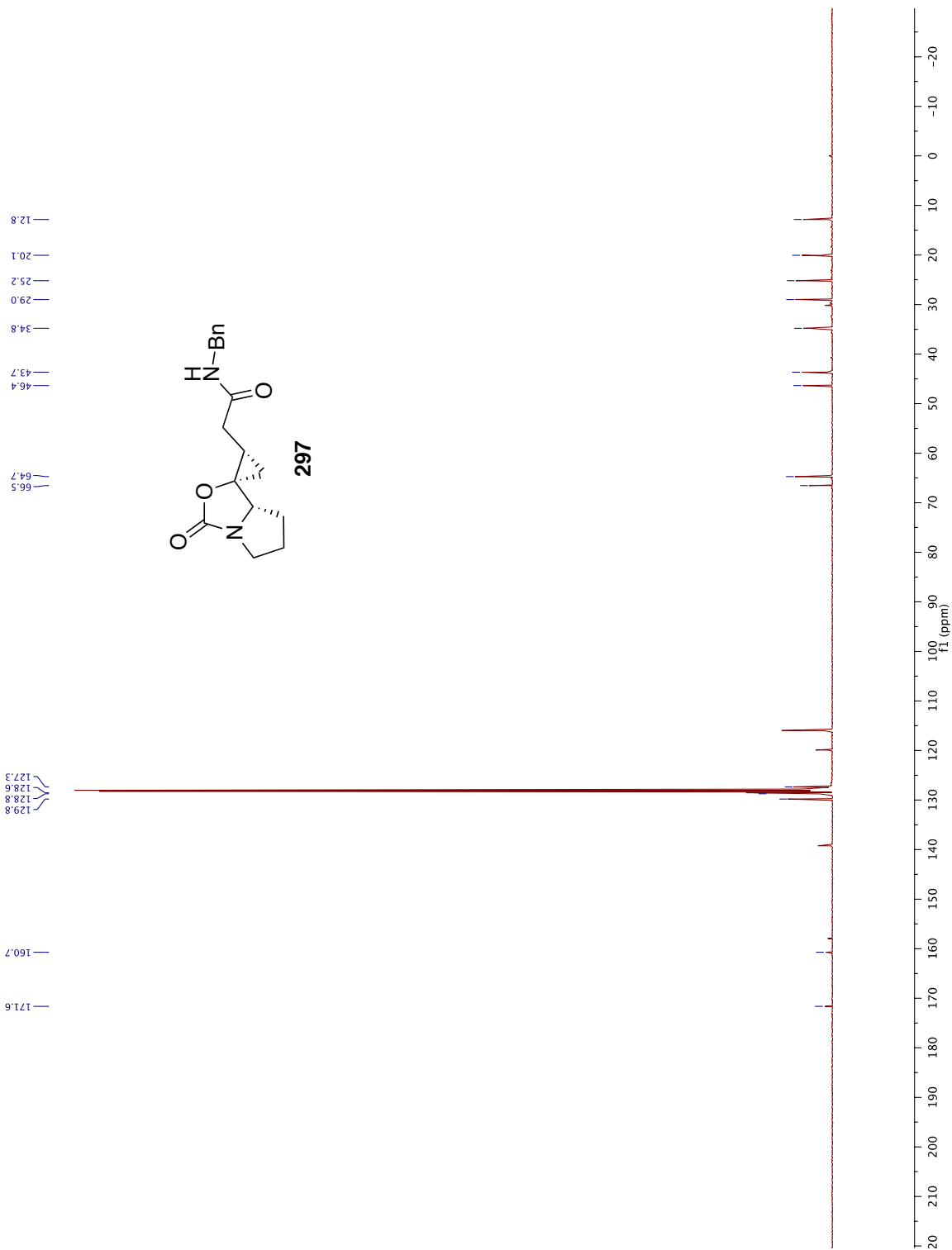
CH

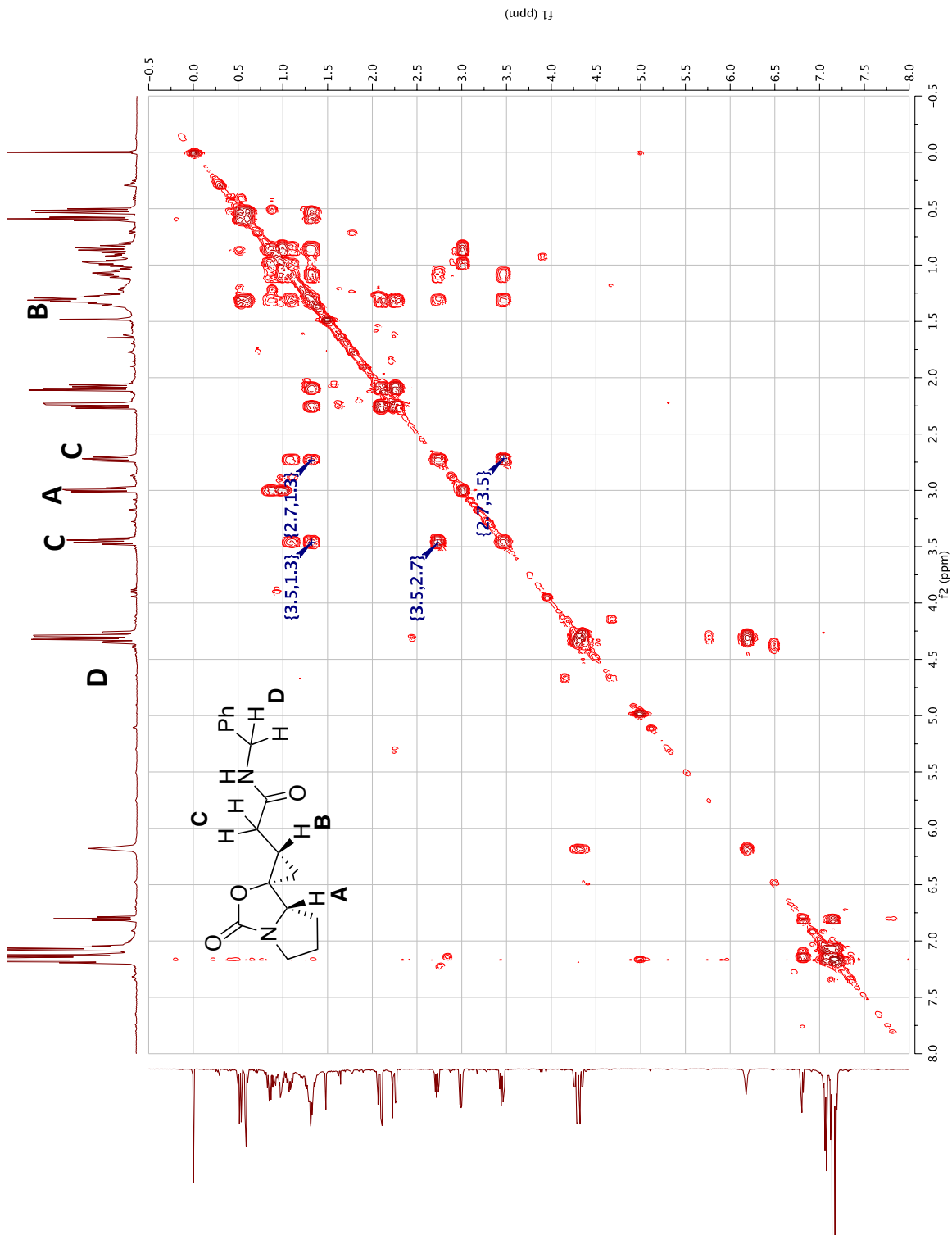
All protonated carbons

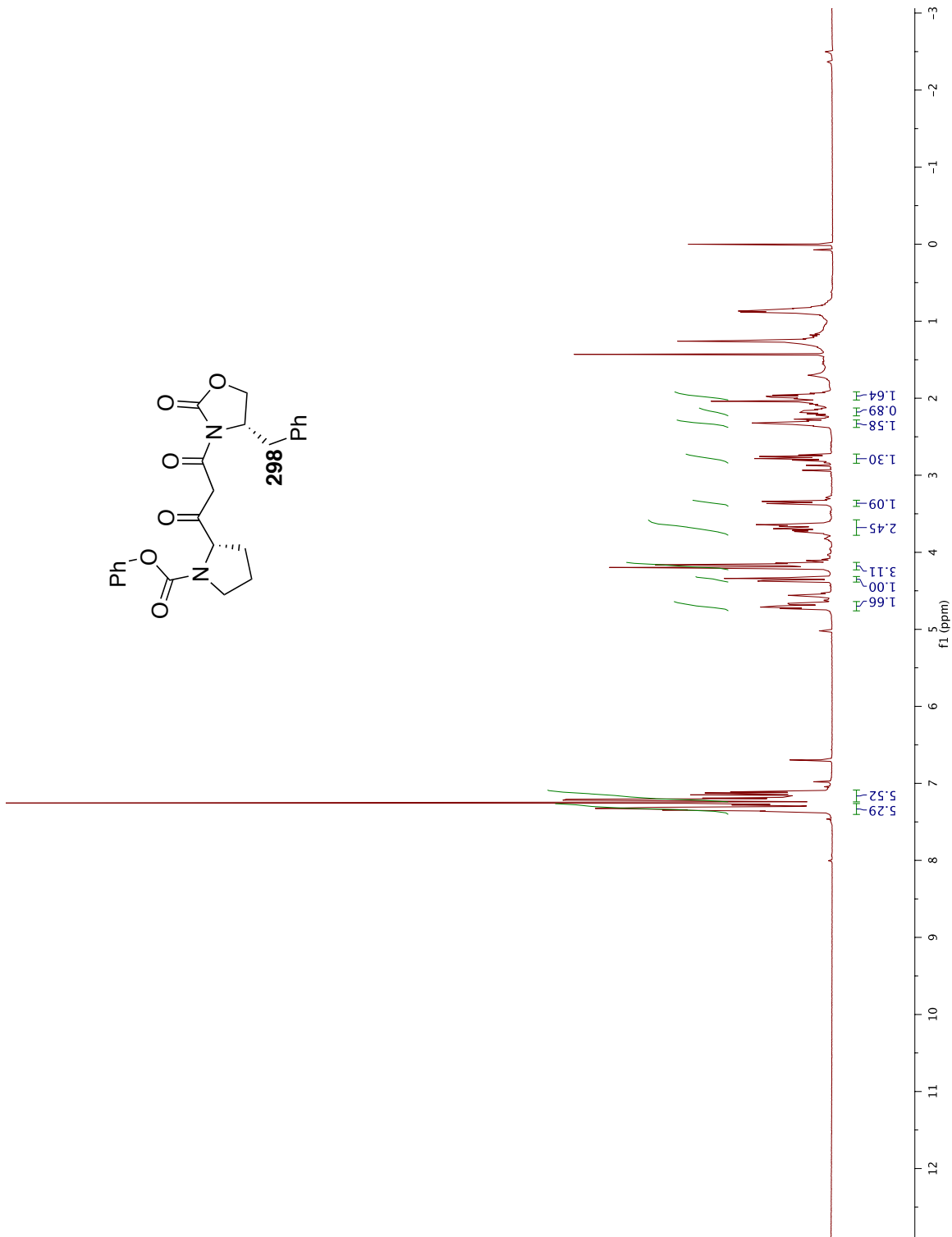
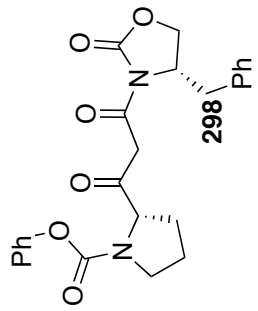


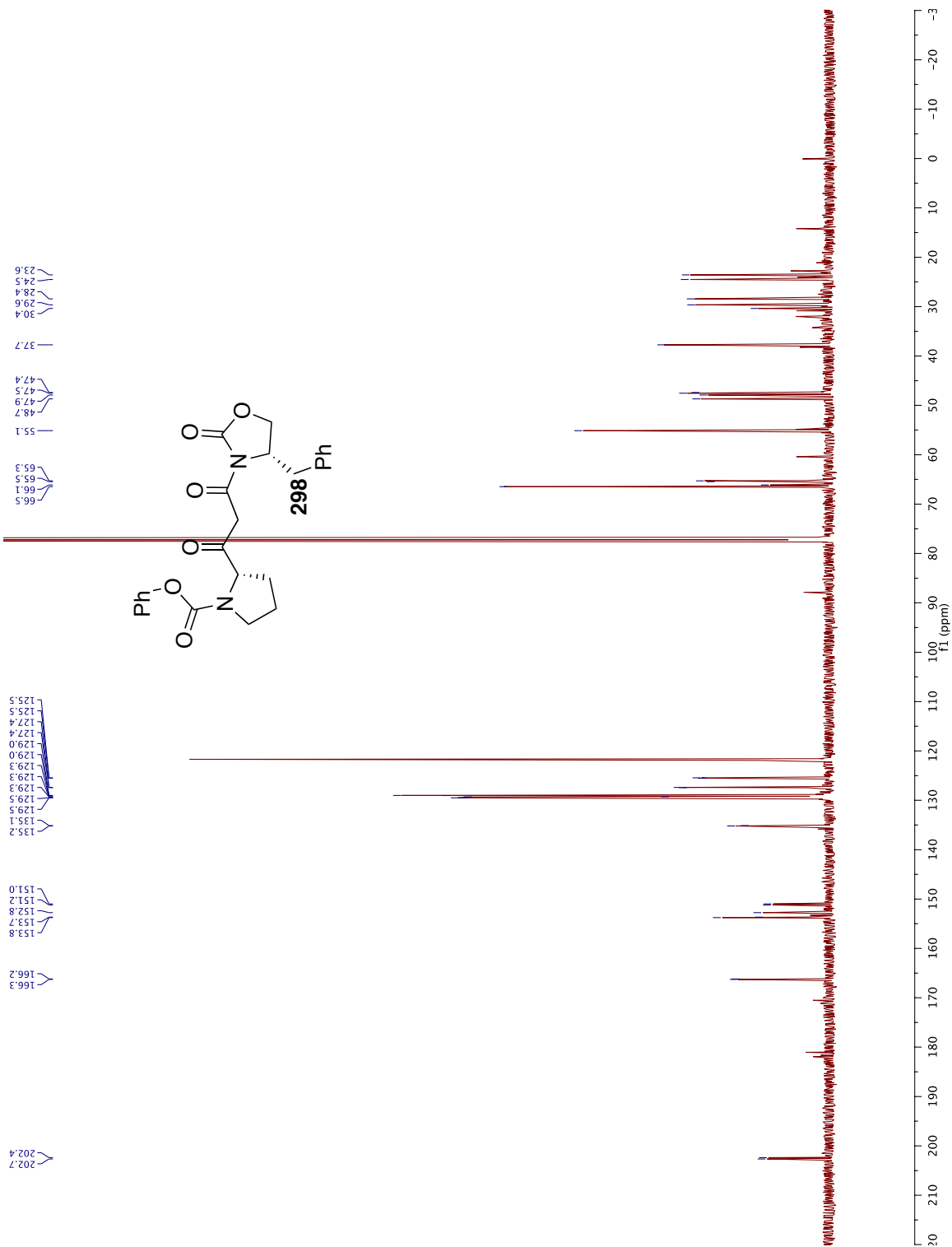


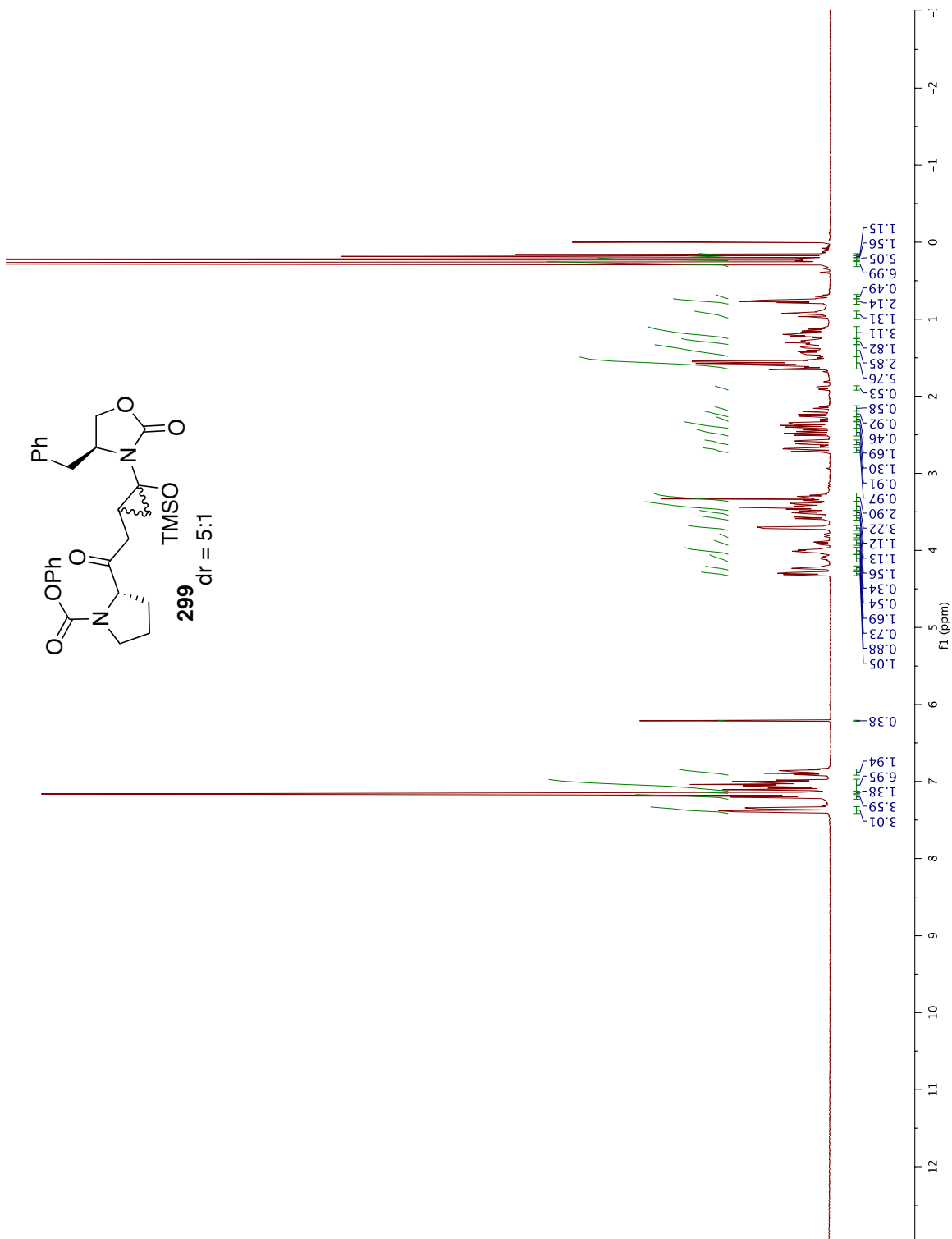


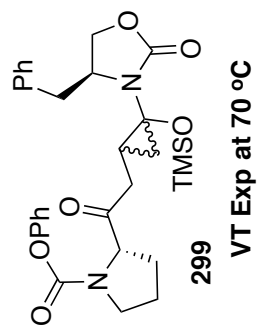




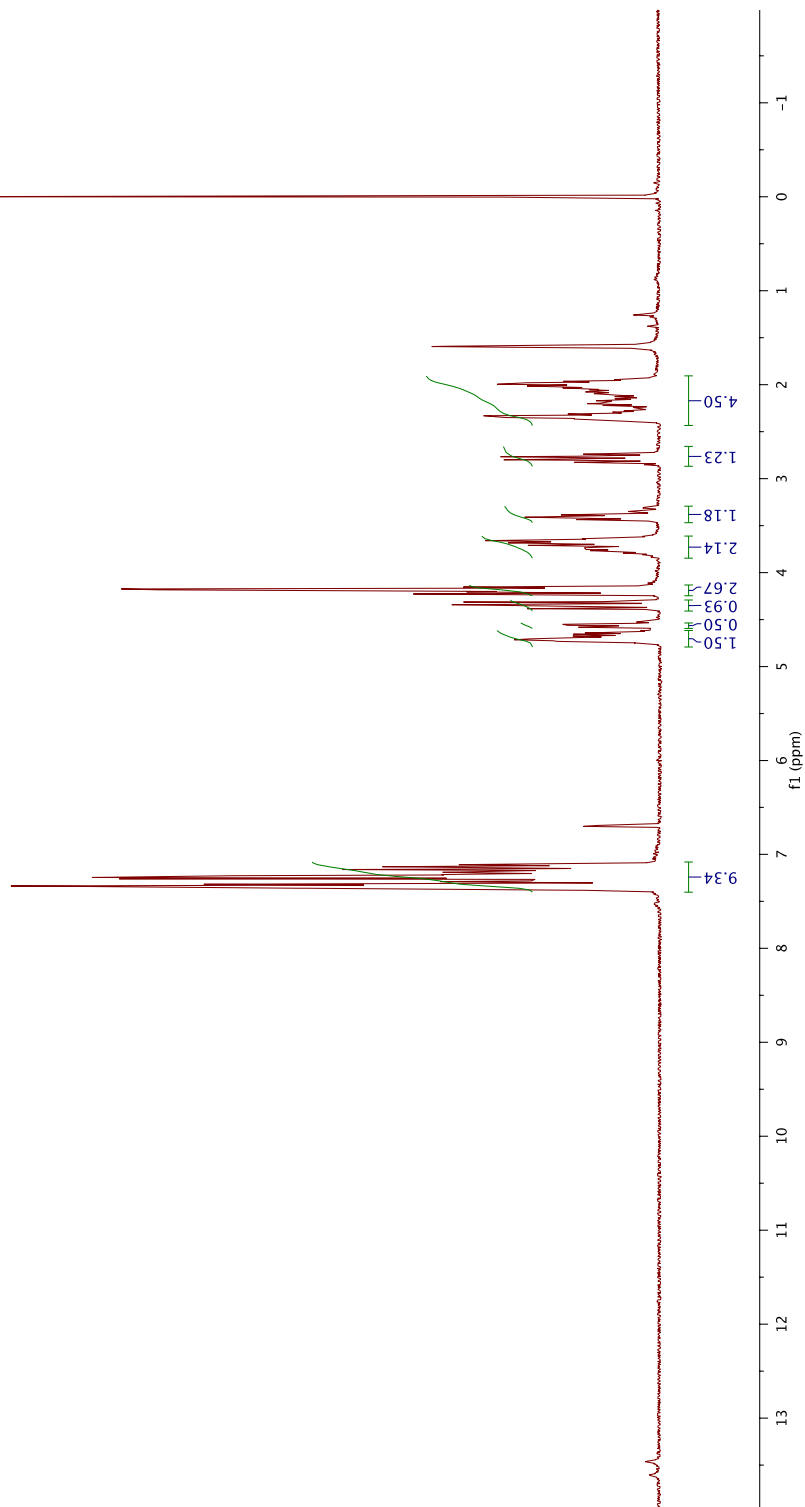


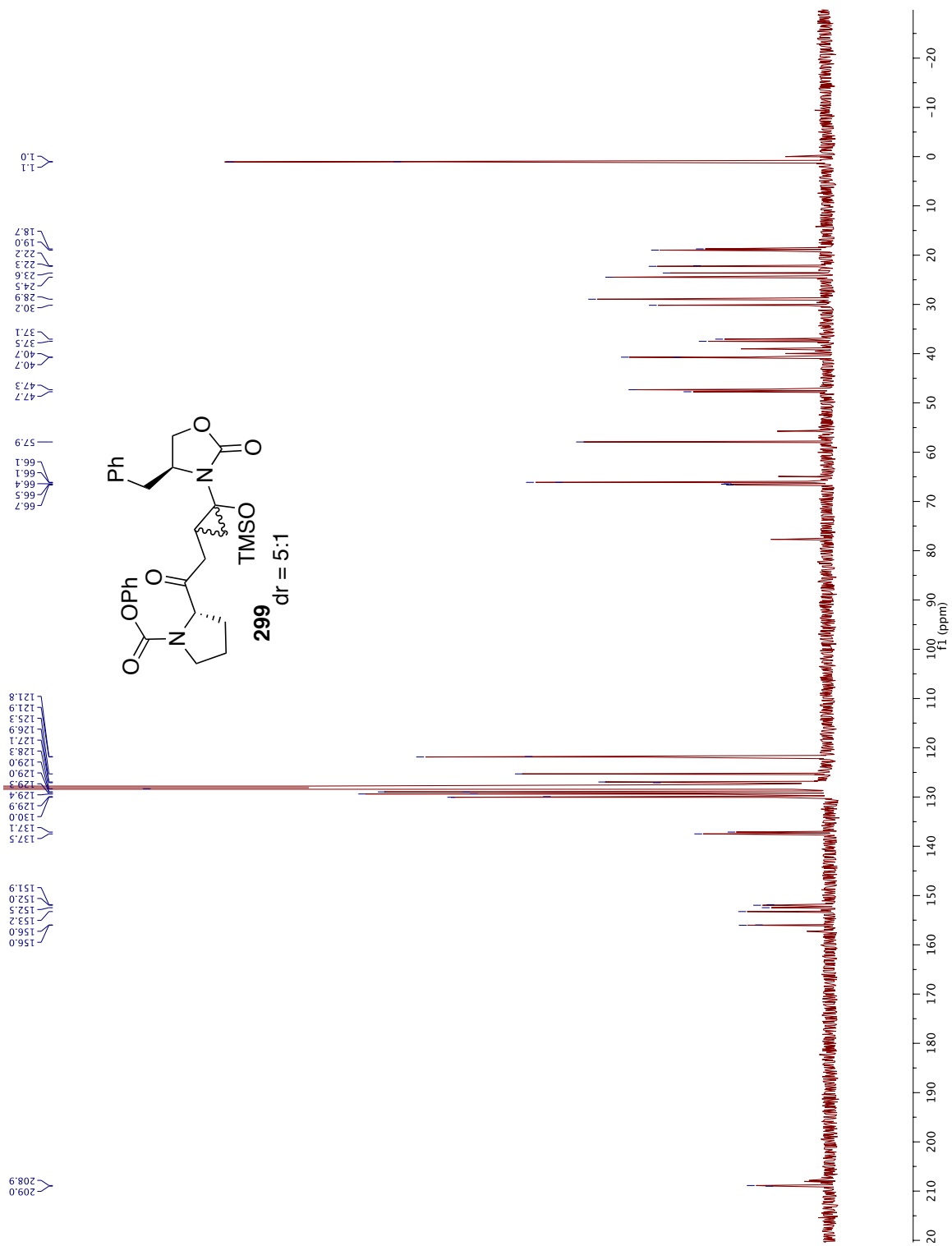


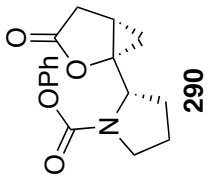
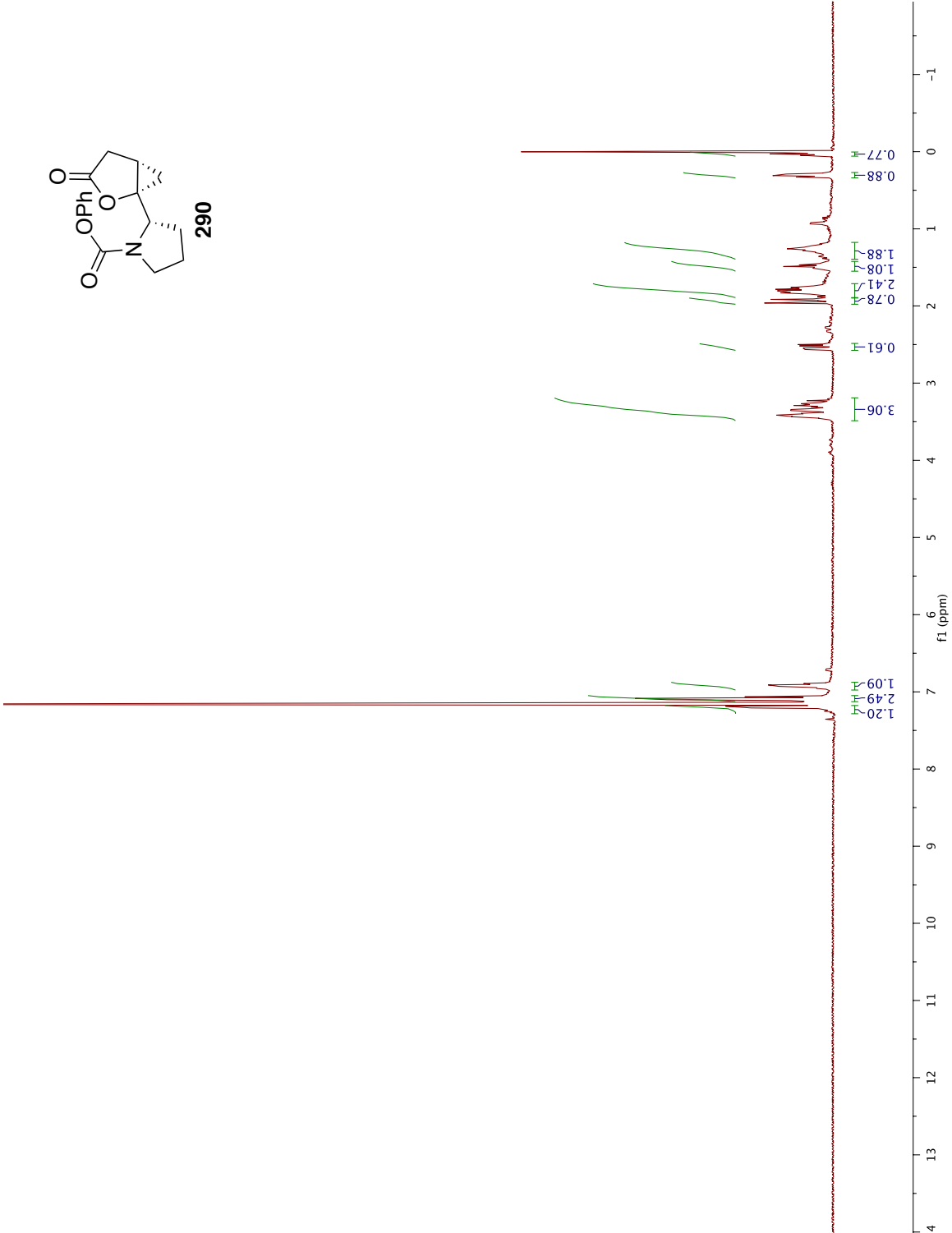


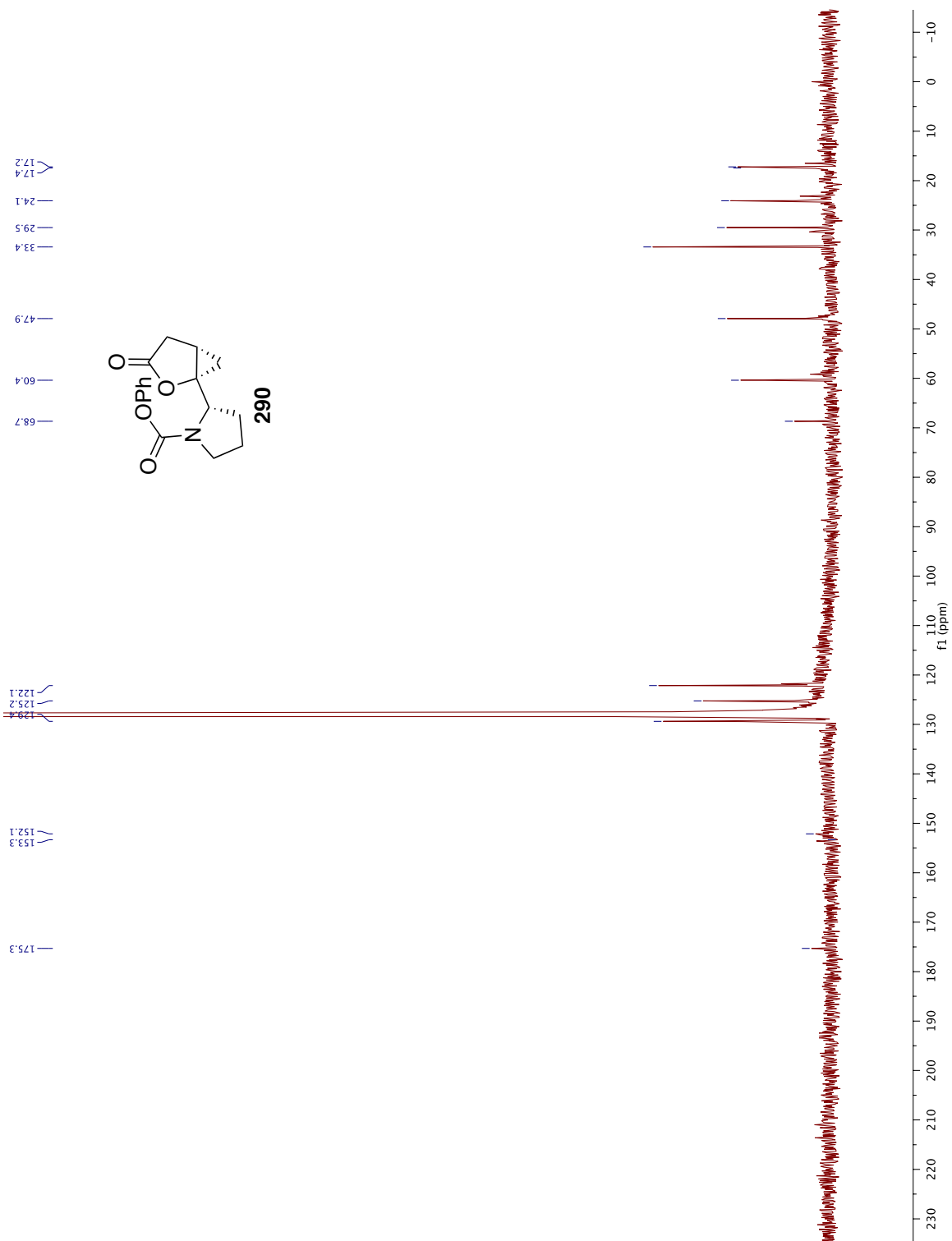


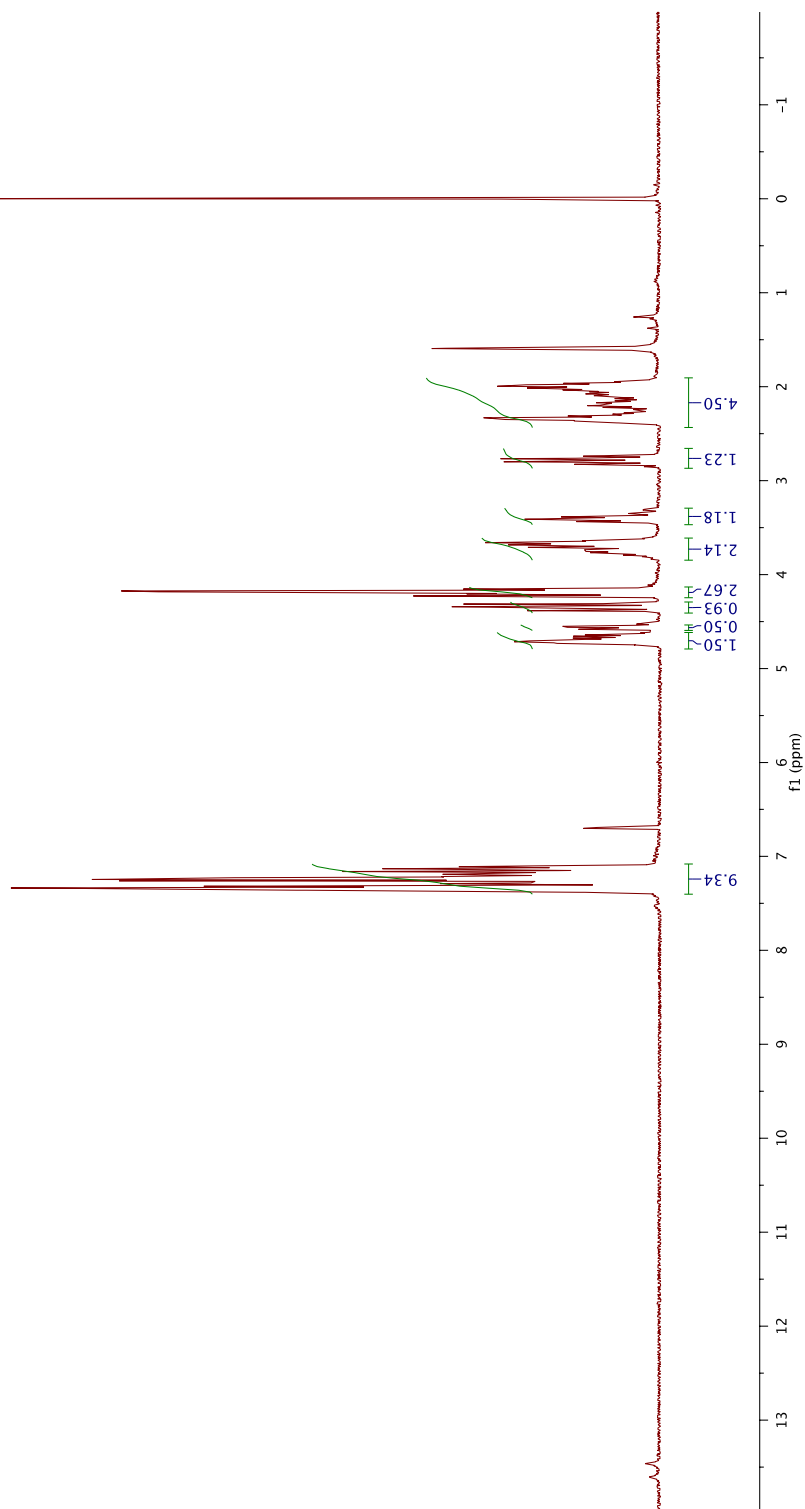
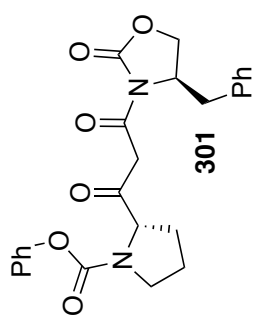
VT Exp at 70 °C

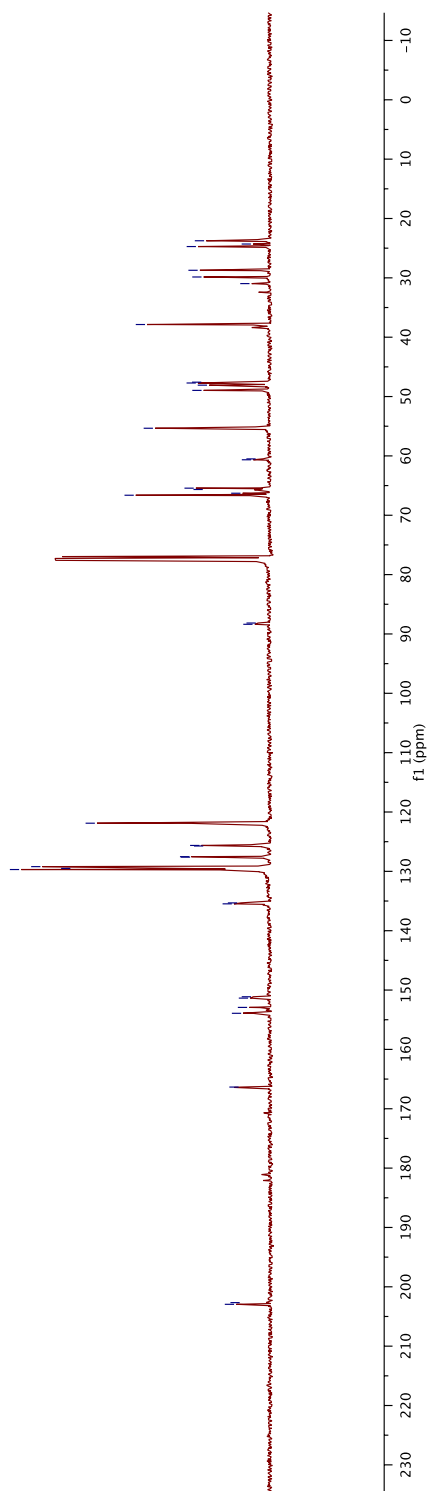
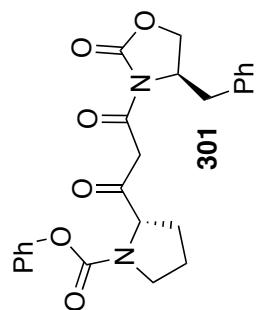


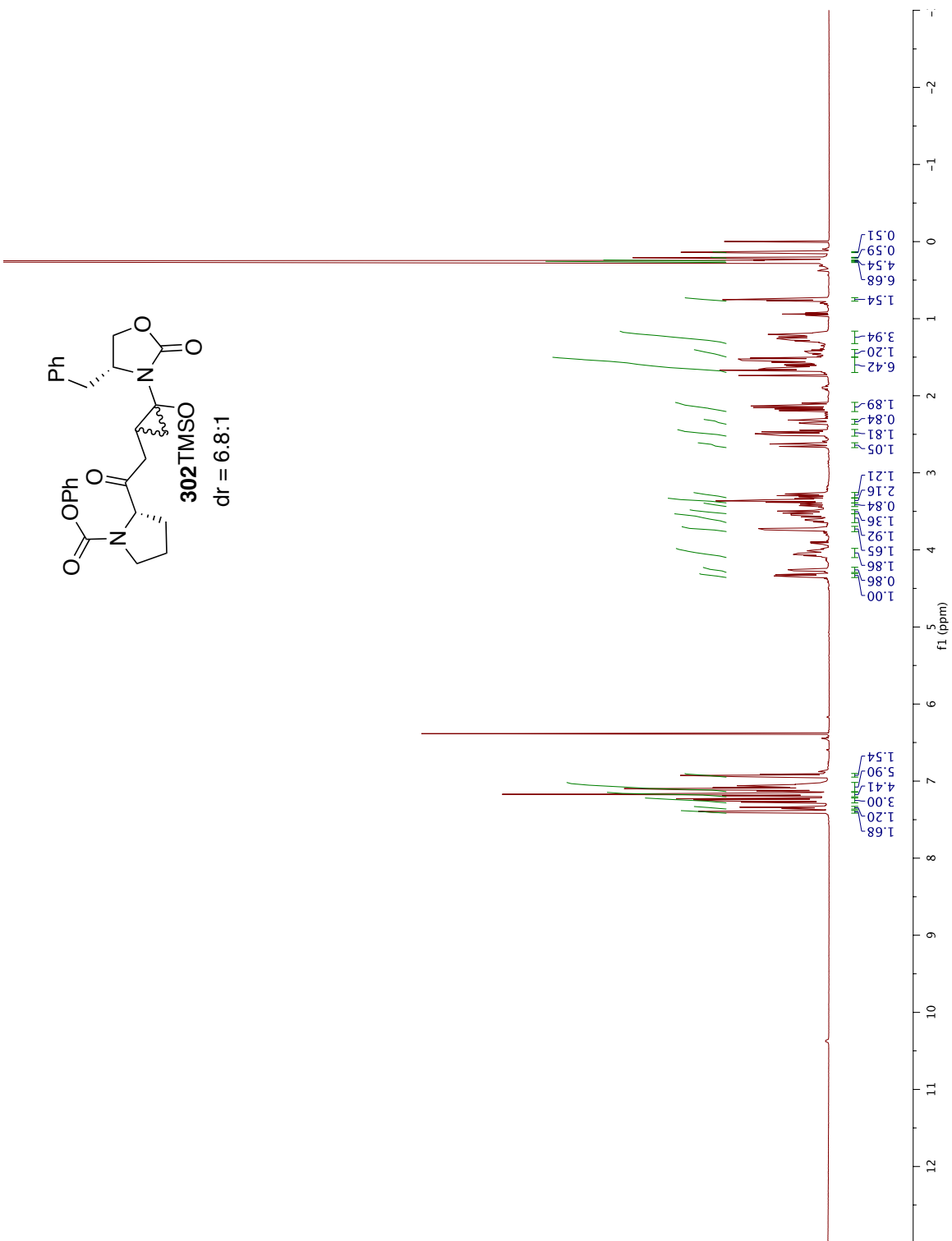


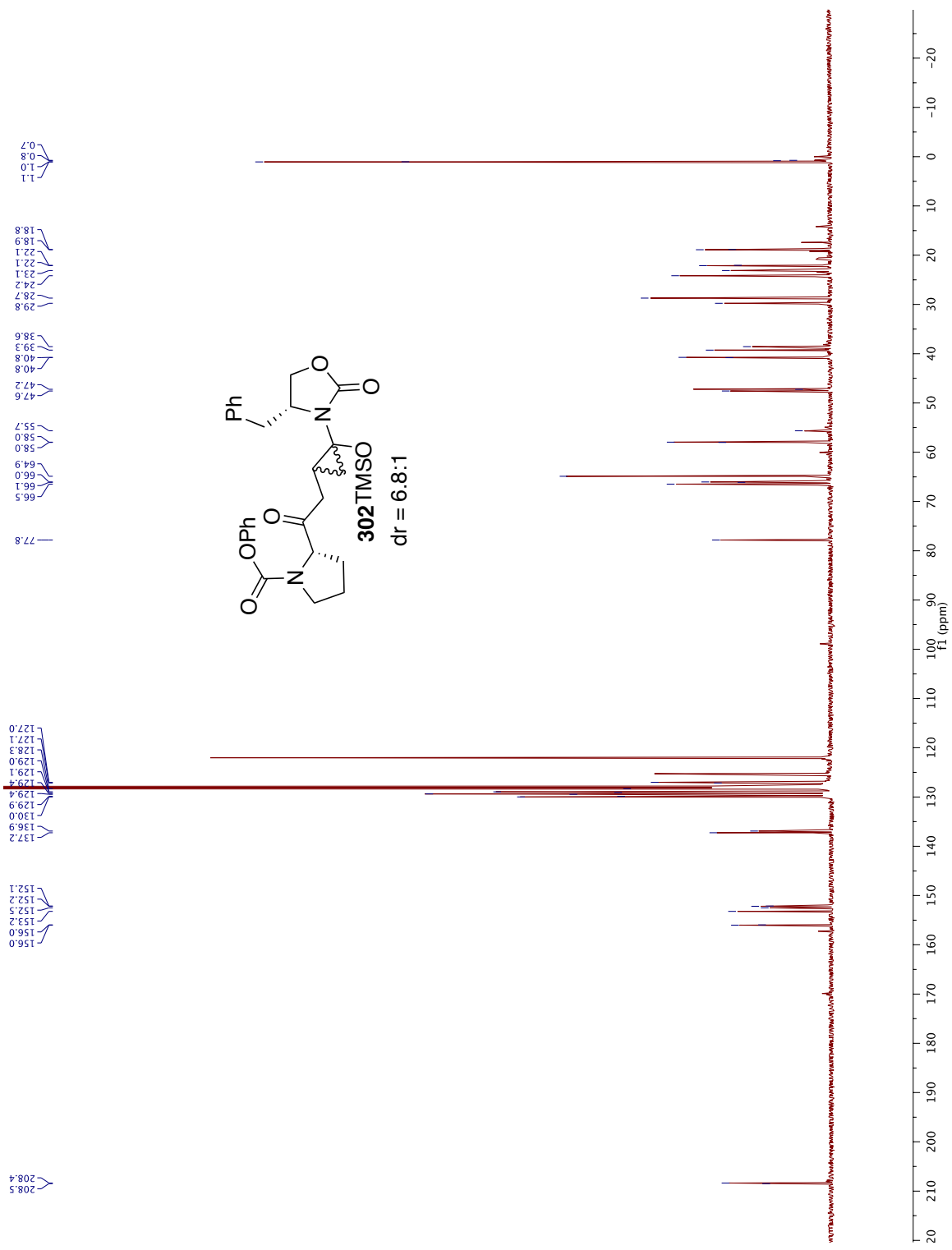


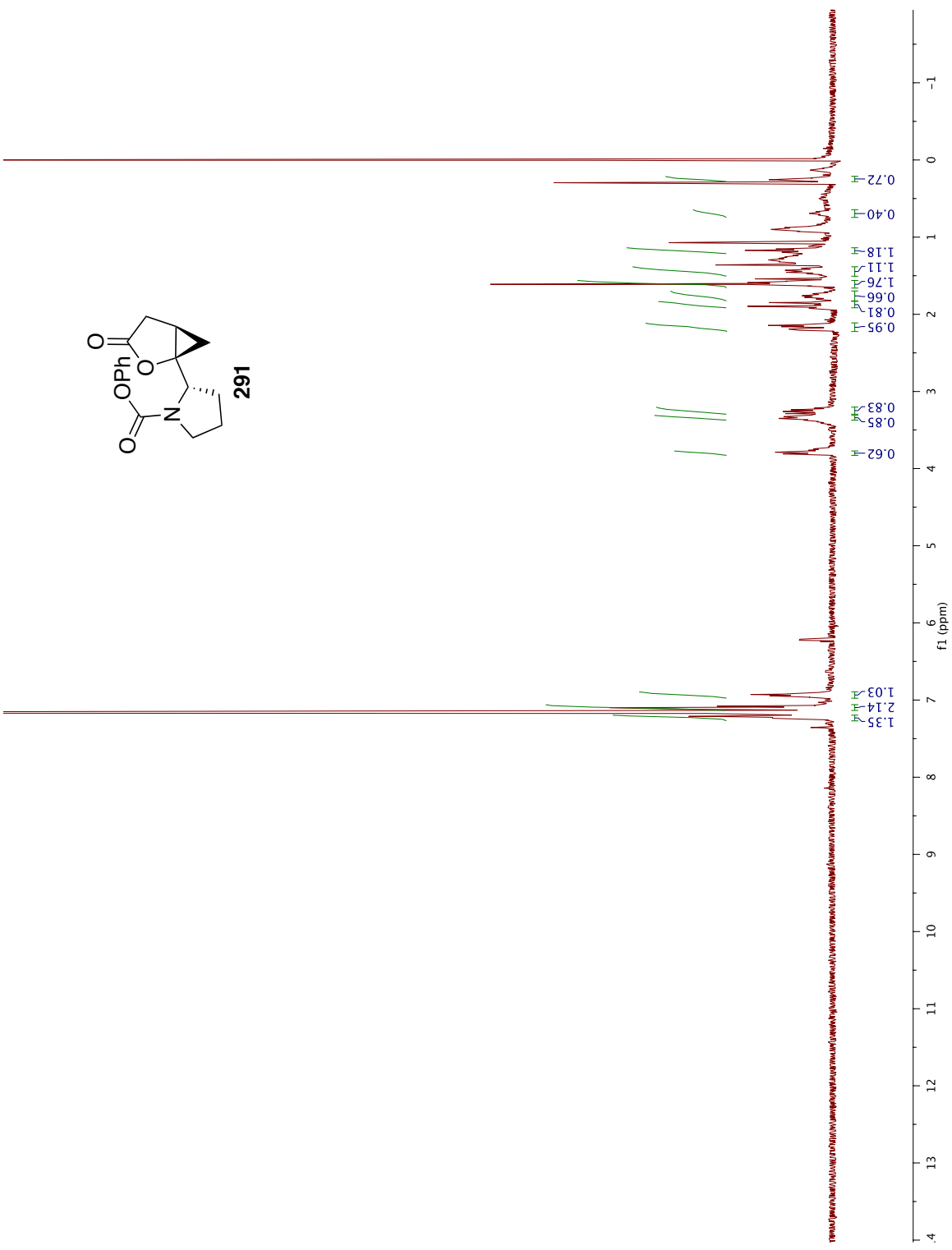
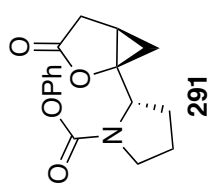


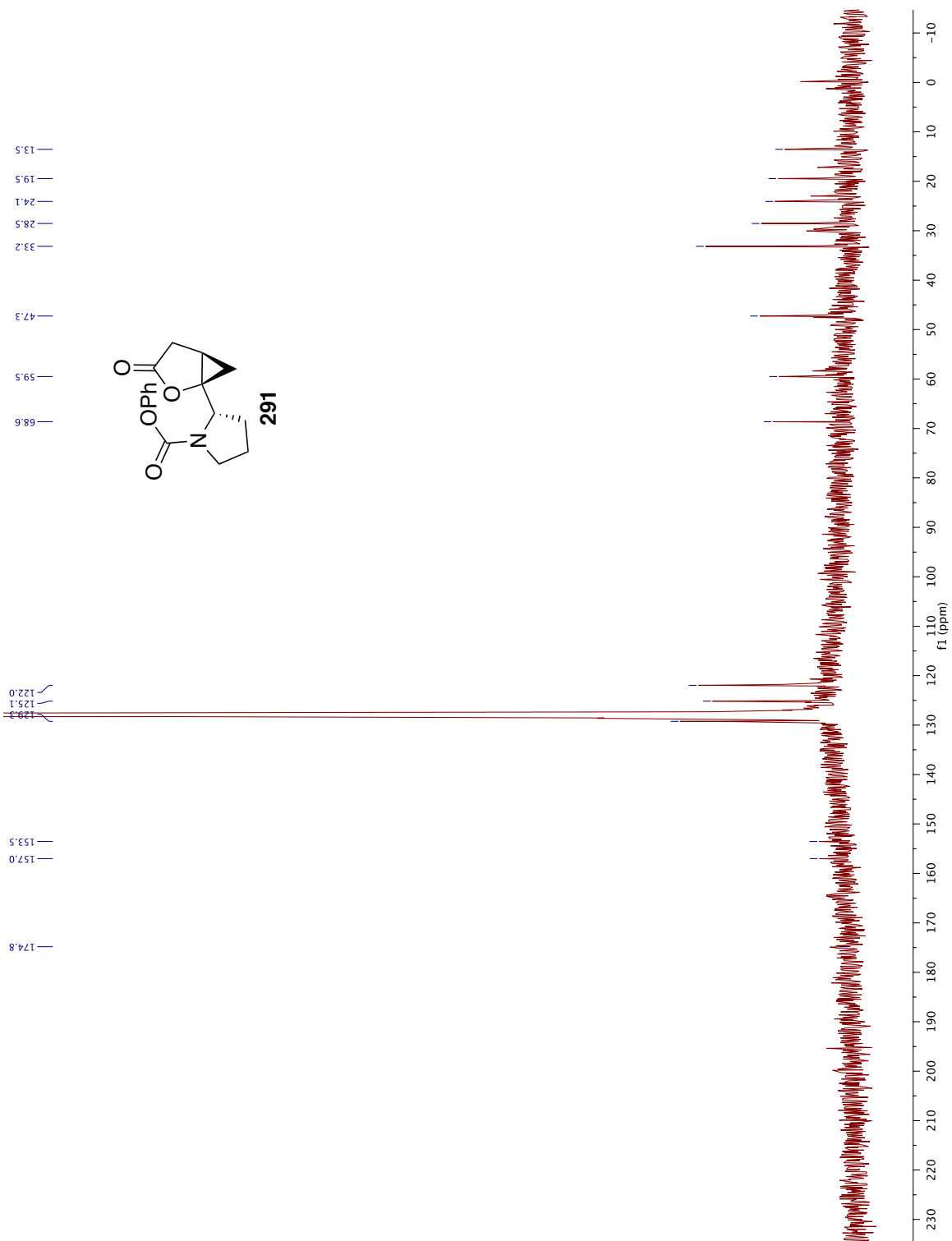


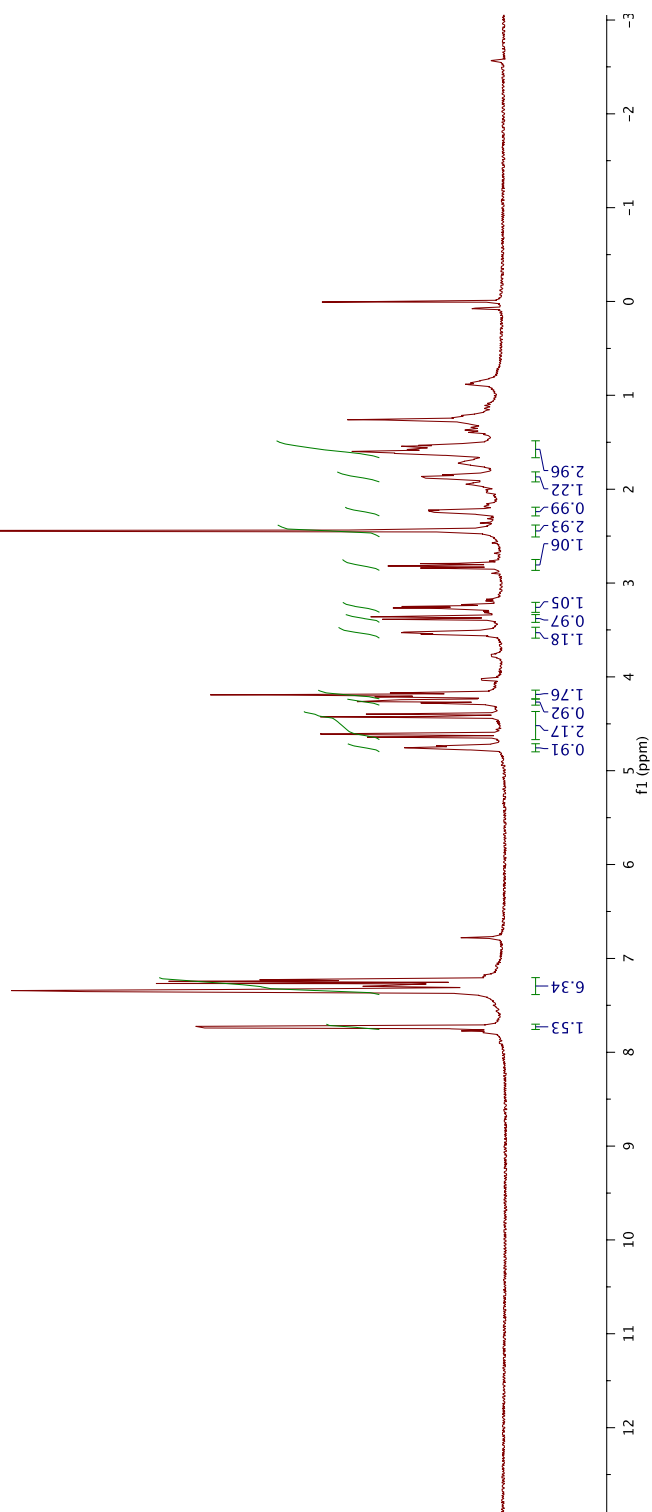
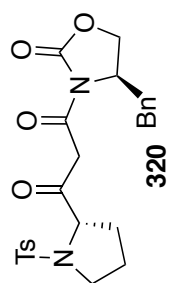


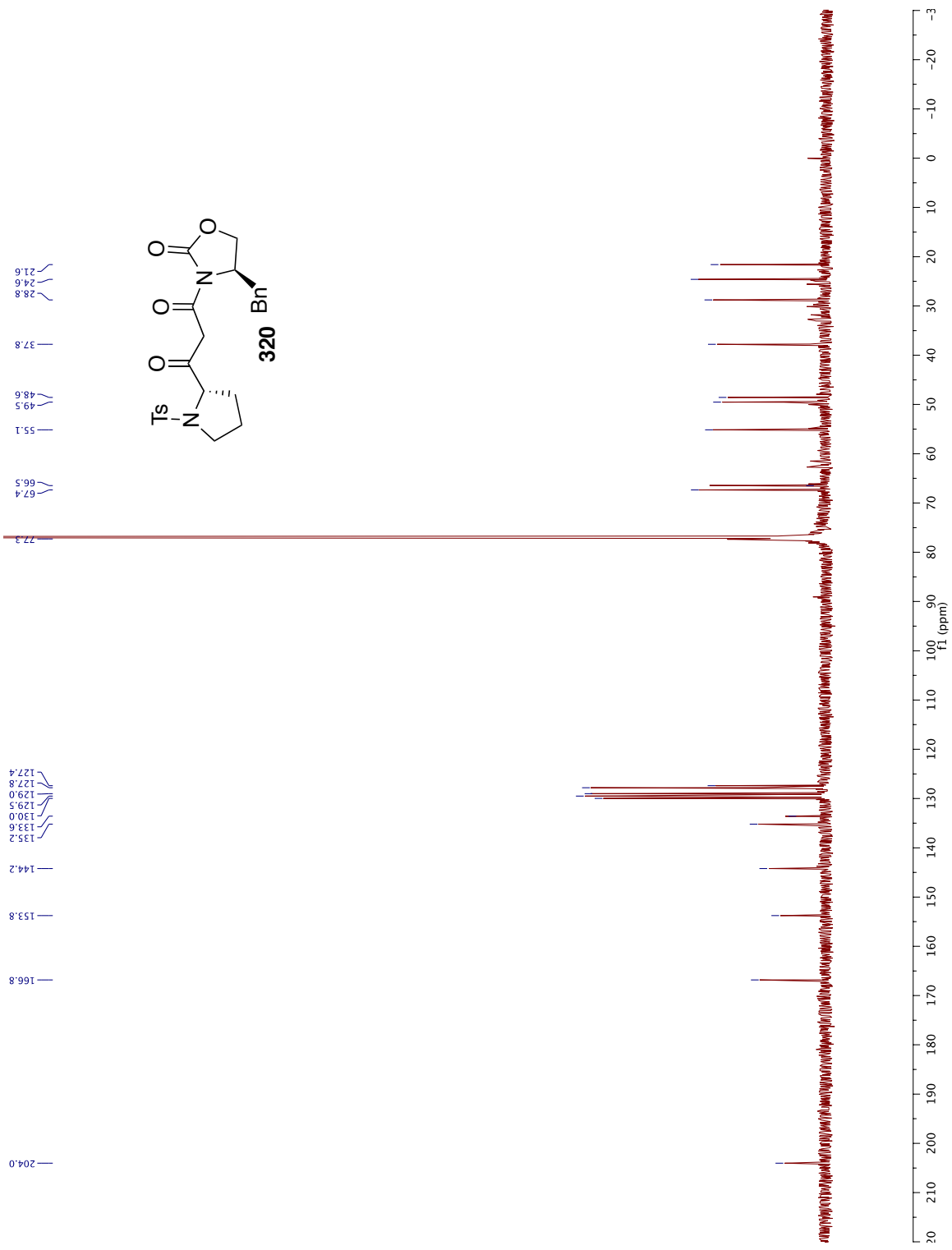












APPENDIX B
Crystal Structure

